HIGHLIGHTS IN CARDIAC RHYTHMOLOGY: 2021

EDITED BY: Matteo Anselmino
PUBLISHED IN: Frontiers in Cardiovascular Medicine

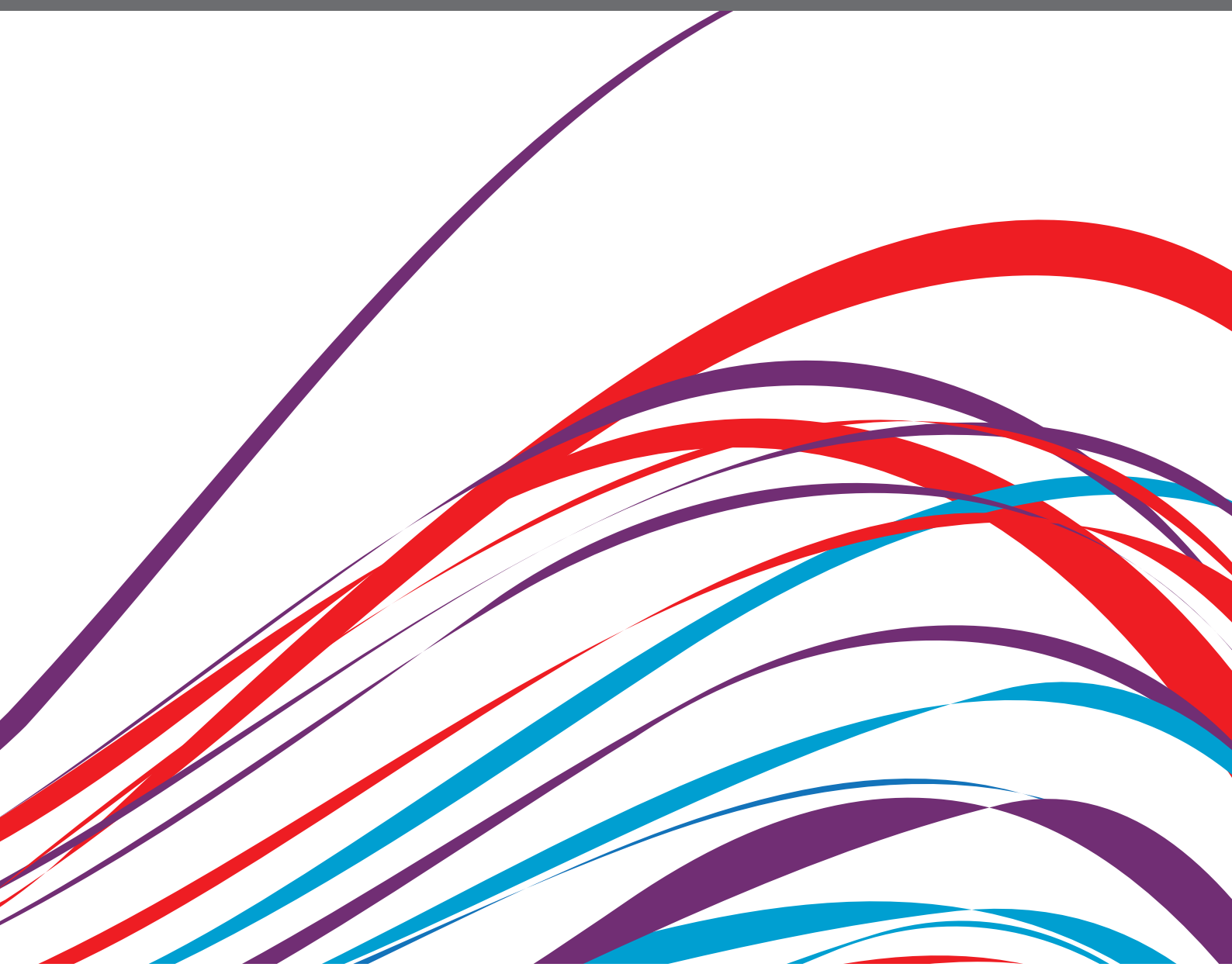

frontiers Research Topics

ISSN 1664-8714
ISBN 978-2-88974-831-0
DOI 10.3389/978-2-88974-831-0

About Frontiers

Frontiers is more than just an open-access publisher of scholarly articles: it is a pioneering approach to the world of academia, radically improving the way scholarly research is managed. The grand vision of Frontiers is a world where all people have an equal opportunity to seek, share and generate knowledge. Frontiers provides immediate and permanent online open access to all its publications, but this alone is not enough to realize our grand goals.

Frontiers Journal Series

The Frontiers Journal Series is a multi-tier and interdisciplinary set of open-access, online journals, promising a paradigm shift from the current review, selection and dissemination processes in academic publishing. All Frontiers journals are driven by researchers for researchers; therefore, they constitute a service to the scholarly community. At the same time, the Frontiers Journal Series operates on a revolutionary invention, the tiered publishing system, initially addressing specific communities of scholars, and gradually climbing up to broader public understanding, thus serving the interests of the lay society, too.

Dedication to Quality

Each Frontiers article is a landmark of the highest quality, thanks to genuinely collaborative interactions between authors and review editors, who include some of the world's best academicians. Research must be certified by peers before entering a stream of knowledge that may eventually reach the public - and shape society; therefore, Frontiers only applies the most rigorous and unbiased reviews.
Frontiers revolutionizes research publishing by freely delivering the most outstanding research, evaluated with no bias from both the academic and social point of view. By applying the most advanced information technologies, Frontiers is catapulting scholarly publishing into a new generation.

What are Frontiers Research Topics?

Frontiers Research Topics are very popular trademarks of the Frontiers Journals Series: they are collections of at least ten articles, all centered on a particular subject. With their unique mix of varied contributions from Original Research to Review Articles, Frontiers Research Topics unify the most influential researchers, the latest key findings and historical advances in a hot research area! Find out more on how to host your own Frontiers Research Topic or contribute to one as an author by contacting the Frontiers Editorial Office: frontiersin.org/about/contact

HIGHLIGHTS IN CARDIAC RHYTHMOLOGY: 2021

Topic Editor:
Matteo Anselmino, University of Turin, Italy

Citation: Anselmino, M., ed. (2022). Highlights in Cardiac Rhythmology: 2021. Lausanne: Frontiers Media SA. doi: 10.3389/978-2-88974-831-0

Table of Contents

frontiers in Cardiovascular Medicine

EDITORIAL
published: 11 March 2022
doi: 10.3389/fcvm.2022.866883

Editorial: Highlights in Cardiac Rhythmology: 2021

*Matteo Anselmino and Gaetano Maria De Ferrari**

Division of Cardiology, Department of Medical Sciences, Città della Salute e della Scienza di Torino Hospital, University of Turin, Turin, Italy

Keywords: arrhythmias, electrophysiology, technologies, innovation, cardiac

Editorial on the Research Topic

Editorial: Highlights in Cardiac Rhythmology: 2021

The World Health Organization declared the outbreak of severe acute respiratory syndrome coronavirus 2 (COVID-19) a pandemic state on 11 March 2020, and, ever since, healthcare professionals have promptly invested all efforts into fighting against COVID-19 with the goal of saving the lives of patients, friends, and family members. Every day, physicians fight against diseases, from those limiting quality of life to those threatening survival. Taking the Hippocratic Oath, they respect scientific obligations, profess warmth and empathy, and take full responsibility for their patients' bettering. Nevertheless, physicians are not used to facing a long-lasting health crisis. Reactions to the unexpected scenario have been palpable. A small group of people are being squeezed by a gigantic enemy and simply remain petrified. A few, guided by feelings of inferiority towards the unprecedented situation, have shifted their energies toward personal or domestic matters, limiting professional duties. The majority, however, have "only" felt disoriented. There is a need for corporate guidance and a sense of the strength of a community moving together towards a common goal, favoring collaborations and team or network formation; these are crucial elements of great 2021's scientific production in all fields, Cardiac Rhythmology included (**Figure 1**).

Out of the most creative and original topics, few emerge. Conduction system pacing (CSP), including left bundle branch pacing, is emerging as a promising pacing modality to prevent electrical and mechanical delay through direct capture of the original conduction system (Chen et al.; Liu P. et al.; Liu J. et al.; Ye, Wu et al.). The challenges related to the restricted number of tools initially confined CSP to small single-center experiences. As new tools are becoming available, the use of CSP is now spreading rapidly, even being used for distal conduction disturbances and, eventually, dealing with cardiac resynchronization. The clinical benefits of CSP are no longer in doubt, and apical pacing, particularly in patients with expected high pacing burden and initial structural heart disease, will soon be banded to avoid pacing-induced cardiomyopathy.

The same year a temporary, fully implantable pacemaker undergoing complete dissolution and clearance by natural biological processes was designed (1), the technology for continuous ECG monitoring and heart rhythm analysis by all kinds of wearable or miniaturized devices was validated [(2); Mancinetti et al.; Guo et al.]. Atrial fibrillation occupies a significant amount of attention due to the social and clinical burden of the arrhythmia. From thromboembolic risk markers, clinical management optimization, and new ablation sources and tools, innovations appear on a daily basis [Hämmerle et al.; Bohm et al.; Ye, Liu et al.; (3, 4)]. Early rhythm control, compared to usual care, has proved to decrease the risk of adverse cardiovascular outcomes (5) suggesting transcatheter ablation even as a first-line therapy option (Saglietto et al.).

Also, ventricular tachycardia management is experiencing a paradigm shift. Novel imaging protocols permit thorough tissue characterization and standardization of the origin depiction of arrhythmias. Insights into the candidate selection, safety, and

OPEN ACCESS

Edited and reviewed by:
Philipp Sommer,
Herz- und Diabeteszentrum NRW,
Clinic for Electrophysiology, Germany

***Correspondence:**
Gaetano Maria De Ferrari
gaetanomaria.deferrari@unito.it

Specialty section:
This article was submitted to Cardiac Rhythmology, a section of the journal Frontiers in Cardiovascular Medicine

Received: *31 January 2022*
Accepted: *07 February 2022*
Published: *11 March 2022*

Citation:
Anselmino M and De Ferrari GM (2022) Editorial: Highlights in Cardiac Rhythmology: 2021. Front. Cardiovasc. Med. 9:866883. doi: 10.3389/fcvm.2022.866883

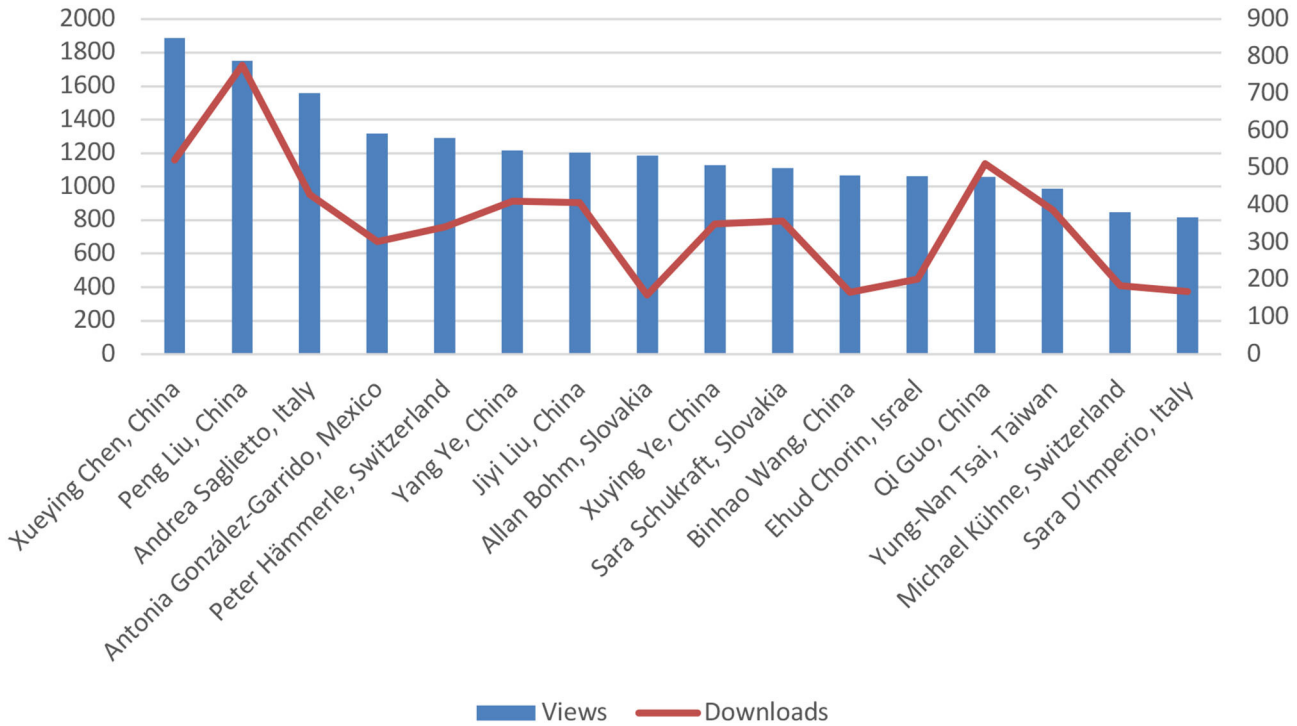

FIGURE 1 | Metrics (at January 12th 2022) of the best-performing articles (First Author, Country) published in Frontiers in Cardiovascular Medicine, Rhythmology section, in 2021.

efficacy of classical and innovative tools hold the potential to improve the outcome of this dreadful arrhythmia.

This issue includes a selection of the accomplishments of the Cardiac Rhythmology section from 2021; there is no time to rest—the wind blows strong in several directions. We do not yet know the future of parasternal access for substernal, less invasive, shock and pacing lead implantation, sympathetic nerve activity (measured at the skin or auditory canal levels), and alternative oxygen delivery and its impact on cardiac arrhythmias; however, we foresee good reasons to keep in touch also during 2022!

AUTHOR CONTRIBUTIONS

MA conceived the editorial. MA and GD revised the text. Both authors contributed to the article and approved the submitted version.

REFERENCES

1. Choi YS, Yin RT, Pfenniger A, Koo J, Avila R, Lee KB, et al. Fully implantable and bioresorbable cardiac pacemakers without leads or batteries. *Nat Biotechnol.* (2021) 39:1228–38. doi: 10.1038/s41587-021-00948-x
2. Chorin E, Hochstadt A, Schwartz AL, Matz G, Viskin S, Rosso R. Continuous Heart Rate Monitoring for Automatic Detection of Life-Threatening Arrhythmias With Novel Bio-Sensing Technology. *Front Cardiovasc Med.* (2021) 8:707621. doi: 10.3389/fcvm.2021.707621
3. Kühne M, Knecht S, Spies F, Aeschbacher S, Haaf P, Zellweger M, et al. Cryoballoon Ablation of Atrial Fibrillation Without Demonstration of Pulmonary Vein Occlusion-The Simplify Cryo Study. *Front Cardiovasc Med.* (2021) 8:664538. doi: 10.3389/fcvm.2021.664538
4. Wang B, Wang Z, Fu G, He B, Wang H, Zhuo W, et al. Left Atrial Spontaneous Echo Contrast and Ischemic Stroke in Patients Undergoing Percutaneous Left Atrial Appendage Closure. *Front Cardiovasc Med.* (2021) 8:723280. doi: 10.3389/fcvm.2021.723280
5. Kirchhof P, Camm AJ, Goette A, Brandes A, Eckardt L, Elvan A, et al. Early rhythm-control therapy in patients with atrial fibrillation. *N Engl J Med.* (2020) 383:1305–16. doi: 10.1056/NEJMoa2019422

Conflict of Interest: MA has received educational grants from Abbott, is consultant for Biosense Webster and proctor for Medtronic.

The remaining authors declare that the research was conducted in the absence of any commercial or financial relationships that could be construed as a potential conflict of interest.

frontiers in Cardiovascular Medicine

ORIGINAL RESEARCH
published: 22 February 2021
doi: 10.3389/fcvm.2021.625449

Compound Heterozygous *KCNQ1* Mutations Causing Recessive Romano–Ward Syndrome: Functional Characterization by Mutant Co-expression

*Antonia González-Garrido [1,2], Mayra Domínguez-Pérez [1], Leonor Jacobo-Albavera [1], Omar López-Ramírez [3], José Guadalupe Guevara-Chávez [1], Oscar Zepeda-García [1], Pedro Iturralde [4], Alessandra Carnevale [5] and Teresa Villarreal-Molina [1]**

[1] Laboratorio de Genómica de Enfermedades Cardiovasculares, Instituto Nacional de Medicina Genómica, Mexico City, Mexico, [2] Cátedras CONACyT, Consejo Nacional de Ciencia y Tecnología, Mexico City, Mexico, [3] Department of Neurobiology, University of Chicago, Chicago, IL, United States, [4] Departamento de Electrofisiología, Instituto Nacional de Cardiología "Ignacio Chávez", Mexico, Mexico, [5] Laboratorio de Enfermedades Mendelianas, Instituto Nacional de Medicina Genómica, Mexico, Mexico

OPEN ACCESS

Edited by:
Shimon Rosenheck,
Hebrew University of Jerusalem, Israel

Reviewed by:
Lee L. Eckhardt,
University of Wisconsin-Madison, United States
Elizabeth S. Kaufman,
The MetroHealth System, United States

***Correspondence:**
Teresa Villarreal-Molina
mvillareal@inmegen.gob.mx

Specialty section:
This article was submitted to Cardiac Rhythmology, a section of the journal Frontiers in Cardiovascular Medicine

Received: 03 November 2020
Accepted: 11 January 2021
Published: 22 February 2021

Citation:
González-Garrido A, Domínguez-Pérez M, Jacobo-Albavera L, López-Ramírez O, Guevara-Chávez JG, Zepeda-García O, Iturralde P, Carnevale A and Villarreal-Molina T (2021) Compound Heterozygous KCNQ1 Mutations Causing Recessive Romano–Ward Syndrome: Functional Characterization by Mutant Co-expression. Front. Cardiovasc. Med. 8:625449. doi: 10.3389/fcvm.2021.625449

Next Generation Sequencing has identified many *KCNQ1* genetic variants associated with type 1 long QT or Romano-Ward syndrome, most frequently inherited in an autosomal dominant fashion, although recessive forms have been reported. Particularly in the case of missense variants, functional studies of mutants are of aid to establish variant pathogenicity and to understand the mechanistic basis of disease. Two compound heterozygous *KCNQ1* mutations (p.A300T and p.P535T) were previously found in a child who suffered sudden death. To provide further insight into the clinical significance and basis for pathogenicity of these variants, different combinations of wildtype, A300T and P535T alleles were co-expressed with the accessory β-subunit minK in HEK293 cells, to analyze colocalization with the plasma membrane and some biophysical phenotypes of homo and heterotetrameric channels using the patch-clamp technique. A300T homotetrameric channels showed left-shifted activation $V_{1/2}$ as previously observed in *Xenopus* oocytes, decreased maximum conductance density, slow rise-time$_{300ms}$, and a characteristic use-dependent response. A300T slow rise-time$_{300ms}$ and use-dependent response behaved as dominant biophysical traits for all allele combinations. The P535T variant significantly decreased maximum conductance density and Kv7.1-minK-plasma membrane colocalization. P535T/A300T heterotetrameric channels showed decreased colocalization with plasma membrane, slow rise-time$_{300ms}$ and the A300T characteristic use-dependent response. While A300T left shifted activation voltage dependence behaved as a recessive trait when co-expressed with WT alleles, it was dominant when co-expressed with P535T alleles.

Conclusions: The combination of P535T/A300T channel biophysical properties is compatible with recessive Romano Ward syndrome. Further analysis of other biophysical traits may identify other mechanisms involved in the pathophysiology of this disease.

Keywords: *KCNQ1*, long-QT syndrome, IKs, electrophysiology, A300T, P535T, recessive Romano-Ward syndrome

INTRODUCTION

In mammalian hearts, the slow delayed potassium rectifier current (IKs) largely contributes to shape the repolarization phase of the ventricular action potential. IKs results from the co-assembly of the Kv7.1 channel complex, consisting of four pore-forming α subunits encoded by the *KCNQ1* gene and accessory β minK subunits encoded by *KCNE1,* with variable stoichiometry (1:4–4:4) (1–5). Heterozygous *KCNQ1* mutations resulting in decreased or total loss of function of the Kv7.1 channel cause autosomal dominant Romano-Ward or type 1 long QT syndrome (LQTS). These patients are susceptible to malignant cardiac arrhythmia, which may cause syncope, seizures, and sudden death, frequently in young and/or apparently healthy individuals (6). Homozygous or compound heterozygous *KCNQ1* mutations cause Jervell Lange-Nielsen syndrome, a recessive form of LQTS with severe QT prolongation and congenital sensorineural deafness (7–11). Patients with mutations on both *KCNQ1* alleles, a prolonged QT interval and normal hearing suffer from recessive Romano-Ward syndrome and are considered a high-risk subgroup (12).

Next Generation Sequencing has identified many *KCNQ1* genetic variants associated with type 1 LQTS. However, particularly in the case of missense variants, establishing pathogenicity remains challenging. The American College of Medical Genetics and Genomics and the Association for Molecular Pathology (ACMG/AMP) published and recently updated guidelines to standardize the interpretation of genetic variants (13, 14), which include functional characterization as a criterion to help define pathogenicity. The standard method to study functional consequences of ion channel genetic variants is the electrophysiological characterization of mutant channels in heterologous expression systems using patch clamp.

We recently reported the case of a child with normal hearing who suffered sudden death, found to be compound heterozygous for *KCNQ1* mutations (P535T/A300T), suggesting recessive Romano-Ward syndrome (15). Some of the electrophysiological properties of the A300T Kv7.1 channel were previously studied in *Xenopus* oocytes, and this mutation was considered as pathogenic only in the homozygous state (16). The P535T mutation was initially classified as of unknown clinical significance (VUS) according to the ACMG/AMP criteria (14). Protein modeling had predicted that the P535T mutation would disrupt the formation of a calmodulin-binding site by steric hindrance, which might prevent trafficking to the plasma membrane (15). To provide further insight into the clinical significance and the mechanistic basis for pathogenicity of these mutations, we studied some biophysical phenotypes of Kv7.1, A300T, and P535T homotetrameric and heterotetrameric channels, and the colocalization of these channels with minK and the plasma membrane. The P535T mutation was found to decrease Kv7.1-minK-plasma membrane colocalization and maximum conductance density. In addition, we further explored possible electrophysiological mechanisms by which the A300T mutation may contribute to the LQTS phenotype, and characterized biophysical properties of P535T/A300T heterotetrameric channels, leading us to conclude that these mutations are compatible with recessive Romano-Ward syndrome in the compound heterozygous child.

MATERIALS AND METHODS

The family of the compound heterozygous *KCNQ1* P535T/A300T child who suffered sudden death was previously described (15). The mother was an asymptomatic P535T heterozygous carrier, with a QTc that was borderline at rest, but prolonged during exercise. The father and only sibling were A300T heterozygous carriers, asymptomatic, and had normal QTc intervals on the ECG. The biophysical properties of IKs currents produced by different Kv7.1 channels were analyzed by co-expressing WT, A300T, and P535T homo and heterotetrameric channels in HEK293 cells.

Site-Directed Mutagenesis

KCNQ1 (NM_000218) tagged with GFP and *KCNE1* (NM_001127670) tagged with RFP plasmids were acquired from Origene (Rockville, MD, USA). The A300T and P535T mutations were cloned in the *KCNQ1* plasmid using QuickChange II XL Site-Directed Mutagenesis Kit (Agilent Technologies; Santa Clara, CA, USA) following manufacturer's instructions. Mutant primers were designed using QuikChange Primer Design tool: A300T-FW: 5′-ccaccacagcgcatccgtgtagctgccgaactc-3′; A300T-RV: 5′-gagttcggcagctacacggatgcgctgtggtgg-3′; P535T-FW: 5′-ccgca catcgtaagtcttccgcgcttgct-3′, and P535T-RV: 5′-agcaagcgcggaagac ttacgatgtgcgg-3′. The presence of the mutations was confirmed by Sanger sequencing.

Cell Culture and Transfection

Human embryonic kidney cells (HEK293) were kindly provided by Dr. Ricardo Félix Grijalva. Cells were maintained in Dulbecco's modified Eagle's medium (DMEM) supplemented with 10% FBS (Hyclone Laboratories Inc; Logan, UT, USA), 100 U/ml penicillin and 100 μg/ml streptomycin (Gibco; Waltham, MA, USA), in a humidified 5% CO_2 atmosphere at 37°C. Cells at 60–80% of confluence were used to transiently transfect both channel complex subunits (*KCNQ1* and *KCNE1*) in a 1:1 ratio, using 1.5 μg of each construct. Transfection was made with Lipofectamine™ LTX Reagent with PLUS™ Reagent (Invitrogen; Carlsbad, CA, USA) according to manufacturer's instructions. Twenty-four hours after transfection, cells were seeded on poly-D-lysine-coated glass coverslips at 2×10^4 cells. Electrophysiological recordings were performed 2 h after seeded to ensure adhesion to coverslip.

Electrophysiological Recordings

Whole-cell recordings were made at room temperature using borosilicate pipettes (WPI; Worcester, MA, USA) with 3–5 MΩ resistance in standard solutions. All reagents were purchased from Sigma Aldrich (St. Louis, MO, USA) unless otherwise indicated. In all experiments, the external solution was (in mM) 145 NaCl, 5 KCl, 1.3 $CaCl_2$, 1 $MgCl_2$, 0.7 NaH_2PO_4, and 10 HEPES; plus ∼6.5 mM NaOH to bring pH to 7.4 and osmolality to ∼295 mmol/kg. The pipette (internal) solution was a conventional KCl solution: (in mM) 135 KCl, 7 NaCl,

0.1 $CaCl_2$, 2 $MgCl_2$, 3 Na_2ATP, 10 EGTA, and 10 HEPES; plus ∼33 mM KOH to bring pH to 7.3 and osmolality to ∼300 mmol/kg. The patch clamp amplifier Multiclamp-700B and D-A/A-D converter Digidata 1550A (Molecular Devices; San Jose, CA, USA) were controlled by pClamp 10.5 (Molecular Devices). Capacitive currents were electronically nulled. Series resistances ranged from 3 to 15 MΩ (mean 6 ± 0.4 MΩ, $n = 61$) and were compensated 76 ± 0.4% for a mean residual value of ∼1.45 MΩ. Potentials were corrected for a liquid junction potential of −0.5 mV, calculated with JPCalc software (17) as implemented by Clampex 10.5 (Molecular Devices). Cells were held at −80.5 mV.

Whole-Cell Current Analyses

Voltage dependence of whole-cell currents was quantified by constructing activation (conductance density-voltage) curves from data collected using a voltage protocol consisting of an iterated series of 5.5 s test steps from a holding potential of −80.5 to 99.5 mV, that activates the slow outwardly rectifying K current (IKs). Steady-state conductances of IKs were calculated from tail currents at −40.5 mV, divided by driving force (the difference between V step and the current's reversal potential), mean across all cells, plotted against the test step voltage, and fitted with a Boltzmann function (Equation 1).

$$G(V) = \frac{G_{\min} - G_{\max}}{1 + e^{(V - V_{1/2})/S}} + G_{\max}$$

where G(V) is conductance at voltage V, Gmin, and Gmax are minimum and maximum conductances, $V_{1/2}$ is the voltage corresponding to half-maximal activation, and S is the voltage corresponding to an e-fold increase in G(V). Curve-fitting and statistical analyses were performed with OriginPro software (OriginLab; Northampton, MA, USA). Parameters of curve fits ($V_{1/2}$, Gmax/Cm, S) were compared for all experimental series, number of cells per group varied from 6 to 14. Gmax/Cm represents the maximum conductance density.

Rise Time

Rise time refers to the time required for a signal to change from a given low value to a given high value. Here, these values were 10 and 90% of the step height, as typically applied. To compare current activation time courses (kinetics) of different homo and heterotetrameric channels, rise time of currents activated from 0 to 100 mV steps was measured during the first 300 ms (rise-time$_{300ms}$), within the physiological human ventricular action potential duration range.

Use-Dependent Response

To assess the response of all multimeric channels during a stimulation at a normal heart rate, a 300 ms step at 49.5 mV from a holding potential of −80.5 mV was delivered 70 times during 1 min, 1.17 Hz. Plots of the end-step normalized current as a function of the step number were built to measure the rise-time of the response.

Confocal Microscopy and Image Analysis

To investigate the colocalization of Kv7.1 WT, A300T, and P535T homo and heterotetrameric channels with minK and the plasma membrane, HEK293 cells transiently transfected with *KCNE1* and different combinations of WT, A300T, and P535T *KCNQ1* plasmids were seeded on poly-D-lysine-treated coverslips at 2×10^4 cells per coverslip. Twenty-four hours after transfection, cells were washed with 1X PBS and fixed in 4% PFA. Fixed cells were treated with CellMaskTM Plasma Membrane Stain-Deep Red fluorophore (ThermoFisher Scientific; Waltham, MA, USA) following the manufacturer's protocol, and were observed with an LSM 780 NLO confocal microscope (Carl Zeiss; Jena, Germany). All images are representative of at least three independent experiments.

As previously mentioned, *KCNQ1* and *KCNE1* plasmids were tagged with GFP and RFP, respectively. Only cells expressing both GFP and RFP were selected for image analysis. Colocalization of the three signals (GFP, RFP, and Deep-Red) was quantified using the threshold overlap score (TOS), where TOS = 1 indicates colocalization, TOS = 0 indicates non-colocalization and TOS = −1 indicates anti-colocalization (18). Images were analyzed with Fiji software (https://imagej.net/Fiji) and EZColocalization plugin (19).

Statistical Analysis

Data are expressed as mean ± SEM. The significance of differences between means was assessed with one-way ANOVA for individual parameters and Two-way ANOVA for curves, both followed by *post-hoc* Tukey's tests of significance.

RESULTS

Activation Parameters

Activation curves and kinetics are presented assuming the possible combinations of Kv7.1 homo and heterotetrameric channels (**Figure 1A**) expressed for three different genotypes (P535T/WT representing the mother, A300T/WT representing the father, and P535T/A300T representing the index case).

P535T/WT Kv7.1-minK Channel Complexes (Mother)

Activation curves for WT, P535T, and P535T/WT channels were similar in terms of their voltage dependence (mean $V_{1/2}$ and S values were not significantly different, **Figures 1B1,C1**). Nonetheless, mean maximum conductance density (Gmax/Cm) of the P535T channels (1.11 ± 0.15 nS/pF, $n = 6$) was lower than WT channels (2.72 ± 0.48 nS/pF, $n = 13$; $p = 0.04$), but not significantly different from P535T/WT channels (1.68 ± 0.29 nS/pF; $p = 0.9$. **Figures 1B1,C2**; **Table 1**). No significant differences in S were found among mutant and WT proteins (**Figure 1**C3).

A300T/WT Kv7.2-minK Channel Complexes (Father)

Voltage dependence of the A300T homotetrameric channel was significantly left-shifted ($V_{1/2}$: −0.21 ± 3.26 mV, $n = 10$) compared with WT homotetrameric ($V_{1/2} = 32.96 \pm 2.26$ mV, $n = 13$; $p = 3.07E\text{-}8$) and A300T/WT heterotetrameric channels ($V_{1/2}$: 21.17 ± 3.46 mV, $p = 7.64E\text{-}4$) (**Figures 1B2,C1**; **Table 1**).

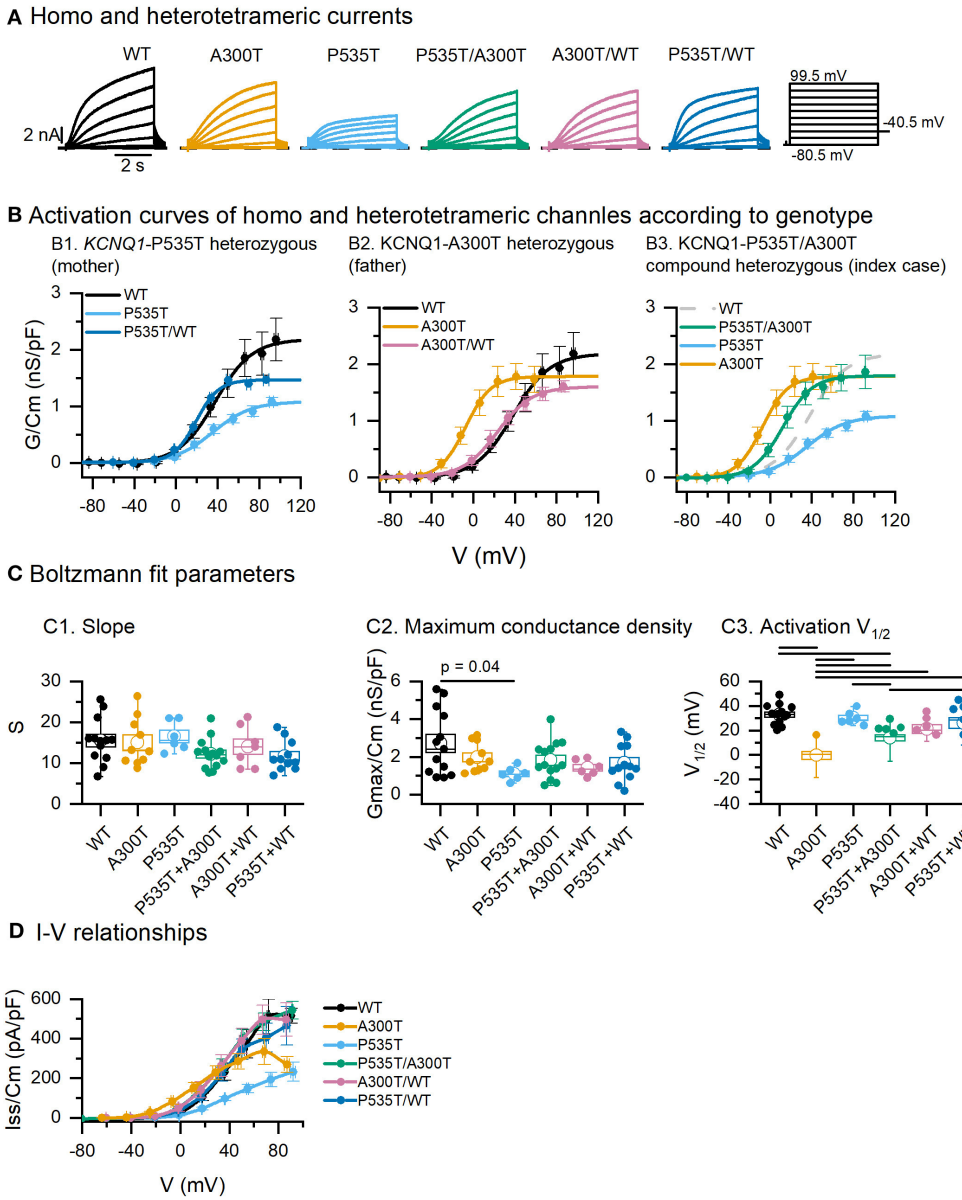

FIGURE 1 | Activation parameters of homo and heterotetrameric channels. **(A)** Exemplar current traces resulting from co-expression of minK and WT, A300T and/or P535T Kv7.1 α subunits. **(B)** Activation curves obtained from tail currents. Circles represent mean ± SEM values and lines represent Boltzmann equation fits. **(C)** Boltzmann fit parameters for tetrameric channels. Empty circles represent means and boxes represent SEM values; full circles represent raw data. **(D)** Averaged steady-state I–V relationships of tetrameric channels. All differences marked in C1 were significant, *p* values for significant differences in C1 and D are shown in **Table 1**. Conductance-voltage (G-V) curves fitted to averaged data from WT ($n = 13$), A300T ($n = 10$), P535T ($n = 6$), P535T/A300T ($n = 14$), A300T/WT ($n = 7$), and P535T/WT ($n = 11$) cells.

No significant differences in the voltage dependence of WT and A300T/WT channels were observed. No significant differences in S or Gmax/Cm were found among mutant and WT proteins (**Figures 1C2,3**).

P535T/A300T Kv7.1-minK Channel Complexes (Index Case)

The activation of P535T/A300T channels was significantly left-shifted ($V_{1/2}$: 13.96 ± 2.31 mV, $n = 14$) compared with WT ($V_{1/2}$ 32.96 ± 2.26 mV, $n = 13$; $p = 9.93E\text{-}5$) and P535T channels ($V_{1/2}$: 30.22 ± 2.27, $n = 6$; $p = 0.017$); but significantly more positive than A300T channels ($V_{1/2}$: −0.21 ± 3.26 mV, $n = 10$; $p = 0.013$) (**Figures 1B3,C1**; **Table 1**).

Activation Kinetics

Rise-time$_{300ms}$ of currents from A300T-containing channels were significantly slower than those from WT, P535T, and P535T/WT channels (**Figure 2**; **Table 2**). On the other hand, rise-time$_{300ms}$

of currents from P535T and P535T/WT channels were similar to those from WT channels.

WT and Mutant IKs Responses to Normal Heart Rate-Like Stimulation

Two different types of use-dependent responses were observed (**Figure 3A**). First, the WT use-dependent response can be described as a constant current amplitude during the step and the 70 repetitions, which was also observed in P535T and P535T/WT channels. Second, an A300T use-dependent response, characterized by a current that increases in amplitude with step duration, and with each step repetition. This response was found in A300T, P535T/A300T, and A300T/WT channels.

We then plotted the end-step normalized current as a function of the step number (**Figures 3B–D**). To evaluate the kinetics of these responses, rise time was measured for all homo and heterotetrameric channels. WT use-dependent responses were estimated as zero because the amplitude was constant and not included in the analysis (**Figure 3E**). Rise time was slowest for A300T homotetrameric currents (31.89 ± 1.84 s, $n = 3$), followed by P535T/A300T (18.14 ± 3.18 s, $n = 8$) and by A300T/WT heterotetrameric currents (10.33 ± 3.86 s, $n = 3$); however, only differences between A300T homotetrameric and A300T/WT heterotetrameric channels reached statistical significance ($p = 0.016$, **Figure 3E**).

The P535T Mutation Decreases Kv7.1-Plasma Membrane Colocalization

Our previous Kv7.1-A300T and -P535T protein model predicted defective trafficking of the Kv7.1-P535T potassium channel (15). We used colocalization assays to further investigate if the decreased conductance density of P535T channels (**Figure 1**) could be due to channel density reduction at the plasma membrane (**Figure 4**). **Table 3** describes TOS for colocalization of Kv7.1-minK-plasma membrane, Kv7.1-plasma

TABLE 1 | *P* values for activation $V_{1/2}$ and Iss/Cm comparisons among different channels.

$V_{½}$ comparisons	*p*	Iss/Cm comparisons	*p*
A300T vs. WT	3.07E-8	A300T vs. WT	0.008
A300T vs. A300T/WT	7.64E-4	A300T vs. P535T/A300T	3.73E-4
A300T vs. P535T	3.07E-6	P535T vs. WT	5.91E-8
A300T vs. P535T/WT	1.92E-6	P535T vs. P535T/A300T	2.07E-10
A300T vs. P535T/A300T	0.01	P535T vs. A300T/WT	2.63E-5
P535T/A300T vs. WT	9.93E-5	P535T vs. P535T/WT	4.29E-4
P535T/A300T vs. P535T/WT	0.04		
P535T/A300T vs. P535T	0.02		

Only statistically significant comparisons are shown.

TABLE 2 | *P* values for rise-time300$_{ms}$ comparisons among different channels.

Rise-time$_{300ms}$ comparisons	p
WT vs. A300T	2.4E-7
WT vs. A300T/WT	0.0086
WT vs. P535T/A300T	0.0001
A300T vs. P535T	6.3E-7
P535T vs. P535T/A300T	0.0001

Only statistically significant comparisons are shown.

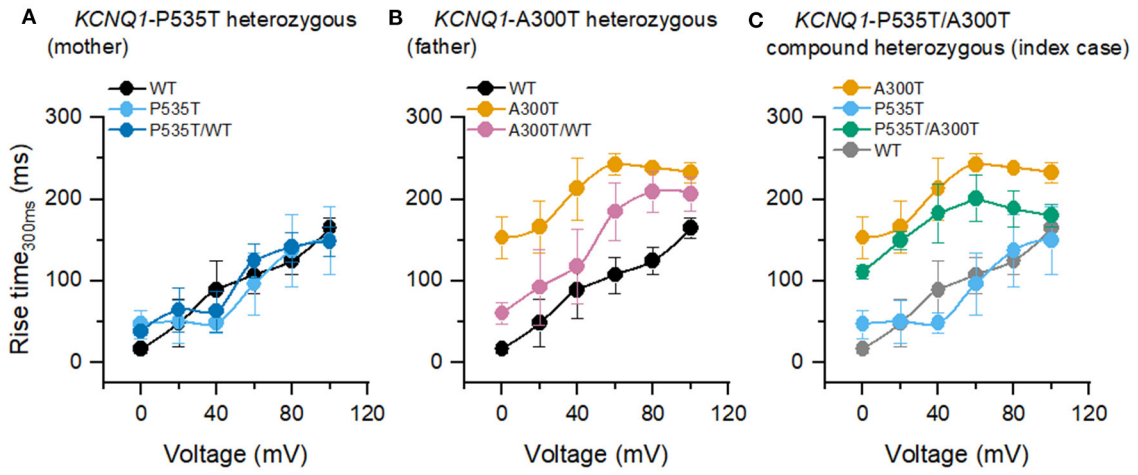

FIGURE 2 | Rise time$_{300ms}$ of homo and heterotetrameric channels. **(A)** P535T ($n = 6$) and P535T/WT ($n = 7$) currents shared similar rise-time$_{300ms}$ values with WT ($n = 13$) currents. **(B)** A300T ($n = 5$) and A300T/WT ($n = 8$) currents were significantly slower than WT currents. **(C)** A300T and P535T/A300T ($n = 8$) currents were significantly slower than P535T and WT currents. WT rise-time$_{300ms}$ values are shown in gray for comparison only.

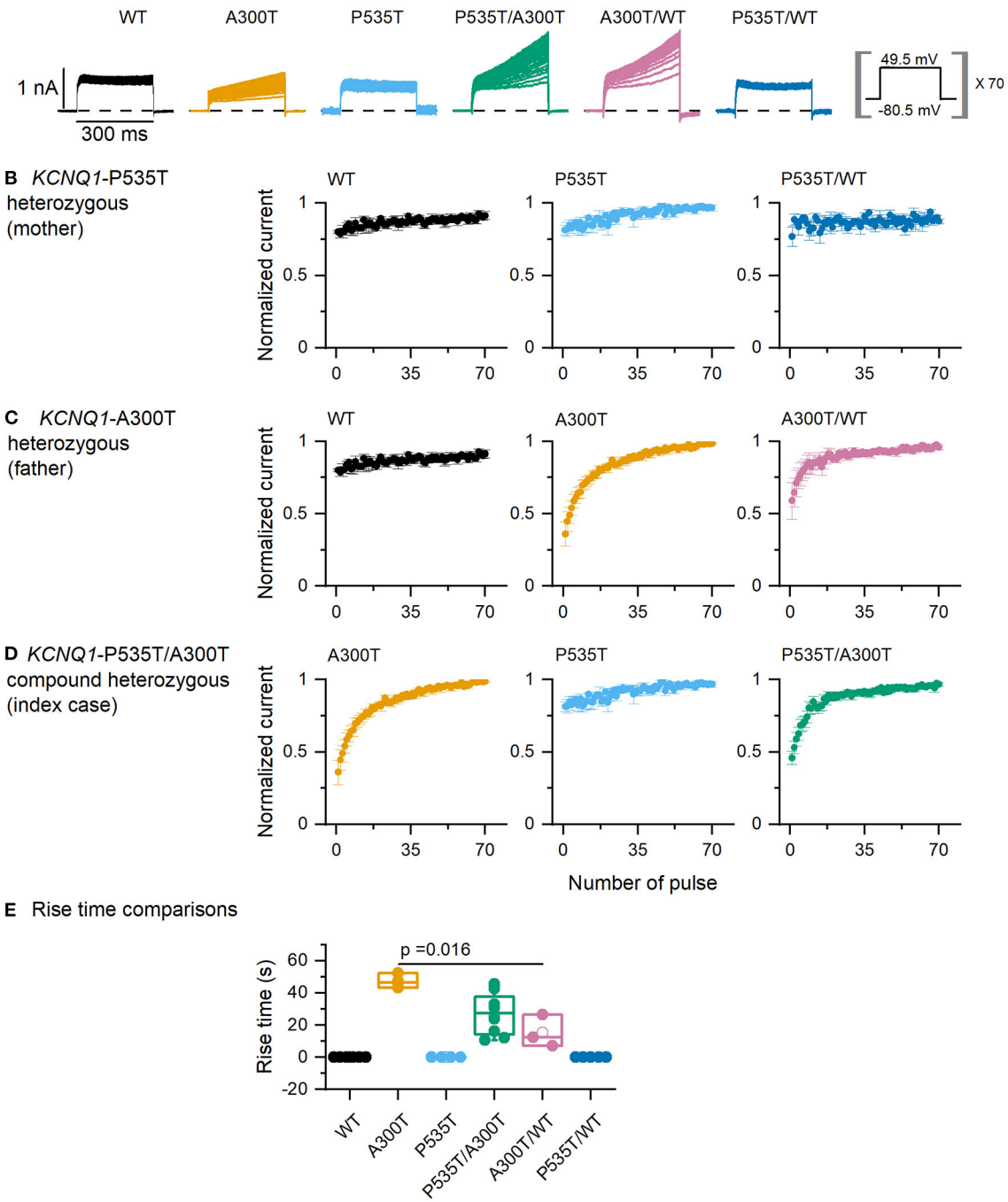

FIGURE 3 | Current responses to normal heart rate-like stimulation. **(A)** Currents from homo and heterotetrameric channels. **(B–D)** End-step normalized current as a function of step number for P535T heterozygous (WT, P535T, and P535T/WT channels, all curves were similar), A300T heterozygous (WT and A300T and A300T/WT channels) and P535T/A300T compound heterozygous (P535T, A300T, and P535T/WT channels) genotypes. **(E)** Rise-time comparisons for A300T-containing channels. Empty circles represent mean values, boxes represent SEM values; full circles represent raw data from WT ($n = 6$), A300T ($n = 3$), P535T ($n = 4$), P535T/A300T ($n = 8$), A300T/WT ($n = 3$), and P535T/WT ($n = 5$) cells.

membrane, Kv7.1-minK and mink-plasma membrane for all different homo and heterotetrameric channels. First, Kv7.1, minK, and plasma membrane (Kv7.1-minK-Mem) colocalization scores were similar for WT, A300T, and A300T/WT channels. However, all P535T-containing channels had significantly lower colocalization scores ($p < 0.04$) compared with WT, A300T,

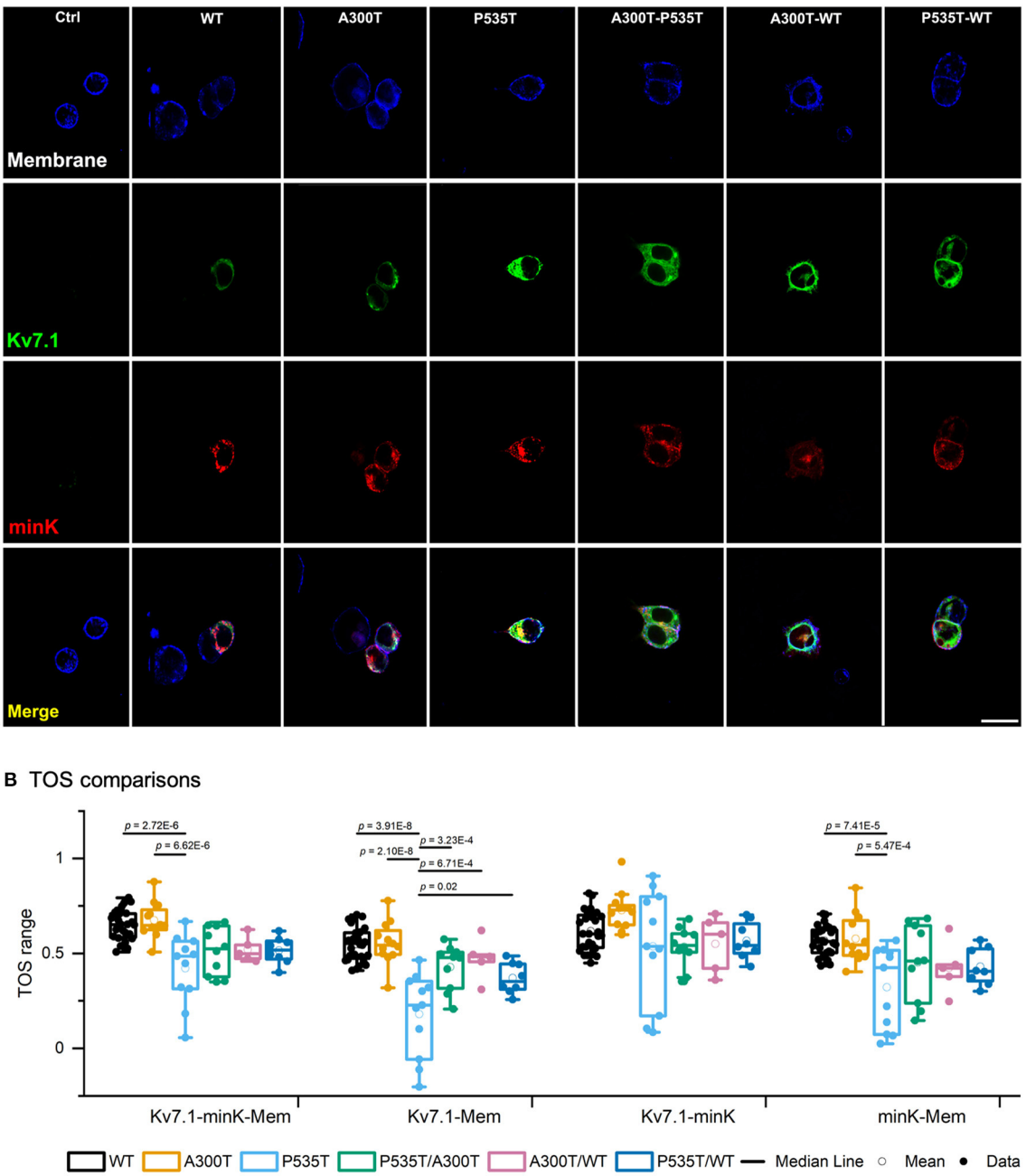

FIGURE 4 | Kv7.1-plasma membrane colocalization. **(A)** Confocal images of representative HEK293 cells transiently transfected with WT-GFP, A300T-GFP, or P535T-GFP (homo and heterotetrameric channels), KCNE1-RFP and stained plasma membrane (blue signal). The final row shows all 3 signals merged. 20 μm scale applies to all panels. **(B)** Box plots of multiple threshold overlap score (TOS) comparisons of Kv7.1, minK and plasma membrane colocalizations. Full circles represent raw data, empty circles mean and boxes ± SEM; *p* values of significant differences are indicated.

and A300T/WT channels. Second, for Kv7.1-plasma membrane (Kv7.1-Mem) colocalization, P535T channels clearly had the lowest score, being significantly lower than all other homo and heterotetrameric channels ($p < 0.02$). P535T/WT channels showed an intermediate colocalization score between WT and P535T channels, being significantly lower than the WT and A300T channels. Third, TOS comparisons of Kv7.1 and minK subunit colocalization (Kv7.1-minK) showed that all channels containing P535T monomers (P535T, P535T/WT, and P535T/A300T) were slightly lower than WT channels,

TABLE 3 | Threshold overlap score (TOS) (mean values ± SEM) for multiple colocalization comparisons.

	Kv7.1-MinK-Mem	Kv7.1-Mem	Kv7.1-MinK	MinK-Mem	*n*
WT	0.65 ± 0.02	0.55 ± 0.02	0.62 ± 0.02	0.57 ± 0.02	28
A300T	0.67 ± 0.03	0.56 ± 0.03	0.73 ± 0.03	0.58 ± 0.04	12
P535T	0.42 ± 0.06†	0.18 ± 0.07*	0.54 ± 0.09	0.32 ± 0.07†	11
P535T/A300T	0.51 ± 0.04	0.43 ± 0.04	0.54 ± 0.03	0.45 ± 0.06	10
A300T/WT	0.52 ± 0.03	0.47 ± 0.05	0.55 ± 0.07	0.42 ± 0.06	5
P535T/WT	0.52 ± 0.03	0.37 ± 0.03	0.57 ± 0.03	0.43 ± 0.04	8

**P535T homomeric channel colocalization scores for Kv7.1-Mem were significantly lower than those of all other homo and heterotetrameric channels ($p < 0.02$). †P535T homo and heterotetrameric channel colocalization scores for Kv7.1-MinK-Mem and MinK-Mem were significantly lower than those of WT and A300T homotetrameric channels ($p < 5.4E\text{-}4$).*

however differences were not statistically significant. Finally, minK subunit-plasma membrane colocalization scores (minK-Mem) were highest for WT and A300T channels and lowest for P535T channels. Only comparisons between P535T and WT or A300T channels showed statistically significant differences (**Figure 4**).

DISCUSSION

Next generation sequencing has facilitated the identification of genetic mutations of cardiac ion channels as a possible cause of arrhythmias. Functional information of identified genetic mutations is of aide for classification of pathogenicity, that will impact diagnosis, prognosis, and risk stratification. Moreover, molecular diagnosis may have implications in clinical decisions and is crucial for the identification of relatives at risk of sudden death (20, 21). Unfortunately, missense genetic variants are frequently classified as VUS, meaning there are insufficient data to define whether they are disease-causal or benign. We recently reported the case of a child with sudden death, who was compound heterozygous for *KCNQ1* mutations (P535T/A300T). The P535T mutation was initially classified as of unknown clinical significance, and although the electrophysiological properties of A300T channels in *Xenopus* oocytes showed clear anomalies, interpretations of these anomalies and the clinical implications of the A300T mutation have been inconsistent (16, 22–24).

Remarkably, it has been observed that mutations that are dysfunctional at the molecular level may not cause clinical disease, and alternatively, some *KCNQ1* mutations reported in LQTS patients do not show electrophysiological alterations (22). In the latter case, it is important to establish whether the variant is in fact not causal of disease, or whether the variant affects other yet unassessed biophysical properties and thus contributes to the phenotype. Most functional studies only analyze IKs amplitude and activation $V_{1/2}$, and few include activation and deactivation time constant (τ) values. We thus further characterized the biophysical properties of A300T and P535T homo and heterotetrameric channels, analyzing prototypical activation curve parameters, current density, rise-time$_{300ms}$, and use-dependent responses, in an effort to gain further insight into how these mutations affect the IKs and may cause LQTS.

Kv7.1 A300T Electrophysiological Phenotype

The *KCNQ1*-A300T mutation (rs120074187) is located at the pore domain, in the P-loop between S5 and S6 transmembrane domains, a topological location with high probability of pathogenicity (25). Previously functional data in *Xenopus* oocytes indicated that the A300T Kv7.1 channel was normally transported to the cell surface but activates IKs more rapidly, left-shifts the activation voltage dependence and decreases current amplitude (16, 23), suggesting that the A300 residue plays an important role in the activation voltage dependence as predicted by structural models (26). Our colocalization data are in agreement with findings in *Xenopus* oocytes as the TOS were similar for A300T and WT channels (**Figure 4**). Our findings in HEK293 cells also agreed with a left-shifted activation and decreased end-step current density (**Figure 1D**). A300T voltage dependence was rescued when expressed together with the WT subunit (A300T/WT, **Figure 1**B2), compatible with a recessive biophysical trait.

We observed that tail maximum conductance density was similar in WT and A300T channels (**Figure 1**C2). Thus, decreased steady state current density (Iss/Cm) and normal tail maximum conductance density suggest higher deactivation extent of A300T compared with WT currents. According to our data, reduction in current density of A300T channels was not as prominent as previously reported by Priori et al. (16). This discrepancy is most likely due to differences between heterologous expression systems (*Xenopus* oocytes vs. HEK293 cells). Post-translational processing, plasma membrane composition, and multimeric protein assembly in *Xenopus* oocytes can be different from mammalian cells (27, 28). These differences should be considered for studies aimed at understanding the mechanism of native human ion channels, receptors, and their modulators.

A previous study in *Xenopus* oocytes described that A300T activation assessed over a 4–5 s period is faster (16). In the present study, we assessed WT and mutant channel IKs activation within the physiological human ventricular action potential duration range (rise-time$_{300ms}$). This analysis revealed an A300T dominant trait described here for the first time. We observed that currents from all A300T-containing channels had significantly slower activation than WT and P535T homo and heterotetrameric channels (**Figure 2**). Since slower

A300T activation would be expected to delay action potential repolarization, this trait can be considered as decreased function. Moreover, A300T homomeric current activation is left-shifted, meaning that it is prematurely activated during the ventricular action potential, but because this premature activation is slow, the final result could be a delayed repolarization. Additionally, on repeated activation simulating a normal heart rate, the A300T channels showed use-dependent current potentiation, which slowly reached a steady state (**Figure 3**). The latter characteristic was also dominant, as it was observed in currents from both A300T/WT and P535T/A300T channels (**Figure 3**).

Summarizing, A300T causes a recessive, increased function biophysical trait (left-shifted activation voltage), concurrently with two dominant, decreased function biophysical traits (slow 300 ms activation and use-dependent response), likely resulting in a mild overall effect. It was first described as causal of a recessive form of Romano Ward in a homozygous child with normal hearing (16). To date, all reported heterozygous A300T mutation carriers have normal QTc intervals, even after exercise (15, 16). Although the 300T allele is rare, it is most frequent in Latino populations (0.00026, https://gnomad.broadinstitute.org/).

P535T Reduces Kv7.1 Function and Colocalization With the Plasma Membrane

The P535T mutation was originally reported by our group (15). Although it was not functionally characterized, an *in silico* model predicted that P535T disrupts a calmodulin binding site by steric hindrance, most likely causing co-assembly and/or trafficking defects. P535T is localized within the C-terminus domain (15, 29), considered with high probability for pathogenicity (25), and lies within a highly conserved protein region (22). Calmodulin is essential for correct channel folding, assembly, and trafficking, and the Kv7.1 C-terminus includes two calmodulin binding sites (30–33). Altogether, these data suggest that mutations located at this region could disrupt Kv7.1-calmodulin interactions resulting in defective trafficking. In consistency with the model predictions, we observed decreased colocalization of P535T-containing channels with the plasma membrane (**Figure 4**).

Although P535T-plasma membrane colocalization score was considerably lower for homotetrameric channels, colocalization analysis and electrophysiological recordings indicated the P535T mutation does not abolish Kv7.1 channel function. First, colocalization scores with plasma membrane suggested that P535T and P535T/WT channel densities were ∼1/3 and 2/3 that of WT channels, respectively. Second, maximum conductance density of P535T channels was ∼2/5 of that of WT channels, likely due to the lower P535T channel density in the plasma membrane. This was a recessive trait, as P535T/WT, P535T/A300T, and WT channels showed similar Gmax/Cm values (**Figures 1B1,B3,C2**). Similarly, other *KCNQ1* genetic mutations within this region have been associated with recessive Romano-Ward syndrome (30, 34). Finally, P535T did not alter activation voltage dependence, rise-time$_{300ms}$ or use-dependent response. In physiological conditions, adrenergic stimulation enhances IKs and shortens ventricular repolarization, providing physiological protection against the possibility of reentrant arrhythmias at fast heart rates (35). Thus, partial IKs impairment is compatible with QT prolongation only during exercise, as observed in P535T/WT heterozygous mother (15).

KCNQ1 P535T/A300T Compound Heterozygosity

Because an undiagnosed child with sudden death was found to be compound heterozygous for *KCNQ1* mutations (P535T/A300T) (15), we functionally characterized the IKs of HEK293 cells expressing both mutations to establish whether she was affected with a form of recessive Romano-Ward syndrome.

Biophysical P535T/A300T Phenotypes

While A300T left shifted activation voltage dependence behaved as a recessive trait when co-expressed with WT alleles, it was dominant when co-expressed with P535T alleles. Although A300T/WT and WT channels showed similar activation $V_{1/2}$ values, P535T/A300T channels showed intermediate activation $V_{1/2}$ values, with a left-shift of 16.3 mV ($p = 0.017$) compared with P535T channels, and a right-shift of 13.8 mV compared with A300T ($p = 0.013$). Because P535T channels showed significantly lower colocalization scores with membrane than WT and A300T channels, it is likely that in a compound heterozygous state, a lower proportion of P535T and higher proportions of P535T/A300T and A300T channels will be assembled at the plasma membrane. This is compatible with the dominance of left-shifted activation voltage only in the compound heterozygous state. Finally, while P535T channels had significantly lower Gmax/Cm compared with WT channels, Gmax/Cm of P535T/A300T channels was also lower, although the difference did not reach statistical significance. These characteristics would most likely lead to abnormal repolarization and low possibilities of functional recovery since no Kv7.1-WT monomers can compensate the effects of the mutations.

Study Limitations

Although HEK293 cells have been widely used as host for heterologous expression and functional characterization of ion channels, they do not resemble the native cardiomyocyte environment where other ion channels and intracellular molecules interact to generate action potentials. For this reason, we cannot rule out that ion channels in their native environment are subject to regulation and interactions not considered in our model. Moreover, characterization of other yet unexplored biophysical traits such as response to PKA activators simulating adrenergic stimulation will provide further insight to better understand the mechanisms by which genetic mutations cause disease, and need to be performed in future studies.

Concluding Remarks

Co-expression of different combinations of WT, A300T, and P535T Kv7.1 with minK in mammalian cells revealed two previously undescribed biophysical phenotypes of the A300T mutation (slow rise-time$_{300ms}$, and a characteristic use-dependent response) that behaved as dominant traits.

The A300T left-shifted activation $V_{1/2}$ previously observed in *Xenopus* oocytes behaved as a recessive trait when co-expressed with WT alleles, but as a dominant trait when co-expressed with P535T alleles. The P535T variant significantly decreased maximum conductance density and Kv7.1-minK-plasma membrane colocalization, although how the P535T mutation affects trafficking remains to be elucidated. A lower density of P535T Kv7.1 monomers at the plasma membrane is compatible with the lower current density of P535T channels and with the dominance of A300T left shift voltage activation observed only when combined with P535T. The biophysical properties of P535T/A300T IKs are compatible with recessive Romano-Ward syndrome. Further analysis of other biophysical traits may identify other mechanisms involved in the pathophysiology of this disease.

DATA AVAILABILITY STATEMENT

The datasets presented in this study can be found in online repositories. The names of the repository/repositories and accession number(s) can be found at: https://www.ncbi.nlm.nih.gov/snp/, rs120074187; https://www.ncbi.nlm.nih.gov/clinvar/variation/3128/, rs120074187; https://gnomad.broadinstitute.org/, rs120074187; https://varsome.com, rs120074187; https://varsome.com, chr11-2797202-C-A (KCNQ1:p.P535T).

AUTHOR CONTRIBUTIONS

TV-M and AC conceptualized and designed the study. TV-M and AG-G designed the experimental approach and drafted the manuscript. AG-G performed all experiments and analyzed the data. MD-P performed confocal experiments. OL-R contributed to the data analysis and comments to the manuscript. LJ-A, JG-C, and OZ-G performed the experiments. MD-P, LJ-A, PI, and AC contributed to the manuscript. All authors contributed to the article and approved the submitted version.

FUNDING

The research was funded by the Consejo Nacional de Ciencia y Tecnología (Cátedras -CONACYT, Grant Number 1703) and Fondo Sectorial de Investigación en Salud y Seguridad Social (FOSISS, Grant Number 261670).

ACKNOWLEDGMENTS

We would like to thank Dr. Ricardo Félix Grijalva for providing the HEK294 cells; Dr. Froylán Gómez Lagunas, Dr. Carolina Barriga Montoya, and Dr. Ricardo Gonzalez Ramirez for their valuable technical advice; and Dr. Enrique Soto for his comments on confocal analysis.

REFERENCES

1. Barhanin J, Lesage F, Guillemare E, Fink M, Lazdunski M, Romey G. K(V)LQT1 and IsK (minK) proteins associate to form the I(Ks) cardiac potassium current. *Nature.* (1996) 384:78–80. doi: 10.1038/384078a0
2. Sanguinetti MC, Curran ME, Zou A, Shen J, Spector PS, Atkinson DL, et al. Coassembly of K(V)LQT1 and minK (IsK) proteins to form cardiac I(Ks) potassium channel. *Nature.* (1996) 384:80–3. doi: 10.1038/384080a0
3. Cui J, Kline RP, Pennefather P, Cohen IS. Gating of IsK expressed in *Xenopus* oocytes depends on the amount of mRNA injected. *J Gen Physiol.* (1994) 104:87–105. doi: 10.1085/jgp.104.1.87
4. Yu H, Lin Z, Mattmann ME, Zou B, Terrenoire C, Zhang H, et al. Dynamic subunit stoichiometry confers a progressive continuum of pharmacological sensitivity by KCNQ potassium channels. *Proc Natl Acad Sci USA*. (2013) 110:8732–7. doi: 10.1073/pnas.1300684110
5. Wang W, Xia J, Kass RS. MinK-KvLQT1 fusion proteins, evidence for multiple stoichiometries of the assembled I(sK) channel. *J Biol Chem.* (1998) 273:34069–74. doi: 10.1074/jbc.273.51.34069
6. Wang Q, Curran ME, Splawski I, Burn TC, Millholland JM, VanRaay TJ, et al. Positional cloning of a novel potassium channel gene: KVLQT1 mutations cause cardiac arrhythmias. *Nat Genet.* (1996) 12:17–23. doi: 10.1038/ng0196-17
7. Liu Z, Zheng R, Grushko MJ, Uversky VN, McDonald TV. Functionally aberrant mutant KCNQ1 with intermediate heterozygous and homozygous phenotypes. *Can J Cardiol.* (2018) 34:1174–84. doi: 10.1016/j.cjca.2018.06.015
8. Jackson HA, McIntosh S, Whittome B, Asuri S, Casey B, Kerr C, et al. LQTS in Northern BC: homozygosity for *KCNQ1* V205M presents with a more severe cardiac phenotype but with minimal impact on auditory function. *Clin Genet.* (2014) 86:85–90. doi: 10.1111/cge.12235
9. Novotny T, Kadlecova J, Janousek J, Gaillyova R, Bittnerova A, Florianova A, et al. The homozygous KCNQ1 gene mutation associated with recessive Romano-Ward syndrome. *Pacing Clin Electrophysiol.* (2006) 29:1013–5. doi: 10.1111/j.1540-8159.2006.00478.x
10. Neyroud N, Denjoy I, Donger C, Gary F, Villain E, Leenhardt A, et al. Heterozygous mutation in the pore of potassium channel gene KvLQT1 causes an apparently normal phenotype in long QT syndrome. *Eur J Hum Genet.* (1998) 6:129–33. doi: 10.1038/sj.ejhg.5200165
11. Zafari Z, Dalili M, Zeinali S, Saber S, Fazeli Far AF, Akbari MT. Identification and characterization of a novel recessive KCNQ1 mutation associated with Romano-Ward long-QT syndrome in two Iranian families. *J Electrocardiol.* (2017) 50:912–8. doi: 10.1016/j.jelectrocard.2017.07.012
12. Giudicessi JR, Ackerman MJ. Genotype- and phenotype-guided management of congenital long QT syndrome. *Curr Probl Cardiol.* (2013) 38:417–55. doi: 10.1016/j.cpcardiol.2013.08.001
13. Nykamp K, Anderson M, Powers M, Garcia J, Herrera B, Ho YY, et al. Sherloc: a comprehensive refinement of the ACMG-AMP variant classification criteria. *Genet Med.* (2017) 19:1105–17. doi: 10.1038/gim.2017.37
14. Richards S, Aziz N, Bale S, Bick D, Das S, Gastier-Foster J, et al. Standards and guidelines for the interpretation of sequence variants: a joint consensus recommendation of the American College of Medical Genetics and Genomics and the Association for Molecular Pathology. *Genet Med.* (2015) 17:405–24. doi: 10.1038/gim.2015.30
15. Antúnez-Argüelles E, Rojo-Domínguez A, Arregui-Mena AL, Jacobo-Albavera L, Márquez MF, Iturralde-Torres P, et al. Compound heterozygous KCNQ1 mutations (A300T/P535T) in a child with sudden unexplained death: insights into possible molecular mechanisms based on protein modeling. *Gene.* (2017) 627:40–8. doi: 10.1016/j.gene.2017.06.011
16. Priori SG, Schwartz PJ, Napolitano C, Bianchi L, Dennis A, De Fusco M, et al. A recessive variant of the Romano-Ward long-QT syndrome? *Circulation.* (1998) 97:2420–5. doi: 10.1161/01.CIR.97.24.2420
17. Barry PH. JPCalc, a software package for calculating liquid junction potential corrections in patch-clamp, intracellular, epithelial and bilayer measurements and for correcting junction potential measurements. *J Neurosci Methods.* (1994) 51:107–16. doi: 10.1016/0165-0270(94)90031-0
18. Sheng H, Stauffer W, Lim HN. Systematic and general method for quantifying localization in microscopy images. *Biol Open.* (2016) 5:1882–93. doi: 10.1242/bio.019893
19. Stauffer W, Sheng H, Lim HN. EzColocalization: an ImageJ plugin for visualizing and measuring colocalization in cells and organisms. *Sci Rep.* (2018) 8:1–13. doi: 10.1038/s41598-018-33592-8

20. Schwartz PJ, Ackerman MJ, George AL, Wilde AAM. Impact of genetics on the clinical management of channelopathies. *J Am Coll Cardiol.* (2013) 62:169–80. doi: 10.1016/j.jacc.2013.04.044
21. Ackerman MJ. Genetic purgatory and the cardiac channelopathies: exposing the variants of uncertain/unknown significance issue. *Hear Rhythm.* (2015) 12:2325–31. doi: 10.1016/j.hrthm.2015.07.002
22. Li B, Mendenhall JL, Kroncke BM, Taylor KC, Huang H, Smith DK, et al. Predicting the functional impact of KCNQ1 variants of unknown significance. *Circ Cardiovasc Genet.* (2017) 10:5. doi: 10.1161/CIRCGENETICS.117.001754
23. Bianchi L, Priori SG, Napolitano C, Surewicz KA, Dennis AT, Memmi M, et al. Mechanisms of I(Ks) suppression in LQT1 mutants. *Am J Physiol Heart Circ Physiol.* (2000) 279:48–56. doi: 10.1152/ajpheart.2000.279.6.H3003
24. Paquin A, Ye D, Tester DJ, Kapplinger JD, Zimmermann MT, Ackerman MJ. Even pore-localizing missense variants at highly conserved sites in KCNQ1-encoded Kv7.1 channels may have wild-type function and not cause type 1 long QT syndrome: do not rely solely on the genetic test company's interpretation. *Hear Case Rep.* (2018) 4:37–44. doi: 10.1016/j.hrcr.2017.04.006
25. Kapa S, Tester DJ, Salisbury BA, Harris-Kerr C, Pungliya MS, Alders M, et al. Genetic testing for long-qt syndrome: distinguishing pathogenic mutations from benign variants. *Circulation.* (2009) 120:1752–60. doi: 10.1161/CIRCULATIONAHA.109.863076
26. Smith JA, Vanoye CG, George AL, Meiler J, Sanders CR. Structural models for the KCNQ1 voltage-gated potassium channel. *Biochemistry.* (2007) 46:14141–52. doi: 10.1021/bi701597s
27. Smith-Maxwell C, Papke R. High throughput electrophysiology with *Xenopus* oocytes. *Comb Chem High Throughput Screen.* (2009) 12:38–50. doi: 10.2174/138620709787047975
28. Nelson ME, Kuryatov A, Choi CH, Zhou Y, Lindstrom J. Alternate stoichiometries of α4β2 nicotinic acetylcholine receptors. *Mol Pharmacol.* (2003) 63:332–41. doi: 10.1124/mol.63.2.332
29. Yus-Nájera E, Santana-Castro I, Villarroel A. The identification and characterization of a noncontinuous calmodulin-binding site in noninactivating voltage-dependent KCNQ potassium channels. *J Biol Chem.* (2002) 277:28545–53. doi: 10.1074/jbc.M204130200
30. Chouabe C, Neyroud N, Richard P, Denjoy I, Hainque B, Romey G, et al. Novel mutations in KvLQT1 that affect I(ks) activation through interactions with Isk. *Cardiovasc Res.* (2000) 45:971–80. doi: 10.1016/S0008-6363(99)00411-3
31. Sachyani D, Dvir M, Strulovich R, Tria G, Tobelaim W, Peretz A, et al. Structural basis of a Kv7.1 potassium channel gating module: studies of the intracellular C-terminal domain in complex with calmodulin. *Structure.* (2014) 22:1582–94. doi: 10.1016/j.str.2014.07.016
32. Shamgar L, Ma L, Schmitt N, Haitin Y, Peretz A, Wiener R, et al. Calmodulin is essential for cardiac IKS channel gating and assembly: impaired function in long-QT mutations. *Circ Res.* (2006) 98:1055–63. doi: 10.1161/01.RES.0000218979.40770.69
33. Ghosh S, Nunziato DA, Pitt GS. KCNQ1 assembly and function is blocked by long-QT syndrome mutations that disrupt interaction with calmodulin. *Circ Res.* (2006) 98:1048–54. doi: 10.1161/01.RES.0000218863.44140.f2
34. Larsen LA, Fosdal I, Andersen PS, Kanters JK, Vuust J, Wettrell G, et al. Recessive Romano-Ward syndrome associated with compound heterozygosity for two mutations in the KVLQT1 gene. *Eur J Hum Genet.* (1999) 7:724–8. doi: 10.1038/sj.ejhg.5200323
35. Goldenberg I, Thottathil P, Lopes CM, Moss AJ, McNitt S, O-Uchi J, et al. Trigger-specific ion-channel mechanisms, risk factors, and response to therapy in type 1 long QT syndrome. *Heart Rhythm.* (2012) 9:49–56. doi: 10.1016/j.hrthm.2011.08.020

Conflict of Interest: The authors declare that the research was conducted in the absence of any commercial or financial relationships that could be construed as a potential conflict of interest.

frontiers in Cardiovascular Medicine

REVIEW
published: 23 March 2021
doi: 10.3389/fcvm.2021.630399

Left Bundle Branch Pacing: Current Knowledge and Future Prospects

Peng Liu[1], Qiaozhu Wang[1], Hongke Sun[1], Xinghua Qin[2] and Qiangsun Zheng[1]**

[1] Department of Cardiology, The Second Affiliate Hospital of Xi'an Jiaotong University, Xi'an, China, [2] School of Life Sciences, Northwestern Polytechnical University, Xi'an, China

Cardiac pacing is an effective therapy for treating patients with bradycardia due to sinus node dysfunction or atrioventricular block. However, traditional right ventricular apical pacing (RVAP) causes electric and mechanical dyssynchrony, which is associated with increased risk for atrial arrhythmias and heart failure. Therefore, there is a need to develop a physiological pacing approach that activates the normal cardiac conduction and provides synchronized contraction of ventricles. Although His bundle pacing (HBP) has been widely used as a physiological pacing modality, it is limited by challenging implantation technique, unsatisfactory success rate in patients with wide QRS wave, high pacing capture threshold, and early battery depletion. Recently, the left bundle branch pacing (LBBP), defined as the capture of left bundle branch (LBB) via transventricular septal approach, has emerged as a newly physiological pacing modality. Results from early clinical studies have demonstrated LBBP's feasibility and safety, with rare complications and high success rate. Overall, this approach has been found to provide physiological pacing that guarantees electrical synchrony of the left ventricle with low pacing threshold. This was previously specifically characterized by narrow paced QRS duration, large R waves, fast synchronized left ventricular activation, and correction of left bundle branch block. Therefore, LBBP may be a potential alternative pacing modality for both RVAP and cardiac resynchronization therapy with HBP or biventricular pacing (BVP). However, the technique's widespread adaptation needs further validation to ascertain its safety and efficacy in randomized clinical trials. In this review, we discuss the current knowledge of LBBP.

Keywords: left bundle branch pacing, physiological pacing, pacemaker, right ventricular apical pacing, cardiac resynchronization therapy

OPEN ACCESS

Edited by:
Matteo Anselmino, University of Turin, Italy

Reviewed by:
Lina Marcantoni, Hospital Santa Maria Della Misericordia of Rovigo, Italy
Osmar Antonio Centurion, National University of Asunción, Paraguay

****Correspondence:***
Qiangsun Zheng
zhengqiangsun@126.com
Xinghua Qin
xinghuaqin@nwpu.edu.cn

Specialty section:
This article was submitted to Cardiac Rhythmology, a section of the journal Frontiers in Cardiovascular Medicine

Received: *17 November 2020*
Accepted: *05 February 2021*
Published: *23 March 2021*

Citation:
Liu P, Wang Q, Sun H, Qin X and Zheng Q (2021) Left Bundle Branch Pacing: Current Knowledge and Future Prospects. Front. Cardiovasc. Med. 8:630399. doi: 10.3389/fcvm.2021.630399

INTRODUCTION

Cardiac conduction disease is a serious health issue caused by the impairment to the integrity of conduction system. The molecular mechanisms of cardiac conduction disease have not been well-understood. To date, cardiac pacing is the only effective therapy for patients with symptomatic bradycardia. Traditional right ventricular apical pacing (RVAP) has been widely used for more than half a century, although the approach has been shown to cause electric and mechanical dyssynchrony, which exacerbates the risk of atrial fibrillation (AF), heart failure (HF), and even mortality (1–4).

Moreover, other ventricular pacing sites, such as the right ventricular septal and right ventricular outflow tract, have been developed and applied to minimize the aforementioned potential adverse outcomes. However, their long-term outcomes have not been demonstrated to be superior to RVAP (5, 6). Cardiac resynchronization therapy (CRT), via biventricular pacing (BVP), is another pacing modality employed for treatment of HF. Clinical studies have demonstrated that CRT promotes left ventricular reverse remodeling, confers exercise tolerance, and reduces morbidity as well as mortality in patients with systolic HF (7). Although CRT's benefits are well demonstrated, the therapy has been associated with significantly high non-response rate (30–40%) (8). Furthermore, the BVP is a non-physiological approach that requires two leads to activate the ventricular myocardium and not the specialized conduction system.

Therefore, the physiological pacing technique that directly activates conduction systems becomes the focus of attention. Deshmukh et al. (10) first demonstrated feasibility of the permanent His bundle pacing (HBP) in patients with AF and dilated cardiomyopathy. Thereafter, multiple studies have confirmed the clinical benefits of permanent HBP (11, 12). Consequently, HBP has been recommended as a rescue modality for failed BVP and even a primary treatment for CRT (11, 13, 14). However, its clinical application in some patients has been limited by concerns associated with its technicalities, high pacing threshold, low R-wave amplitudes, and the potential to cause distal conduction block (12). Moreover, HBP cannot normalize the QRS duration in almost half of patients with left bundle branch block (LBBB) in the His Bundle Pacing vs. Coronary Sinus Pacing for Cardiac Resynchronization Therapy (His-SYNC) study (15). To address the above issues, researchers have recently developed the left bundle branch pacing (LBBP) therapy, as a novel pacing modality for delivering physiological pacing and ensure electrical synchrony of the left ventricle. Benefits of the LBBP technique, first reported by Huang et al. (16) in patients with dilated cardiomyopathy, have been demonstrated across several studies (17–21). Given the growing interest in pacing at the left bundle branch (LBB) region, we will summarize the current knowledge in LBBP, from anatomy to definition, implantation technique, complication, short-term clinical outcomes, potential advantages, and future directions, in order to provide comprehensive insights to help in understanding of this pacing modality.

ANATOMY OF THE LBB

The His bundle and its branches were first described by Tawara in 1906 (22). The bundle of His, a thin cylindrical fascicle that connects the atrioventricular node with bundle branches, has two segments, namely, the penetrating portion (PHB) and the branching portion (BHB). LBB originates from the BHB of His, located below the membranous septum (MS) (**Figure 1A**). All the fibers forming the LBB lie on the same plane giving a ribbon-like appearance beneath the endocardium of the subaortic septal

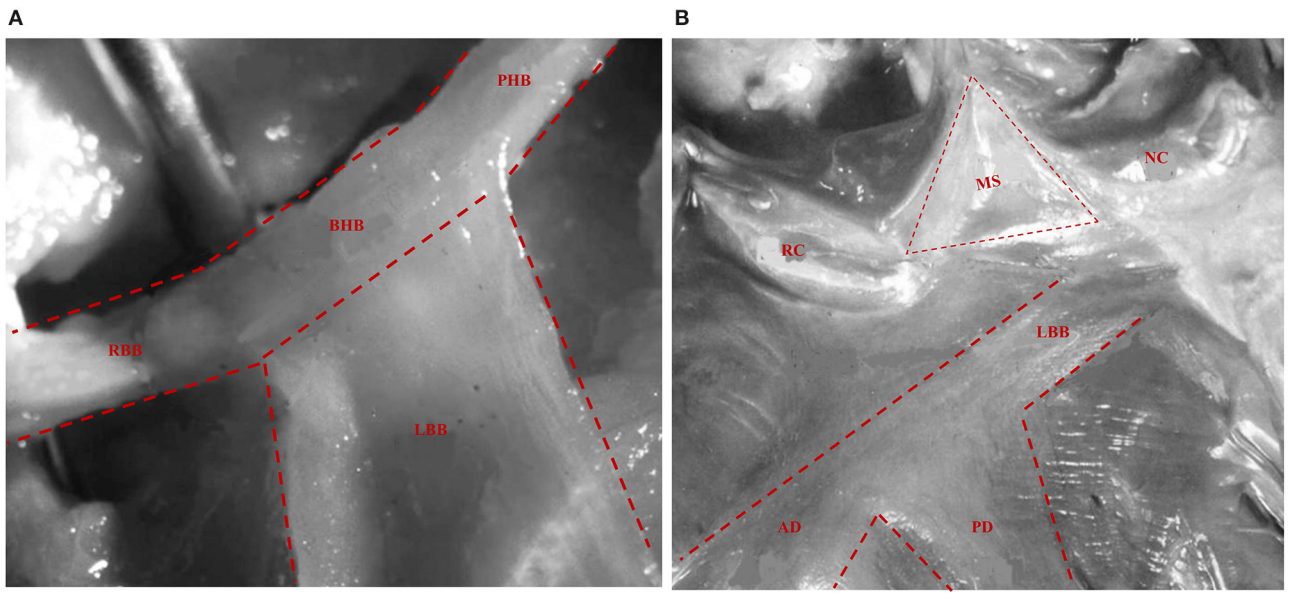

FIGURE 1 | The anatomy of His bundle and LBB. **(A)** The His bundle comprises two segments: PHB and BHB. LBB originates from the BHB of His located below the MS. The RBB appears as a continuation of the bundle of His after the LBB has been given off. **(B)** LBB can be seen underlying the endocardium below the MS, which is encompassed between the NC and RC aortic cusps and the summit of the ventricular septum. Then, it produces its two main divisions, AD and PD, both heading the anterior and posterior papillary muscles, respectively (23). LBB, left bundle branch; PHB, penetrating portion of His bundle; BHB, branching portion of His bundle; MS, membranous septum; RBB, right bundle branch; NC, non-coronary aortic cusps; RC, right coronary aortic cusps; AD, anterior division; PD, posterior division.

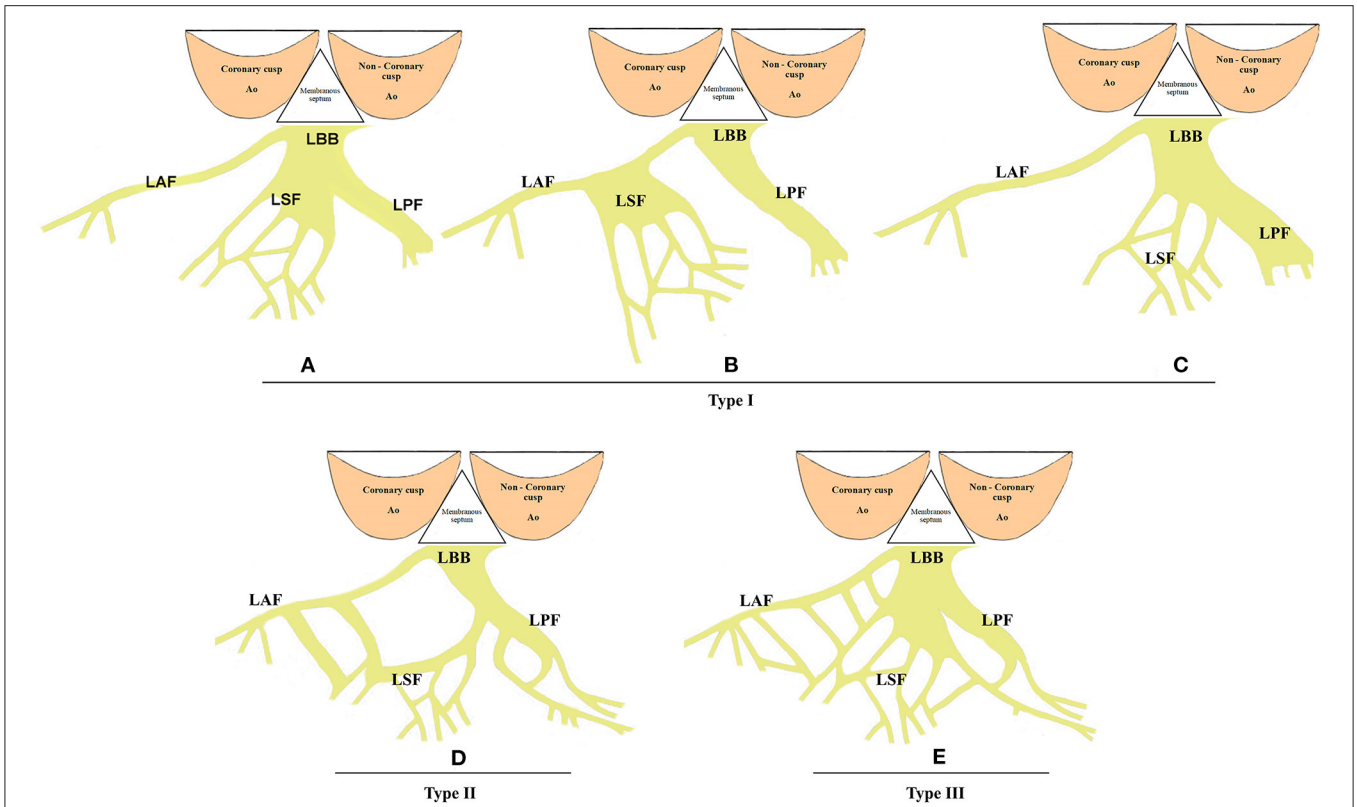

FIGURE 2 | The anatomical variants of LSF. **(A–C)** The most common LSF pattern, known as type I. In this type, LSF may originate from the main LBB or any of its division (PD or AD). **(D)** Type II anatomical variants of LSF. The LSF branches concomitantly from the AD and PD. **(E)** In type III, LSF is a "fan-like interconnecting network." LSF, left septal fascicle; LBB, left bundle branch; AD, anterior division; PD, posterior division.

region below the pars membranacea at the angle formed by the non-coronary and right coronary aortic cusps (23). The LBB's initial section is the narrowest, reaching its maximal width after extending about 10–15 mm (23). Its composition and distribution considerably vary across individuals. In some cases, two main divisions, anterior and posterior, that both head the anterior and posterior papillary muscles, respectively, appear soon after the origin of LBB (**Figure 1B**). Generally, the posterior division (PD) is thicker and shorter than the anterior division (AD) (24, 25), and in some cases, there are also well-defined left septal fascicle (LSF), which can arise from the PD and less frequently from the AD. Demoulin and Kulbertus (26) described the LSF's anatomical variants in 20 normal human hearts, with the most common pattern, which they called type I, showing a definite septal division. In this type, the LSF may originate from the main LBB or its division (PD or AD). In type II, the LSF branches concomitantly from AD and PD, whereas in type III, it appears as a "fan-like interconnecting network" (**Figure 2**) (11, 26–28). The existence and importance of LSF cannot be ignored. Particularly, these fibers are known to produce a network of interwoven strands that cover the inferior third of the septum, which avoids the widening of QRS when one of the divisions of the LBB is blocked (26, 28, 29). Overall, LBB's anatomical characteristics determine the feasibility of LBBP as a potential physiological pacing modality.

LBBP DEFINITION

LBBP is defined as capture of the LBB, usually with septal myocardium capture at low output (<1.0 V at 0.4 ms pulse width) (9, 30). In LBBP, the ventricular pacing lead is placed deep inside the interventricular septum 10–15 mm apical and ventricular to the distal His bundle region in the vicinity of the left bundle or its branches (**Figures 3A,B**) (9). The capture of LBB can be confirmed by some criteria described below, such as paced QRS morphology, peak left ventricular activation time (pLVAT), LBB potential, retrograde His or anterograde distal LBB potentials, programmed stimulation, and selective or non-selective LBBP.

Paced QRS Morphology

The paced QRS morphology, during unipolar LBBP, shows the pattern of right bundle branch block (RBBB) in V1 lead (qR or Qr) or improving the LBB conduction in patients with LBBB (**Figure 3C**) (31, 32). The RBBB pattern is usually incomplete and is influenced by the level of capture of the distal His bundle or proximal left bundle, distal conduction system disease,

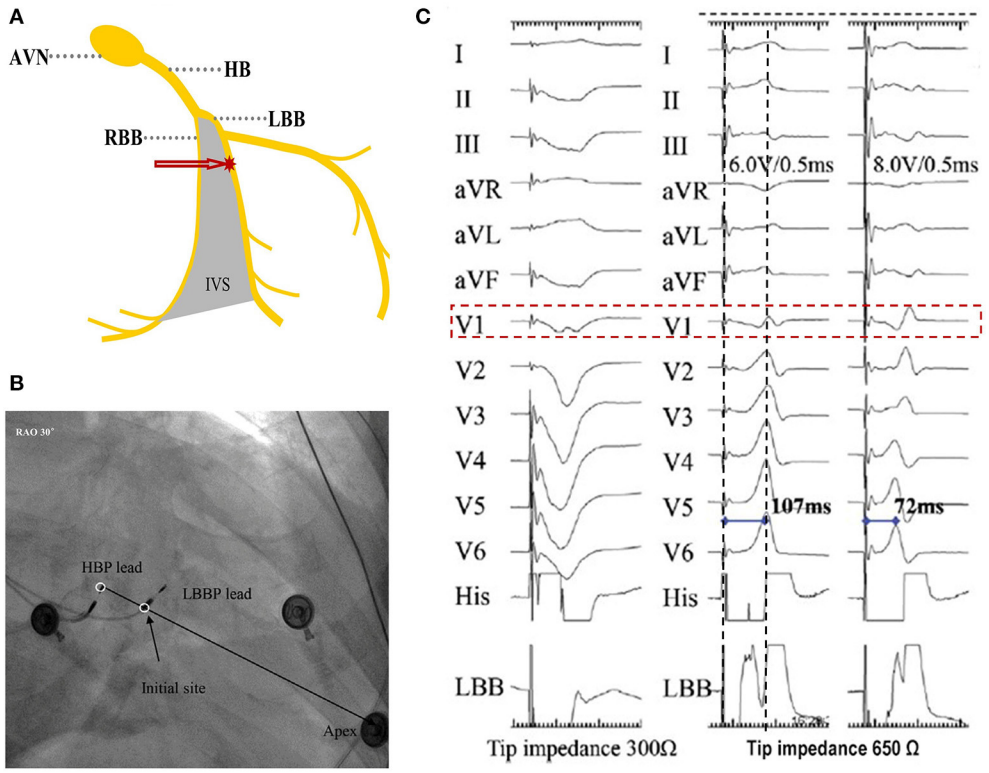

FIGURE 3 | How to locate the site for LBBP and electrogram characteristics. **(A)** A photographic representation of LBBP. **(B)** Location of the HBP lead and LBBP leads in the right anterior oblique 30° view. **(C)** Paced morphology of "W" pattern with a notch at the nadir of the QRS in lead V1 and impedance of 300 Ω by unipolar tip pacing before fixation (left). Screwing the lead ~6–8 mm deep, the notch in lead V1 moved up and toward the end of the QRS with impedance of 650 Ω. Increased output, from 6.0 V/0.5 ms (middle) to 8.0 V/0.5 ms (right), caused the paced morphology to change to RBBB and the pLVAT to be shortened from 107 to 72 ms (9). HBP, His-bundle pacing; HB, His bundle; LBB, left bundle branch; LBBP, left bundle branch pacing; RBBB, right bundle branch block; pLVAT, peak left ventricular activation time; AVN, atrioventricular node; RBB, right bundle branch; IVS, interventricular septum.

and septal-Purkinje connections. However, the QRS morphology alone is not a good predictor of left bundle capture, because RBBB pattern may not be observed if the pacing site is located in the superior septum or near the distal His bundle or proximal left bundle (33). Furthermore, the left ventricle septal pacing (LVSP) without capturing the left bundle can also produce an RBBB pattern. The difference is that the LVSP has prolonged left ventricle (LV) free-wall activation compared with LBBP.

pLVAT

The pLVAT is measured from the onset of the pacing spike to the peak of the R wave in the lead V5–6 (9). pLVAT is an indicator of the rapidity of LV free-wall activation used to identify the depth of pacing lead and capture of the LBB. Upon left bundle capture, pLVAT always remains short (<80 ms) and stable across different pacing outputs (**Figure 3C**). An increase in pLVAT, from high (10 V) to low (2 V) output, indicates the lead is away from the left bundle region and hence has to be carefully advanced slightly further to reach the left bundle. The current experience suggests a pLVAT < 80 ms indicates LBB capture (9). However, pLVAT can be influenced by intraventricular conduction defects and ischemic cardiomyopathy with significant scar, necessitating further refinement of pLVAT's cut-off point.

LBB Potential

LBB potential should always be recorded in patients without complete heart block (CHB) or complete LBBB. It is a sharp high-frequency deflection distance 15–30 ms to the onset of surface QRS (His potential to the ECG QRS onset is about 50 ms) (**Figures 4A,B**) (30, 34). LBB potential can help confirm lead depth and the level of conduction block. Interestingly, LBB potential can also be recorded in patients with LBBB, although it is limited to LBB conduction restoration via the HBP technique (**Figures 4C,D**) (35).

Retrograde His or Anterograde Distal LBB Potentials

Reverse His potential can be recorded during low-output LBBP, via direct capture of LBB, in patients without conduction disease (**Figure 5A**). Alternatively, stimulus to atrial intervals can be assessed during unipolar pacing from the LBBP lead tip (cathode at the LBB) and unipolar ring (anode at right ventricular septum).

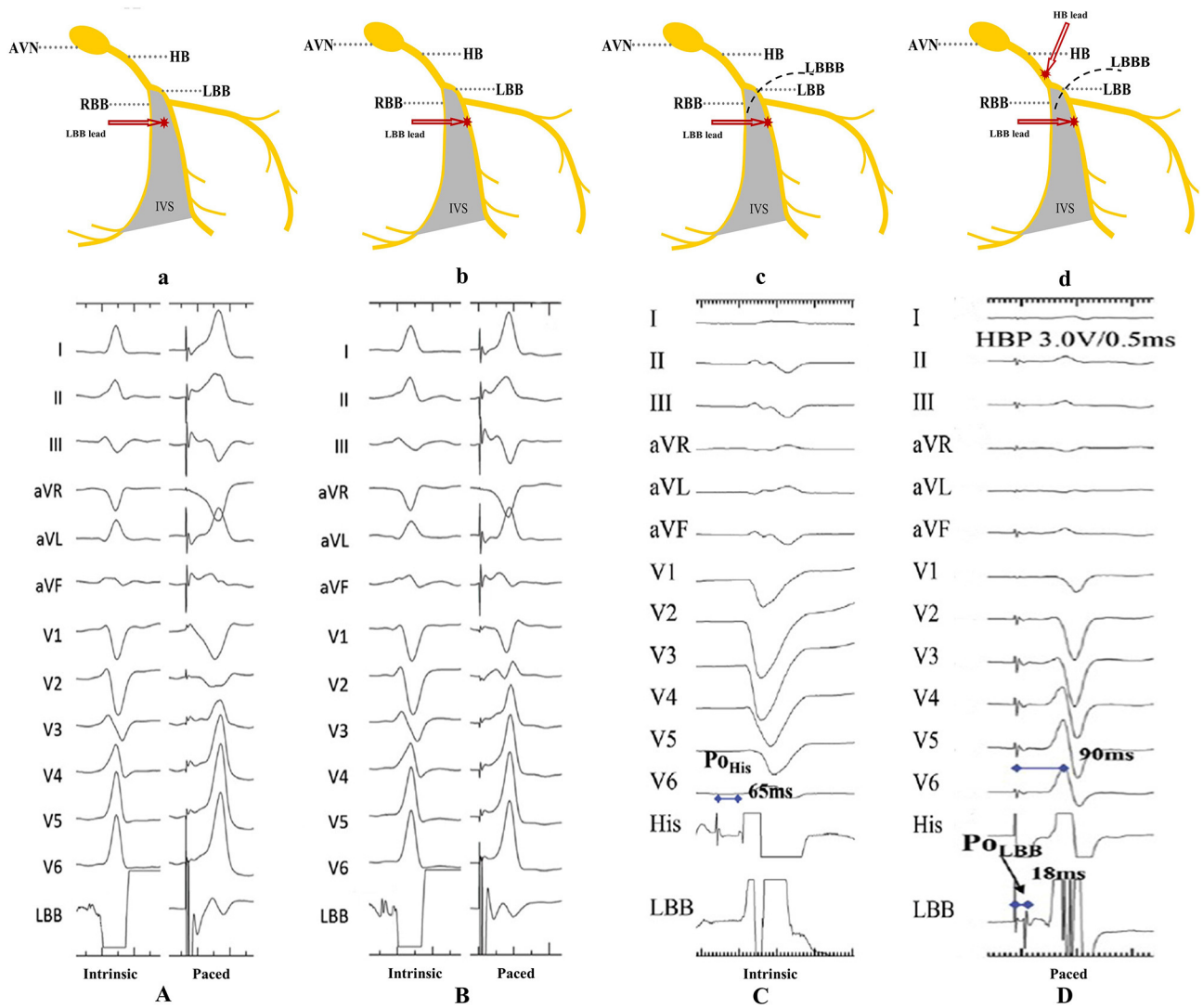

FIGURE 4 | Recording of the LBB potential. **(A)** The LBB potential can be recorded when the pacing lead helix is approaching the LBB. **(B)** The LBB potential becomes larger when the lead is closer to or at the LBB. **(C,D)** The LBB potential cannot be recorded in patients with LBBB, unless LBB is corrected by HBP (9). AVN, atrioventricular node; HB, His bundle; LBB, left bundle branch; LBBB, left bundle branch block; RBB, right bundle branch; IVS, interventricular septum; Po_{His}, His potential; Po_{LBB}, left bundle branch potential.

Here, the stimulus to atrial intervals would be markedly shorter than right ventricular septal pacing (RVSP) (36). Moreover, the anterograde distal LBB potential can also be considered as an indicator of LBB capture and can be recorded by multipolar catheter placed distal to the LBBP lead (**Figure 5B**) (9).

Programmed Stimulation

In some cases, the abovementioned criteria may not be observed during lead implantation. Thus, programmed stimulation may be adopted, as an alternative method, for differentiating septal and LBB capture. For example, Jastrzebski et al. (37) demonstrated that programmed deep septal stimulation with a 600-ms basic drive train could identify 79.7% LBB capture in patients. Their results further showed that the average septal-myocardial refractory period was shorter than the LBB refractory period (263.0 ± 34.4 vs. 318.0 ± 37.4) (37). However, this approach is not applicable to patients with LBBB (37).

Selective or Non-selective LBBP

LBBP can either be selective or non-selective, in a similar fashion to HBP. Selective LBBP captures only the LBB as a direct LBB capture sign. In fact, capturing both LBB and the adjacent local septal myocardium causes non-selective LBBP. While selective LBBP guarantees an isoelectric interval, between the pacing spike and the onset of surface QRS, this is not the case in non-selective LBBP (**Figure 6C**) (31). Moreover, a discrete local ventricular

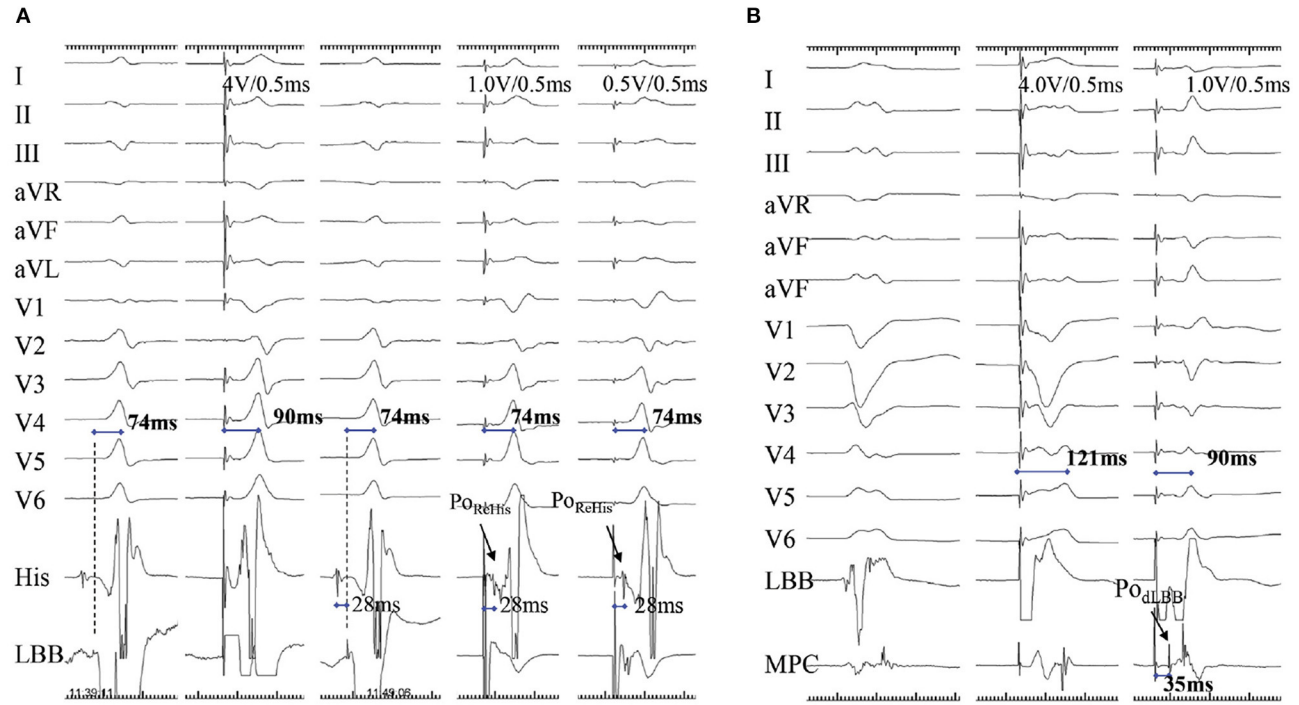

FIGURE 5 | A demonstration of direct LBB capture using retrograde His potential and anterograde distal left conduction system potential. **(A)** A case with narrow QRS wave. There is a small Po_{LBB} and long pLVAT (90 ms) with septal pacing (first two beats). When the lead is advanced at a deeper site of septum, the non-selective and selective LBBP (last three beats) are visible, with larger Po_{LBB}, shorter and constant pLVAT (74 ms), and Po_{Rehis} with stimulus to Po_{Rehis} interval of 28 ms at low and high outputs. **(B)** The Po_{dLBB} can be recorded after the ventricular EGM with MCP distal to the LBBP lead (first beat). The second beat shows the Po_{dLBB} remains after the ventricular EGM with 121 ms pLVAT during septal pacing, whereas the last indicates achievement of selective LBBP at a deeper site, Po_{dLBB} recorded ahead of ventricular EGM with shorter pLVAT (90 ms) (9). LBB, left bundle branch; pLVAT, peak left ventricular activation time; LBBP, left bundle branch pacing; MCP, multipolar placed; EGM, electrogram; Po_{dLBB}, distal left bundle branch potential; Po_{Rehis}, retrograde His potential.

electrogram (EGM), separate from the pacing artifact, can only be seen on the LBBP lead at low pacing output (**Figure 6C**) (35). Apart from the aforementioned indicators, pLVAT duration in non-selective LBBP may be prolonged when the output changes from high to low (32). Moreover, there are also longer stimulus–His interval and stimulus-to-right atrial interval, compared to the selective LBBP (32, 34). However, Chen et al. (35) found that both selective and non-selective LBBP resulted in constant pLVAT at different pacing outputs, implying that pLVAT may be not a powerful indicator of selective or non-selective LBBP.

LBBP IMPLANTATION

Evaluating the structure of the heart, especially the thickness of the basal interventricular septum and the presence of septal scars, is a crucial requirement before surgery. The SelectSecure lead (model 3830, Medtronic Inc., Minneapolis, USA) and Select Site C315 His or C304 His sheaths (Medtronic Inc., Minneapolis, USA) are used in operation, while an electrophysiological multichannel recorder is used to simultaneously document intracardiac EGMs and 12-lead ECG. Moreover, the Pacing System Analyzer (PSA) is used to test the pacing parameters and record intracardiac EGMs via the pacing lead. Generally, the operation process can be summarized as follows: (1) establishment of the venous access and determination of the initial LBBP site; (2) introducing a pacing lead into the right ventricle and screwing it into the interventricular septum (IVS) until the left ventricular septum is reached in the LBB areas; (3) assessing the lead depth into ventricular septum and confirming LBB capture; (4) removing the sheath and providing the slack; and (5) programming the pulse generator.

The Initial Site for LBBP

In LBBP, the His bundle region or tricuspid valve annulus can be used as anatomic markers for the pacing site. The target site is about 10–15 mm below the His bundle region, based on an imaginary line drawn from the distal extent of the His bundle to the RV apex in right anterior oblique (RAO) 30° fluoroscopic view (**Figure 3B**). The use of fluoroscopic landmarks, such as quadripolar catheter or another 3830 lead, to locate LBBP's initial site is possibly helpful for beginners, while it is not a general recommendation. Pace mapping, at this site, will often show a "W" pattern in lead V1 with a notch at the nadir of the QS complex, a positive QRS in lead II, and biphasic QRS in lead III

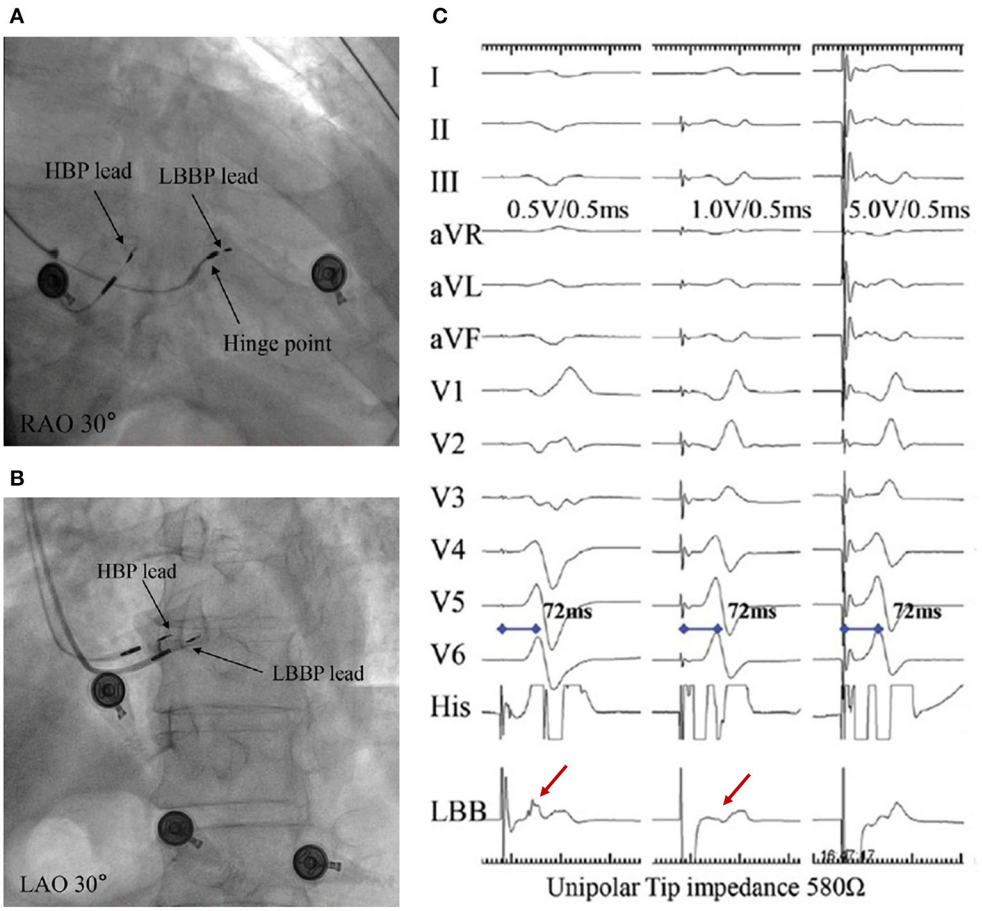

FIGURE 6 | A demonstration of selective and non-selective LBBP and the depth of its lead in the septum. **(A)** Fulcrum sign. **(B)** Sheath angiography in the LAO 30° view demonstrating the depth of the LBBP lead inside the septum. **(C)** The presence of a discrete local EGM with short pLVAT (72 ms) during selective LBBP (first beat). The last two beats indicate a constant pLVAT at different pacing outputs without discrete component, which is considered as non-selective LBBP (9). LBBP, left bundle branch pacing; LAO, left anterior oblique; RAO, right anterior oblique; EGM, electrogram; pLVAT, peak left ventricular activation time.

(**Figure 3C**) (31). It should be noted that the "W" pattern in lead V1 may not appear in ∼20% of patients (38).

Fixing the Lead

Once the site is confirmed, the C315 sheath (Medtronic Inc.) is rotated counterclockwise to maintain orientation of the lead tip perpendicular to the septal surface, thereby providing adequate support to allow screwing of the lead into the septum. Rapid lead rotations, three–four turns at a time by one or both hands, are suggested to achieve penetration of the lead body behind the screw into the septum. Thereafter, the lead is released and the rapid rotations are repeated. Advancing the lead deep inside the septum is expected to reveal the following parameters; (1) the notch on the nadir of "W" in lead V1 will gradually ascend up to form an R wave (**Figure 3C**); (2) unipolar pacing impedance gradually increases, before dropping by 100–200 Ω as the lead reaches the LV subendocardium; and (3) the left bundle branch injury current is present in 70% of the cases (20).

Determining the Optimal Position of the Lead

The ultimate ideal lead location depends on parameters of pLVAT, unipolar pacing lead impedance, and the presence of LBB potential. Generally, the paced pLVAT duration measured in lead V5 or V6 is short and constant (<80 ms) at differential pacing output, whereas the paced QRS morphology indicates qR or rSR in lead V1 (**Figure 3C**). Moreover, LBB potential is an important marker in patients with narrow complex or RBBB at baseline (**Figures 4A,B**). Interestingly, premature complexes of RBBB pattern can appear during lead fixation, suggesting the presence of Purkinje potentials in patients with complete heart block or LBBB (38). The unipolar pacing impedance is preferably >500 Ω. Further rotations need to be avoided if pLVAT is short and constant (<80 ms), LBB potential recorded, or unipolar pacing impedance of around 500–550 Ω with low capture threshold (<1.0 V at 0.5 ms pulse width). The septum's lead depth is ∼1.4 ± 0.23 cm (32). However, in cases where the LV is perforated, simply withdrawing the lead is not adequate

and must be repositioned at a different location. During the procedure, lead depth can be determined by contrast injection and echocardiography (**Figure 6B**), whereas 3D mapping system can also be used to assess the depth of lead after lead fixation. Therefore, 3D mapping may be a valuable tool for LBBP if it could monitor lead depth in real-time (39).

Removing the Sheath and Providing the Slack

When the lead is fixed, the sheath is pulled back into the right atrium, and the lead gently advanced to provide adequate slack. Improper and excessive slacks can cause lead dislodgement and late perforation, respectively. Furthermore, the pacing parameters need to be checked in both unipolar and bipolar modes, prior to slitting the sheath. The pacing lead can easily format an alpha loop after slitting the sheath, which can then be redressed by slowly retracting the lead, by applying a slight counterclockwise torque in RAO view (38).

Programming the Pulse Generator

Unipolar, bipolar, and anodal capture thresholds need to be recorded, prior to programming the pulse generator. Additionally, atrioventricular (AV) delay programming should be individualized based on native AV conduction and bundle branch block, while the automatic AV search function is routinely turned on in patients with sinus node dysfunction and intermittent AVB. The RBB conduction delay, caused by LBB capture, can also be partly compensated via two means (38): (1) programming the output above the anodal threshold, as the anode captures the septum's right side, and (2) optimizing the AV delay to allow native fusion through RBB. However, the programming above anodal capture is optional when battery life is considered.

Failure of LBBP

LBBP guarantees a high success rate, between 80 and 97% (18, 19, 32). LBBP's failure to advance the lead in the septum has been attributed to the difficulty in lead fixation, as well as other factors, including septal scar/fibrosis at the fixation site, tissue lodging into the helix, deformed sheath or helix, and, most commonly, inadequate sheath support or incorrect sheath orientation. In these cases, removing the tissue from the helix, using a 22–24 G needle, replacing the sheath or lead, and distally and inferiorly repositioning the lead may be helpful (9).

LBBP-ASSOCIATED COMPLICATIONS

Septal Perforation and Thromboembolism

Septal perforation and thromboembolism represent the most common complications associated with LBBP. Specifically, septal perforation comprises acute and late lead perforation, with the acute condition reported in 3% of patients following LBBP implantation (32). Acute lead perforation into the LV cavity can be discerned by the diminution of R wave amplitude, increase in capture threshold, or an immediate fall in unipolar impedance below 500 Ω. To avoid perforation, it is important to evaluate the thickness of the basal interventricular septum and lead length (the lead helix is 1.8 mm long and is 9 mm away from the anode tip) (**Figure 6A**). Moreover, a contrast injection can be used to assess lead depth during operation in the left anterior oblique (LAO) 30° (**Figure 6B**). In cases where acute septal perforation occurs, the lead needs to be re-implanted at a different site. Although late septal perforation is rare, it is a potential LBBP complication. To date, only a single case of late septal perforation, which has similar characteristics to acute septal perforation, has been reported during follow-up (40). In addition, exposure of the helix to the LV cavity is thought to be a theoretical risk of thromboembolism, although this has not been experimentally proven. Thus, there is a need to carefully monitor patients during follow-up.

RBB and Septal Arterial Injury

The RBB may be injured due to manipulation of the sheath at the basal septum below the His bundle region. Notably, ventricular backup pacing is recommended prior to LBBP lead implantation in patients with LBBB, because RBB injury may cause the AV to be completely blocked during the procedure. Moreover, injury to the coronary artery may also occur when the lead is placed deep in the proximal septum (41). To minimize this complication, clinicians are encouraged to place the lead at least 10 mm below the His bundle region.

Lead Dislodgement

The risk of lead dislodgement is slightly higher than HBP. Previous studies have reported acute lead dislodgement in LBBP, with Vijayaraman et al. (32) demonstrating its occurrence in three out of 97 patients who underwent LBBP. To minimize the risk of dislodgement, it is imperative to ensure appropriate slack and satisfactory pacing parameters are put in place. Furthermore, follow-up is encouraged to confirm the risk of late lead prominence.

SHORT-TERM CLINICAL OUTCOMES OF LBBP

Early Case Reports That Employed LBBP

Although research on LBBP is still at the exploratory phase, results from recent clinical explorations have been encouraging. For example, Huang et al. (16) were the first group to report LBBB and dilated cardiomyopathy in a 72-year-old HF woman treated with LBBP. Specifically, they used a low pacing output to correct the LBBB with accompanying RBBB on the electrocardiogram. At 1-year follow-up, they found a 62% increase in the left ventricular ejection fraction (LVEF), from a baseline 32%. Moreover, the left ventricular end-diastolic diameter (LVEDD) had decreased from 76 to 42 mm, whereas the New York Heart Association (NYHA) class had improved from a baseline IV to I (16). Similarly, Li et al. (42) reported a patient who accepted LBBP because of symptomatic systolic HF and complete LBBB. LBBB was corrected (QRS duration $<$120 ms) by a capture threshold 0.5 V, with the authors observing a significant improvement in exercise tolerance, reduction in ventricular size, and recovery of left bundle branch conduction after 1 year of LBBP therapy (42).

Furthermore, Wu et al. (43) reported the use of LBBP on a 74-years-old patient, with a LVEF and LVEDD of 34% and 62 mm, respectively, because of the RVAP-induced cardiomyopathy. They found that the patient's LVEF had increased to 63%, his LVEDD had decreased to 46 mm, and NYHA class had improved from III to I, after 6 months of LBBP. Moreover, they recorded a LBB capture threshold and R-wave amplitude of 0.5 V/0.5 ms and 20 mV, respectively (43). Vijayaraman and Panikkath (44) reported the successful application of LBBP in a patient who underwent bioprosthetic tricuspid valve replacement and whose proximal His bundle in the right atrium could not be located.

Comparison of Short-Term Clinical Outcomes of LBBP and RVAP

Several prospective studies have demonstrated that permanent LBBP guarantees a stable threshold, a narrow QRS duration, and preserved left ventricular synchrony, with only a few complications (18–21, 32, 34, 35, 37, 45). For example, Hasumi et al. (46) attempted to implant LBBP in 21 patients with HBP failure in atrioventricular block and obtained a success rate of 81% (17/21). Particularly, the mean procedure time of LBBP implantation was <15 min, whereas the QRS duration was reduced from 116 ± 8.3 ms to 108 ± 4.2 ms. Moreover, the group achieved a significant narrowing of the QRS duration in four patients with LBBB (from 151 ± 4.0 to 122 ± 6.7 ms, $P = 0.01$), with a mean capture and LBBB correction thresholds of 0.77 ± 0.07 V/0.4 and 0.89 ± 0.14 V/0.4 ms, respectively. The speckle tracking echocardiogram revealed no significant deterioration in the left ventricular total longitudinal strain, relative to intrinsic rhythm, during LBBP. Moreover, the researchers observed no complications during the 6-month follow-up (46). On the other hand, Li et al. (19) evaluated the LBBP in 87 patients with sinus node dysfunction and atrioventricular conduction disease and achieved an 80.5% LBBP implantation success rate, with an average procedure time of 18.0 ± 8.8 min. Notably, the LBBP's QRS duration was significantly narrower than RVAP (113.2 ± 9.9 ms vs. 144.4 ± 12.8 ms, $P < 0.001$), whereas the pacing threshold was low and stable (0.76 ± 0.22 V). Moreover, the researchers observed no adverse events during 3-month follow-up (19). Vijayaraman et al. (32) recorded 93 (93/100) and 88% (21/24) LBBP implantation success rates in bradycardia and LBBB patients, respectively. From their findings, it was evident that LBBP could significantly lower QRS duration in patients with LBBB (137 ± 19 ms vs. 162 ± 21 ms, $P < 0.001$). Notably, the authors reported that three patients had acute lead dislodgments within 24 h, three others had ventricular septal lead perforation, whereas one developed pericardial effusion. However, they did not observe transient ischemic attacks or thromboembolism in any of the patients during the short-term follow-up (32). Chen et al. (18) compared ECG parameters between LBBP and RVAP and found significantly narrower QRS duration in LBBP than RVAP (111.85 ± 10.77 ms vs. 160.15 ± 15.04 ms, $P < 0.001$). Two patients, with LBBB correction by LBBP, exhibited reduced QRS durations, from 178 and 168 ms during intrinsic rhythm to 120 and 128 ms during LBBP, respectively. In addition, one patient with RBBB exhibited lower QRS duration, from 188 to 130 ms by LBBP. Notably, the researchers found neither significant differences between the pacing thresholds (0.73 ± 0.20 V vs. 0.61 ± 0.23 V) nor adverse events during 3-month follow-up (18).

Application of LBBP in CRT

Hou et al. (45) compared cardiac synchrony of LBBP with RVAP and HBP in bradycardia patients and found that QRS duration of LBBP was located between the other two (HBP vs. LBBP vs. RVSP; 99.7 ± 15.6 ms vs. 117.8 ± 11.0 ms vs. 158.1 ± 11.1 ms, $P < 0.0001$). Their results further revealed that LBBP patients with recorded LBB potential had the similar phase standard deviation (PSD) and phase histogram bandwidth (PHB) to those with HBP patients (PSD, 15.1° ± 5.3° vs. 13.9° ± 5.8°, $P = 0.80$; PHB, 46.2° ± 13.4° vs. 41.3° ± 12.6°, $P = 0.51$). In addition, LBBP resulted in lower pacing threshold (0.5 ± 0.1 V vs. 1.4 ± 0.8 V, $P < 0.0001$) and higher R-wave amplitude (17.0 ± 6.7 mV vs. 4.4 ± 4.3 mV, $P < 0.0001$) (45). Furthermore, Zhang et al. (20) performed LBBP in 11 HF patients with LBBB. Their results revealed significant narrowing of QRS duration following LBBP (139.09 ± 17.44 ms vs. 180.00 ± 15.86 ms), whereas the pacing threshold was low and stable. Moreover, all 11 patients exhibited a 5% improvement in their LVEF, relative to the baseline value, whereas seven of them had a 20% increase in LVEF and a 15% decrease in left ventricular end-systolic diameter (LVESD), respectively, relative to the baseline value (20). Wu et al. (21) reported the gratifying outcomes of CRT with LBBP in a non-randomized treatment comparison with HBP and BVP. Specifically, they analyzed a total of 137 patients with LVEF ≤ 40% and typical LBBB referred for CRT who received BVP, HBP, or LBBP and found mean paced QRS durations of 100.7 ± 15.3, 110.8 ± 11.1, and 135.4 ± 20.2 ms, respectively. Meanwhile, patients in the LBBP group had higher R-wave amplitude (11.2 ± 5.1 vs. 3.8 ± 1.9 mV) and lower pacing thresholds (0.49 ± 0.13 V/0.5 ms vs. 1.35 ± 0.73 V/0.5 ms) relative to those in the HBP group. Generally, both HBP and LBBP groups exhibited a similar absolute increase (Δ) in LVEF (+23.9 vs. +24%) and rate of normalized final LVEF (74.4 vs. 70.0%) at 1-year follow-up, which was significantly higher than those observed in the BVP group (ΔLVEF +16.7 and 44.9% rate of normalized final LVEF) (21). Moreover, Ravi et al. (47) reported that LBBP could significantly improve the left ventricular dysfunction in patients with HF during 6-month follow-up. Their results revealed significant improvement of LVEF (from 30 ± 11% to 42 ± 15%) following LBBP in 21 patients with cardiomyopathy. Among seven patients with LBBB and cardiomyopathy, the LVEF improved from 27 ± 4% to 36 ± 11%. In addition, there was a significant reduction in QRS duration (30–46 ms) in patients with baseline QRS duration > 120 ms. Recently, Huang et al. (48) also demonstrated that LBBP was a feasible and effective method for achieving electric resynchronization in patients with LBBB and non-ischemic cardiomyopathy in a prospective, multicenter study. Specifically, they recorded 97% (61/63) LBBP implantation success rates, with stable pacing threshold and R-wave amplitude at 1-year follow-up compared with implantation values (0.5 ± 0.15 V/0.5 ms vs. 0.58 ± 0.14 V/0.5 ms and 11.1 ± 4.9 mV vs. 13.3 ± 5.3 mV, respectively). Notably, the QRS duration narrowed from 169 ±

16 to 118 ± 12 ms during LBBP. In addition, patients exhibited a significant improvement in their LVEF (33 ± 8% vs. 55 ± 10%, $P < 0.001$) and a decrease in left ventricular end-systolic volume (123 ± 61 ml vs. 67 ± 39 ml, $P < 0.001$), relative to the baseline value (48).

ADVANTAGES OF LBBP

RVAP and LBBP

Clinical practice has associated previous cardiac pacing strategies with deficiencies (49). RVAP is clearly non-physiological with regard to ventricular activation, with the creation of a LBBB-like sactivation sequence, and is associated with the risk of HF and AF as well as all-cause mortality (50). Alternative RV pacing sites, such as the right septum and right ventricular outflow tracts, have been attempted in the right ventricle, while their clinical outcomes remain controversial (5). Some studies have showed that LBBP confers better electrical and mechanical synchrony with RVAP and comparable R-wave amplitude and pacing threshold (18, 45), and its operation is safe and with few serious complications (18–20, 45). However, it is not known whether this approach's long-term clinical outcomes are superior to these of RVAP.

HBP and LBBP

Theoretically, HBP is an ideal method for ventricular stimulation through the His–Purkinje conduction system. Numerous studies have demonstrated HBP's clinical benefits relative to those from RVAP in patients with preservation of LVEF (12). For example, permanent HBP has been proposed as an alternative to BVP for CRT (13). However, the His bundle is only ∼1–2 mm in diameter, while HBP technique remains challenging (51). The His bundle is located in the central fibrous body and is minimally surrounded by myocardial tissue, which generates a high His capture threshold that may progressively increase during follow-up. Studies have also shown that HBP guarantees a higher 5-year generator replacement rate than RVAP (9 vs. 1%) (52). Capture thresholds required to correct underlying BBB are often higher in patients undergoing CRT with HBP, and their early battery depletion can still be a major obstacle (11). The mechanism through which HBP reverses LBBB is based on the concept of longitudinal dissociation with specific fibers within the His bundle committed to the left bundle. Thus, local lesions within the His bundle can result in LBBB, although this condition can be overcome by pacing at a location near or distal to the His bundle (53). Previous studies have shown that the mechanisms of LBBB are not restricted to the longitudinal dissociation of His. For instance, Upadhyay et al. (54) studied 85 patients with LBBB. They found that the cause of LBBB in 64% of cohort was localized conduction block, with no specific block but intraventricular conduction delay (IVCD) with intact Purkinje activation (IPA) in the remainder of the cohort. Patients with conduction block exhibited blockade, either at the level of the His bundle at the left septum (72%) or proximally within the left bundle (28%). Moreover, a majority of the patients with His block (94%) responded to HBP, compared to 64% of those with block in left bundle and none of the patients with IPA (54), indicating that LBBB may not be corrected by permanent HBP in 10–30% of patients (51). Notably, LBBP can bypass the pathological or disease-vulnerable region in the cardiac conduction system to produce near physiological or true conduction system pacing. In addition, a comparison with HBP indicates that LBBP operation is simple. Particularly, the entire LBB distribution area is similar to a "fan plane," while the His bundle distribution is more restricted, in a similar fashion to a "point" (23). In fact, LBBP implantation guarantees a high success rate, between 80 and 97% (19, 34). Clinical studies have demonstrated that LBBP preserves better electrical and mechanical synchrony than RVAP, in a similar fashion to HBP. LBBP's R-wave amplitude and pacing threshold are reportedly more satisfactory and stable than those obtained in HBP (45). Furthermore, pacing at the LBB may also prevent later deterioration at the proximal His bundle or AV node, which may be caused by progression of AV conduction delay, and also provide more space for AV node ablation (17).

BVP and LBBP

Currently, the application of BVP is the most common way of reversing or preventing pacing-induced dyssynchrony. Improvements in clinical applications have predisposed CRT to various shortcomings, with about 30% of patients reportedly not responding to the therapy (55, 56). Another problem associated with CRT via BVP is the use of epicardial LV pacing, which reverses physiologic activation of the ventricular wall. Functionally, this change increases transmural dispersion of repolarization (TDR) and QT interval, thereby creating a substrate for the development of torsade de pointe (TdP) (57). To date, the role of CRT in patients with preserved LV systolic function has not been elucidated. In addition, intravenous CRT implants are challenging, and diverse coronary sinus anatomy provides a limited choice of LV pacing sites. Consequently, research efforts have been directed to LV endocardial pacing. Mills et al. (58) demonstrated the benefits of LV endocardial pacing relative to traditional BVP, both acutely and chronically, and found that LV septal or apical pacing resulted in cardiac efficiency similar to that seen with native conduction. Other clinical studies have also demonstrated that LV pacing produces equivalent or even superior effects than conventional CRT via BVP (59, 60). However, LV endocardial pacing, via percutaneous atrial transseptal route, is complex and can influence mitral valve function and predispose patients to infections and stroke (61). Betts et al. (62) and Mafi-Rad et al. (63) reported a new feasible and safe route of LV endocardial pacing via ventricular septal puncture. Although LBBP can also be operated via transvenous approach through the interventricular septum, some differences have been reported between LVSP and LBBP. For instance, LBBP's lead position was higher than that of LVSP. The LBB potential, recorded in LBBP, shows that the pacing site is close to its torso and the Purkinje network, and this has not been reported in LVSP. In fact, LBBP's mean pacing QRS duration is narrower than the LVSP's, indicating the former's superiority with regard to ventricular synchrony (18, 19, 32, 45, 63). Apart from this, Li et al. (34) found that mechanical dispersion seemed to worsen over a 3-month follow-up period in three patients who received LVSP. However, LBBP could correct ventricular dyssynchrony, shorten

QRS duration, promote LV reverse remodeling, and improve clinical symptoms in patients with HF (20, 21, 48).

WHAT IS THE FUTURE OF LBBP THERAPY?

Although early studies have demonstrated LBBP's potential as a physiologic pacing modality with stable and low threshold, numerous aspects of this therapy remain unknown, necessitating future explorations. For instance, what is the long-term safety and efficacy of the procedure? How can we accurately determine the depth of lead implantation to avoid the occurrence of interventricular septal perforation? Will the risk of thromboembolism and lead dislodgement increase? What is the long-term effect on interventricular septum and LBB when they are traumatized by the screw on the tip of the lead? Can a second LBBP lead be successfully placed if the earlier one fails in the long run? Beyond pacing hemodynamics, what is the impact of LBBP on arrhythmia? Since LBBP is also considered as a potential alternative to CRT, which patients with heart failure are best suited for LBBP, compared with either HBP or BVP? Apart from these areas, considerable efforts need to be directed to improving the design and structure of the lead as well as the delivery tools that will allow easier implantation and stabilization of the lead. Despite the technique's great potential for physiological pacing, further validation using studies with large numbers of participants and longer follow-up periods is required.

CONCLUSIONS

Left bundle branch pacing is a novel pacing modality that can bypass the pathological or disease-vulnerable region in the cardiac conduction system, to provide physiological pacing modality for patients. LBBP guarantees a narrow paced QRS complex and fast LVAT, with a low pacing capture threshold. Previous studies have shown that LBBP can be applied to circumvent the limitations of HBP or RV pacing and can acts as a potential alternative to CRT in patients with typical LBBB. Future studies are expected to validate LBBP's safety, reliability, and long-term performance using large prospective trials and affirm its potential as an alternative option for physiological pacing in several groups of patients.

AUTHOR CONTRIBUTIONS

QZ and XQ provided the idea and technical guidance for the manuscript. PL wrote the manuscript. QW and HS made the figures. All authors have read and agreed to the published version of the manuscript.

FUNDING

This work was supported by the National Natural Science Foundation of China (Grant Numbers 81870257 and 31871172).

REFERENCES

1. Lamas GA, Lee KL, Sweeney MO, Silverman R, Leon A, Yee R, et al. Ventricular pacing or dual-chamber pacing for sinus-node dysfunction. *N Engl J Med.* (2002) 346:1854–62. doi: 10.1056/NEJMoa013040
2. Wilkoff BL, Cook JR, Epstein AE, Greene HL, Hallstrom AP, Hsia H, et al. Dual-chamber pacing or ventricular backup pacing in patients with an implantable defibrillator: the Dual Chamber and VVI Implantable Defibrillator (DAVID) Trial. *JAMA.* (2002) 288:3115–23. doi: 10.1001/jama.288.24.3115
3. Sweeney MO, Hellkamp AS, Ellenbogen KA, Greenspon AJ, Freedman RA, Lee KL, et al. Adverse effect of ventricular pacing on heart failure and atrial fibrillation among patients with normal baseline QRS duration in a clinical trial of pacemaker therapy for sinus node dysfunction. *Circulation.* (2003) 107:2932–7. doi: 10.1161/01.CIR.0000072769.17295.B1
4. Slotwiner DJ, Raitt MH, Del-Carpio Munoz F, Mulpuru SK, Nasser N, Peterson PN. Impact of physiologic pacing versus right ventricular pacing among patients with left ventricular ejection fraction greater than 35%: a systematic review for the 2018 ACC/AHA/HRS guideline on the evaluation and management of patients with bradycardia and cardiac conduction delay: a report of the American College of Cardiology/American Heart Association Task Force on Clinical Practice Guidelines and the Heart Rhythm Society. *Circulation.* (2019) 140:e483–503. doi: 10.1161/CIR.0000000000000629
5. Da Costa A, Gabriel L, Romeyer-Bouchard C, Geraldine B, Gate-Martinet A, Laurence B, et al. Focus on right ventricular outflow tract septal pacing. *Arch Cardiovasc Dis.* (2013) 106:394–403. doi: 10.1016/j.acvd.2012.08.005
6. Zografos TA, Siontis KC, Jastrzebski M, Kutyifa V, Klein HU, Zareba W, et al. Apical vs. non-apical right ventricular pacing in cardiac resynchronization therapy: a meta-analysis. *Europace.* (2015) 17:1259–66. doi: 10.1093/europace/euv048
7. Ponikowski P, Voors AA, Anker SD, Bueno H, Cleland JGF, Coats AJS, et al. 2016 ESC guidelines for the diagnosis and treatment of acute and chronic heart failure: the task force for the diagnosis and treatment of acute and chronic heart failure of the European Society of Cardiology (ESC)Developed with the special contribution of the Heart Failure Association (HFA) of the ESC. *Eur Heart J.* (2016) 37:2129–200. doi: 10.1093/eurheartj/ehw128
8. Daubert C, Behar N, Martins RP, Mabo P, Leclercq C. Avoiding non-responders to cardiac resynchronization therapy: a practical guide. *Eur Heart J.* (2017) 38:1463–72. doi: 10.1093/eurheartj/ehw270
9. Huang W, Chen X, Su L, Wu S, Xia X, Vijayaraman P. A beginner's guide to permanent left bundle branch pacing. *Heart Rhythm.* (2019) 16:1791–6. doi: 10.1016/j.hrthm.2019.06.016
10. Deshmukh P, Casavant DA, Romanyshyn M, Anderson K. Permanent, direct His-bundle pacing: a novel approach to cardiac pacing in patients with normal His-Purkinje activation. *Circulation.* (2000) 101:869–77. doi: 10.1161/01.CIR.101.8.869
11. Lustgarten DL, Crespo EM, Arkhipova-Jenkins I, Lobel R, Winget J, Koehler J, et al. His-bundle pacing versus biventricular pacing in cardiac resynchronization therapy patients: a crossover design comparison. *Heart Rhythm.* (2015) 12:1548–57. doi: 10.1016/j.hrthm.2015.03.048
12. Sharma PS, Ellenbogen KA, Trohman RG. Permanent His Bundle pacing: the past, present, and future. *J Cardiovasc Electrophysiol.* (2017) 28:458–65. doi: 10.1111/jce.13154
13. Sharma PS, Dandamudi G, Herweg B, Wilson D, Singh R, Naperkowski A, et al. Permanent His-bundle pacing as an alternative to biventricular pacing for cardiac resynchronization therapy: a multicenter experience. *Heart Rhythm.* (2018) 15:413–20. doi: 10.1016/j.hrthm.2017.10.014
14. Huang W, Su L, Wu S, Xu L, Xiao F, Zhou X, et al. Long-term outcomes of His bundle pacing in patients with heart failure with left bundle branch block. *Heart.* (2019) 105:137–43. doi: 10.1136/heartjnl-2018-313415
15. Upadhyay G, Vijayaraman P, Nayak H, Verma N, Dandamudi G, Sharma P, et al. His corrective pacing or biventricular pacing for cardiac

resynchronization in heart failure. *J Am Coll Cardiol*. (2019) 74:157–9. doi: 10.1016/j.jacc.2019.04.026
16. Huang W, Su L, Wu S, Xu L, Xiao F, Zhou X, et al. A novel pacing strategy with low and stable output: pacing the left bundle branch immediately beyond the conduction block. *Can J Cardiol*. (2017) 33:1736.e1–1736.e3. doi: 10.1016/j.cjca.2017.09.013
17. Huang W, Su L, Wu S, Xu L, Xiao F, Zhou X, et al. Benefits of permanent His bundle pacing combined with atrioventricular node ablation in atrial fibrillation patients with heart failure with both preserved and reduced left ventricular ejection fraction. *J Am Heart Assoc*. (2017) 6:e005309. doi: 10.1161/JAHA.116.005309
18. Chen K, Li Y, Dai Y, Sun Q, Luo B, Li C, et al. Comparison of electrocardiogram characteristics and pacing parameters between left bundle branch pacing and right ventricular pacing in patients receiving pacemaker therapy. *Europace*. (2019) 21:673–80. doi: 10.1093/europace/euy252
19. Li Y, Chen K, Dai Y, Li C, Sun Q, Chen R, et al. Left bundle branch pacing for symptomatic bradycardia: Implant success rate, safety, and pacing characteristics. *Heart Rhythm*. (2019) 16:1758–65. doi: 10.1016/j.hrthm.2019.05.014
20. Zhang W, Huang J, Qi Y, Wang F, Guo L, Shi X, et al. Cardiac resynchronization therapy by left bundle branch area pacing in patients with heart failure and left bundle branch block. *Heart Rhythm*. (2019) 16:1783–90. doi: 10.1016/j.hrthm.2019.09.006
21. Wu S, Su L, Vijayaraman P, Zheng R, Cai M, Xu L, et al. Left bundle branch pacing for cardiac resynchronization therapy: non-randomized on treatment comparison with His bundle pacing and biventricular pacing. *Can J Cardiol*. (2020) 37:319–28. doi: 10.1016/j.cjca.2020.04.037
22. Knorre, GHV. The 100(th) anniversary of "The Conduction System of the Mammalian Heart" by Sunao Tawara. *Herzschrittmacherther Elektrophysiol*. (2006) 17:140–5. doi: 10.1007/s00399-006-0525-x
23. Elizari MV. The normal variants in the left bundle branch system. *J Electrocardiol*. (2017) 50:389–99. doi: 10.1016/j.jelectrocard.2017.03.004
24. Hudson RE. Surgical pathology of the conducting system of the heart. *Br Heart J*. (1967) 29:646–70. doi: 10.1136/hrt.29.5.646
25. Anderson RH, Ho SY, Becker AE. The surgical anatomy of the conduction tissues. *Thorax*. (1983) 38:408–20. doi: 10.1136/thx.38.6.408
26. Demoulin JC, Kulbertus HE. Histopathological examination of concept of left hemiblock. *Br Heart J*. (1972) 34:807–14. doi: 10.1136/hrt.34.8.807
27. Kulbertus HE, Demoulin JC. Histopathological correlates of sinoatrial disease. *Br Heart J*. (1978) 40:1384–9. doi: 10.1136/hrt.40.12.1384
28. Perez-Riera AR, Barbosa-Barros R, Daminello-Raimundo R, de Abreu LC, Nikus K. The tetrafascicular nature of the intraventricular conduction system. *Clin Cardiol*. (2019) 42:169–74. doi: 10.1002/clc.23093
29. MacAlpin RN. In search of left septal fascicular block. *Am Heart J*. (2002) 144:948–56. doi: 10.1067/mhj.2002.125503
30. Zhang S, Zhou X, Gold MR. Left bundle branch pacing: jacc review topic of the week. *J Am Coll Cardiol*. (2019) 74:3039–49. doi: 10.1016/j.jacc.2019.10.039
31. Chen K, Li Y. How to implant left bundle branch pacing lead in routine clinical practice. *J Cardiovasc Electrophysiol*. (2019) 30:2569–77. doi: 10.1111/jce.14190
32. Vijayaraman P, Subzposh FA, Naperkowski A, Panikkath R, John K, Mascarenhas V, et al. Prospective evaluation of feasibility and electrophysiologic and echocardiographic characteristics of left bundle branch area pacing. *Heart Rhythm*. (2019) 16:1774–82. doi: 10.1016/j.hrthm.2019.05.011
33. Wu S, Su L, Zheng R, Xu L, Huang W. New-onset intrinsic and paced QRS morphology of right bundle branch block pattern after atrioventricular nodal ablation: longitudinal dissociation or anatomical bifurcation? *J Cardiovasc Electrophysiol*. (2020) 31:1218–21. doi: 10.1111/jce.14469
34. Li X, Li H, Ma W, Ning X, Liang E, Pang K, et al. Permanent left bundle branch area pacing for atrioventricular block: feasibility, safety, and acute effect. *Heart Rhythm*. (2019) 16:1766–73. doi: 10.1016/j.hrthm.2019.04.043
35. Chen X, Wu S, Su L, Su Y, Huang W. The characteristics of the electrocardiogram and the intracardiac electrogram in left bundle branch pacing. *J Cardiovasc Electrophysiol*. (2019) 30:1096–101. doi: 10.1111/jce.13956
36. Sundaram S, Vijayaraman P. Left bundle branch pacing. *Herzschrittmacherther Elektrophysiol*. (2020) 31:124–34. doi: 10.1007/s00399-020-00694-8
37. Jastrzebski M, Moskal P, Bednarek A, Kiełbasa G, Kusiak A, Sondej T, et al. Programmed deep septal stimulation: a novel maneuver for the diagnosis of left bundle branch capture during permanent pacing. *J Cardiovasc Electrophysiol*. (2020) 31:485–93. doi: 10.1111/jce.14352
38. Ponnusamy SS, Arora V, Namboodiri N, Kumar V, Kapoor A, Vijayaraman P. Left bundle branch pacing: a comprehensive review. *J Cardiovasc Electrophysiol*. (2020) 31:2462–73. doi: 10.1111/jce.14681
39. Vijayaraman P, Panikkath R, Mascarenhas V, Bauch TD. Left bundle branch pacing utilizing three dimensional mapping. *J Cardiovasc Electrophysiol*. (2019) 30:3050–6. doi: 10.1111/jce.14242
40. Ravi V, Larsen T, Ooms S, Trohman R, Sharma PS. Late-onset interventricular septal perforation from left bundle branch pacing. *HeartRhythm Case Rep*. (2020) 6:627–31. doi: 10.1016/j.hrcr.2020.06.008
41. Ponnusamy SS, Vijayaraman P. Aborted ST-elevation myocardial infarction-an unusual complication of left bundle branch pacing. *HeartRhythm Case Rep*. (2020) 6:520–2. doi: 10.1016/j.hrcr.2020.05.010
42. Li Y, Chen K, Dai Y, Li C, Sun Q, Chen R, et al. Recovery of complete left bundle branch block following heart failure improvement by left bundle branch pacing in a patient. *J Cardiovasc Electrophysiol*. (2019) 30:1714–7. doi: 10.1111/jce.14034
43. Wu S, Su L, Wang S, Vijayaraman P, Ellenbogen KA, Huang W. Peri-left bundle branch pacing in a patient with right ventricular pacing-induced cardiomyopathy and atrioventricular infra-Hisian block. *Europace*. (2019) 21:1038. doi: 10.1093/europace/euz031
44. Vijayaraman P, Panikkath R. Intracardiac echocardiography-guided left bundle branch pacing in a patient with tricuspid valve replacement. *J Cardiovasc Electrophysiol*. (2019) 30:2525–7. doi: 10.1111/jce.14205
45. Hou X, Qian Z, Wang Y, Qiu Y, Chen X, Jiang H, et al. Feasibility and cardiac synchrony of permanent left bundle branch pacing through the interventricular septum. *Europace*. (2019) 21:1694–702. doi: 10.1093/europace/euz188
46. Hasumi E, Fujiu K, Nakanishi K, Komuro I. Impacts of left bundle/peri-left bundle pacing on left ventricular contraction. *Circ J*. (2019) 83:1965–7. doi: 10.1253/circj.CJ-19-0399
47. Ravi V, Hanifin JL, Larsen T, Huang HD, Trohman RG, Sharma PS. Pros and cons of left bundle branch pacing: a single-center experience. *Circ Arrhythm Electrophysiol*. (2020) 13:e008874. doi: 10.1161/CIRCEP.120.008874
48. Huang W, Wu S, Vijayaraman P, Su L, Chen X, Cai B, et al. Cardiac resynchronization therapy in patients with nonischemic cardiomyopathy using left bundle branch pacing. *JACC Clin Electrophysiol*. (2020) 6:849–58. doi: 10.1016/j.jacep.2020.04.011
49. Vijayaraman P, Bordachar P, Ellenbogen KA. The continued search for physiological pacing: where are we now? *J Am Coll Cardiol*. (2017) 69:3099–114. doi: 10.1016/j.jacc.2017.05.005
50. Healey JS, Toff WD, Lamas GA, Andersen HR, Thorpe KE, Ellenbogen KA, et al. Cardiovascular outcomes with atrial-based pacing compared with ventricular pacing: meta-analysis of randomized trials, using individual patient data. *Circulation*. (2006) 114:11–7. doi: 10.1161/CIRCULATIONAHA.105.610303
51. Vijayaraman P, Chung MK, Dandamudi G, Upadhyay GA, Krishnan K, Crossley G, et al. His bundle pacing. *J Am Coll Cardiol*. (2018) 72:927–47. doi: 10.1016/j.jacc.2018.06.017
52. Vijayaraman P, Naperkowski A, Subzposh FA, Abdelrahman M, Sharma PS, Oren JW, et al. Permanent his-bundle pacing: long-term lead performance and clinical outcomes. *Heart Rhythm*. (2018) 15:696–702. doi: 10.1016/j.hrthm.2017.12.022
53. Narula OS. Longitudinal dissociation in the His bundle. Bundle branch block due to asynchronous conduction within the His bundle in man. *Circulation*. (1977) 56:996–1006. doi: 10.1161/01.CIR.56.6.996
54. Upadhyay GA, Cherian T, Shatz DY, Beaser AD, Aziz Z, Ozcan C, et al. Intracardiac delineation of septal conduction in left bundle-branch block patterns. *Circulation*. (2019) 139:1876–88. doi: 10.1161/CIRCULATIONAHA.118.038648
55. Cleland JGF, Daubert JC, Erdmann E, Freemantle N, Gras D, Kappenberger L, et al. The effect of cardiac resynchronization on morbidity and mortality

in heart failure. *N Engl J Med.* (2005) 352:1539–49. doi: 10.1056/NEJMoa050496
56. Hanley A, Heist EK. Left ventricular endocardial pacing/leadless pacing. *Card Electrophysiol Clin.* (2019) 11:155–64. doi: 10.1016/j.ccep.2018.10.001
57. Fish JM, Di Diego JM, Nesterenko V, Antzelevitch C. Epicardial activation of left ventricular wall prolongs QT interval and transmural dispersion of repolarization: implications for biventricular pacing. *Circulation.* (2004) 109:2136–42. doi: 10.1161/01.CIR.0000127423.75608.A4
58. Mills RW, Cornelussen RN, Mulligan LJ, Strik M, Rademakers LM, Skadsberg ND, et al. Left ventricular septal and left ventricular apical pacing chronically maintain cardiac contractile coordination, pump function and efficiency. *Circ Arrhythm Electrophysiol.* (2009) 2:571–9. doi: 10.1161/CIRCEP.109.882910
59. Ginks MR, Shetty AK, Lambiase PD, Duckett SG, Bostock J, Peacock JL, et al. Benefits of endocardial and multisite pacing are dependent on the type of left ventricular electric activation pattern and presence of ischemic heart disease: insights from electroanatomic mapping. *Circ Arrhythm Electrophysiol.* (2012) 5:889–97. doi: 10.1161/CIRCEP.111.967505
60. Sohal M, Shetty A, Niederer S, Chen Z, Jackson T, Sammut E, et al. Delayed trans-septal activation results in comparable hemodynamic effect of left ventricular and biventricular endocardial pacing: insights from electroanatomical mapping. *Circ Arrhythm Electrophysiol.* (2014) 7:251–8. doi: 10.1161/CIRCEP.113.001152
61. Graham AJ, Providenica R, Honarbakhsh S, Srinivasan N, Sawhney V, Hunter R, et al. Systematic review and meta-analysis of left ventricular endocardial pacing in advanced heart failure: clinically efficacious but at what cost? *Pacing Clin Electrophysiol.* (2018) 41:353–61. doi: 10.1111/pace.13275
62. Betts TR, Gamble JHP, Khiani R, Bashir Y, Rajappan K. Development of a technique for left ventricular endocardial pacing via puncture of the interventricular septum. *Circ Arrhythm Electrophysiol.* (2014) 7:17–22. doi: 10.1161/CIRCEP.113.001110
63. Mafi-Rad M, Luermans JG, Blaauw Y, Janssen M, Crijns HJ, Prinzen FW, et al. Feasibility and acute hemodynamic effect of left ventricular septal pacing by transvenous approach through the interventricular septum. *Circ Arrhythm Electrophysiol.* (2016) 9:e003344. doi: 10.1161/CIRCEP.115.003344

Conflict of Interest: The authors declare that the research was conducted in the absence of any commercial or financial relationships that could be construed as a potential conflict of interest.

frontiers in Cardiovascular Medicine

ORIGINAL RESEARCH
published: 24 March 2021
doi: 10.3389/fcvm.2021.645947

Procedure-Related Complications of Left Bundle Branch Pacing: A Single-Center Experience

Xueying Chen[1†], Lanfang Wei[2†], Jin Bai[1], Wei Wang[1], Shengmei Qin[1], Jingfeng Wang[1], Yixiu Liang[1], Yangang Su[1] and Junbo Ge[1]*

[1] Department of Cardiology, Zhongshan Hospital of Fudan University, Shanghai Institute of Cardiovascular Diseases, National Clinical Research Center for Interventional Medicine, Shanghai, China, [2] Department of Cardiology, Xiamen Branch, Zhongshan Hospital, Fudan University, Xiamen, China

Background: Although left bundle branch pacing (LBBP) has emerged as a novel physiological pacing strategy with a low and stable threshold, its safety has not been well-documented. In the present study, we included all the patients with procedure-related complications at our centre to estimate these LBBP cases with unique complications.

Methods: We enrolled 612 consecutive patients who received the procedure in Zhongshan Hospital, Fudan University, between January 2018 and July 2020. Regular follow-ups were conducted (at 1, 3, and 6 months in the first year and every 6–12 months from the second year), and the clinical data of the patients with complications were collected and analyzed.

Results: With a mean follow-up period of 12.32 ± 5.21 months, procedure-related complications were observed in 10 patients (1.63%) that included two postoperative septum perforations (2/612, 0.33%), two postoperative lead dislodgements (2/612, 0.33%), four intraoperative septum injuries (4/612, 0.65%), and two intraoperative lead fractures (2/612, 0.33%). Pacing parameters were stable during follow-up, and no major complications were observed after lead repositioning in the cases of septum perforation and lead dislodgement.

Conclusion: The incidence of procedure-related complications for LBBP, namely postoperative septum perforation, postoperative lead dislodgement, intraoperative septum injury, and intraoperative lead fracture, were low. No adverse clinical outcomes were demonstrated after successful repositioning of the lead and appropriate treatment.

Keywords: left bundle branch pacing, His-Purkinje conduction system pacing, procedure-related complications, septal perforation, lead dislodgement, septum injury, lead fracture, safety

OPEN ACCESS

Edited by:
Pietro Mesirca, INSERM U1191 Institut de Génomique Fonctionnelle (IGF), France

Reviewed by:
Richard Hauer, ICIN Netherlands Heart Institute (KNAW), Netherlands
Antonio Sorgente, EpiCURA, Belgium

***Correspondence:**
Yangang Su
yangangsu@yeah.net;
su.yangang@zs-hospital.sh.cn

[†] *These authors have contributed equally to this work*

Specialty section:
This article was submitted to Cardiac Rhythmology, a section of the journal Frontiers in Cardiovascular Medicine

Received: *24 December 2020*
Accepted: *01 March 2021*
Published: *24 March 2021*

Citation:
Chen X, Wei L, Bai J, Wang W, Qin S, Wang J, Liang Y, Su Y and Ge J (2021) Procedure-Related Complications of Left Bundle Branch Pacing: A Single-Center Experience. Front. Cardiovasc. Med. 8:645947. doi: 10.3389/fcvm.2021.645947

INTRODUCTION

Left bundle branch pacing (LBBP) has emerged as a novel physiological pacing strategy with low pacing threshold and high R wave amplitude (1, 2). Several small size observational studies have reported that LBBP offers narrow QRS duration and superior mechanical synchrony (1–5). Moreover, the feasibility and efficacy of LBBP have also been demonstrated in candidates for cardiac resynchronisation therapy with heart failure and left bundle branch block (1, 6, 7). However, as a novel pacing technique, the safety of LBBP has not been well-documented. To capture the left

conduction system, the LBBP lead should be screwed deep enough into the subendomyocardium of the left ventricle (8), which differs from the conventional right ventricular (RV) pacing lead. Consequently, unique procedure-related complications, such as interventricular septum perforation, lead dislodgement, septum injury, and lead fracture, of LBBP are observed. To date, only limited case reports (9, 10) and small observational studies (4, 5, 11) on these complications are available. However, these observations have been limited by indefinite criteria of LBBP, relatively short follow-up, and lack of the specific analysis of the complications. Therefore, in the present study, we attempted to collect and evaluate LBBP cases with unique complications from a consecutive large population in our center.

METHODS

Study Population

The present retrospective single-centre observational study was conducted in all patients with procedure-related complications including septum perforation, lead dislodgement, septum injury and lead fracture from 612 consecutive patients who received LBBP in Zhongshan Hospital, Fudan University, between January 2018 and July 2020. Septum perforation was defined as the lead's tip penetrated the entire interventricular septum into the left ventricular cavity. While septum injury was defined as contrast agent retention during angiography through the delivery sheath. All the patients were discharged 1–2 days after the procedure in case of no evidence of complications, and they were asked to follow-up at 1, 3, and 6 months in the first year and every 6–12 months from the second year after the procedure for the assessment of device function and complications. Medical history, pacing parameters, 12-lead paced electrocardiogram, and fluoroscopic images of the patients with complications were recorded and analyzed. Written informed consent was obtained from all the enrolled participants, and the study was approved by the Institutional Review Board of Zhongshan Hospital, Fudan University, Shanghai, China.

Implantation Procedure of LBBP

The LBBP was performed according to the procedure described in literature (1, 2, 11). The pacing lead (Model 3830 69-cm, Medtronic, Minneapolis, USA) and C315 His sheath were used to map the potential of the His bundle by connecting the lead to an electrophysiology (EP) recording system (GE CardioLab EP Recording System 2000 GE Inc. Wisconsin, USA). Then the lead was placed 1–2 cm distal the His bundle location and in the direction of the RV apex under the fluoroscopic image of the right anterior oblique (RAO) 30 degree. The lead was screwed deeply into the interventricular septum until the paced QRS complex changed from an LBBB to a RBBB morphology. LBB capture was confirmed using RBBB paced morphology and one of the following signs: (1) selective LBBP (SLBBP) (paced morphology as a typical RBBB shape with a discrete component in intracardiac electrogram); (2) stimulus to left ventricular activation time (Sti-LVAT) shortening abruptly by >10 ms with increasing output or remaining shortest and constant at the final site (2, 12–14). When LBB capture threshold was lower than the local myocardium capture threshold, SLBBP could be achieved at low output while nonselective LBBP (NSLBBP) at high output (**Figures 1A,B**). On the contrary, when LBB capture threshold was higher than that of the myocardium, abrupt shortening of Sti-LVAT by >10 ms could be achieved by increasing output at the same site with left ventricular septum pacing (LVSP) at low output and NSLBBP at high output (**Figures 2A,B**). The LBB capture threshold ≤1.5 V/0.5 ms was recognized as acceptable (12).

Statistical Methods

Continuous variables were reported as means ± standard deviation (SD) and compared by Student's *t*-test. Categorical variables were expressed as percentages and compared by using Pearson's $\chi 2$ test. *P*-values < 0.05 was considered statistically significant. All analyses were done by SPSS version 17 (SPSS Inc., Chicago, IL, USA).

RESULTS

Of the 612 patients who received LBBP at our center, with a mean follow-up of 12.32 ± 5.21 months, procedure-related complications were observed in 10 patients (1.63%); the complications included two postoperative septum perforations (2/612, 0.33%), two postoperative lead dislodgements (2/612, 0.33%), four intraoperative septum injuries (4/612, 0.65%), and two intraoperative lead fractures (2/612, 0.33%). The characteristics at baseline between the LBBP cases with and without complications were not significantly different **(Table 1)**. During the procedure, there was no significant difference concerning the percentage of SLBBP in cases with and without complications (80.00 vs. 71.43%, $P = 0.733$) **(Table 1)**. After lead repositioning in cases of postoperative septum perforation and lead dislodgement, pacing parameters were stable during follow-up, and no major complications such as transient ischemic attack or stroke, thrombus, infection, ventricular septal defect, and pericardial effusion were observed.

Postoperative Septum Perforation

Of the 612 patients, two patients with postoperative septum perforation (one at the second day and one at 1 month) were observed (**Table 2**). Details of the cases are described as follows:

Case 1

A 78-year-old male received LBBP due to sick sinus syndrome with paroxysmal atrial fibrillation. Nonselective LBBP (NSLBBP) and selective LBBP (SLBBP) were achieved at different outputs during the procedure, and the LBB potential (Po_{LBB}) was mapped (**Figures 1A–C**). The pacing parameters were normal, and the angiography through the sheath revealed the lead depth inside the septum (**Figure 1E**). At the 1-month postoperative follow-up, the pacing threshold of the LBBP lead increased dramatically (>5.0 V/0.5 ms during unipolar pacing and 2.5 V/0.5 ms during bipolar pacing), and impedance reduced to <300 Ω during unipolar pacing. Computed tomography (CT) imaging and echocardiogram demonstrated LBBP lead perforation into the left ventricular cavity for ∼1.5 cm (**Figure 1**). The lead was repositioned to a more distal LBB area at the posterior septum

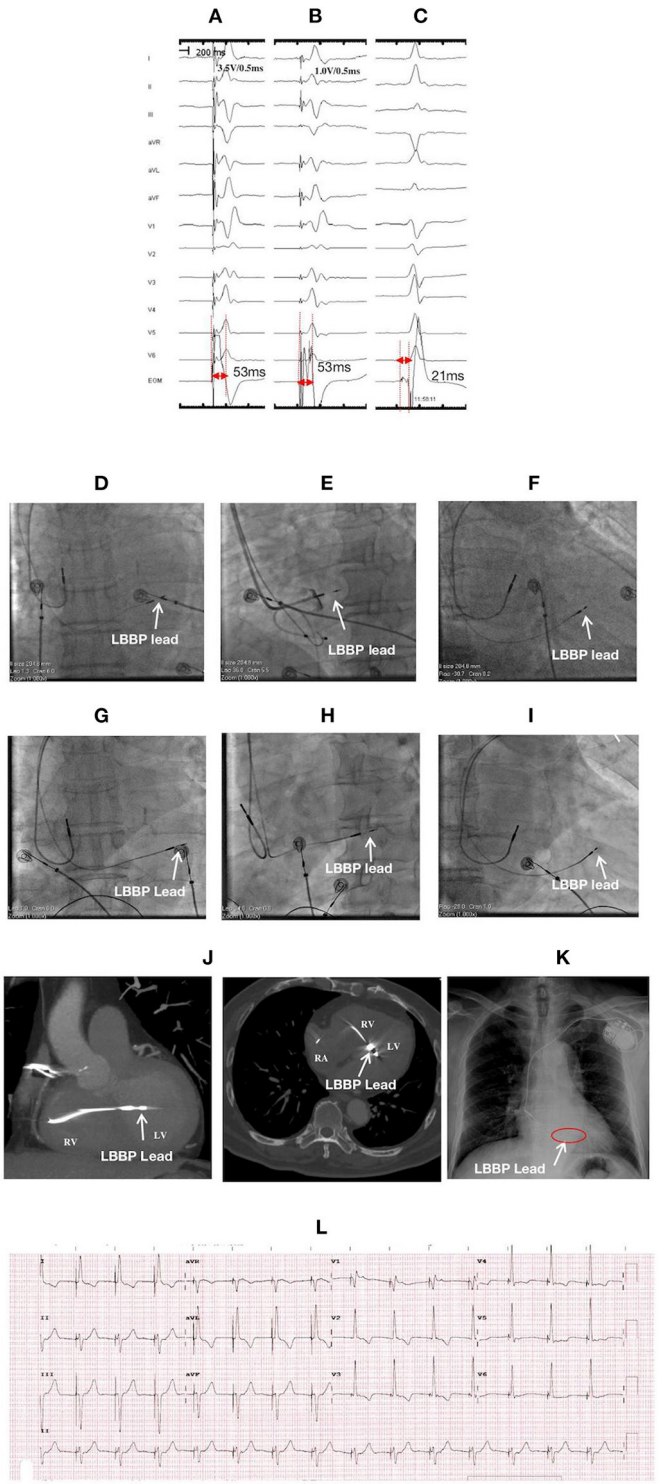

FIGURE 1 | ECGs, EGMs, and fluroscopic images of a 78-year-old male with LBBP lead perforation to the left ventricular (LV) chamber at 1-month postoperative follow-up: During the first procedure: NSLBBP at 3.5 V/0.5 ms **(A)** and SLBBP at 1.0 V/0.5 ms **(B)** with the same Sti-LVAT of 53 ms, **(C)** Po_{LBB} during intrinsic rhythm with a Po_{LBB}-V interval of 21 ms; Fluoroscopic images during the first procedure: **(D)** at PA, **(E)** at LAO 35° with angiography through the sheath exhibiting the LBBP lead depth inside the septum (white arrow), and **(F)** at RAO 30°; Fluoroscopic images before lead reposition: **(G)** at PA; **(H)** at LAO 35°, **(I)** at RAO 30°, and **(J)** CT imaging illustrating the lead perforation to LV chamber for approximately 1.5 cm (white arrow); After lead repositioning: **(K)** X-ray film illustrating lead location and **(L)** ECG. ECG, electrocardiogram; EGM, electrogram; LBBP, left bundle branch pacing; NSLBBP, nonselective left bundle branch pacing; SLBBP, selective left bundle branch pacing; Sti-LVAT, stimulus to left ventricular activivation time; PoLBB, left bundle branch potential; PoLBB-V, left bundle branch potential to ventricle; PA, posteroanterior; LAO, left anterior oblique; RAO, right anterior oblique; CT, Computed Tomography.

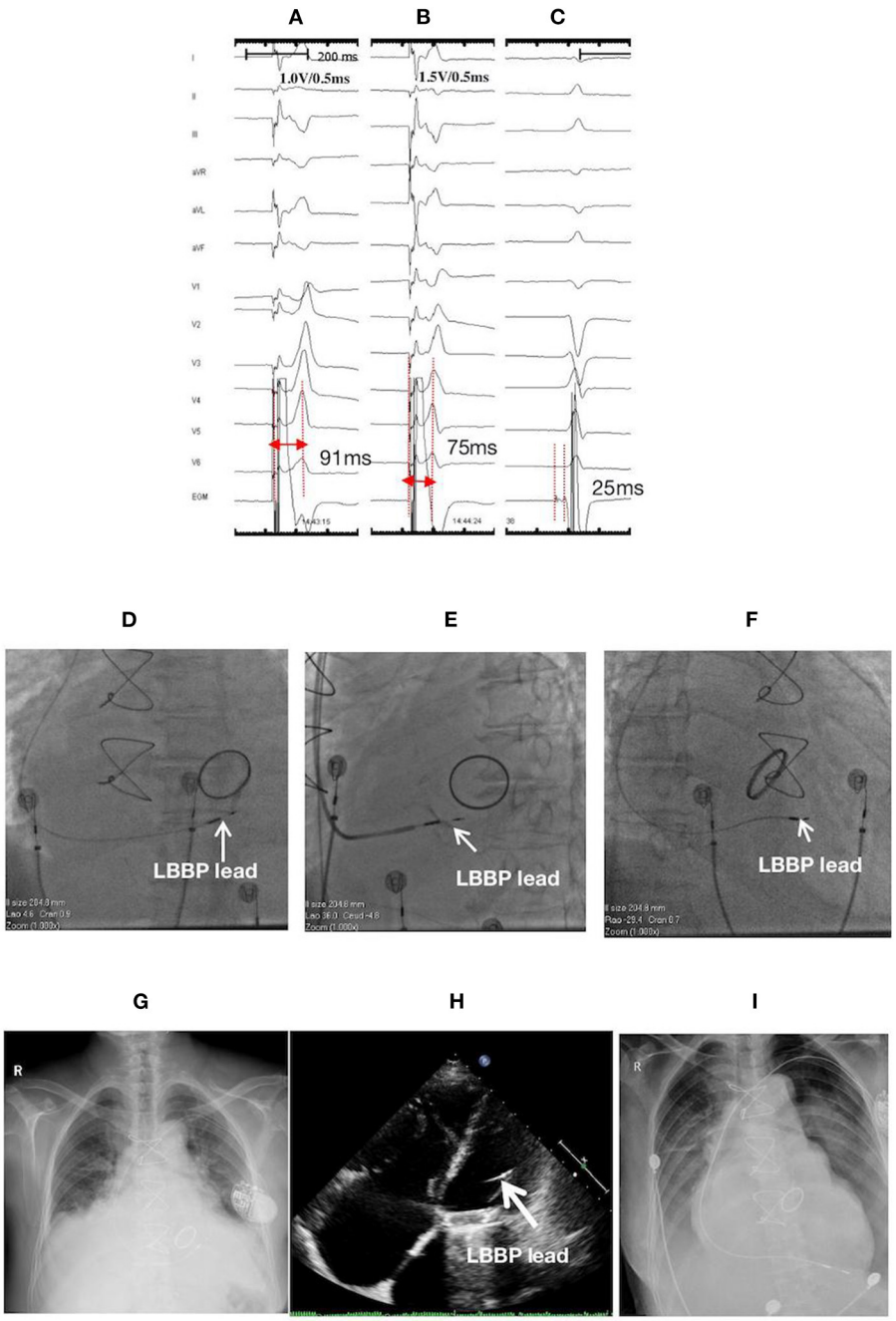

FIGURE 2 | ECGs, EGMs, and fluoroscopic images of a 76-year-old female with LBBP lead perforation to the LV chamber on the second postoperative day: **(A)** LVSP at 1.0 V/0.5 ms with a Sti-LVAT of 91 ms; **(B)** NSLBBP at the same site with abrupt shortening of Sti-LVAT to 75 ms with increasing output (1.5 V/0.5 ms); **(C)** Po_{LBB} during intrinsic rhythm with a Po_{LBB}-V interval of 25 ms; Fluoroscopic images during the first procedure: **(D)** at PA, **(E)** at LAO 35° with angiography through the sheath displaying the LBBP lead depth inside the septum (white arrow), and **(F)** at RAO 30°; At the second postoperative day: **(G)** X-ray film, and **(H)** Echocardiographic image illustrating lead perforation to the LV chamber (white arrow); **(I)** X-ray film after lead reposition to the RV apex. ECG, electrocardiogram; EGM, electrogram; LBBP, left bundle branch pacing; LV, left ventricle; LVSP, left ventricular septum pacing; NSLBBP, nonselective left bundle branch pacing; Sti-LVAT, stimulus to left ventricular activation time; Po_{LBB}, left bundle branch potential; Po_{LBB}-V, left bundle branch potential to ventricle; PA, posteroanterior; LAO, left anterior oblique; RAO, right anterior oblique; RV, right ventricle.

with confirmation of LBB capture and paced QRS with left axis deviation. The pacing parameters were stable at the 1-year follow-up.

Case 2

A 76-year-old female with low body mass index (BMI) (18.02 kg/m^2) and having atrial fibrillation with low ventricular rate and

dilated atrium received LBBP with a single-chamber pacemaker. The screwing of the lead deep inside the septum was challenging in this case probably due to lack of support from the sheath. After multiple attempts, the lead was finally screwed into the LBB area by using the "sheath in sheath" technique (C315 His sheath in CS sheath) (**Figures 2D–F**). The thresholds of the left ventricular septal pacing (LVSP) and nonselective LBBP were 1.0 V/0.5 ms and 1.5 V/0.5 ms, with Sti-LVAT of 91 and 75 ms, respectively (**Figures 2A–C**). Septum perforation was demonstrated through X-ray film, echocardiogram (**Figures 2G,H**), and loss of capture at high output (>7.5 V/0.5 ms) during both unipolar and bipolar pacing at the second postoperative day. The lead was withdrawn, and a new lead (Model 5076, Medtronic, Inc.) was implanted and repositioned at the RV apex (**Figure 2I**).

TABLE 1 | Comparisons between LBBP with and without complications.

	LBBP without complications ($n = 602$)	LBBP with complications ($n = 10$)	*P*-value
Age	70.08 ± 10.21	72.90 ± 6.81	0.385
Female	289 (48.00)	4 (40.00)	0.754
Hypertension	256 (42.53)	5 (50.00)	0.751
Diabetes	72 (11.96)	1 (10.00)	0.346
Atrial fibrillation	92 (15.28)	2 (20.00)	0.656
Pacemaker types			0.062
Single chamber pacemaker, *n* (%)	138 (22.92)	4 (40.00)	
Dual chamber pacemaker, *n* (%)	288 (47.84)	6 (60.00)	
CRT/CRTD	176 (29.23)	0 (0.00)	
Pacemaker indication			0.093
SSS, *n* (%)	116 (19.27)	3 (30.00)	
AVB, *n* (%)	280 (46.51)	6 (60.00)	
Heart failure indicated for CRT/CRTD	176 (29.23)	0 (0.00)	
Atrial fibrillation with low ventricular rate, *n* (%)	30 (4.98)	1 (10.00)	
SLBBP (%)	430 (71.43)	8 (80.00)	0.733

Postoperative Lead Dislodgement

Of the 612 cases who received LBBP, two cases of postoperative lead dislodgement were observed [one at 1 month, and one at 1 month with recurrence of dislodgement 5 months after repositioning (**Table 2**)].

Case 3

A 77-year-old female with complete atrioventricular block (AVB) received LBBP with a dual-chamber pacemaker. The LBBP was confirmed by achieving NSLBBP and SLBBP at different outputs, with a constant Sti-LVAT of 65 ms and recording Po_{LBB} (**Figures 3A–C**). The X-ray film taken before discharge displayed less slack. However, the pacing parameters were stable. Lead dislodgement was confirmed by a high pacing threshold (>7.5 V/0.5 ms) and through X-ray film at the 1-month follow-up (**Figure 3G**). The lead was repositioned to another LBB region with appropriate slack (**Figures 3D,E,H**), and the pacing parameters were stable at the 1-year follow-up.

Case 4

A 64-year-old male with complete AVB and atrial fibrillation received LBBP with a single-chamber pacemaker. The echocardiogram displayed enlargement of the right atrium (78 × 69 mm) and increase in diameter of the basal segment of the right ventricle (49 mm) with severe tricuspid regurgitation. LBBP was finally achieved with optimum pacing parameters after multiple attempts. At 1-month after the procedure, the lead dislodgement to the RV apex was confirmed by a high pacing threshold (>7.5 V/0.5 ms) and through X-ray film (**Figure 4**). The lead was repositioned to another LBB region with superior pacing threshold and R wave amplitude.

TABLE 2 | Septum perforation and lead dislodgement cases.

Case No.	Age	Gender	Diagnosis	Complication	Abnormal pacing parameters	Treatment and outcome
1	78	Male	Sick sinus syndrome with paroxysmal atrial fibrillation	Septum perforation at 1-month follow-up	Threshold: >5.0 V/0.5 ms (unipolar) 2.5 V/0.5 ms (bipolar) Impedance: <300 Ω (unipolar)	The lead was repositioned to a more distal LBB area at posterior septum
2	76	Female	Atrial fibrillation with low ventricular rate	Septum perforation at the second day post-procedure	loss of capture at the high output (>7.5 V/0.5 ms)	A new lead (Model 5076) was implanted and replaced at RV apex
3	77	Female	Complete AVB	Lead dislodgement	loss of capture at the high output (>7.5 V/0.5 ms)	The lead was replaced to another LBB region with proper slack
4	64	Male	Complete AVB and atrial fibrillation	Lead dislodgement at 1-month follow-up and the lead dislodgement occurred again at 5-month after reposition.	loss of capture at the high output (>7.5 V/0.5 ms)	The lead was replaced to another LBB region but dislodged again Finally another lead (Model 5076) was repositioned at RV septum

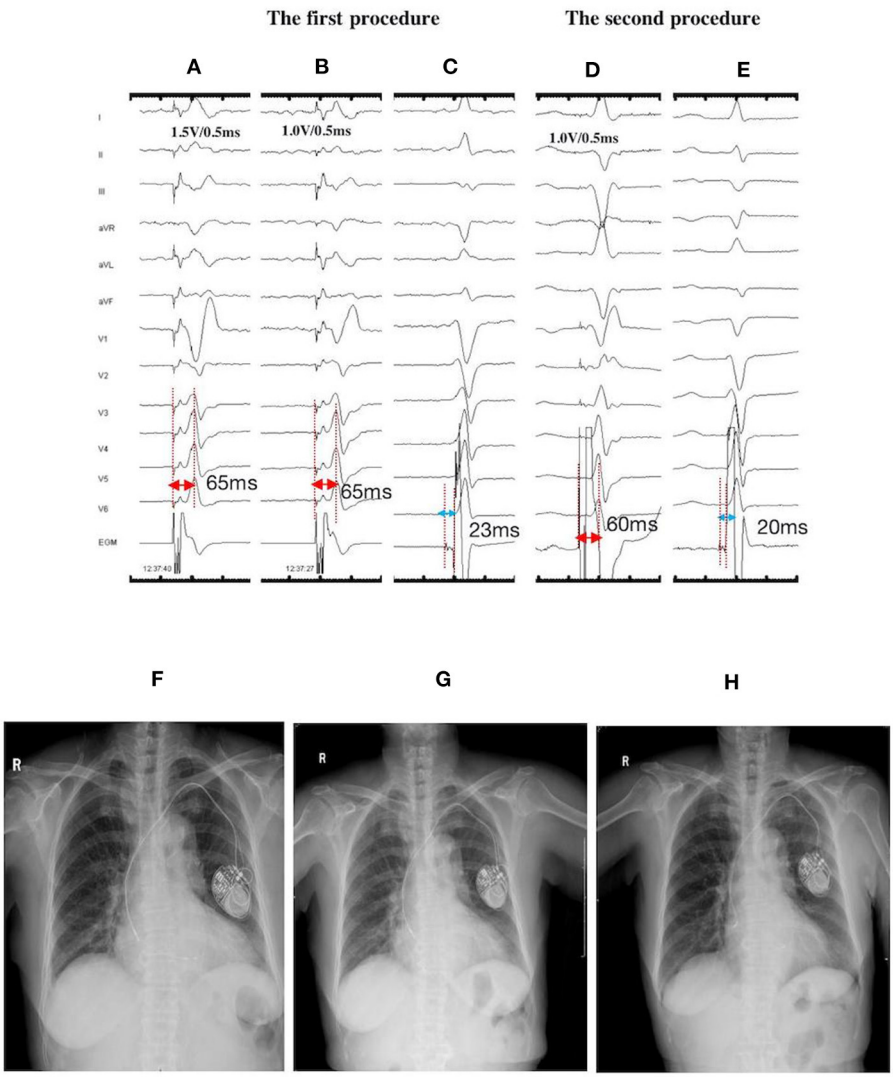

FIGURE 3 | ECGs, EGMs, and fluoroscopic images of a 77-year-old female with LBBP lead dislodgement at the 1-month postoperative follow-up: During the first procedure: NSLBBP at 1.5 V/0.5 ms **(A)** and SLBBP at 1.0 V/0.5 ms **(B)** with the same Sti-LVAT of 65 ms; **(C)** Po_{LBB} during intrinsic rhythm with the Po_{LBB}-V interval of 23 ms; During the second procedure: **(D)** NSLBBP at 1.0 V/0.5 ms, with the Sti-LVAT of 60 ms; **(E)** Po_{LBB} during intrinsic rhythm, with the PoLBB-V interval of 20 ms; X-ray films illustrating lead locations: **(F)** on the second day after the first procedure, **(G)** at the 1-month follow-up exhibiting lead dislodgement, and **(H)** on the second day after lead repositioning. ECG, electrocardiogram; EGM, electrogram; LBBP, left bundle branch pacing; NSLBBP, nonselective left bundle branch pacing; SLBBP, selective left bundle branch pacing; Sti-LVAT, stimulus to left ventricular activivation time; Po_{LBB}, left bundle branch potential; Po_{LBB}-V, left bundle branch potential to ventricle.

However, the pacing impedance was relatively low (∼300–400 Ω). Pacing parameters remained stable until 2-months after the procedure. Lead dislodgement recurred 5 months after repositioning. The lead was withdrawn, and another lead (Model 5076, Medtronic Inc., Minneapolis, MN, USA) was repositioned at the RV septum. The pacing parameters remained stable afterwards.

Intraoperative Septum Injury

Of the 612 cases, four cases of intraoperative ventricular septum injury were identified **(Figure 5)**. Approximately 5 mL of contrast agent was injected through the delivery sheath (C315 His; Medtronic Inc., Minneapolis, MN, USA) and placed close to the right side of the interventricular septum to determine the exact depth of the lead inside the septum after the lead was confirmed to have achieved LBBP. High pressure was determined during the contrast injection in these four cases, and the contrast agent retention was recorded to detect intraoperative septum injury. The patients did not complain of any symptoms such as chest pain and shortness of breath, and the electrocardiogram did not exhibit ST-segment elevation or depression in any leads. Pacing parameters were measured several times and were found to be stable after contrast injection. No obvious septal abnormalities were observed in the echocardiogram of the four cases during

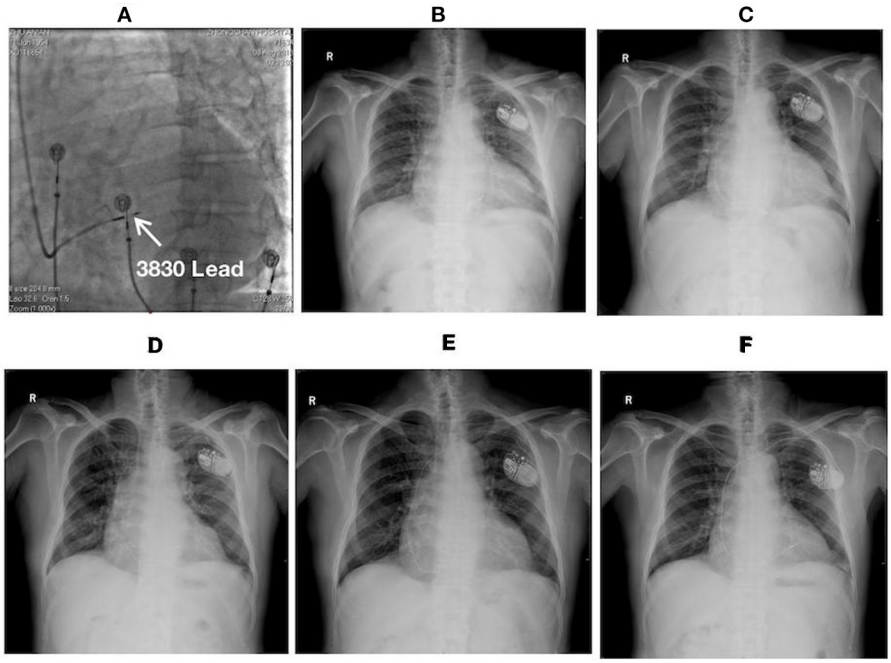

FIGURE 4 | Fluoroscopic images of a 64-year-old male with LBBP lead dislodgement: **(A)** The fluoroscopic image at LAO 30° during the procedure illustrating the lead depth inside the septum (white arrow); **(B)** Postoperative X-ray film; **(C)** X-ray film at the 1-month postoperative follow-up illustrating lead dislodgement; **(D)** X-ray film after lead reposition; **(E)** X-ray film at 5 months after lead reposition demonstrating the recurrence of lead dislodgement; **(F)** X-ray film on the 2nd day after the 2nd lead repositioning demonstrating the repositioning of a new lead (Model 5076, Medtronic Inc., Minneapolis, MN, USA) at the RV septum. LAO, left anterior oblique.

procedure. LBBP leads of all four cases were not repositioned afterwards. Cardiac troponin T (CTNT) levels on the second postoperative day were found to be mildly elevated compared with the preoperative levels (**Table 3**). During the follow-up, no evidence of myocardial infarction, septum perforation, and lead dislodgement was identified, and pacing parameters remained acceptable and stable (**Table 3**).

Lead Fracture

Of the 612 cases, two cases of LBBP lead (model 3830, 69 cm; Medtronic, Inc.) fracture were identified during the procedure when it was hard to advance the leads. After multiple attempts, the leads were withdrawn, and disconnection between the lead body and end of the ring was demonstrated (**Figure 6**). The lead was subsequently abandoned, and new leads were implanted to another site to achieve LBBP. **Figure 6** represent the image of lead fracture between the lead body and the end of the ring.

DISCUSSION

LBBP is an emerging alternative physiological technique to His bundle pacing. Although the definitions and characteristics of this procedure have been established and its short-term safety profile has been demonstrated, the long-term safety remains unknown. In the present study, we demonstrated the possible procedure-related LBBP complications, including ventricular septum perforation (two cases), lead dislodgement (two cases), septum injury (four cases), and lead fracture (two cases) in a relatively large population during a mean follow-up of 12.32 ±5.21 months.

Lead Dislodgement and Septum Perforation

Of the 530 published cases in literature, 6 (1.1%) lead dislodgements (one intraoperative, three within 24 h, one at 2 months, and one at 4 months) and 9 (1.7%) septal perforations (eight intraoperative and one at 1 month) have been identified (4, 5, 15–17). In the present study, two cases of lead dislodgement were identified by the high threshold, low impedance, and X-ray film at the 1-month follow-up. One of these two cases received LBBP lead replacement to a more distal LBB site, and the pacing parameters were stable during follow-up. LBB is a wide network beneath the endomyocardium of the left septum (18). Thus, positioning of the lead at this area could easily capture the left conduction system (8). In case of lead dislodgement and perforation, repositioning of the lead to a distal LBB area could probably prevent the recurrence of these complications because the original area might be injured by the lead, and the fixation of lead in posterior septum through the C315 His sheath is simple. Similar to the conventional RV lead, the risk of myocardial perforation would be high for an older woman with low BMI (19). In case 2, the large atrium might have lead to heart transposition, which causes difficulties in screwing the lead into the septum. Multiple attempts might cause injury to the septum and increase the

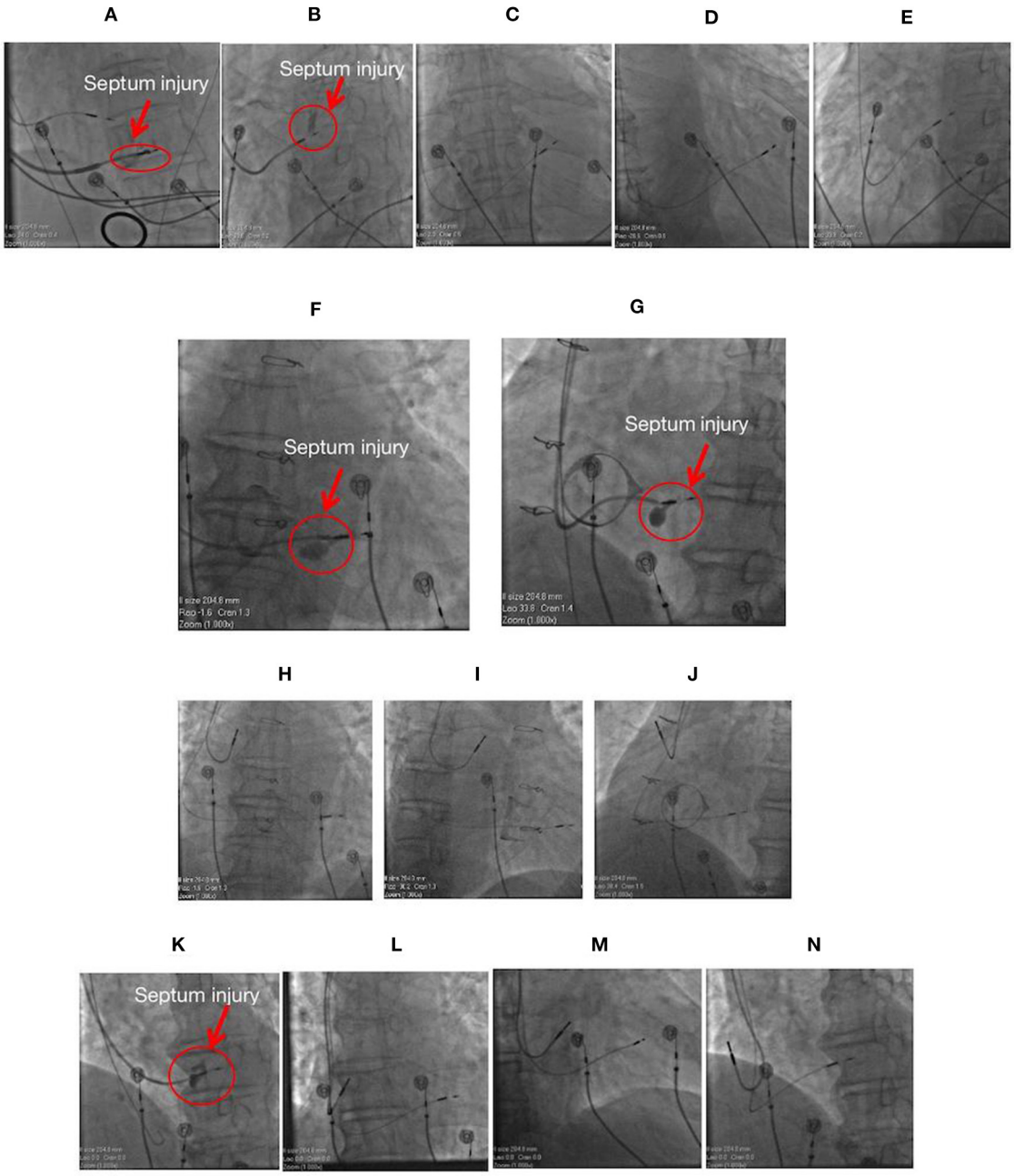

FIGURE 5 | Images of four cases with septum injury during the procedure. **(A)** The fluoroscopic image of a 71-year-old female having mitral regurgitation and sick sinus syndrome with ventricular septum injury (red arrow) during LBBP lead implantation at LAO 35°. **(B)** The fluoroscopic image of a 77-year-old male with atrial fibrillation and complete AVB with septum injury (red arrow) during LBBP lead implantation with a single-chamber pacemaker at LAO 35°. The lead was not repositioned, and its location is illustrated at PA **(C)**, RAO30° **(D)**, and LAO 35° **(E)**. Fluoroscopic images of a 64-year-old male with sick sinus syndrome post-bioprosthetic tricuspid valve replacement having septum injury (red arrow) during LBBP lead implantation with a dual-chamber pacemaker at PA **(F)** and LAO 35° **(G)**. The lead was not repositioned, and its location is illustrated at PA **(H)**, RAO30° **(I)**, and LAO 35° **(J)**. **(K)** The fluoroscopic image of an 85-year-old male with complete AVB and atrial fibrillation having septum injury (red arrow) during LBBP lead implantation with a dual-chamber pacemaker at LAO 35°. The lead was not repositioned, and its location is illustrated at PA **(L)**, RAO30° **(M)**, and LAO 35° **(N)**. LBBP, left bundle branch pacing; AVB, atrioventricular block; PA, posteroanterior; LAO, left anterior oblique; RAO, right anterior oblique.

risk of perforation. Additionally, heart contraction is an axial twisting movement (20). The torsion between the large atrium and septum might result in perforation after removal of the sheath. This might be a possible explanation for the recurrence of lead dislodgement after lead repositioning to another LBB area. The lead dislodgement in case 3 might be attributed to less slack

TABLE 3 | Characteristics of four cases with septum injury during procedure.

Case No.	Age	Gender	Diagnosis	CTNT level (ng/ml) post-procedure	CTNT level (ng/ml) at 2rd day post-procedure	Pacing parameters (unipolar) during procedure	Pacing parameters (unipolar) during follow-up
1	71	Female	Sick sinus syndrome	0.084	0.143	Threshold: 1.0 V/0.5 ms R wave amplitude: 10 mV Impedance: 510 Ω	Threshold: 0.75 V/0.5 ms R wave amplitude: 12 mV Impedance: 436 Ω (at 18-month follow-up)
2	77	Male	Atrial fibrillation with AVB	0.015	0.05	Threshold: 0.8 V/0.5 ms R wave amplitude: 15 mV Impedance: 620 Ω	Threshold: 0.5 V/0.5 ms R wave amplitude: 14 mV Impedance: 490 Ω (at 18-month follow-up)
3	66	Male	Sick sinus syndrome	0.01	0.07	Threshold: 0.5 V/0.5 ms R wave amplitude: 17 mV Impedance: 464 Ω	Threshold: 0.5 V/0.5 ms R wave amplitude: 15 mV Impedance: 386 Ω (at 24-month follow-up)
4	85	Male	Atrial fibrillation with AVB	0.065	0.074	Threshold: 0.8 V/0.5 ms R wave amplitude: 5 mV Impedance: 680 Ω	Threshold: 0.75 V/0.5 ms R wave amplitude: 8 mV Impedance: 512 Ω (at 12-month follow-up)

(Figure 3F). Proper slack is crucial to acute and chronic lead dislodgement and perforation.

Septum Injury

Multiple attempts at positioning the lead inside the septum and the procedure of the contrast injection itself might be the possible causes of septum injury, and these were the probable reason of septum injury of the four cases in the present study. During the contrast injection, the sheath should be pulled slightly backwards from the right septum to avoid septum injury due to the sheath or pressure of contrast injection. Under this circumstance, the repositioning of lead to another site might not be required, if the pacing parameters remain stable and no evidence of myocardial ischaemia is observed.

Lead Fracture

The LBBP lead must be screwed deep enough into the subendomyocardium of the left septum. VJ et al. reported that the average lead depth inside the septum is 1.4 ± 0.23 cm (5), whereas the helix length of the lead is only 1.8 mm, which is designed for conventional RV pacing. To reach the desired LBB area, the lead needs to be screwed at least 10 turns, which is much more than that recommended by the manufacturer (4–6 turns). Thus, the possibility of lead fracture would be higher than than that with conventional RV pacing. We observed two cases of intraoperative lead fracture and successfully performed LBBP with another new lead. Lead check should be considered, if screwing of the lead during the procedure becomes difficult. Long-term lead performance of LBBP has not been demonstrated yet. Thus, to identify chronic lead fracture during follow-up, a more frequent lead check than the conventional RV pacing in LBBP is recommended.

Although LBBP complications may occur intraoperatively or postoperatively, the incidence is slightly low in the present study (1.63%). No adverse clinical outcomes were demonstrated with these complications after appropriate treatment. However, due to lack of long-term follow-up, the complications should be carefully detected both intraoperatively and postoperatively. Evaluation of the preoperative septal thickness and characteristics, minimization of multiple attempts in the same region, adequate lead slack, and frequent follow-ups could be helpful in avoiding complications. Postoperative follow-up, particularly more frequent monitoring, could also help in promptly detecting possible complications and administering clinical interventions as early as possible to avoid adverse outcomes.

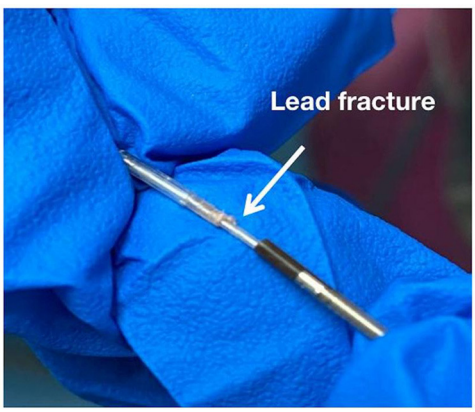

FIGURE 6 | Image of lead fracture between the lead body and the end of the ring.

Limitation

The present study was a retrospective observational study performed at a single centre with a short- to mid-term follow-up. The follow-up period was not sufficiently long to draw a conclusion on the long-term safety of LBBP. Lead performance during long-term follow-up is unknown at present. Moreover, operator experience might influence the incidence of complications. Consequently, long-term, multi-centre, case–control, and randomized trials are required to confirm the safety of LBBP relative to the conventional ventricular pacing.

CONCLUSION

The incidence of procedure-related LBBP complications including postoperative septum perforation, postoperative lead dislodgement, intraoperative septum injury, and intraoperative lead fracture was low. Additionally, no adverse clinical outcomes of these complications were observed after successful repositioning of leads and appropriate treatment.

DATA AVAILABILITY STATEMENT

The datasets generated during and analyzed during the current study are available from the corresponding author on reasonable request.

ETHICS STATEMENT

This study is a retrospective single-center study. Written informed consent was obtained from the individual(s) to publish any potentially identifiable images or data included in this article. All patients signed informed consent to participate in the study.

AUTHOR CONTRIBUTIONS

XC, YS, and JG designed the research. XC, JB, WW, JW, SQ, and YL performed operations on the above-mentioned patients. XC and LW collected and analyzed data and wrote the papers. All authors contributed to the article and approved the submitted version.

FUNDING

The research was funded by the Clinical Research Plan of Shanghai Hospital Development Center (SHDC) (No. SHDC2020CR4003).

ACKNOWLEDGMENTS

The authors would like to thank Dr. Weijian Huang (the First Affiliated Hospital of Wenzhou Medical University) for his technical assistance in the LBBP procedure.

REFERENCES

1. Huang W, Su L, Wu S, Xu L, Xiao F, Zhou X, et al. A novel pacing strategy with low and stable output: pacing the left bundle branch immediately beyond the conduction block. *Can J Cardiol.* (2017) 33:1736.e1–1736.e3. doi: 10.1016/j.cjca.2017.09.013
2. Chen X, Wu S, Su L, Su Y, Huang W. The characteristics of the electrocardiogram and the intracardiac electrogram in left bundle branch pacing. *J Cardiovasc Electrophysiol.* (2019) 30:1096–101. doi: 10.1111/jce.13956
3. Cai B, Huang X, Li L, Guo J, Chen S, Meng F, et al. Evaluation of cardiac synchrony in left bundle branch pacing: insights from echocardiographic research. *J Cardiovasc Electrophysiol.* (2020) 31:560–9. doi: 10.1111/jce.14342
4. Hou X, Qian Z, Wang Y, Qiu Y, Chen X, Jiang H, et al. Feasibility and cardiac synchrony of permanent left bundle branch pacing through the interventricular septum. *Europace.* (2019) 21:1694–702. doi: 10.1093/europace/euz188
5. Vijayaraman P, Subzposh FA, Naperkowski A, Panikkath R, John K, Mascarenhas V, et al. Prospective evaluation of feasibility and electrophysiologic and echocardiographic characteristics of left bundle branch area pacing. *Heart Rhythm.* (2019) 16:1774–82. doi: 10.1016/j.hrthm.2019.05.011
6. Huang W, Wu S, Vijayaraman P, Su L, Chen X, Cai B, et al. Cardiac resynchronization therapy in patients with nonischemic cardiomyopathy using left bundle branch pacing. *JACC Clin Electrophysiol.* (2020) 6:849–58. doi: 10.1016/j.jacep.2020.04.011
7. Wu S, Su L, Vijayaraman P, Zheng R, Cai M, Xu L, et al. Left bundle branch pacing for cardiac resynchronization therapy: nonrandomized on-treatment comparison with his bundle pacing and biventricular pacing. *Can J Cardiol.* (2020) 37:319–28. doi: 10.1016/j.cjca.2020.04.037
8. Chen X, Jin Q, Li B, Jia J, Sharma PS, Huang W, et al. Electrophysiological parameters and anatomical evaluation of left bundle branch pacing in an in vivo canine model. *J Cardiovasc Electrophysiol.* (2020) 31:214–9. doi: 10.1111/jce.14300
9. Qi P, Li XX, Tian Y, Shi L, Wang YJ, Liu XP. Injection of contrast medium through a delivery sheath reveals interventricular septal vascular injury in a case of left bundle branch pacing. *J Int Med Res.* (2020) 48:300060520947880. doi: 10.1177/0300060520947880
10. Ponnusamy SS, Vijayaraman P. Aborted ST elevation myocardial infarction – an unusual complication of left bundle branch pacing. *HeartRhythm Case Rep.* (2020) 6:520–22. doi: 10.1016/j.hrcr.2020.05.010
11. Padala S, Ellenbogen K. Left bundle branch pacing is the best approach to physiological pacing. *Heart Rhythm.* (2020) 1:59–67. doi: 10.1016/j.hroo.2020.03.002
12. Huang W, Chen X, Su L, Wu S, Xia X, Vijayaraman P. A beginner's guide to permanent left bundle branch pacing. *Heart Rhythm.* (2019) 16:1791–6. doi: 10.1016/j.hrthm.2019.06.016
13. Su L, Wang S, Wu S, Xu L, Huang Z, Chen X, et al. Long-term safety and feasibility of left bundle branch pacing in a large single center study. *Circ Arrhythm Electrophysiol.* (2021) 14:e009261. doi: 10.1161/CIRCEP.120.009261
14. Xueying C, Qinchun J, Jin B, Wang W, Qin S, Wang J, et al. The feasibility and safety of left bundle branch pacing vs. right ventricular pacing after mid-long-term follow-up: a single-centre experience. *EP Europace.* (2020) 22(Suppl.2):36–44. doi: 10.1093/europace/euaa294
15. Jiang Z, Chang Q, Wu Y, Ji L, Zhou X, Shan Q. Typical BBB morphology and implantation depth of 3830 electrode predict QRS correction by left bundle branch area pacing. *Pacing Clin Electrophysiol.* (2020) 43:110–7. doi: 10.1111/pace.13849
16. Wang J, Liang Y, Wang W, Chen X, Bai J, Chen H, et al. Left bundle branch area pacing is superior to right ventricular septum pacing concerning depolarization-repolarization reserve. *J Cardiovasc Electrophysiol.* (2020) 31:313–22. doi: 10.1111/jce.14295
17. Li X, Li H, Ma W, Ning X, Liang E, Pang K, et al. Permanent left bundle branch area pacing for atrioventricular block: feasibility, safety, and acute effect. *Heart Rhythm.* (2019) 16:1766–73. doi: 10.1016/j.hrthm.2019.04.043
18. Sedmera, D, Gourdie RG. Why do we have purkinje fibers deep in our heart? *Physiol Res.* (2014) 63:S9–18. doi: 10.33549/physiolres.932686
19. Mahapatra S, Bybee KA, Bunch TJ, Espinosa RE, Sinak LJ, McGoon MD, et al. Incidence and predictors of cardiac perforation after permanent pacemaker placement. *Heart Rhythm.* (2005) 2:907–11. doi: 10.1016/j.hrthm.2005.06.011

20. Hoeland K, Kloppe A, Hexamer M, Nowack G, Werner J. New sensor based on fibre optics for measurement of heart movement. *Med Biol Eng Comput*. (2002) 40:571–5. doi: 10.1007/BF02345457

Conflict of Interest: The authors declare that the research was conducted in the absence of any commercial or financial relationships that could be construed as a potential conflict of interest.

frontiers in Cardiovascular Medicine

CLINICAL TRIAL
published: 04 May 2021
doi: 10.3389/fcvm.2021.681890

Handheld ECG Tracking of in-hOspital Atrial Fibrillation (HECTO-AF): A Randomized Controlled Trial

Marco Mancinetti[1†], *Sara Schukraft*[2*†], *Yannick Faucherre*[2], *Stéphane Cook*[2], *Diego Arroyo*[2‡] *and Serban Puricel*[2‡]

[1] Department of General Internal Medicine, University and Hospital Fribourg, Fribourg, Switzerland, [2] Department of Cardiology, University and Hospital Fribourg, Fribourg, Switzerland

Background: Atrial fibrillation (AF) is frequent and causes substantial morbidity through AF-related strokes. Given the increasing prevalence of AF, screening methods are of interest given the potential to initiate timely appropriate anticoagulation.

Aims: The HECTO-AF trial aims to determine the efficacy of AF screening with a single-lead electrocardiogram (ECG) handheld device in naïve in-hospital patients.

Methods: The HECTO-AF is a single-center, open label, randomized controlled trial. Patients admitted to the general internal medicine ward of the University and Hospital Fribourg without previous diagnosis of AF were invited to participate in a screening program with a 1:1 allocation to either the screening group with intermittent single-lead handheld ECG recordings vs. a control group undergoing detection of AF as per routine clinical practice. The primary outcome was the prevalence of newly diagnosed AF during the hospital stay. Enrolment was terminated for poor patient recruitment and apparent futility before a sufficient sample for powered efficacy comparisons was enrolled.

Results: A total of 804 patients were included of whom 381 were allocated to the intervention and 423 to the control group. Mean age was 65 ± 16 and 464 (58%) were male. Median CHA_2DS_2-VASc score was 3 (13% heart failure, 57% hypertension, 19% diabetes mellitus, 14% prior stroke/transient ischemic attack, and 29% arterial disease) and all CHA_2DS_2-VASc risk factors were equally distributed between groups. The incidence of newly detected AF was 1.4% over a median of 6 hospitalized days. Seven patients (1.8%) were diagnosed with AF in the intervention group vs. 3 (0.7%) in the control group ($p = 0.20$).

Conclusion: There was a trend toward a higher AF detection over a median of 6 hospitalized days in the intervention group, but a definitive conclusion cannot be drawn due to the early termination of the present study. Systematic screening for AF in the hospital setting is resource-consuming, and of uncertain clinical benefit. The interpretation of single-lead handheld ECG is challenging and may result in inaccurate AF diagnosis.

Clinical Trial Registration: ClinicalTrials.gov, identifier [NCT03197090].

Keywords: atrial fibrillation, ECG handheld device, prevention, screening, stroke

OPEN ACCESS

Edited by:
Marina Cerrone,
New York University, United States

Reviewed by:
Silvia Magnani,
New York University, United States
Jacqueline Joza,
McGill University Health Centre, Canada

****Correspondence:***
Sara Schukraft
sara.schukraft@yahoo.com

[†]These authors share co-first authorship

[‡]These authors share co-senior authorship

Specialty section:
This article was submitted to Cardiac Rhythmology, a section of the journal Frontiers in Cardiovascular Medicine

Received: *17 March 2021*
Accepted: *12 April 2021*
Published: *04 May 2021*

Citation:
Mancinetti M, Schukraft S, Faucherre Y, Cook S, Arroyo D and Puricel S (2021) Handheld ECG Tracking of in-hOspital Atrial Fibrillation (HECTO-AF): A Randomized Controlled Trial. Front. Cardiovasc. Med. 8:681890. doi: 10.3389/fcvm.2021.681890

INTRODUCTION

Atrial fibrillation (AF) affects over 5 million people in Europe, with projected estimates up to 14 million by 2060 making it the most common arrhythmia (1). AF patients have a two-fold increase in mortality and a five-fold increase in risk of stroke compared with the general population (2). It is estimated that one third of AF patients will be hospitalized at least once a year due to worsening heart failure or cardioembolic events (3). Asymptomatic or "silent" AF is present in close to 33% of patients and conveys a risk of stroke identical to symptomatic patients (2). There is evidence that even short episodes of silent AF (of at least 6 min) have an increased thromboembolic risk (4).

The 2016 European Society of Cardiology (ESC) guidelines encourage opportunistic AF screening programs in at-risk populations by pulse palpation (5). To date there is insufficient evidence for a systematic screening strategy (6). However, a number of randomized controlled trials have investigated the effectiveness of routine screening for AF in outpatients using different devices. Among them, is the Zenicor single-lead electrocardiogram (ECG) recording device which appropriately detects AF with a sensitivity of 96%, and a specificity of 92% (7). Data on AF screening strategies and clinical benefit in hospitalized patients are lacking.

HECTO-AF is the first study to assess the effectiveness of systematic screening for silent-AF using a single-lead ECG handheld device vs. routine clinical practice in patients hospitalized in the general internal medicine ward.

METHODS

In this single center, open label, randomized controlled trial, we randomly assigned patients in a 1:1 ratio to a systematic screening strategy using the Zenicor (Medical Systems AB) single-lead handheld ECG recording device vs. a control group with standard clinical care. The study methods and design have been published previously (8). The study was conducted in accordance with the Declaration of Helsinki and was approved by the regional ethics committee (ClinicalTrials.gov, ID: NCT03197090, first registration on 23/06/2017). All patients provided written, informed consent for participation.

All patients 18 years or older admitted to the general internal medicine ward were eligible. Patients with known or previously documented AF, patients with cardiac pacemakers or implantable cardioverter-defibrillators, length of stay <48 h, life expectancy <6 months, and those unable to provide written-informed consent, were excluded (**Figure 1**).

Randomization was performed as soon as written consent was provided, using a computer-generated allocation sequence (www.randomizer.org) and concealment until assignment. Research nurses generated the random allocation sequence, enrolled participants and assigned the patients to the study groups according to the previously generated randomization sequence. There was no blinding.

ECG Recording

Patients included in the Zenicor group were instructed to use the handheld ECG recorder for intermittent ECG recordings during the hospitalization period. Recordings were planned twice daily under supervision of specially trained nurses. Patients had to apply their thumbs over the captors of the device during 30-s to yield a single-lead ECG recording which was stored, and subsequently transmitted to a central server for analysis. In the control group, 12-lead ECG were performed and interpreted by the treating physicians as per standard clinical care (i.e., in case of palpitations, chest pain, suspicion of arrhythmia during physical examination).

ECG Analysis

All single-lead ECGs were stored in a web-based interface analysis system (Zenicor-ECG Doctor System) and independently reviewed on the same day by the investigators to assess the presence of AF (**Figure 2**). A 12-lead ECG was performed in all cases of suspected AF in the Zenicor group. Additional recordings, including 24–48 h Holter monitoring or 7-day R-Test were performed in case of uncertainty. Finally, two cardiologists reviewed every case of suspected new AF.

Outcomes

The primary outcome was the incidence of new-onset AF defined as a 30-s recording of irregular rhythm without p waves (5). Each patient with newly diagnosed AF was treated according to the 2016 ESC guidelines on the management of atrial fibrillation (i.e., regarding anticoagulation, rhythm, and/or rate control therapy). Additional workup including 12-lead ECG, laboratory investigations, and further cardiological workup such as echocardiography, were organized as per guidelines.

Statistics

We calculated that a total of 1,600 patients would yield a power of 80% to detect superiority with an estimated event rate of 3% in the Zenicor group and 1% in the control group, allowing a 9% loss to follow-up. The trial was interrupted at interim analysis after 50% of patients were enrolled ($n = 804$), due to poor patient recruitment and limited resources. The premature interruption of the trial was responsible for patient number differences between groups. The inclusion of 804 patients yields a power of 53% for the presumed event rate of 3 and 1%, respectively. Because of the potential for type I error due to incomplete patient enrollment, the reported analyses should be interpreted as exploratory.

Categorical variables are reported as counts and percentages; continuous variables are reported as means and SD. Normality was assessed by visual inspection of histograms and computation of Q-Q plots. Continuous variables were analyzed using the Student *t*-test or the Wilcoxon rank-sum test according to their distribution. Categorical variables were compared using chi-square or Fisher exact test as appropriate. All statistical analyses

Abbreviations: AF, atrial fibrillation; ECG, electrocardiogram; FUP, follow-up; HECTO-AF, Handheld ECG Tracking of in-hOspital Atrial Fibrillation; IQR, interquartile range; NSAID, nonsteroidal anti-inflammatory drug; OAC, oral anticoagulation; SD, standard deviation; TIA, transient ischemic attack.

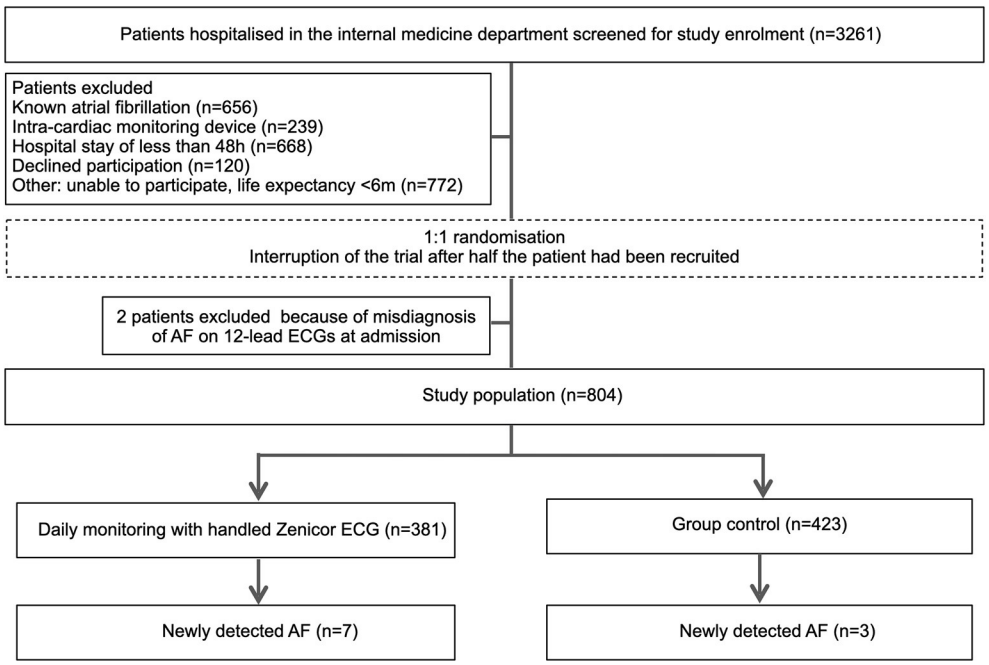

FIGURE 1 | Study flowchart. Participants are 1:1 randomized to either handheld single-lead ECG (Zenicor) screening or control group.

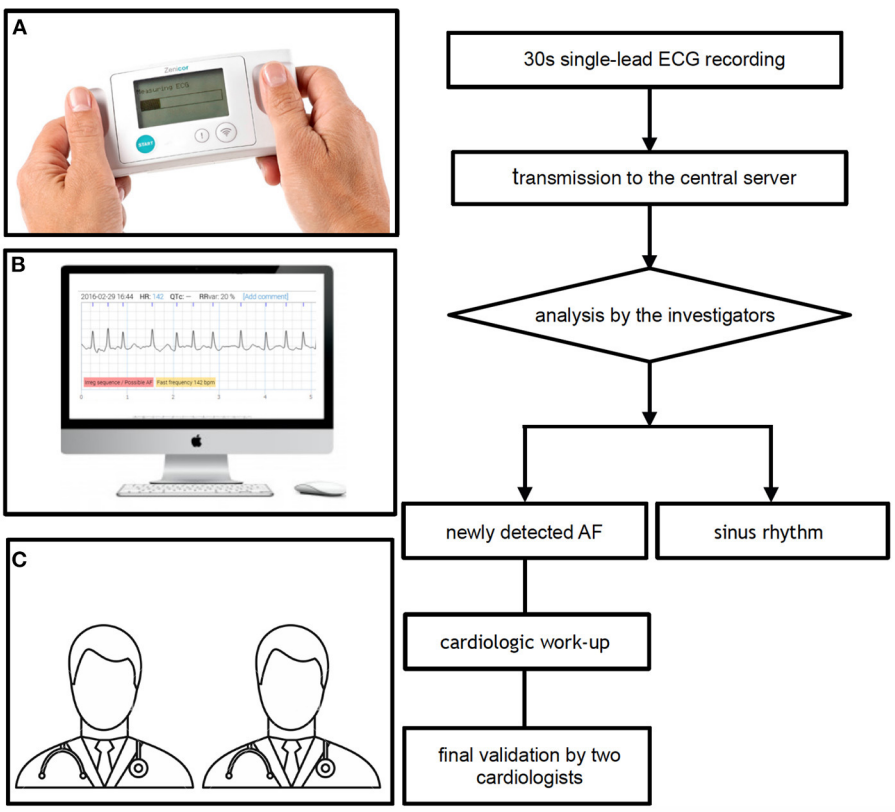

FIGURE 2 | Single-lead ECG recording and interpretation with the Zenicor device. **(A)** Thirty second single-lead ECG handheld device recording, **(B)** analysis of the ECG on the central server, and **(C)** final validation by two cardiologists in case of newly detected AF. AF, atrial fibrillation; ECG, electrocardiogram.

TABLE 1 | Baseline patient characteristics.

	Zenicor ($n = 381$)	Control group ($n = 423$)	p-value
Male	216 (57)	248 (59)	0.62
Age, years	66.16 ± 14.79	64.57 ± 17.03	0.56
Hypertension	219 (57)	229 (54)	0.35
Diabetes mellitus	71 (19)	78 (18)	1.00
Dyslipidemia	145 (38)	134 (31)	0.06
Smoker or previous smoker	175 (46)	177 (42)	0.26
Positive family history for cardiovascular disease	66 (17)	81 (19)	0.52
Ischemic heart disease	72 (19)	69 (16)	0.35
Congestive heart failure	48 (13)	49 (12)	0.67
Previous stroke	55 (14)	52 (12)	0.40
Vascular disease (MI, peripheral artery disease, complex aortic plaque)	112 (29)	119 (28)	0.70
Age (>75 years)	215 (33)	135 (32)	0.82
CHA_2DS_2-VASc risk score (categorical)			
0–1	121 (32)	141 (33)	0.65
2–4	181 (48)	203 (48)	0.94
>4	79 (21)	79 (19)	0.48
CHA_2DS_2-VASc risk score (quantitative)	2.80 ± 1.93	2.69 ± 1.89	0.52
Medication predisposing to bleeding (aspirin, clopidogrel, and NSAID)	224 (59)	226 (53)	0.14
Length of hospitalization, days			
Mean ± SD	10 ± 7	10 ± 8	0.78
Median (IQR)	8 (6–12)	8 (6–11)	

Values are mean ± SD or n (%).

were performed using dedicated software (Stata 14, College Station, Texas) at a 2-tailed significance level of alpha = 0.05.

RESULTS

Participation

From March 2018 and August 2019, 3,261 patients were screened for eligibility of which 806 (25%) underwent randomization. Among the main exclusion criteria, 656 patients were known to have AF, 239 patients had a cardiac pacemaker or implantable cardioverter-defibrillator, 668 had a length of stay <48 h and 120 patients declined participation. While were was no systematic analysis of consent refusals, frequent reasons for declining participation were anxiety about being labeled with an unexpected diagnosis and the risk of undergoing further investigations. Two patients were excluded from the analysis because of AF on 12-lead ECGs at admission. A total of 804 patients were included of whom 381 were assigned to intermittent single-lead handheld ECG recordings, and 423 to routine clinical practice. Patient flow-chart is depicted in **Figure 1**.

Patient Characteristics

Baseline characteristics are summarized in **Table 1**. Mean age was 65 ± 16 years and 464 (58%) were male. Median CHA_2DS_2-VASc score was three of which: 13% heart failure, 57% hypertension, 19% diabetes mellitus, 14% prior stroke/transient ischemic attack, and 29% vascular disease (including myocardial infarction, peripheral artery disease, and complex aortic plaque). CHA_2DS_2-VASc risk factors were equally distributed between groups. All main diagnoses were well-balanced between the groups (**Table 2**). The most common primary diagnosis was malignancy (14%). Moreover, 34 patients (8%) were hospitalized due to an ischaemic stroke in the Zenicor group vs. 24 patients (6%) in the control group ($p = 0.08$).

TABLE 2 | Main diagnosis during hospitalization.

	Zenicor ($n = 381$)	Control ($n = 423$)	p-value
Heart failure	19 (5)	21 (5)	1.00
Ischaemic heart disease	22 (6)	16 (4)	0.19
Pneumonia	31 (8)	43 (10)	0.33
Chronic obstructive pulmonary disease	12 (3)	8 (2)	0.27
Pulmonary embolism	15 (4)	6 (1)	0.28
Other lung disease	16 (4)	14 (3)	0.58
Ischemic stroke or TIA	34 (8)	24 (6)	0.08
Gastrointestinal bleed	11 (3)	12 (3)	1.00
Malignancy	47 (12)	65 (15)	0.22
Minor trauma	21 (5)	22 (5)	0.88
Vascular disease	6 (2)	6 (1)	1.00
Infection/sepsis	39 (10)	60 (14)	0.11
Kidney failure	8 (2)	5 (1)	0.40
Miscellaneous	100 (26)	121(29)	0.48

Values are n (%).
TIA, transient ischemic attack.

Atrial Fibrillation Screening in the Zenicor Group

Systematic single-lead ECG screening was performed in 381 patients. Although single-lead ECG were scheduled twice daily, compliance with study protocol was incomplete. Median number of ECG recordings per individual was 6 (IQR: 3–10), over a median screening period of 6 days (IQR: 4–10). A total of 3,015 records were made using the Zenicor device. The time required for the screening strategy was 1 h per patient for identification of inclusion/exclusion criteria, explanation of device use and recording of one-lead ECGs. The time required for post-recording interpretation of the ECG was variable (between 1 and 5 min per ECG), requiring single-lead ECG review 7 days a week.

Primary Outcome

The overall incidence of newly detected AF was 1.4% ($n = 10$) over the 17 months inclusion period. A total of 7 AF episodes were detected in the Zenicor group vs. 3 AF events in the control group (1.8 vs. 0.7%, $p = 0.20$).

Management of Newly Detected AF

Oral anticoagulation was initiated in seven newly detected AF patients with a median CHA_2DS_2-VASc score of 3 (1–4), of which four in the Zenicor group, and three in the control group. Amongst the three non-anticoagulated patients in the Zenicor group [median HAS-BLED score of 2.5 (1.5–4)], OAC therapy was withheld because of risk of fall, risk of bleeding, and advanced malignancy. History and follow-up of patients with newly detected AF is summarized in **Table 3**.

Harms and Misdiagnosis of AF

A total of four patients in the Zenicor group were initially considered to have AF, but were subsequently reclassified as no AF by two independent cardiologists. None of the latter were started on OAC as two were already anticoagulated for other indications (mesenteric venous thrombosis, pulmonary embolism), and two refused anticoagulation. All patients were correctly reclassified in the final analysis.

DISCUSSION

The HECTO-AF trial was designed to determine whether a systematic screening strategy using daily recordings with a single-lead handheld ECG device increases the detection rate of AF compared to standard clinical practice in the hospital setting. The main findings of the HECTO-AF randomized trial are: (a) the overall incidence of newly detected AF was 1.4% over a median of 6 hospitalized days; (b) in the systematic screening group, a total of seven AF episodes were detected of which 4 (57%) were started on OAC; (c) the systematic screening for AF in the hospital setting is resource-consuming, and of uncertain clinical benefit.

Rational for AF Screening

The European Society of Cardiology Guidelines recommend opportunistic screening of AF using pulse palpation based on a randomized controlled trial which found 1.64% incidence of new AF in patients >75 years-old (9). Recently a number of studies have assessed the effect of systematic screening on the detection of AF, with the idea that even brief (30 s or longer) episodes of AF detected during a limited period are clinically relevant. Four randomized controlled trials (RCTs) have compared screening programs to routine care. The Screening for Atrial Fibrillation in the Elderly (SAFE) trial including 14,802 patients demonstrated that active screening for AF (invitation for a 12-lead ECG) was more effective than routine care (pulse palpation and ECG in case of pulse irregularity). This study conducted in 50 primary care centers in England found a detection rate of new AF of 1.63% a year in the intervention group vs. 1.04% in the control group (difference 0.59%, 95% CI: 0.20–0.98) (10). Another RCT comparing opportunistic pulse palpation to systematic screening with 12-lead ECG in outpatient primary care, reported, in 3,001 patients, a greater AF detection rate in the intervention group (4.5 vs. 1.3%, OR, 3.7; 95% IC: 2.2–1.6) (11). In the REHEARSE-AF Study which randomized patients with CHA_2DS_2-VASc score $\geq$2 and $\geq$65 years old, to an AliveCor Kardia monitoring vs. routine care, in 1,001 patients, showed a statistically significant increase in detection of AF in the monitoring arm over a 12-month period (3.8 vs. 0.9%, HR, 3.9; 95% IC: 1.4–10.4; $P = 0.007$) (12). Finally, the STROKESTOP trial (Systematic ECG screening for Atrial Fibrillation Among) has reported a prevalence of AF of 3% in 7,625 outpatients from Sweden undergoing a 2-week intermittent recording using the Zenicor device (13).

More recently, there has been a paradigm shift in clinical trial design with the Apple Heart Study, in which photoplethysmography was used to detect irregularity in 419,297 participants wearing the Apple Watch (14). Of these, 2,161 participants (0.52%) received a notification of pulse irregularity, and were assessed for the necessity to wear a 7-day ECG patch. Of those notified and wearing the ECG-patch, 153 patients were diagnosed with AF (0.036% of the total population). It must be stressed that Apple Watch-like devices attract younger populations with uncertainty about the clinical value of detecting AF in low-risk individuals.

The place of AF screening is widely debated, and despite meta-analyses pointing to an apparent benefit in patients > 40 years-old (15), a recent US Preventive Services Task Force (USPSTF) has concluded that the evidence on the benefits for AF screening with ECG is insufficient (16).

Screening for Atrial Fibrillation in the Hospital Setting

HECTO-AF is the first randomized study to assess a systematic screening strategy using a handheld device in the hospital setting. The incidence of newly diagnosed AF episodes (1.8%, $n = 7$) in the Zenicor group was lower than expected in hospitalized patients compared to outpatients. Factors that could explain a lower detection rate in the internal medicine ward include a younger population, short hospitalization stay (median 6 days) resulting in shorter screening periods as compared with the 2-weeks in the STROKESTOP trial. All patients were considered to have paroxysmal AF, none required neither rhythm nor rate control.

TABLE 3 | Clinical characteristics of patients with newly detected atrial fibrillation.

Patient	AF detection group	Main diagnosis	Possible trigger factor	Time to detection (days)	OAC	Type of AF	CHA2DS2-VASc/ HAS-BLED	Relevant FUP	Time to FUP (months)
82 years-old women	Control	Interstitial pneumonia	Unknown	7	Yes	Paroxysmal	4/2	Ischemic stroke after OAC interruption (reason for interruption unknown)	12
83 years-old women	Control	Lumbar trauma	Hyperthyroidism	7	Yes	Paroxysmal	4/2	No known AF recurrence	6
80 years-old women	Control	Kidney failure	Unknown	5	Yes	Paroxysmal	6/4	No known AF recurrence	7
50 years-old man	Zenicor	Skin infection	Infection	1	Yes (for planned electrical cardioversion, but not long term)*	Paroxysmal	0/0	No known AF recurrence	12
74 years-old man	Zenicor	Pneumonia	Unknown	2	Yes	Paroxysmal	1/2	No known AF recurrence	8
78 years-old man	Zenicor	Gastro-intestinal bleeding	Bleeding	0	Yes (after resolution of gastrointestinal bleeding)	Paroxysmal	3/3	Death from septic shock	5
74 years-old man	Zenicor	Malignancy	Mild hypokalaemia, severe hypomagnesemia	1	No, advanced malignancy	Paroxysmal	1/3	Death from malignancy	1
90 years-old man	Zenicor	Cholecystitis	Infection, mild hypokalaemia	9	No, high risk of fall	Paroxysmal	3/3	Pulmonary embolism requiring OAC	1
88 years-old women	Zenicor	TIA	n/a	1	Yes	Paroxysmal	7/5	AF recurrence	24
68 years-old man	Zenicor	Malignancy	Mild hypomagnesemia	0	No, bleeding risk (esophageal cancer)	Paroxysmal	2/2	No known AF recurrence	12

OAC, oral anticoagulation; TIA, transient ischemic attack; FUP, follow-up.

**instead, patient had spontaneous cardioversion and anticoagulation was stopped at 1 month in the absence of AF recurrence after 24-h Holter.*

Recording and Interpretation of ECGs

Single-lead ECG recordings were performed at rest under direct supervision of nurses to ensure optimal quality. Nonetheless, single-lead ECG quality was variable, and in some situations uninterpretable. Poor quality has been described due to the electric disturbance caused by movements, or high thumb pressures during recordings (7). Overall, and after review by expert cardiologists, initial AF misdiagnosis was considered in four patients. 12-lead ECGs were performed in all cases of suspected AF in the Zenicor group. The most common reason for discrepancy between single-lead ECG and 12-lead ECG was the presence of atrial or ventricular premature beats.

As mentioned, a previous study in patients with known AF, calculated ECG Zenicor sensitivity at 96% and specificity 92% which points toward AF overdiagnosis (7). It must be stressed however, that this was done in a context of 10-s recordings and not 30 s. Our trial results also indicated potential AF overdiagnosis. Although our aim was not to test for sensitivity, nor specificity we hypothesize that they may have differed from previous reports.

Potential Harms of AF Misdiagnosis

A recent meta-analysis suggests that there is a lack of data regarding potential harms of AF screening vs. no screening (15). Indeed, AF misdiagnosis can lead to the initiation of unnecessary treatment with potential complications, and unwarranted tests. We strived to reduce this harm by requiring confirmation of every suspected AF single-lead recording by two senior cardiologists. Additional 24-h Holter monitoring were necessary in four patients from the Zenicor group (57%) with suspected AF. None of them detected a recurrence of AF.

Treatment of AF and Initiation of OAC Treatment in the Acute Setting

There is a lack of evidence on the benefit of anticoagulation initiation in newly diagnosed AF in the acute setting. Prior studies have shown that AF in sepsis is associated with higher in-hospital and 5-year stroke risk when compared with patients with no AF (17). Gundlund et al. (18) found a greater recurrence of AF among patients with infection-related AF and twice the risk of thromboembolic events compared to infections without AF at 1 year's follow-up. Conversely, a retrospective study (19) did not demonstrate a lower risk of ischemic stroke following anticoagulation in patients with new-onset AF associated with sepsis, acute pulmonary disease and myocardial infarction. Meanwhile, anticoagulant use was associated with a higher risk of bleeding in patients with acute pulmonary disease (6.8 vs. 11.8%, $p < 0.05$). In our study, anticoagulation was not started in 3 (43%) patients in the intervention group because of bleeding risk. Overall, the uncertainty of initiating long-term OAC in the acute setting, limits the indication for systematic AF screening in the hospital setting. Finally, AF was paroxysmal in all patients, and none required rhythm nor rate control therapy on the long term.

LIMITATIONS

The most important study limitation was the lack of statistical power caused by prematurely discontinuing patient enrolment. Bias may have occurred due to fluctuations of AF detection during the study. The time to inclusion was not standardized for each patient and may have led to underdetection of AF in patients with very short hospital stays. There was a potential selection bias as only patients capable of performing a proper single-lead handheld recording were eligible. Therefore, the most vulnerable and fragile patients who may have been at even higher risk of AF were excluded. This may have underestimated the overall AF rate, but the benefit of introducing OAC in this population is debatable. In some cases, the presence of artifacts has limited the interpretation of ECG. The sensitivity and specificity as well as positive and negative predictive values in the in-hospital setting were not assessed as no systematic simultaneous 12-lead ECG were performed with each one-lead ECG. Finally, this was a monocentric study with results that may not be applicable to a more general population.

CONCLUSION

There was a trend toward a higher AF detection over a median of 6 hospitalized days in the intervention group, but a definitive conclusion cannot be drawn because of the insufficient statistical power of the present study. A systematic screening program with daily single-lead handheld ECG recordings is resource-consuming. The interpretation of single-lead handheld ECG is challenging and may result in inaccurate AF diagnosis. The long-term benefit of oral anticoagulation in patients with accurate detection of AF during acute illness is uncertain.

DATA AVAILABILITY STATEMENT

The raw data supporting the conclusions of this article will be made available by the authors, without undue reservation.

ETHICS STATEMENT

The studies involving human participants were reviewed and approved by Cantonal Ethics Committee of Vaud (CER-VD). The patients/participants provided their written informed consent to participate in this study.

AUTHOR CONTRIBUTIONS

MM and SC conceived the original idea and planned the study. YF contributed to the implementation of the research and data management. SS contributed to

the study design, analyzed the data, and wrote the manuscript with support from DA, SP, and MM. DA and SP contributed to data analysis. SC supervised the project. All authors contributed to the article and approved the submitted version.

FUNDING

The trial was supported by an unrestricted grant from Fond Scientifique Cardiovasculaire Fribourg.

ACKNOWLEDGMENTS

The authors would like to thank the nursing staff of the Department of Internal Medicine, University and Hospital of Fribourg.

SUPPLEMENTARY MATERIAL

The Supplementary Material for this article can be found online at: https://www.frontiersin.org/articles/10.3389/fcvm.2021.681890/full#supplementary-material

REFERENCES

1. Di Carlo A, Bellino L, Consoli D, Mori F, Zaninelli A, Baldereschi M, et al. Prevalence of atrial fibrillation in the Italian elderly population and projections from 2020 to 2060 for Italy and the European Union: the FAI Project. *Europace.* (2019) 21:1468–75. doi: 10.1093/europace/euz141
2. Miyasaka Y, Barnes Marion E, Gersh Bernard J, Cha Stephen S, Bailey Kent R, Abhayaratna Walter P, et al. Secular trends in incidence of atrial fibrillation in Olmsted County, Minnesota, 1980 to 2000 and implications on the projections for future prevalence. *Circulation.* (2006) 114:119–25. doi: 10.1161/CIRCULATIONAHA.105.595140
3. Kim MH, Johnston SS, Chu B-C, Dalal MR, Schulman KL. Estimation of total incremental health care costs in patients with atrial fibrillation in the United States. *Circ Cardiovasc Qual Outcomes.* (2011) 4:313–20. doi: 10.1161/CIRCOUTCOMES.110.958165
4. Healey JS, Connolly SJ, Gold MR, Israel CW, Van Gelder IC, Capucci A, et al. Subclinical atrial fibrillation and the risk of stroke. *N Engl J Med.* (2012) 366:120–9. doi: 10.1056/NEJMoa1105575
5. Kirchhof P, Benussi S, Kotecha D, Ahlsson A, Atar D, Casadei B, et al. 2016 ESC Guidelines for the management of atrial fibrillation developed in collaboration with EACTS. *Eur Heart J.* (2016) 37:2893–962. doi: 10.5603/KP.2016.0172
6. Jones NR, Taylor CJ, Hobbs FDR, Bowman L, Casadei B. Screening for atrial fibrillation: a call for evidence. *Eur Heart J.* (2019) 41:1075–85. doi: 10.1093/eurheartj/ehz834
7. Doliwa PS, Frykman V, Rosenqvist M. Short-term ECG for out of hospital detection of silent atrial fibrillation episodes. *Scand Cardiovasc J.* (2009) 43:163–8. doi: 10.1080/14017430802593435
8. Schukraft S, Mancinetti M, Hayoz D, Faucherre Y, Cook S, Arroyo D, et al. Handheld ECG Tracking of in-hOspital Atrial Fibrillation the HECTO-AF trial Clinical Study Protocol. *Trials.* (2019) 20:92. doi: 10.1186/s13063-019-3189-7
9. Gargiulo G, Goette A, Tijssen J, Eckardt L, Lewalter T, Vranckx P, et al. Safety and efficacy outcomes of double vs. triple antithrombotic therapy in patients with atrial fibrillation following percutaneous coronary intervention: a systematic review and meta-analysis of non-vitamin K antagonist oral anticoagulant-based randomized clinical trials. *Eur Heart J.* (2019) 40:3757–67. doi: 10.1093/eurheartj/ehz732
10. Fitzmaurice DA, Hobbs FDR, Jowett S, Mant J, Murray ET, Holder R, et al. Screening versus routine practice in detection of atrial fibrillation in patients aged 65 or over: cluster randomised controlled trial. *BMJ.* (2007) 335:383. doi: 10.1136/bmj.39280.660567.55
11. Morgan S, Mant D. Randomised trial of two approaches to screening for atrial fibrillation in UK general practice. *Br J Gen Pract.* (2002) 52:373–80.
12. Halcox JPJ, Wareham K, Cardew A, Gilmore M, Barry JP, Phillips C, et al. Assessment of remote heart rhythm sampling using the AliveCor heart monitor to screen for atrial fibrillation: the REHEARSE-AF study. *Circulation.* (2017) 136:1784–94. doi: 10.1161/CIRCULATIONAHA.117.030583
13. Svennberg E, Engdahl J, Al-Khalili F, Friberg L, Frykman V, Rosenqvist M. Mass screening for untreated atrial fibrillation: the STROKESTOP study. *Circulation.* (2015) 131:2176–84. doi: 10.1161/CIRCULATIONAHA.114.014343
14. Perez MV, Mahaffey KW, Hedlin H, Rumsfeld JS, Garcia A, Ferris T, et al. Large-scale assessment of a smartwatch to identify atrial fibrillation. *N Engl J Med.* (2019) 381:1909–17. doi: 10.1056/NEJMoa1901183
15. Jonas DE, Kahwati LC, Yun JDY, Middleton JC, Coker-Schwimmer M, Asher GN. Screening for atrial fibrillation with electrocardiography: evidence report and systematic review for the US Preventive Services Task Force. *JAMA.* (2018) 320:485–98. doi: 10.1001/jama.2018.4190
16. Curry SJ, Krist AH, Owens DK, Barry MJ, Caughey AB, Davidson KW, et al. Screening for atrial fibrillation with electrocardiography: US Preventive Services Task Force Recommendation Statement. *JAMA.* (2018) 320:478–84. doi: 10.1001/jama.2018.10321
17. Walkey AJ, Hammill BG, Curtis LH, Benjamin EJ. Long-term outcomes following development of new-onset atrial fibrillation during sepsis. *Chest.* (2014) 146:1187–95. doi: 10.1378/chest.14-0003
18. Gundlund A, Olesen JB, Butt JH, Christensen MA, Gislason GH, Torp-Pedersen C, et al. One-year outcomes in atrial fibrillation presenting during infections: a nationwide registry-based study. *Eur Heart J.* (2020) 41:1112–9. doi: 10.1093/eurheartj/ehz873
19. Quon MJ, Behlouli H, Pilote L. Anticoagulant use and risk of ischemic stroke and bleeding in patients with secondary atrial fibrillation associated with acute coronary syndromes, acute pulmonary disease, or sepsis. *JACC Clin Electrophysiol.* (2018) 4:386–93. doi: 10.1016/j.jacep.2017.08.003

Conflict of Interest: The authors declare that the research was conducted in the absence of any commercial or financial relationships that could be construed as a potential conflict of interest.

frontiers in Cardiovascular Medicine

OPINION
published: 11 May 2021
doi: 10.3389/fcvm.2021.688875

Early Morning QT Prolongation During Hypoglycemia: Only a Matter of Glucose?

Sara D'Imperio[1†], *Michelle M. Monasky*[1†], *Emanuele Micaglio*[1], *Gabriele Negro*[1] *and Carlo Pappone*[1,2*]

[1] Arrhythmology Department, IRCCS Policlinico San Donato, Milan, Italy, [2] Vita-Salute San Raffaele University, Milan, Italy

Keywords: QT prolongation, hypoglycemia, Brugada syndrome, diabetes, sudden cardiac death, glucose, glucose - insulin

QT is the surface ECG equivalent of the time it takes for the ventricular myocardium to repolarize after its depolarization. The prolongation of the QT interval is a dangerous ECG abnormality that can be inherited or acquired and is a risk for sudden cardiovascular events due to its potential arrhythmogenicity. The prevalence of QT prolongation has been investigated in both type 1 and type 2 diabetes mellitus (DM) (1). It has been demonstrated that QT prolongation is a risk factor for sudden cardiac death in the presence of hypoglycemia (2), including when it is insulin-induced (3).

We read with great interest the retrospective study by Tsujimoto et al. reporting that in the early morning (4 a.m.−10 a.m.) severe hypoglycemia was associated with a significant incidence of abnormal QT prolongation in a cohort of 287 Japanese patients, regardless of whether the patients were diabetic or not (4). This study focused on the relationship between QT prolongation and severe hypoglycemia, which is a common and deleterious effect of diabetes and has been associated with adverse cardiovascular outcomes, such as fatal cardiac arrhythmic events (5, 6) and mortality (7). Indeed, several studies support that there is a strict correlation between hypoglycemia and arrhythmic events during bedtime in diabetic patients (6, 8–10), with a significant increase in prolonged QT interval (11–13). Of note, in the human species, the length of the QT interval has been shown to depend upon the circadian rhythm, which is controlled by the autonomous nervous system and was shown to have marked variability in patients with type 1 diabetes mellitus (14). We are aware that maturity onset diabetes of the young (MODY) is not a common cause of diabetes worldwide, although an excellent study by Yorifuji et al. (15) reported 103 mutations in MODY genes (39%) in a cohort of 263 Japanese diabetic patients. Therefore, we suggest the analysis of at least the genes *GCK*, *HNF1A*, *HNF1B*, and *HNF4A* in the cohort presented by Tsujimoto and coworkers.

Lengthened QT interval is associated with ventricular arrhythmias and sudden cardiac death (16). It can be caused by genetic variations, mineral imbalance, or QT-prolonging medications (17, 18). Moreover, a higher incidence of QT prolongation has been described in metabolic syndrome (19), eating disorders, such as anorexia nervosa (20), and obesity (21). Therefore, it is very important to identify the underlying conditions of the patients that influence their QT interval and risk of mortality.

Multiple regulatory mechanisms are implicated in balancing the serum glucose concentration with the circadian rhythm. Therefore, when this balance is disrupted, hypoglycemia can occur. This condition usually occurs in diabetic patients due to the administration of hypoglycemic agents, such as insulin or sulfonylurea. However, hypoglycemia can develop due to several clinical complications, such as metabolic diseases (22), insulinoma (23), and non-islet tumors (24). Moreover, regardless of a patient's diet, hypoglycemia can also manifest due to an excess intake of alcohol, because it inhibits both hepatic gluconeogenesis and glycogenolysis (25–27). Autoimmunity is another important cause of both hypoglycemia and QT interval prolongation.

OPEN ACCESS

Edited by:
Marina Cerrone, New York University, United States

Reviewed by:
Pier Leopoldo Capecchi, University of Siena, Italy
David Auerbach, Upstate Medical University, United States

***Correspondence:**
Carlo Pappone
carlo.pappone@af-ablation.org

[†] *These authors have contributed equally to this work*

Specialty section:
This article was submitted to Cardiac Rhythmology, a section of the journal Frontiers in Cardiovascular Medicine

Received: *31 March 2021*
Accepted: *19 April 2021*
Published: *11 May 2021*

Citation:
D'Imperio S, Monasky MM, Micaglio E, Negro G and Pappone C (2021) Early Morning QT Prolongation During Hypoglycemia: Only a Matter of Glucose? Front. Cardiovasc. Med. 8:688875. doi: 10.3389/fcvm.2021.688875

Type 1 diabetes is characterized by the presence of many different antibodies (28). Those antibodies provoke autoimmune destruction of insulin-producing β cells (29) and can be detected in the patients' plasma. Thus, it is very important to exclude the presence of such mechanisms in the studied cohort.

Of note, in the present article by Tsujimoto et al., we did not find any information regarding the clinical status of non-DM patients, in particular the prevalence of potentially QT prolonging conditions [hypokalemia, QT prolonging drugs, metabolic disorders others than diabetes, or inflammation (30)]. Therefore, it would be better to understand the etiology of the severe hypoglycemia, because it may be the cause or a contributing cause of the QT prolongation. This ECG abnormality happens spontaneously in the hereditary form, but can be triggered by drugs (https://www.crediblemeds.org), such as antiarrhythmics, antihistamines, antipsychotics, antibiotics (18), cancer treatments, and alcohol intake (25, 26). Furthermore, no genetic testing is presented about the most common long QT syndrome (LQTS) genes (*KCNQ1*, *KCNH2*, *SCN5A*, or possible modulating polymorphisms).

Moreover, we noticed that Tsujimoto et al. only took into consideration the QT interval and no other important electrocardiogram (ECG) information, such as ST-segment and T wave. Clinical similarities exist among patients with prolonged QT interval and Brugada syndrome (BrS), and the majority of these patients are asymptomatic, yet they can be at risk of sudden cardiac death (31–33).

BrS and LQTS are both life-threatening inherited arrhythmic disorders that usually manifest in the nighttime. LQTS type-3 and BrS also share the same *SCN5A* variant (34, 35), and several instances of an overlap syndrome have been described (34, 36). Therefore, the evaluation of the ST-segment could have been useful to unveil an overlap syndrome.

We understand why cardiopulmonary arrest patients were excluded from the study, however, it would have been useful to evaluate, if available, the ECGs of those patients, since they showed the worst phenotype. Therefore, it would have been interesting if those patients had prior clinical evaluations of their health conditions. Specifically, it would have been useful to know if they have ever had any symptoms like syncope, palpitations, seizures, or family history related to BrS, and more importantly, whether the ST-segment from a standard 12-precordial lead ECG had ever been evaluated. Notably, the patients presented to a hospital in Japan, which has a relatively high incidence of BrS, ranging from 0.1 to 0.2% in the general population (37).

It is known that many cardiovascular outcomes vary in prevalence depending the time of the day. Indeed, the cardiac circadian rhythm is involved in different cardiac functions and it may contribute to HF and SCD (38). We noticed that in the study conducted by Tsujimoto et al., the QT prolongation was only assessed in patients with severe hypoglycemia. It would have been helpful to have QT prolongation records of the same patients or a matched cohort, during periods of non-hypoglycemia. Moreover, to better understand the relationship between QT prolongation and hypoglycemia events, it would also be important to know the QT baseline at different times of day in order to determine the effect of the circadian fluctuations on the QT interval. In fact, two types of circadian clocks exist: a central clock that acts on the heart by various neurohumoral factors, and a local clock in the heart that alters the expression of cardiac ion channels (39). At night, the QT interval (as well as the PR interval and QRS duration) is lengthened, indicating slower ventricular repolarization. A possible mechanism for this may include ion channel remodeling, including Na^+, Ca^{2+}, and K^+ channels, as well as connexins, as a result of circadian rhythm, as demonstrated in animal models (39). Therefore, in the study by Tsujimoto et al., it is not clear how it is possible to distinguish the role of hypoglycemia vs. the role of the time of day impacting the QT when the study included only data investigating hypoglycemia during early morning.

On another note, only patients with hypoglycemia were included in the study, but the relationship between blood glucose and QT prolongation was not discussed. A strict temporal relationship has been described between hypoglycemia and QT prolongation, stressing the proarrhythmic harm related to dynamic changes of heart repolarization (40). Thus, it would have been optimal to understand the duration of QT prolongation at different blood glucose concentrations. Indeed, this issue would have been better understood if several blood glucose values, including non-hypoglycemic readings, could have been included.

In conclusion, according to current literature, it is not possible to consider an abnormal QT prolongation during the early morning as just an expression of severe hypoglycemia. In fact, QT trait prolongation can be an expression of a concealed channelopathy (possibly overlap syndrome), a sign of non-alcoholic fatty liver disease, regardless of the presence of diabetes (41), or the onset of metabolic dysregulation, potentially associated with several different cardiomyopathies with preserved ejection fraction (HFpEF) (42).

AUTHOR CONTRIBUTIONS

SD'I and MM decided on the project, drafted the original version, and revised the manuscript. EM and GN provided expertise and revised the manuscript. CP provided resources and funding. All authors contributed to the article and approved the submitted version.

FUNDING

This study was partially supported by Ricerca Corrente funding from Italian Ministry of Health to IRCCS Policlinico San Donato.

REFERENCES

1. Kumar R, Fisher M, Macfarlane PW. Review: diabetes and the QT interval: time for debate. *Br J Diabetes Vasc Dis.* (2004) 4:146–50. doi: 10.1177/14746514040040030201
2. Nordin C. The proarrhythmic effect of hypoglycemia: evidence for increased risk from ischemia and bradycardia. *Acta Diabetol.* (2014) 51:5–14. doi: 10.1007/s00592-013-0528-0
3. Kacheva S, Karges B, Göller K, Marx N, Mischke K, Karges W. QT prolongation caused by insulin-induced hypoglycaemia - an interventional

study in 119 individuals. *Diabetes Res Clin Pract.* (2017) 123:165–72. doi: 10.1016/j.diabres.2016.11.021
4. Tsujimoto T, Yamamoto-Honda R, Kajio H, Kishimoto M, Noto H, Hachiya R, et al. High risk of abnormal QT prolongation in the early morning in diabetic and non-diabetic patients with severe hypoglycemia. *Ann Med.* (2015) 47:238–44. doi: 10.3109/07853890.2015.1017528
5. Clus S, Crețeanu G, Popa A. Nocturnal hypoglycemia in type 2 diabetes. *Romanian J Diabetes Nutr Metab Dis.* (2018) 25:99–103. doi: 10.2478/rjdnmd-2018-0011
6. Andersen A, Jørgensen PG, Knop FK, Vilsbøll T. Hypoglycaemia and cardiac arrhythmias in diabetes. *Ther Adv Endocrinol Metab.* (2020) 11:2042018820911803. doi: 10.1177/2042018820911803
7. Amiel SA, Aschner P, Childs B, Cryer PE, de Galan BE, Frier BM, et al. Hypoglycaemia, cardiovascular disease, and mortality in diabetes: epidemiology, pathogenesis, and management. *Lancet Diabetes Endocrinol.* (2019) 7:385–96. doi: 10.1016/S2213-8587(18)30315-2
8. Stahn A, Pistrosch F, Ganz X, Teige M, Koehler C, Bornstein S, et al. Relationship between hypoglycemic episodes and ventricular arrhythmias in patients with type 2 diabetes and cardiovascular diseases: silent hypoglycemias and silent arrhythmias. *Diabetes Care.* (2014) 37:516–20. doi: 10.2337/dc13-0600
9. Reno CM, Daphna-Iken D, Chen YS, VanderWeele J, Jethi K, Fisher SJ. Severe hypoglycemia-induced lethal cardiac arrhythmias are mediated by sympathoadrenal activation. *Diabetes.* (2013) 62:3570–81. doi: 10.2337/db13-0216
10. Chow E, Bernjak A, Williams S, Fawdry RA, Hibbert S, Freeman J, et al. Risk of cardiac arrhythmias during hypoglycemia in patients with type 2 diabetes and cardiovascular risk. *Diabetes.* (2014) 63:1738–47. doi: 10.2337/db13-0468
11. Robinson RT, Harris ND, Ireland RH, Macdonald IA, Heller SR. Changes in cardiac repolarization during clinical episodes of nocturnal hypoglycaemia in adults with Type 1 diabetes. *Diabetologia.* (2004) 47:312–5. doi: 10.1007/s00125-003-1292-4
12. Marques JL, George E, Peacey SR, Harris ND, Macdonald IA, Cochrane T, et al. Altered ventricular repolarization during hypoglycaemia in patients with diabetes. *Diabet Med J Br Diabet Assoc.* (1997) 14:648–54. doi: 10.1002/(SICI)1096-9136(199708)14:8<648::AID-DIA418>3.0.CO;2-1
13. Ko S-H, Park Y-M, Yun J-S, Cha S-A, Choi E-K, Han K, et al. Severe hypoglycemia is a risk factor for atrial fibrillation in type 2 diabetes mellitus: Nationwide population-based cohort study. *J Diabetes Complications.* (2018) 32:157–63. doi: 10.1016/j.jdiacomp.2017.09.009
14. Kardelen F, Akçurin G, Ertu,g H, Akcurin S, Bircan I. Heart rate variability and circadian variations in type 1 diabetes mellitus. *Pediatr Diabetes.* (2006) 7:45–50. doi: 10.1111/j.1399-543X.2006.00141.x
15. Yorifuji T, Higuchi S, Kawakita R, Hosokawa Y, Aoyama T, Murakami A, et al. Genetic basis of early-onset, maturity-onset diabetes of the young-like diabetes in Japan and features of patients without mutations in the major MODY genes: dominance of maternal inheritance. *Pediatr Diabetes.* (2018) 19:1164–72. doi: 10.1111/pedi.12714
16. Algra A, Tijssen JG, Roelandt JR, Pool J, Lubsen J. QTc prolongation measured by standard 12-lead electrocardiography is an independent risk factor for sudden death due to cardiac arrest. *Circulation.* (1991) 83:1888–94. doi: 10.1161/01.CIR.83.6.1888
17. Castiglione A, Odening K. QT-Zeit – was fange ich eigentlich damit an? *Dtsch Med Wochenschr.* (2020) 145:536–42. doi: 10.1055/a-0969-6312
18. Nachimuthu S, Assar MD, Schussler JM. Drug-induced QT interval prolongation: mechanisms and clinical management. *Ther Adv Drug Saf.* (2012) 3:241–53. doi: 10.1177/2042098612454283
19. Guo X, Li Z, Guo L, Yu S, Yang H, Zheng L, et al. Effects of metabolically healthy and unhealthy obesity on prolongation of corrected QT interval. *Am J Cardiol.* (2017) 119:1199–204. doi: 10.1016/j.amjcard.2016.12.033
20. Takimoto Y, Yoshiuchi K, Kumano H, Yamanaka G, Sasaki T, Suematsu H, et al. QT interval and QT dispersion in eating disorders. *Psychother Psychosom.* (2004) 73:324–8. doi: 10.1159/000078850
21. Kumar T, Jha K, Sharan A, Sakshi P, Kumar S, Kumari A. Study of the effect of obesity on QT-interval among adults. *J Fam Med Prim Care.* (2019) 8:1626–9. doi: 10.4103/jfmpc.jfmpc_168_19
22. Douillard C, Mention K, Dobbelaere D, Wemeau J-L, Saudubray J-M, Vantyghem M-C. Hypoglycaemia related to inherited metabolic diseases in adults. *Orphanet J Rare Dis.* (2012) 7:26. doi: 10.1186/1750-1172-7-26
23. Kandaswamy L, Raghavan R, Pappachan JM. Spontaneous hypoglycemia: diagnostic evaluation and management. *Endocrine.* (2016) 53:47–57. doi: 10.1007/s12020-016-0902-0
24. Bodnar TW, Acevedo MJ, Pietropaolo M. Management of non-islet-cell tumor hypoglycemia: a clinical review. *J Clin Endocrinol Metab.* (2014) 99:713–22. doi: 10.1210/jc.2013-3382
25. van de Wiel A. Diabetes mellitus and alcohol. *Diabetes Metab Res Rev.* (2004) 20:263–7. doi: 10.1002/dmrr.492
26. Oba-Yamamoto C, Takeuchi J, Nakamura A, Takikawa R, Ozaki A, Nomoto H, et al. Combination of alcohol and glucose consumption as a risk to induce reactive hypoglycemia. *J Diabetes Investig.* (2021) 12:651–7. doi: 10.1111/jdi.13375
27. Spoke C, Malaeb S. A case of hypoglycemia associated with the ketogenic diet and alcohol use. *J Endocr Soc.* (2020) 4:bvaa045. doi: 10.1210/jendso/bvaa045
28. Kahaly GJ, Hansen MP. Type 1 diabetes associated autoimmunity. *Autoimmun Rev.* (2016) 15:644–8. doi: 10.1016/j.autrev.2016.02.017
29. Bluestone JA, Herold K, Eisenbarth G. Genetics, pathogenesis and clinical interventions in type 1 diabetes. *Nature.* (2010) 464:1293–300. doi: 10.1038/nature08933
30. Lazzerini PE, Acampa M, Laghi-Pasini F, Bertolozzi I, Finizola F, Vanni F, et al. Cardiac arrest risk during acute infections: systemic inflammation directly prolongs QTc interval via cytokine-mediated effects on potassium channel expression. *Circ Arrhythm Electrophysiol.* (2020) 13:e008627. doi: 10.1161/CIRCEP.120.008627
31. Obeyesekere MN, Antzelevitch C, Krahn AD. Management of ventricular arrhythmias in suspected channelopathies. *Circ Arrhythm Electrophysiol.* (2015) 8:221–31. doi: 10.1161/CIRCEP.114.002321
32. Haïssaguerre M, Extramiana F, Hocini M, Cauchemez B, Jaïs P, Cabrera JA, et al. Mapping and ablation of ventricular fibrillation associated with long-QT and brugada syndromes. *Circulation.* (2003) 108:925–8. doi: 10.1161/01.CIR.0000088781.99943.95
33. Romero D, Behar N, Mabo P, Hernandez AI. Differences in brugada syndrome patients through ventricular repolarization analysis during sleep. In: *2019 41st Annual International Conference of the IEEE Engineering in Medicine Biology Society (EMBC). Presented at the 2019 41st Annual International Conference of the IEEE Engineering in Medicine & Biology Society (EMBC)*. Berlin: IEEE (2019). p. 5638–41.
34. Hasebe H, Yokoya T, Murakoshi N, Kurebayashi N. Pilsicainide administration unmasks a phenotype of Brugada syndrome in a patient with overlap syndrome due to the E1784K SCN5A mutation. *Intern Med Tokyo Jpn.* (2020) 59:83–7. doi: 10.2169/internalmedicine.3430-19
35. Sandhu A, Borne RT, Mam C, Bunch TJ, Aleong RG. Double jeopardy: long QT3 and Brugada syndromes. *Clin Case Rep.* (2017) 5:1315–9. doi: 10.1002/ccr3.1064
36. Bezzina C, Veldkamp MW, van Den Berg MP, Postma AV, Rook MB, Viersma JW, et al. A single Na(+) channel mutation causing both long-QT and Brugada syndromes. *Circ Res.* (1999) 85:1206–13. doi: 10.1161/01.RES.85.12.1206
37. Hiraoka M. Brugada syndrome in Japan. *Circ J.* (2007) 71(Suppl. A):A61–8. doi: 10.1253/circj.71.A61
38. Bernardi J, Aromolaran KA, Zhu H, Aromolaran AS. Circadian mechanisms: cardiac ion channel remodeling and arrhythmias. *Front Physiol.* (2020) 11:611860. doi: 10.3389/fphys.2020.611860
39. Black N, D'Souza A, Wang Y, Piggins H, Dobrzynski H, Morris G, et al. Circadian rhythm of cardiac electrophysiology, arrhythmogenesis, and the underlying mechanisms. *Heart Rhythm.* (2019) 16:298–307. doi: 10.1016/j.hrthm.2018.08.026

40. Lee AS, Brooks BA, Simmons L, Kilborn MJ, Wong J, Twigg SM, et al. Hypoglycaemia and QT interval prolongation: detection by simultaneous Holter and continuous glucose monitoring. *Diabetes Res Clin Pract.* (2016) 113:211–4. doi: 10.1016/j.diabres.2016.01.005
41. Hung C-S, Tseng P-H, Tu C-H, Chen C-C, Liao W-C, Lee Y-C, et al. Nonalcoholic fatty liver disease is associated with QT prolongation in the general population. *J Am Heart Assoc*. (2015) 4:e001820. doi: 10.1161/JAHA.115.001820
42. Tune JD, Goodwill AG, Sassoon DJ, Mather KJ. Cardiovascular consequences of metabolic syndrome. *Transl Res J Lab Clin Med.* (2017) 183:57–70. doi: 10.1016/j.trsl.2017.01.001

Conflict of Interest: The authors declare that the research was conducted in the absence of any commercial or financial relationships that could be construed as a potential conflict of interest.

frontiers in Cardiovascular Medicine

ORIGINAL RESEARCH
published: 14 May 2021
doi: 10.3389/fcvm.2021.577742

Heart Rate Fluctuation and Mortality in Critically Ill Myocardial Infarction Patients: A Retrospective Cohort Study

Qi Guo [1,2], Hongwei Li [1,2], Huijun Ouyang [1,2], Runlu Sun [1,2], Junjie Wang [1,2], Maoxiong Wu [1,2], Yue Pan [3], Jingfeng Wang [1,2] and Yuling Zhang [1,2]**

[1] Department of Cardiology, Sun Yat-sen Memorial Hospital of Sun Yat-sen University, Guangzhou, China, [2] Guangdong Provincial Key Laboratory of Arrhythmia and Electrophysiology, Sun Yat-sen Memorial Hospital of Sun Yat-sen University, Guangzhou, China, [3] Guangdong Provincial Key Laboratory of Malignant Tumor Epigenetics and Gene Regulation, Sun Yat-Sen Memorial Hospital of Sun Yat-Sen University, Guangzhou, China

OPEN ACCESS

Edited by:
Mehdi Namdar, Geneva University Hospitals (HUG), Switzerland

Reviewed by:
Martin Ibarrola, Independent researcher, Bella Vista, Argentina
Li Zhang, Huazhong University of Science and Technology, China
Yuli Huang, Southern Medical University, China

***Correspondence:**
Yuling Zhang
zhyul@mail.sysu.edu.cn
Jingfeng Wang
wjingf@mail.sysu.edu.cn

Specialty section:
This article was submitted to Cardiac Rhythmology, a section of the journal Frontiers in Cardiovascular Medicine

Received: *10 February 2021*
Accepted: *20 April 2021*
Published: *14 May 2021*

Citation:
Guo Q, Li H, Ouyang H, Sun R, Wang J, Wu M, Pan Y, Wang J and Zhang Y (2021) Heart Rate Fluctuation and Mortality in Critically Ill Myocardial Infarction Patients: A Retrospective Cohort Study. Front. Cardiovasc. Med. 8:577742. doi: 10.3389/fcvm.2021.577742

Background: Whether heart rate (HR) fluctuation after admission has an impact on the outcomes of critically ill myocardial infarction (MI) patients in intensive care unit remains unknown.

Methods: A total of 2,031 MI patients were enrolled from the Medical Information Mart for Intensive Care (MIMIC-III) database. HR fluctuation was calculated as the maximum HR minus the minimum HR in the initial 24 h after admission. Participants were divided into 3 groups, namely, low HR fluctuation [<30 beats per minute (bpm)], medium HR fluctuation (30–49 bpm), and high HR fluctuation (≥ 50 bpm). The main outcomes were 30–day and 1-year mortality. Cox regression and restricted cubic spline model were used.

Results: Each 10-bpm increase in HR fluctuation was associated with a higher risk of 30-day mortality and 1-year mortality, with adjusted hazard ratios of 1.122 (95% CI, 1.083–1.162) and 1.107 (95% CI, 1.074–1.140), respectively. Compared with the low HR fluctuation group, the high HR fluctuation group suffered a significantly higher risk of mortality after adjustment, with hazard ratios of 2.156 (95% CI, 1.483–3.134) for 30-day mortality and 1.796 (95% CI, 1.354–2.381) for 1-year mortality. A typical J-type curve was observed in restricted cubic splines for the association between HR fluctuation and 30-day or 1-year mortality of MI patients, with the lowest risk on the HR fluctuation of 30 bpm. Sensitivity analyses emphasized the robustness of our results.

Conclusions: This retrospective cohort study revealed an independent positive association between HR fluctuation and 30-day and 1-year mortality in critically ill MI patients, which warrants further investigation.

Keywords: myocardial infarction, mortality, heart rate fluctuation, risk factor, intensive care unit

INTRODUCTION

Myocardial infarction (MI) is common in intensive care unit (ICU), resulting to an enormous cost worldwide (1). It is of great importance to perform MI risk stratification to help patients gain benefit and reduce cost. MI patients in the ICU are exposed to different degrees of artificial light, noise, and various organ supports, including ventilation and medications, which might commonly cause

disrupted rhythms of sleep architecture, core body temperature, blood pressure, and heart rate (HR) (2). Besides the ICU environments, severe diseases, and acute stress response might further contribute the fluctuation of vital signs (3). However, whether these fluctuations of vital sings have an impact on the outcomes of critically ill MI patients in the ICU has been poorly investigated.

HR is a widely recognized predictor of cardiovascular diseases and outcomes in numerous cohorts of patients with heart failure or patients at high cardiovascular risk after MI (4, 5). As a common kind of physiological change, HR also shows an obvious fluctuation across 24 h. It has been reported that the fluctuation range of HR was an easily available prognostic predictor for chronic heart failure, which might be correlated with autonomic tone and exercise capacity (6). Recently, we reported that both high and low HR fluctuation were associated with higher mortality in ICU (7). Nevertheless, the association between HR fluctuation and the risk of mortality in MI patients remains unknown. We hypothesized that HR fluctuation might be positively correlated with the risk of mortality in MI patients.

To better clarify the association between HR fluctuation and risk of mortality in MI patients, this retrospective cohort study was designed and conducted using a multivariate Cox hazard ratio regression model and restricted cubic spline model based on the Medical Information Mart for Intensive Care (MIMIC-III) database. In addition, detailed sensitivity analyses were carried out to further evaluate the robustness and reliability of our results under different levels of admission HR and the use of vasopressors, sedatives, or other HR-limiting conditions.

MATERIALS AND METHODS

Data Source

The cohort data were retrieved from the MIMIC-III database. Briefly, MIMIC-III integrated comprehensive and de-identified clinical data of 53,423 distinct ICU stays for 38,597 adult patients in the ICU from 2001 to 2012. The overall information was saved as a relational database, consisting of patient demographics, laboratory tests, discharge summaries, electrocardiographs, imaging examinations, diagnostic information [such as the International Classification of Diseases, Ninth Revision (ICD-9) codes], and in-hospital and out-of-hospital mortality. The use of the MIMIC-III database was approved by the review boards of the Massachusetts Institute of Technology and Beth Israel Deaconess Medical Center (8).

Study Cohort

The Structure Query Language was used for data extraction (9). Patients admitted to the ICU who were diagnosed with MI were eligible for inclusion. After the MIMIC-III database was screened, a total of 2,031 patients with MI were enrolled in our study. For multiple ICU admissions of one patient, only the data of each patient's first ICU admission were extracted. All characteristics were collected in the initial 24-h documents following admission. The following variables for further statistical analysis were included: [1] basic demographics, including age, sex, and weight; [2] HR, sedative use, ventilation use, vasopressor use, simplified acute physiology score (SAPS), and sequential organ failure assessment (SOFA) score; and [3] comorbidities, including hypertension, congestive heart failure (CHF), atrial fibrillation (AF), liver disease, renal disease, chronic obstructive pulmonary disease (COPD), diabetes, depression, and malignancy. Because more than 20% of patients suffered the missing value of height, height and body mass index were not enrolled in this study to avoid bias resulting from missing value.

HR Fluctuation and Outcomes

Admission HR was identified as the first record of HR after ICU admission, while HR fluctuation was calculated as the maximum HR minus the minimum HR in the initial 24 h. According to the level of HR fluctuation, participants were divided into 3 groups, namely, low HR fluctuation [<30 beats per minute (bpm)], medium HR fluctuation (30–49 bpm), and high HR fluctuation ($\geq$ 50 bpm). In this study, we regarded 30-day mortality and 1-year mortality as the outcome events, which were also extracted from the MIMIC-III database.

Statistical Analysis

Normally distributed continuous variables are presented as the mean $\pm$ standard deviation, while non-normally distributed data are presented as the median [interquartile range (IQR)]. Differences in continuous variables were tested using the analysis of variance test or rank-sum test as appropriate. Categorical variables were presented as numbers (percentages) and tested by the chi-square test. Linear regression was used to evaluate *P* value for trend of each variable across 3 groups with different HR fluctuation. Multivariable Cox hazard regression models with backward processes were used to investigate the association between HR fluctuation and outcomes. Model 1 was adjusted for age, male sex, and weight. Model 2 was adjusted for model 1 plus SOFA score. Model 3 was adjusted for model 2 plus admission HR. Model 4 was adjusted for model 3 plus sedative use, ventilation use, and vasopressor use. Model 5 was adjusted for model 4 plus CHF, AF, hypertension, and liver disease. HR fluctuation was analyzed as both a continuous variable and a categorical variable in our study, aiming to show the association between HR fluctuation and mortality of MI patients more particular and comprehensive. For continuous variables, the hazard ratio and 95% confidence interval (CI) corresponded to a 10-bpm increase in HR fluctuation. For categorical variables, hazard ratios and 95% CIs in the high and medium HR fluctuation groups were calculated and compared with those in the low HR fluctuation group.

The crude and adjusted models using restricted cubic spline with 5 knots were constructed to flexibly represent the association between the hazards and HR fluctuation as a continuous variable, using a reference level of 30 bpm (10). We considered that HR fluctuation may be influenced by the use of anti-hypertensives, sedatives, and vasopressors. Thus, sensitivity analyses were conducted to determine whether the results persisted in subgroups with different admission HRs, with or without hypertension, AF, vasopressor use, ventilation use, and sedative use.

TABLE 1 | Baseline characteristics of enrolled participants grouped by HR fluctuation.

	Low HR fluctuation (< 30 bpm)	Medium HR fluctuation (30–49 bpm)	High HR fluctuation (≥ 50 bpm)	*P*	*P* for trend
Number	632	704	695		
Age, years	65.7 ± 14.1	67.3 ± 14.8	70.1 ± 13.4	<0.001	<0.001
Male	426 (67.4)	460 (65.3)	413 (59.4)	0.007	0.170
Weight, kg	82.9 ± 19.8	80.8 ± 19.3	79.0 ± 19.9	0.001	0.001
SAPS score	14.4 ± 4.7	16.0 ± 5.7	20.4 ± 6.2	<0.001	<0.001
SOFA score	2.0 (1.0–3.0)	2.0 (1.0–5.0)	5.0 (2.0–8.0)	<0.001	<0.001
Admission HR, bpm	78.2 ± 13.1	84.1 ± 14.8	91.8 ± 21.2	<0.001	<0.001
Sedative	94 (14.9)	200 (28.4)	367 (52.8)	<0.001	0.105
Ventilation	98 (15.5)	234 (33.2)	406 (58.4)	<0.001	0.064
Vasopressor	104 (16.5)	199 (28.3)	369 (53.1)	<0.001	0.129
Hypertension	388 (61.4)	413 (58.7)	366 (52.7)	0.004	0.137
CHF	181 (28.6)	263 (37.4)	334 (48.1)	<0.001	0.036
AF	85 (13.4)	140 (19.9)	285 (41.0)	<0.001	0.189
Liver disease	14 (2.2)	23 (3.3)	43 (6.2)	0.001	0.162
Renal disease	46 (7.3)	58 (8.2)	58 (8.3)	0.736	0.275
COPD	53 (8.4)	67 (9.5)	72 (10.4)	0.470	0.037
Diabetes	171 (27.1)	186 (26.4)	180 (25.9)	0.892	0.061
Depression	34 (5.4)	36 (5.1)	22 (3.2)	0.100	0.253
Malignancy	35 (5.5)	41 (5.8)	52 (7.5)	0.281	0.245
30-day mortality	41 (6.5)	64 (9.1)	198 (28.5)	<0.001	0.264
1-year mortality	80 (12.7)	121 (17.2)	279 (40.1)	<0.001	0.235

Baseline data were presented by 3 groups, namely, low HR fluctuation (<30 bpm), medium HR fluctuation (30–49 bpm), and high HR fluctuation (≥ 50 bpm). Normally distributed continuous variables are presented as the mean ± standard deviation, while non-normally distributed data are presented as the median (interquartile range). HR, heart rate; bpm, beats per minute; SAPS, simplified acute physiology score; SOFA, sequential organ failure assessment; CHF, congestive heart failure; AF, atrial fibrillation; COPD, chronic obstructive pulmonary disease.

A two-tailed test was performed, and a $P < 0.05$ was considered statistically significant in our study. SPSS software (version 23.0, IBM, NY, USA) and the R tool (version 3.6.3, R Foundation for Statistical Computing, Vienna, Austria) were used for statistical analysis.

RESULTS

Among 2,031 critically ill patients with MI, the mean age was 67.9 ± 14.2 years, and 64.0% of them were male. Patients with high HR fluctuation were significantly older in age, had lower weight and had higher admission HR (P for trend < 0.01). Patients with high HR fluctuation had a higher SAPS score of 20.4 ± 6.2 and a higher SOFA score of 5.0 (IQR, 2.0–8.0) (P for trend < 0.001). Additionally, this group was more likely to have comorbidities of CHF (P for trend < 0.05). Compared with the low HR fluctuation group, the high HR fluctuation group suffered a higher 30-day mortality (28.5 vs. 6.5%) and 1-year mortality (40.1 vs. 12.7%) ($P < 0.001$) (**Table 1**).

As a continuous variable, each 10-bpm increase in HR fluctuation was associated with a higher risk of 30-day mortality and 1-year mortality, with hazard ratios of 1.214 (95% CI, 1.179–1.250) and 1.193 (1.164–1.222), respectively. After further strict adjustment in model 5, the association remained significant, with hazard ratios of 1.122 (95% CI, 1.083–1.162) and 1.107 (95% CI, 1.074–1.140), respectively (**Table 2**).

TABLE 2 | Hazard ratio and 95% CI of HR fluctuation (continuous) for mortality.

	30-day mortality		1-year mortality	
	Hazard ratio (95% CI)	*P*	Hazard ratio (98% CI)	*P*
Model 1	1.214 (1.179–1.250)	<0.001	1.193 (1.164–1.222)	<0.001
Model 2	1.127 (1.089–1.165)	<0.001	1.113 (1.083–1.145)	<0.001
Model 3	1.117 (1.079–1.156)	<0.001	1.104 (1.073–1.136)	<0.001
Model 4	1.122 (1.083–1.162)	<0.001	1.115 (1.082–1.148)	<0.001
Model 5	1.122 (1.083–1.162)	<0.001	1.107 (1.074–1.140)	<0.001

The hazard ratio and 95% CI were calculated along with a 10-bpm HR fluctuation increase by the Cox hazard regression model using a backward process. Model 1 adjusted for age, male sex, and weight. Model 2 adjusted for model 1 plus SOFA score. Model 3 adjusted for model 2 plus admission HR. Model 4 adjusted for model 3 plus sedative use, ventilation use, and vasopressor use. Model 5 adjusted for model 4 plus CHF, AF, hypertension, and liver disease. HR, heart rate; SAPS, simplified acute physiology score; SOFA, sequential organ failure assessment; CHF, congestive heart failure; AF, atrial fibrillation; CI, confidence interval.

To better investigate the potential non-linear association between HR fluctuation and mortality, the relative hazard compared with an HR fluctuation of 30 bpm as a reference

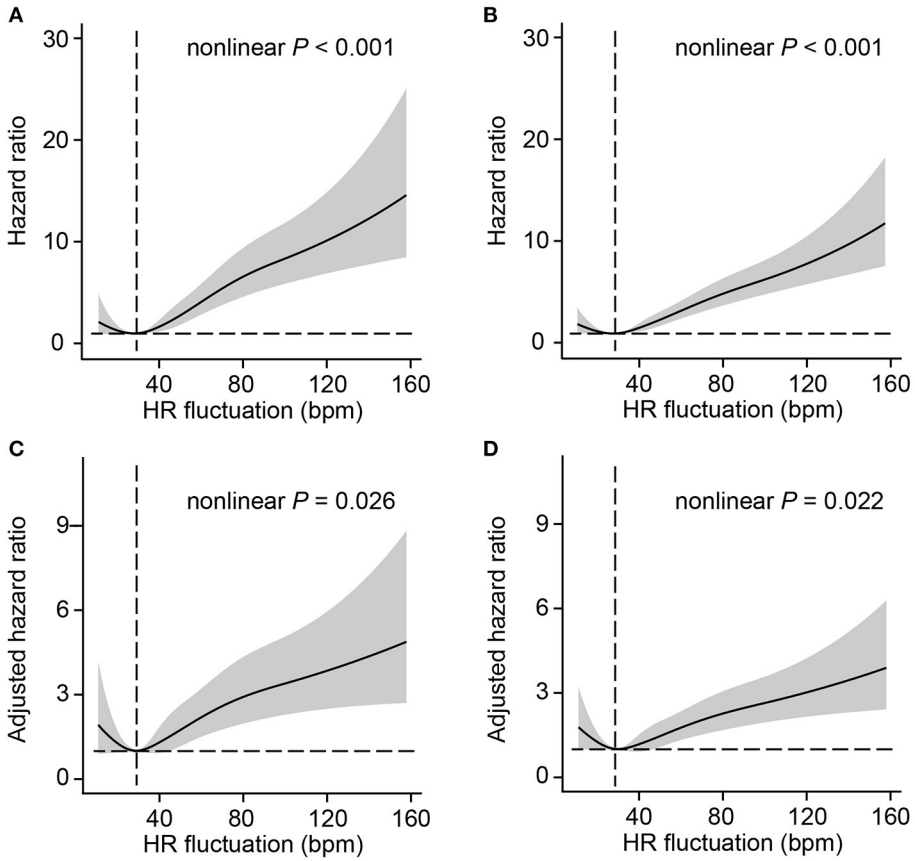

FIGURE 1 | Association between HR fluctuation and outcomes of MI patients. Crude hazard ratio and 95% CI for HR fluctuation in 30-day mortality **(A)** and 1-year mortality **(B)**. Adjusted hazard ratio and 95% CI for HR fluctuation in 30-day mortality **(C)** and 1-year mortality **(D)**. The analyses used a model with restricted cubic splines. The reference (hazard ratio = 1, horizontal dotted line) was an HR fluctuation of 30 bpm (vertical dotted line). Adjusted variables included age, male sex, weight, SOFA score, admission HR, sedative use, ventilation use, vasopressor use, CHF, AF, hypertension, and liver disease, namely, model 5 described above. HR, heart rate; SOFA, sequential organ failure assessment; CHF, congestive heart failure; AF, atrial fibrillation; CI, confidence interval.

was calculated. The association between HR fluctuation and mortality was similar in crude and adjusted models, with an increased risk in patients with HR fluctuation > 30 bpm. There was a typical J-type curve observed in restricted cubic splines for the association between HR fluctuation and 30-day or 1-year mortality of MI patients, with the lowest risk on the HR fluctuation of 30 bpm (**Figure 1**).

The survival rates were presented by 3 groups with different levels of HR fluctuation. Compared with the low HR fluctuation group, the high HR fluctuation group suffered a significantly higher risk of mortality after adjustment, with hazard ratios of 2.156 (95% CI, 1.483–3.134) for 30-day mortality and 1.796 (95% CI, 1.354–2.381) for 1-year mortality (**Figure 2**).

Subsequently, to determine the influence of admission HR on our results, all participants were divided into 2 subgroups with a cut-off value of admission HR at 85 bpm for further sensitivity analysis. In the subgroup with admission HR ≥ 85 bpm, each 10-bpm increase in HR fluctuation was correlated with an increased risk of 30-day mortality (hazard ratio, 1.112, 95% CI, 1.062–1.165) and 1-year mortality (hazard ratio, 1.099, 95% CI, 1.056–1.144). This result was also observed in participants who had an admission HR < 85 bpm. Furthermore, sensitivity analyses were also conducted for comorbidities of hypertension, AF, vasopressor use, ventilation use, and sedative use, which showed that the positive correlation between HR fluctuation and the risk of mortality was still statistically significant (each $P < 0.05$) (**Figure 3**).

DISCUSSION

In this retrospective cohort study with critically ill MI patients in the ICU, we found that the HR fluctuation was significantly associated with 30-day mortality and 1-year mortality, even after a broad array of potential confounders were taken into account. This association was independent of admission resting HR, comorbidities of hypertension or AF, or the use of ventilation or sedatives. Furthermore, a typical J-type curve was observed in restricted cubic splines for the association between HR fluctuation and 30-day or 1-year mortality of MI patients, indicating the lowest hazard on the HR fluctuation of 30 bpm. To the best of our knowledge,

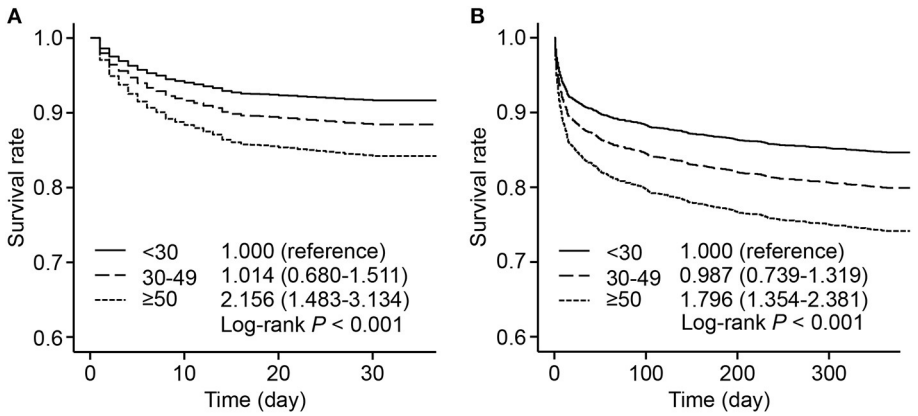

FIGURE 2 | Adjusted survival rate by 3 HR fluctuation groups. Survive curves presented adjusted survival rates of 30-day mortality **(A)** and 1-year mortality **(B)** by 3 HR fluctuation groups. Adjusted variables included age, male sex, weight, SOFA score, admission HR, sedative use, ventilation use, vasopressor use, CHF, AF, hypertension, and liver disease, namely, model 5 described above. The hazard ratio and 95% CI were calculated compared with those of the low HR fluctuation group. HR, heart rate; SOFA, sequential organ failure assessment; CHF, congestive heart failure; AF, atrial fibrillation; CI, confidence interval.

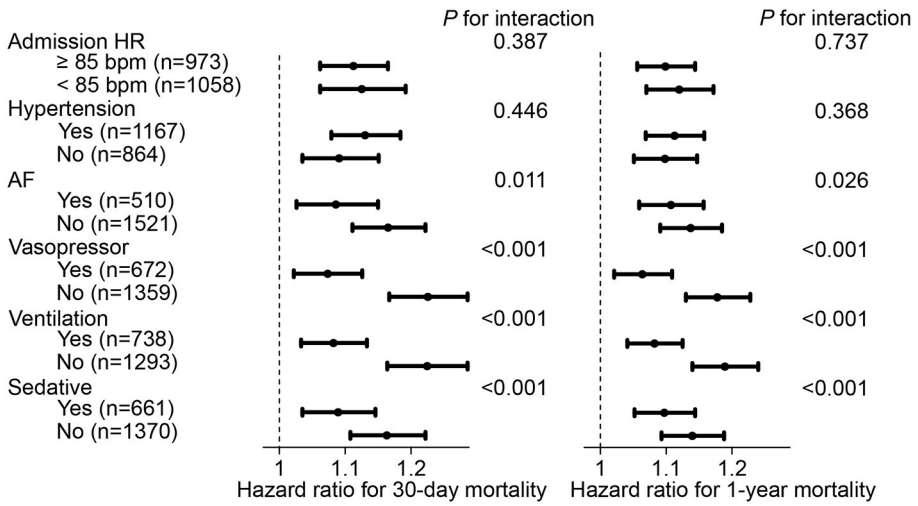

FIGURE 3 | Hazard ratio and 95% CI of HR fluctuation (continuous) for mortality in subgroups. Hazard ratio and 95% CI were calculated along as 10 bpm HR fluctuation increase by Cox hazard regression model using backward process. Model adjusted for age, male, weight, SOFA score, admission HR, sedative, ventilation, vasopressor, CHF, AF, hypertension, liver disease, namely model 5 described above. HR, heart rate; SOFA, sequential organ failure assessment; CHF, congestive heart failure; AF, atrial fibrillation; CI, confidence interval.

this is the first study clearly revealing the association between HR fluctuation and the risk of mortality in MI patients and highlighting that HR fluctuation may be a useful and easily measured marker as well as a prognostic predictor in clinical practice.

HR has been shown to be associated with cardiovascular outcomes in various large cohorts (11, 12). Additionally, beat-to-beat variations in HR have been reported to offer additional prognostic information for chronic heart failure, probably by reflecting autonomic dysfunction (13, 14). However, heart rate variability was complexly measured depending on ambulatory electrocardiography and limited to patients with sustained periods of normal sinus rhythm (15). HR fluctuation, calculated as the maximum minus the minimum HR using the initial 24-h data, showed its strength as a simpler and more generalizable marker. Recently, HR fluctuation was demonstrated to predict mortality and hospitalization in chronic heart failure (6). Another study showed that both high and low HR fluctuation were harmful for survival of critically ill patients in ICU (7). However, this current study focused on MI patients and found that HR fluctuation was positively associated with 30-day mortality and 1-year mortality in MI patients, emphasizing its feasibility and importance for outcome prediction of MI.

Indeed, HR may be easily affected by the use of drugs or other therapies, such as antihypertensives, antiarrhythmics,

vasopressors, ventilation, and sedatives. In a large cohort with 15,680 community participants, β-blocker use at any time during the study could alter the association between HR change from the preceding visit and outcomes, leading to an association that was no longer significant between change in HR and all-cause mortality and incident HF (16). In another cohort of hypertensive patients, HR remained a significant independent risk factor for cardiovascular mortality after correction for HR-limiting therapy (17). In our study, history of hypertension, AF, vasopressor use, ventilation use, and sedative use were included in the sensitivity analysis, showing the consistent correlation between HR fluctuation and the mortality of MI patients in the majority subgroups. Because admission HR was reported to be associated with the severity and complexity of coronary artery disease, a sensitivity analysis was also conducted to determine the potential influence of different admission HRs (18). Surprisingly, our results remained significant in subgroups with different levels of admission HR, demonstrating that HR fluctuation is a reliable risk factor for mortality in MI patients.

It should be noted that the risk correlated with an HR increase is not always strictly fitted to a linear association because it is evident that both too high or too low of an HR could be harmful. A non-linear curve was observed for a trend between the mean HR and incident stroke in diabetes patients, which indicated the lowest risk for the mean HR of 65 bpm (11). However, an increased risk of all-cause mortality, along with an increase in HR changes from the preceding visit, was reported in a community population (16). Our restricted cubic splines clearly showed a J-type curve for the association between HR fluctuation and the 30-day or 1-year mortality of MI patients. According to the restricted cubic spline plots, patients with HR fluctuation of 10 or 20 bpm were with higher risk but this association did not achieve statistical significance. Interestingly, for both the 30-day and 1-year mortality of MI patients, the lowest risk of HR fluctuation was ∼30 bpm, which might be a candidate marker for decision making in HR control strategies.

This study has some limitations. Our study was based on real-world clinical data, in which different intervals between HR monitoring measurements for each patient may exist. We calculated the HR fluctuation using the maximum and minimum HR across the initial 24 h and further adjusted for multiple covariates in the regression models to diminish their potential influence on mortality. Another limitation is that selection bias is inevitable in a retrospective study design, and future randomized controlled trials would help validate our findings.

CONCLUSION

In conclusion, this retrospective cohort study revealed a positive association between HR fluctuation and 30-day and 1-year mortality in critically ill MI patients in the ICU. This association was not affected by the comorbidities of hypertension and AF or by the use of ventilation and sedatives. HR fluctuation might be an accessible and reliable marker and risk factor for mortality in critically ill patients, which is worthy of further investigation.

DATA AVAILABILITY STATEMENT

Publicly available datasets were analyzed in this study. This data can be found here: https://physionet.org/content/mimiciii/1.4/.

ETHICS STATEMENT

Ethical review and approval was not required for the study on human participants in accordance with the local legislation and institutional requirements. Written informed consent for participation was not required for this study in accordance with the national legislation and the institutional requirements.

AUTHOR CONTRIBUTIONS

QG, JiW, and YZ conceived and designed the research protocol. QG, HL, and RS collected and analyzed the data, and wrote the first draft of the manuscript. All authors provided input on data analysis and interpretations, and participated in multiple revisions of the manuscript and approved the final version of the manuscript and agree to be accountable for all aspects of the work.

FUNDING

This study was funded by grants from the National Natural Science Foundation of China (Grant nos. 81700397, 81970388, 81870170, 82070237), Guangdong Basic and Applied Basic Research Foundation (Grant nos. 2019A1515011682, 2020A1515110313), Guangdong Basic and Applied Basic Research Foundation for Distinguished Young Scholars (Grant no. 2020B1515020027), Guangzhou Science and Technology Bureau (Grant nos. 201803040010, 202002020070), Bioland Laboratory (Guangzhou Regenerative Medicine and Health Guangdong Laboratory, Grant no. 2019GZR110406004), Fundamental Research Funds for the Central Universities (Grant no. 19ykpy108), and Yat-sen Start-up Foundation (Grant no. YXQH202014).

REFERENCES

1. Valley TS, Iwashyna TJ, Cooke CR, Sinha SS, Ryan AM, Yeh RW, et al. Intensive care use and mortality among patients with ST elevation myocardial infarction: retrospective cohort study. *BMJ*. (2019) 365:l1927. doi: 10.1136/bmj.l1927
2. Dessap AM, Roche-Campo F, Launay J-M, Charles-Nelson A, Katsahian S, Brun-Buisson C, et al. Delirium and circadian rhythm of melatonin during weaning from mechanical ventilation: an ancillary study of a weaning trial. *Chest*. (2015) 148:1231–41. doi: 10.1378/chest.15-0525
3. Gazendam JAC, Van Dongen HPA, Grant DA, Freedman NS, Zwaveling JH, Schwab RJ. Altered circadian rhythmicity in patients in the ICU. *Chest*. (2013) 144:483–9. doi: 10.1378/chest.12-2405
4. Böhm M, Swedberg K, Komajda M, Borer JS, Ford I, Dubost-Brama A, et al. Heart rate as a risk factor in chronic heart failure. (SHIFT): the association between heart rate and outcomes in a randomised placebo-controlled

trial. *Lancet*. (2010) 376:886–94. doi: 10.1016/S0140-6736(10)61259-7
5. Lonn EM, Rambihar S, Gao P, Custodis FF, Sliwa K, Teo KK, et al. Heart rate is associated with increased risk of major cardiovascular events, cardiovascular and all-cause death in patients with stable chronic cardiovascular disease: an analysis of ONTARGET/TRANSCEND. *Clin Res Cardiol*. (2014) 103:149–59. doi: 10.1007/s00392-013-0644-4
6. Cubbon RM, Ruff N, Groves D, Eleuteri A, Denby C, Kearney L, et al. Ambulatory heart rate range predicts mode-specific mortality and hospitalisation in chronic heart failure. *Heart*. (2016) 102:223–9. doi: 10.1136/heartjnl-2015-308428
7. Guo Q, Xiao Z, Lin M, Yuan G, Qiu Q, Yang Y, et al. Heart rate fluctuation predicts mortality in critically ill patients in the intensive care unit: a retrospective cohort study. *Ann Transl Med*. (2021) 9:334. doi: 10.21037/atm-20-7897
8. Johnson AEW, Pollard TJ, Shen L, Lehman L-WH, Feng M, Ghassemi M, et al. MIMIC-III, a freely accessible critical care database. *Sci Data*. (2016) 3:160035. doi: 10.1038/sdata.2016.35
9. Johnson AE, Stone DJ, Celi LA, Pollard TJ. The MIMIC code repository: enabling reproducibility in critical care research. *J Am Med Inform Assoc*. (2018) 25:32–9. doi: 10.1093/jamia/ocx084
10. Ng R, Kornas K, Sutradhar R, Wodchis WP, Rosella LC. The current application of the Royston-Parmar model for prognostic modeling in health research: a scoping review. *Diagn Progn Res*. (2018) 2:4. doi: 10.1186/s41512-018-0026-5
11. Böhm M, Schumacher H, Teo KK, Lonn EM, Mahfoud F, Ukena C, et al. Resting heart rate and cardiovascular outcomes in diabetic and non-diabetic individuals at high cardiovascular risk analysis from the ONTARGET/TRANSCEND trials. *Eur Heart J*. (2020) 41:231–8. doi: 10.1093/eurheartj/ehy808
12. Dobre D, Kjekshus J, Rossignol P, Girerd N, Benetos A, Dickstein K, et al. Heart rate, pulse pressure and mortality in patients with myocardial infarction complicated by heart failure. *Int J Cardiol*. (2018) 271:181–5. doi: 10.1016/j.ijcard.2018.05.017
13. Nolan J, Batin PD, Andrews R, Lindsay SJ, Brooksby P, Mullen M, et al. Prospective study of heart rate variability and mortality in chronic heart failure: results of the United Kingdom heart failure evaluation and assessment of risk trial. (UK-heart). *Circulation*. (1998) 98:1510–6. doi: 10.1161/01.CIR.98.15.1510
14. Tegegne BS, Man T, van Roon AM, Riese H, Snieder H. Determinants of heart rate variability in the general population: the lifelines cohort study. *Heart Rhythm*. (2018) 15:1552–8. doi: 10.1016/j.hrthm.2018.05.006
15. Huikuri HV, Mäkikallio T, Airaksinen KE, Mitrani R, Castellanos A, Myerburg RJ. Measurement of heart rate variability: a clinical tool or a research toy? *J Am Coll Cardiol*. (1999) 34:1878–83. doi: 10.1016/s0735-1097(99)00468-4
16. Vazir A, Claggett B, Cheng S, Skali H, Shah A, Agulair D, et al. Association of resting heart rate and temporal changes in heart rate with outcomes in participants of the atherosclerosis risk in communities study. *JAMA Cardiol*. (2018) 3:200–6. doi: 10.1001/jamacardio.2017.4974
17. Paul L, Hastie CE, Li WS, Harrow C, Muir S, Connell JMC, et al. Resting heart rate pattern during follow-up and mortality in hypertensive patients. *Hypertension*. (2010) 55:567–74. doi: 10.1161/HYPERTENSIONAHA.109.144808
18. Ma X, Wang Z, Wang J, Liu F, Zhang D, Yang L, et al. Admission heart rate is associated with coronary artery disease severity and complexity in patients with acute coronary syndrome. *Angiology*. (2019) 70:774–81. doi: 10.1177/0003319719832376

Conflict of Interest: The authors declare that the research was conducted in the absence of any commercial or financial relationships that could be construed as a potential conflict of interest.

frontiers in Cardiovascular Medicine

SYSTEMATIC REVIEW
published: 21 May 2021
doi: 10.3389/fcvm.2021.664647

Catheter Ablation vs. Anti-Arrhythmic Drugs as First-Line Treatment in Symptomatic Paroxysmal Atrial Fibrillation: A Systematic Review and Meta-Analysis of Randomized Clinical Trials

Andrea Saglietto[1], *Fiorenzo Gaita*[2], *Roberto De Ponti*[3], *Gaetano Maria De Ferrari*[1]* *and Matteo Anselmino*[1]

[1] Division of Cardiology, Department of Medical Sciences, "Città della Salute e della Scienza di Torino" Hospital, University of Turin, Turin, Italy, [2] Cardiology Unit, J Medical, Turin, Italy, [3] Department of Medicine and Surgery, University of Insubria, Varese, Italy

OPEN ACCESS

Edited by:
Antonio Zaza,
University of Milano-Bicocca, Italy

Reviewed by:
Giannis G. Baltogiannis,
Vrije University Brussel, Belgium
Richard Hauer,
University Medical Center
Utrecht, Netherlands

***Correspondence:**
Gaetano Maria De Ferrari
gaetanomaria.deferrari@unito.it

Specialty section:
This article was submitted to Cardiac Rhythmology, a section of the journal Frontiers in Cardiovascular Medicine

Received: 05 February 2021
Accepted: 14 April 2021
Published: 21 May 2021

Citation:
Saglietto A, Gaita F, De Ponti R, De Ferrari GM and Anselmino M (2021) Catheter Ablation vs. Anti-Arrhythmic Drugs as First-Line Treatment in Symptomatic Paroxysmal Atrial Fibrillation: A Systematic Review and Meta-Analysis of Randomized Clinical Trials.
Front. Cardiovasc. Med. 8:664647.
doi: 10.3389/fcvm.2021.664647

Background: Catheter ablation has become a well-established indication for long-term rhythm control in atrial fibrillation (AF) patients refractory to anti-arrhythmic drugs (AADs). Efficacy and safety of AF catheter ablation (AFCA) before AADs failure are, instead, questioned.

Objective: The aim of the study was to perform a systematic review and meta-analysis of randomized clinical trials (RCTs) comparing first-line AFCA with AADs in symptomatic patients with paroxysmal AF.

Methods: We performed a random-effects meta-analysis of binary outcome events comparing AFCA with AADs in rhythm control-naïve patients. The primary outcomes, also stratified by the type of ablation energy (radiofrequency or cryoenergy), were (1) recurrence of atrial tachyarrhythmias and (2) recurrence of symptomatic atrial tachyarrhythmias. The secondary outcomes included adverse events.

Results: Six RCTs were included in the analysis. AFCA was associated with lower recurrences of atrial tachyarrhythmias [relative risk (RR) 0.58, 95% confidence interval (CI) 0.46–0.72], consistent across the two types of ablation energy (radiofrequency, RR 0.50, 95% CI 0.28–0.89; cryoenergy, RR 0.60, 95% CI 0.50–0.72; *p*-value for subgroup differences: 0.55). Similarly, AFCA was related to less symptomatic arrhythmic recurrences (RR 0.46, 95% CI 0.27–0.79). Overall, adverse events did not differ. A trend toward increased periprocedural cardiac tamponade or phrenic nerve palsy was observed in the AFCA group, while more atrial flutter episodes with 1:1 atrioventricular conduction and syncopal events were reported in the AAD group.

Conclusions: First-line rhythm control therapy with AFCA, independent from the adopted energy source (radiofrequency or cryoenergy), reduces long-term arrhythmic recurrences in patients with symptomatic paroxysmal AF compared with AADs.

Keywords: atrial fibrillation, catheter ablation, rhythm control, anti-arrhythmic drugs, side effects

INTRODUCTION

Atrial fibrillation (AF) is the most common supraventricular arrhythmia, affecting up to 2% of the population (1). Anti-arrhythmic drugs (AADs) are considered as the first-line option for the maintenance of sinus rhythm (rhythm control) in patients with symptomatic AF episodes; however, they are limited by a relatively low efficacy and substantial side effects (2–4). AF catheter ablation (AFCA) has established itself as a superior alternative to AADs in terms of long-term sinus rhythm maintenance and quality of life (5, 6). Accordingly, AFCA has been recommended in case of AAD failure by the most recent guidelines (1, 7).

A possible role for AFCA also as first-line option in paroxysmal AF is emerging. A shorter time between first AF documentation and ablation is associated with lower arrhythmic recurrences, implying a lower probability of disease progression toward persistent AF (4, 8, 9). In the last decade, three randomized clinical trials (RCTs) evaluating radiofrequency (RF) ablation compared with AADs as first-line treatment in rhythm control-naïve patients (10–12) had demonstrated lower recurrence rate by ablation, at the price of transiently exposing the patient to the rare, but not negligible, risk of periprocedural complications (13). More recently, three RCTs comparing cryoballoon ablation and AADs as first-line rhythm control therapy have been published (14–16).

The aim of the present study is to perform an updated systematic review and meta-analysis comparing efficacy and safety of AFCA vs. AADs as first-line rhythm control strategy in patients with paroxysmal AF, also assessing potential differences related to ablation energy source (RF or cryoenergy).

METHODS

The present systematic review and meta-analysis was performed in accordance to Preferred Reporting Items for Systematic Reviews and Meta-Analyses (PRISMA) guidelines (17).

Search Strategy, Study Selection, and Quality Assessment

We screened PubMed/MEDLINE and Embase databases from their inceptions to March 7, 2021, using the following search terms: "atrial fibrillation AND ablation AND first-line."

The inclusion criteria were as follows: (a) prospective RCTs comparing AFCA (RF or cryoballoon ablation) with AADs as first-line rhythm control treatment in symptomatic AF; and (b) availability of data regarding arrhythmic recurrences (symptomatic or asymptomatic).

Two investigators (AS and MA) independently reviewed the titles/abstracts and studies to determine their eligibility based on the inclusion criteria and extracted all the relevant features, including study characteristics, baseline population data, and outcomes (assessment and measures). A third reviewer (GMDF) resolved disagreement. Risk of bias assessment was performed at the study level using the Cochrane bias risk assessment tool (RoB 2) (18).

Outcomes

The primary efficacy outcomes of the present analysis were as follows: (1) recurrence of atrial tachyarrhythmias and (2) recurrence of symptomatic atrial tachyarrhythmias. According to study design, recurrent atrial tachyarrhythmia included AF alone, or AF and/or atrial tachycardia/atrial flutter (AT/AFL).

The secondary outcome endpoints were all-cause death, proportion of crossover to the alternative arm, proportion of patients undergoing ablation after failure of the initial treatment (either AFCA or AADs), stroke/transient ischemic attack (TIA), cardiac tamponade, phrenic nerve palsy, atrioesophageal fistula, pulmonary vein (PV) stenosis >70%, atrial flutter with 1:1 AV conduction, ventricular tachycardia, symptomatic bradycardia requiring pacemaker implantation, and syncope.

Statistical Analysis

Baseline characteristics of pooled study populations were reported as median values between the included studies, along with their interquartile range (IQR). Random-effects model meta-analysis of binary outcome events, taking into account the estimated between-study heterogeneity, was performed for the present analysis using inverse-variance method. The resulting meta-analytic relative risk (RR) of observing the investigated outcomes in AFCA group compared with AAD group, along with their 95% confidence interval (CI), is reported. Forest plots for the primary outcome endpoints are shown, stratified by ablation energy type (RF or cryoenergy). A test for subgroup differences was also performed. Heterogeneity across studies was assessed using the Cochran Q test. Higgins I^2 statistics was used to determine the degree of between-study heterogeneity (I^2 < 25%, low; 25–50%, moderate; and >50%, high degree of heterogeneity). Due to the low number of studies included, we did not investigate publication bias, and we did not performed meta-regression to assess potential source of heterogeneity. *P*-values <0.05 were considered statistically significant. Statistical analyses were performed with R version 4.0.0 (R Foundation for Statistical Computing, Vienna, Austria).

RESULTS

Included Studies and Population Characteristics

A total of 342 studies were identified by literature search. After detailed evaluation, six RCTs (10–12, 14–16) were finally included in the systematic review and meta-analysis (refer to **Supplementary Figure 1** for PRISMA flowchart). The 5-year follow-up data of MANTRA-PAF (19) was not considered since clinical assessment and electrocardiographic monitoring were not performed between the second and 5th year. The main characteristics of the included RCTs are reported in **Table 1**. Ablation energy was RF in RAAFT-1 (10), MANTRA-PAF (11), and RAAFT-2 (12) while cryoenergy in EARLY-AF (14), STOP-AF (15), and Cryo-FIRST (16). Further, details regarding study inclusion/exclusion criteria and study-specific endpoints may be found in the **Supplementary Tables 1, 2**. Risk of bias in the individual studies is reported in **Figure 1**: the overall risk of bias

TABLE 1 | Main characteristics of the included randomized clinical trials comparing first-line catheter ablation with antiarrhythmic drugs in symptomatic atrial fibrillation.

Study	Study type	Enrollment period	No. of patients included in the primary analysis (AFCA/AADs)	Paroxysmal AF (%)	Type of ablation energy used	Follow-up duration (months)
RAAFT-1 [Wazni et al. (10)]	Prospective, randomized, multicenter	2001–2002	32/35	96%	Radiofrequency	12
MANTRA-PAF [Cosedis Nielsen et al. (11)]	Prospective, randomized, multicenter	2005–2009	146/148	100%	Radiofrequency	24
RAAFT-2 [Morillo et al. (12)]	Prospective, randomized, multicenter	2006–2010	66/61	98%	Radiofrequency	24
EARLY-AF [Andrade et al. (14)]	Prospective, randomized, multicenter	2017–2018	154/149	95%	Cryoenergy	12
STOP-AF [Wazni et al. (15)]	Prospective, randomized, multicenter (Canada)	2017–2019	104/99	100%	Cryoenergy	12
Cryo-FIRST [Kuniss et al. (16)]	Prospective, randomized, multicenter	2014–2018	107/111	100%	Cryoenergy	12

AFCA, atrial fibrillation catheter ablation; AADs, anti-arrhythmic drugs; AF, atrial fibrillation.

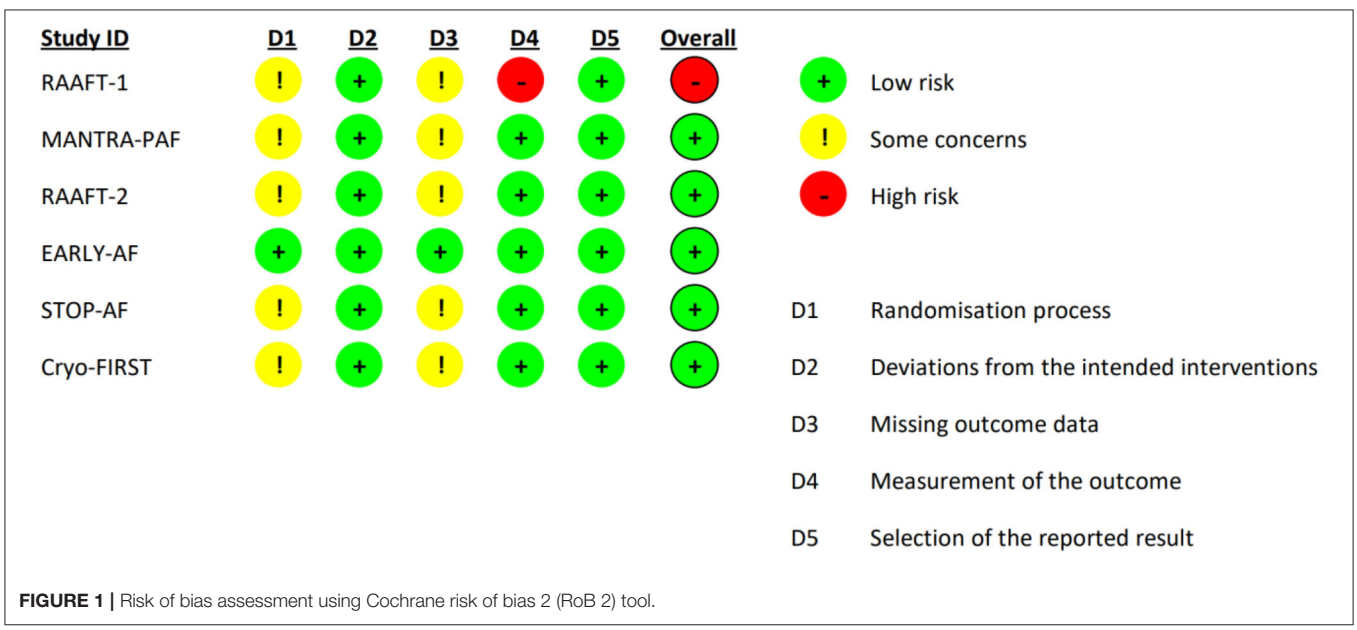

FIGURE 1 | Risk of bias assessment using Cochrane risk of bias 2 (RoB 2) tool.

for five studies was low, while RAAFT-1 trial (10) was considered at high risk of bias due to the unblinded outcome adjudication.

The resulting meta-analytic population encompassed 1,204 patients [603 randomized to AFCA (365 cryoballoon ablation, 61%; 238 RF ablation, 39%) and 601 to AADs], with a median follow-up of 12 (IQR 12–24) months. AF type was paroxysmal in nearly the totality of the patients (99%, IQR 96–100%). Median age was 55 (IQR 54–59) years, with nearly 2:1 male-to-female ratio (male 70%, IQR 68–71%). Hypertension was the most frequent concurrent comorbid condition (37%, IQR 33–41%), while baseline heart failure was rare [2%, IQR 1–6%; left ventricular ejection fraction (LVEF) 61%, IQR 60–61%]. Median left atrial antero-posterior diameter was 40 mm (IQR 38–41 mm). Mean $CHADS_2$ score in MANTRA-PAF (11) and RAAFT-2 (12) was 0.6, while mean CHA_2DS_2-VASc score was 1.9 in EARLY-AF (14); 66% and 86% of the patients in STOP-AF (15) and in Cryo-FIRST (16), respectively, had a CHA_2DS_2-VASc score $\leq$2; and 58% (IQR 51–60%) of the patients were on beta-blocker therapy at the time of randomization.

Table 2 reports study-specific ablation protocol, AAD use in both treatment arms, type of monitoring, and definition of arrhythmic recurrence. All patients underwent PV isolation (PVI). In two RF studies, additional ablation lesion was also allowed at the physician's discretion [MANTRA-PAF (11) and RAAFT-2 (12)], while in Cryo-FIRST study, additional freeze applications were allowed in case of incomplete PVI isolation or focal trigger identification (16). AAD use in AFCA arm was only allowed during post-procedural blanking period in most of the studies. Continuous electrocardiographic monitoring with an implantable loop recorder was only performed in EARLY-AF (14).

Primary Endpoints

The threshold defining an arrhythmic recurrence varied between 15 s in RAAFT-1 (10) and 60 s in MANTRA-PAF (11), with the four remaining studies used a 30-s threshold (12, 14–16).

As illustrated in **Figure 2**, AFCA was associated with a higher probability of freedom from any arrhythmic recurrence compared with AADs (RR 0.58, 95% CI 0.46–0.72, $I^2 = 46\%$), consistent across the two types of ablation energy used (RF, RR 0.50, 95% CI 0.28–0.89, $I^2 = 75\%$; cryoenergy, RR 0.60, 95% CI 0.50–0.72, $I^2 = 0\%$; *p*-value for subgroup differences: 0.55). Similarly, AFCA is related to higher probability of freedom from symptomatic arrhythmic recurrence (**Figure 3**; RR 0.46, 95% CI 0.27–0.79, $I^2 = 71\%$), irrespective of ablation energy used (RF, RR 0.46, 95% CI 0.22–0.98, $I^2 = 76\%$; cryoenergy, RR 0.42, 95% CI 0.25–0.71, $I^2 = 0\%$; *p*-value for subgroup differences: 0.85). Sensitivity analysis only considering studies with low risk of bias gave similar results (**Supplementary Figures 2, 3**).

Secondary Endpoints

Secondary endpoints are detailed in **Table 3**, while forest plots are reported in **Supplementary Figures 4–14**. All-cause deaths

TABLE 2 | Study-specific ablation protocol, AAD use in both treatment arms, type of monitoring, and definition of arrhythmic recurrence.

Study	Ablation protocol	AAD therapy	AAD use after index ablation in AFCA arm	Arrhythmic recurrence monitoring	Definition of arrhythmic recurrence
RAAFT-1 [Wazni et al. (10)]	PVI	Flecainide, propafenone, and sotalol (according to physician preference)	Not permitted	Clinical follow-up and intermittent electrocardiographic monitoring (event recorder, 24-h Holter)	Any recurrence of AF lasting longer than 15 s
MANTRA-PAF [Cosedis Nielsen et al. (11)]	PVI + additional lesions allowed (according to physician preference)	Propafenone, flecainide, sotalol, dofetilide, and amiodarone (according to physician preference)	Only allowed during the 90-day blanking period	Clinical follow-up and intermittent electrocardiographic monitoring (7-day Holter)	Any recurrence of AF lasting longer than 1 min
RAAFT-2 [Morillo et al. (12)]	PVI + additional lesions allowed (according to physician preference)	Flecainide, propafenone, sotalol, and amiodarone (according to physician preference)	Only allowed during the 3-month blanking period	Clinical follow-up and intermittent electrocardiographic monitoring (event recorder, 24-h Holter)	Any recurrence of atrial tachyarrhythmia (AF, AT/AFL) lasting longer than 30 s
EARLY-AF [Andrade et al. (14)]	PVI	Flecainide, propafenone, dronedarone, sotalol, and amiodarone (according to physician preference)	Only allowed during the blanking period (excluding amiodarone); to be discontinued at least five half-lives before the end of the 90-day blanking period	Clinical follow-up and continuous electrocardiographic monitoring (loop recorder)	Any recurrence of atrial tachyarrhythmia (AF, AT/AFL) lasting longer than 30 s
STOP-AF [Wazni et al. (15)]	PVI	Flecainide, propafenone, dronedarone, sotalol, and amiodarone (according to physician preference)	Only allowed for up to 80 days after the procedure (excluding amiodarone), to allow complete washout by the end of the 90-day blanking period	Clinical follow-up and intermittent electrocardiographic monitoring (event recorder, 24-h Holter)	Any recurrence of atrial tachyarrhythmia (AF, AT/AFL) lasting longer than 30 s
Cryo-FIRST [Kuniss et al. (16)]	PVI + additional freeze applications allowed (in case of incomplete PV isolation or focal trigger identification)	Flecainide, propafenone, dronedarone, sotalol, and amiodarone (according to physician preference)	Only allowed during the 3-month blanking period	Clinical follow-up and intermittent electrocardiographic monitoring (7-day Holter)	Any recurrence of atrial tachyarrhythmia (AF, AT/AFL) lasting longer than 30 s

AAD, antiarrhythmic drug; AFCA, atrial fibrillation catheter ablation; AF, atrial fibrillation; PVI, pulmonary vein isolation; AT/AFL, atrial tachycardia/atrial flutter.

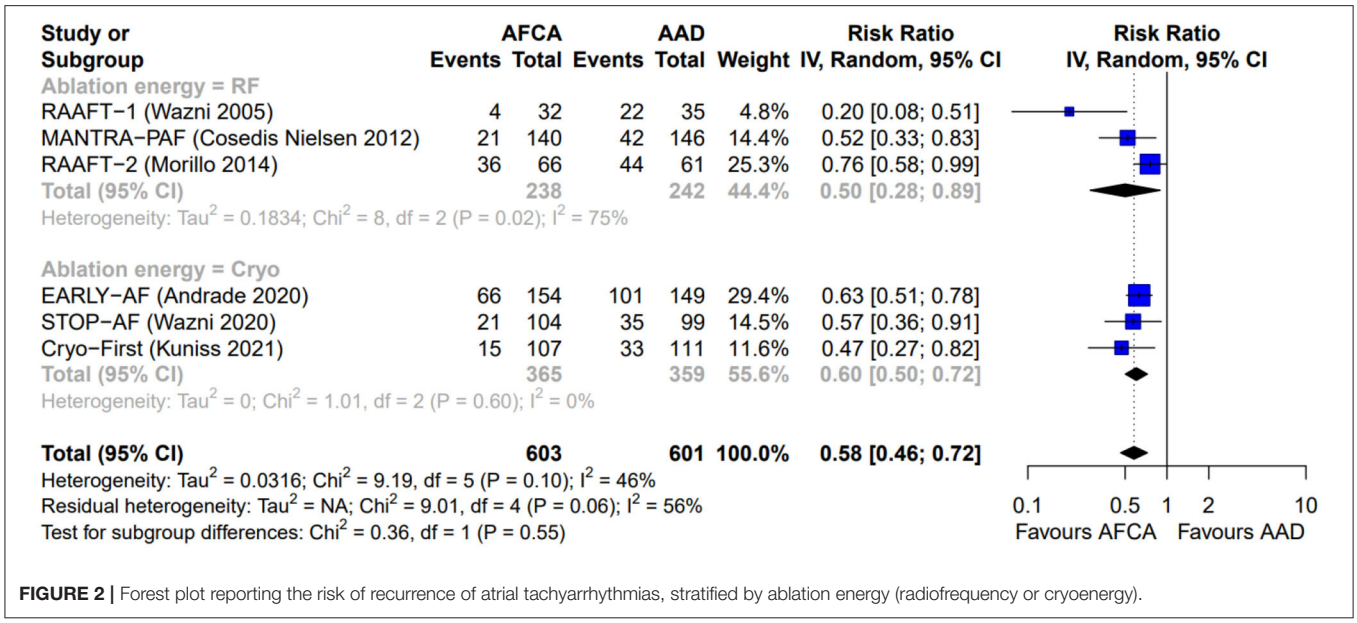

FIGURE 2 | Forest plot reporting the risk of recurrence of atrial tachyarrhythmias, stratified by ablation energy (radiofrequency or cryoenergy).

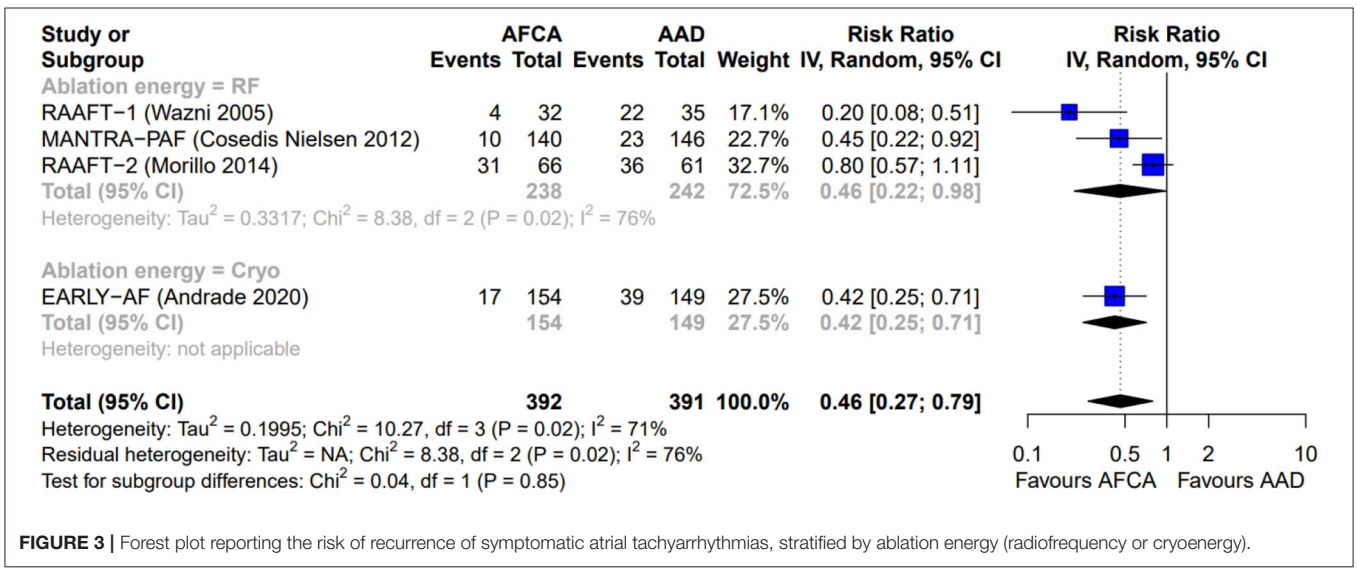

FIGURE 3 | Forest plot reporting the risk of recurrence of symptomatic atrial tachyarrhythmias, stratified by ablation energy (radiofrequency or cryoenergy).

did not differ between AFCA and AAD groups (0.5 vs. 0.7%, RR 0.86, 95% CI 0.28–2.67, $I^2 = 0\%$). Crossover to the alternative arm was significantly less frequent in AFCA compared with AAD group (7.9 vs. 28.2%; RR 0.23, 95% CI 0.10–0.51; $I^2 = 77\%$). No significant differences in terms of stroke/TIA (0.8 vs. 0.8%, RR 0.98, CI 0.33–2.95; $I^2 = 0\%$) were found. Concerning procedural complications, there was a nons-ignificant trend toward more cardiac tamponade/clinically significant pericardial effusion (1.3 vs. 0.2%; RR 2.35, CI 0.62–8.93; $I^2 = 0\%$) or phrenic nerve palsy (1.4 vs. 0.3%; RR 2.42, CI 0.40–14.63; $I^2 = 4\%$) in the AFCA group. No atrio-esophageal fistula were observed, and only one severe PV stenosis was documented after an RF ablation procedure. Conversely, a trend toward more AFL episodes with 1:1 atrioventricular conduction (0 vs. 1.5%; RR 0.25, CI 0.03–2.25; $I^2 = 0\%$) and syncope (0.2 vs. 1.4%; RR 0.30, CI 0.08–1.12; $I^2 = 0\%$) was observed in the AAD group.

DISCUSSION

The present meta-analysis indicates that, compared with AADs, first-line therapy with AFCA reduces arrhythmic recurrences in symptomatic patients with paroxysmal AF independently from the adopted energy source. This result is achieved without exposing the patients to an increase of adverse events. In addition, crossover to the alternative treatment arm is significantly less frequent in patients undergoing AFCA as first-line rhythm management. AFCA, in fact, is candidate gold standard treatment when sinus rhythm maintenance is strongly desired in symptomatic AF patients.

TABLE 3 | Meta-analysis results for pre-specified secondary outcomes.

Secondary outcomes	No. of studies	Included patients (AFCA/AAD)	AFCA (% of included patients)	AADs (% of included patients)	RR (95% CI)
All-cause death	6	1204 (603/601)	3 (0.5%)	4 (0.7%)	0.86 (0.28–2.67)
Crossover to alternative treatment arm	6	1204 (603/601)	48 (7.9%)	169 (28.2%)	0.23 (0.10–0.51)
Ablation during follow-up	6	1204 (603/601)	96 (15.9%)	169 (28.2%)	0.33 (0.12–0.88)
Stroke or transient ischemic attack	6	1204 (603/601)	5 (0.8%)	5 (0.8%)	0.98 (0.33–2.95)
Cardiac tamponade or clinically significant pericardial effusion	6	1204 (603/601)	8 (1.3%)	1 (0.2%)	2.35 (0.62–8.93)
Phrenic nerve palsy	3*	724 (365/359)	5§ (1.4%)	1§ (0.3%)	2.42 (0.40–14.63)
Atrioesophageal fistula	6	1204 (603/601)	0 (0%)	0 (0%)	n.a.
Severe pulmonary vein stenosis	4	683 (342/341)	1 (0.3%)	0 (0%)	1.43 (0.23–9.01)
Atrial flutter with 1:1 atrioventricular conduction	2	413 (206/207)	0 (0%)	3 (1.5%)	0.25 (0.03–2.25)
Ventricular tachycardia	6	1204 (603/601)	2 (0.3%)	3 (0.5%)	0.88 (0.22–3.46)
Bradycardia requiring pacemaker implantation	4	919 (464/455)	3 (0.6%)	5 (1.1%)	0.80 (0.21–3.05)
Syncope	5	1137 (571/566)	1 (0.2%)	8 (1.4%)	0.30 (0.08–1.12)

AFCA, atrial fibrillation catheter ablation; AAD, anti-arrhythmic drug.

**This outcome was evaluated in the three most recent RCTs which used cryoenergy.*

§*In all cases the palsy was reversible.*

Periprocedural risk, mainly characterized by cerebral ischemic events, pericardial effusion (possibly leading to cardiac tamponade requiring urgent pericardiocentesis), and, particularly for cryoballoon ablation, phrenic nerve palsy is of concern. However, AFCA has dramatically improved its safety profile in the last decade. Technological advancement, increased experience, and shared evidence-based protocols (20), despite an increase in patient-specific risk profile (e.g., older patients in the "modern" cohort), have halved periprocedural complications in post-2010 compared with pre-2010 cohorts (2.3 vs. 5%) (21).

Conversely, AADs expose patients to a long-term risk of potential side effects, in particular pro-arrhythmic, which are, differently from AFCA, spread over time rather than concentrated in a specific period (22). The present analysis reports generally low complication rates in both study groups. However, the median 12-month follow-up may have limited collection of AAD-related side effects, while at the same time it likely captures all AFCA complications. Considering that patients initially treated with AADs, due to the overall modest efficacy of AADs in maintaining sinus rhythm (2), frequently undergo AFCA in the following 12 months (approximately one third), first-line AFCA may not only significantly shorten the "diagnosis-to-ablation time" maximizing rhythm outcome but also potentially prevent the sum of AFCA-related periprocedural risk and AADs side effects in drug-refractory patients.

Of note, the meta-analytic population was mainly constituted by relatively young, symptomatic patients, without overt underlying structural heart disease (guaranteed by the strict RCT inclusion criteria). As an example, median age in the CABANA (Catheter Ablation vs. Antiarrhythmic Drug Therapy on Mortality, Stroke, Bleeding, and Cardiac Arrest Among Patients With Atrial Fibrillation) trial (6) was significantly higher compared with the present population (67.5 vs. 55 years), with seven times more patients presenting with heart failure (15 vs. 2%) and higher thromboembolic risk (82% of patients with CHA2DS2-VASc score $\geq$2). Similarly, real-world data (23) indicate that on average AFCA candidates are older, with more comorbid conditions, higher thromboembolic risk profile, and frequent history of treatment failure with AADs. This suggests that particular caution should be used before extrapolating these data to the general AF population; however, it can be speculated that the observed low event rate of side effects in the AAD group might also relate to the healthier population. Unlike AFCA-related adverse events, which are mainly operator- and center-dependent, potential toxicity of AADs is known to increase with patient-related factors such as heart failure and underlying structural heart disease (22).

Finally, the present is the first analysis showing that cryoballoon ablation, previously demonstrating non-inferiority to RF ablation for the treatment of patients with drug-refractory

paroxysmal AF (24), has similar efficacy to RF ablation also as a first-line option. In fact, cryoballoon ablation was reported to have fewer cardiac tamponades than ablation, and the most frequent and specific cryoballoon complication, phrenic nerve palsy, resolved within 1 month in three EARLY-AF (14) patients and was not present at 12-month follow-up in all STOP-AF cases (15); in Cryo-FIRST, the only transient case of phrenic nerve palsy occurred in a patient who crossed to AFCA arm after being randomized to AAD treatment arm (16).

Limitations

Some limitations of the present analysis need to be addressed. First, the threshold defining an arrhythmic event varied between the included studies (from 15 to 60 s) and arrhythmia monitoring during follow-up was heterogeneous, ranging from clinical follow-up visits with intermittent rhythm monitoring to continuous monitoring with implantable loop records in one study (14). These differences may have an influence on the observed recurrent rate, even if a change in the proportional efficacy of the two treatment arms considered is unlikely. Second, also the type of arrhythmia considered as arrhythmic recurrences was variable between the studies, with two studies only including AF and four studies considering both AF and AT/AFL (**Table 2**), Nevertheless, arrhythmic recurrences are mainly AF episodes (25); thus, it is unlikely that the present results would have been affected by the inclusion of AT/AFL as arrhythmic recurrences in RAAFT-1 (10) and MANTRA-PAF (11). Third, we cannot exclude that the unblinded nature of the studies may have contributed to ablation benefit concerning symptomatic recurrences. Fourth, the analysis was not powered to detect potential significant differences in most of the secondary outcomes. Due to the low absolute number of events, we did not perform subgroup meta-analysis (RF or cryoenergy ablation) for the secondary outcomes.

CONCLUSIONS

Compared with AADs, first-line therapy with AFCA, independently from the adopted energy source (RF or cryoenergy), reduces arrhythmic recurrences in symptomatic, paroxysmal AF patients without increasing exposure to complications. First-line AFCA, performed in high-volume experienced centers with low complication rate, candidates as for the preferable choice for sinus rhythm maintenance in relatively young, healthy patients without overt structural heart disease.

DATA AVAILABILITY STATEMENT

The original contributions presented in the study are included in the article/**Supplementary Material**, further inquiries can be directed to the corresponding author/s.

AUTHOR CONTRIBUTIONS

AS and MA conceived the study. AS performed literature search, data extraction, and statistical analysis. AS, FG, RD, GD, and MA critically analyzed the results and wrote the manuscript. All authors contributed to the article and approved the submitted version.

SUPPLEMENTARY MATERIAL

The Supplementary Material for this article can be found online at: https://www.frontiersin.org/articles/10.3389/fcvm.2021.664647/full#supplementary-material

REFERENCES

1. Hindricks G, Potpara T, Dagres N, Arbelo E, Bax JJ, Blomström-Lundqvist C, et al. 2020 ESC guidelines for the diagnosis and management of atrial fibrillation developed in collaboration with the European Association of Cardio-Thoracic Surgery (EACTS): the task force for the diagnosis and management of atrial fibrillation of the European. *Eur Heart J.* (2020) 42:373–498. doi: 10.1093/eurheartj/ehaa612
2. Valembois L, Audureau E, Takeda A, Jarzebowski W, Belmin J, Lafuente-Lafuente C. Antiarrhythmics for maintaining sinus rhythm after cardioversion of atrial fibrillation. *Cochrane Database Syst Rev.* (2019) 2019:CD005049. doi: 10.1002/14651858.CD005049.pub5
3. Calkins H, Reynolds MR, Spector P, Sondhi M, Xu Y, Martin A, et al. Treatment of atrial fibrillation with antiarrhythmic drugs or radiofrequency ablation: two systematic literature reviews and meta-analyses. *Circ Arrhythmia Electrophysiol.* (2009) 2:349–61. doi: 10.1161/CIRCEP.108.824789
4. Chew DS, Black-Maier E, Loring Z, Noseworthy PA, Packer DL, Exner D V., et al. Diagnosis-to-Ablation time and recurrence of atrial fibrillation following catheter ablation: a systematic review and meta-analysis of observational studies. *Circ Arrhythmia Electrophysiol.* (2020) 13:350–7. doi: 10.1161/CIRCEP.119.008128
5. Khan AR, Khan S, Sheikh MA, Khuder S, Grubb B, Moukarbel G V. Catheter ablation and antiarrhythmic drug therapy as first- or second-line therapy in the management of atrial fibrillation: systematic review and meta-analysis. *Circ Arrhythmia Electrophysiol.* (2014) 7:853–60. doi: 10.1161/CIRCEP.114.001853
6. Packer DL, Mark DB, Robb RA, Monahan KH, Bahnson TD, Poole JE, et al. Effect of catheter ablation vs. antiarrhythmic drug therapy on mortality, stroke, bleeding, and cardiac arrest among patients with atrial fibrillation: The CABANA randomized clinical trial. *JAMA.* (2019) 321:1261–74. doi: 10.1001/jama.2019.0693
7. January CT, Wann LS, Alpert JS, Calkins H, Cigarroa JE, Cleveland JC, et al. 2014 AHA/ACC/HRS guideline for the management of patients with atrial fibrillation: A report of the American college of Cardiology/American heart association task force on practice guidelines and the heart rhythm society. *J Am Coll Cardiol.* (2014) 64:e1–76. doi: 10.1016/j.jacc.2014.03.022
8. Bunch TJ, May HT, Bair TL, Johnson DL, Weiss JP, Crandall BG, et al. Increasing time between first diagnosis of atrial fibrillation and catheter ablation adversely affects long-term outcomes. *Hear Rhythm.* (2013) 10:1257–62. doi: 10.1016/j.hrthm.2013.05.013
9. Kawaji T, Shizuta S, Yamagami S, Aizawa T, Komasa A, Yoshizawa T, et al. Early choice for catheter ablation reduced readmission in management of atrial fibrillation: impact of diagnosis-to-ablation time. *Int J Cardiol.* (2019) 291:69–76. doi: 10.1016/j.ijcard.2019.03.036
10. Wazni OM, Marrouche NF, Martin DO, Verma A, Bhargava M, Saliba W, et al. Radiofrequency ablation vs. antiarrhythmic drugs as first-line treatment of symptomatic atrial fibrillation: a randomized trial. *J Am Med Assoc.* (2005) 293:2634–40. doi: 10.1001/jama.293.21.2634

11. Cosedis Nielsen J, Johannessen A, Raatikainen P, Hindricks G, Walfridsson H, Kongstad O, et al. Radiofrequency ablation as initial therapy in paroxysmal atrial fibrillation. *N Engl J Med.* (2012) 367:1587–95. doi: 10.1056/NEJMoa1113566
12. Morillo CA, Verma A, Connolly SJ, Kuck KH, Nair GM, Champagne J, et al. Radiofrequency ablation vs. antiarrhythmic drugs as first-line treatment of paroxysmal atrial fibrillation (RAAFT-2) a randomized trial. *JAMA*. (2014) 311:692–9. doi: 10.1001/jama.2014.467
13. Hakalahti A, Biancari F, Nielsen JC, Raatikainen MJP. Radiofrequency ablation vs. antiarrhythmic drug therapy as first line treatment of symptomatic atrial fibrillation: systematic review and meta-analysis. *Europace.* (2015) 17:370–8. doi: 10.1093/europace/euu376
14. Andrade JG, Wells GA, Deyell MW, Bennett M, Essebag V, Champagne J, et al. Cryoablation or drug therapy for initial treatment of atrial fibrillation. *N Engl J Med.* (2020) 384:305–15. doi: 10.1056/NEJMoa2029980
15. Wazni OM, Dandamudi G, Sood N, Hoyt R, Tyler J, Durrani S, et al. Cryoballoon ablation as initial therapy for atrial fibrillation. *N Engl J Med.* (2020) 384: 316–24. doi: 10.1056/NEJMoa2029554
16. Kuniss M, Pavlovic N, Velagic V, Hermida JS, Healey S, Arena G, et al. Cryoballoon ablation vs. antiarrhythmic drugs: first-line therapy for patients with paroxysmal atrial fibrillation. *EP Eur.* (2021):euab029. doi: 10.1093/europace/euab029
17. Liberati A, Altman DG, Tetzlaff J, Mulrow C, Gøtzsche PC, Ioannidis JPA, et al. The PRISMA statement for reporting systematic reviews and meta-analyses of studies that evaluate healthcare interventions: explanation and elaboration. *BMJ.* (2009) 339:b2700. doi: 10.1136/bmj.b2700
18. Sterne JAC, Savović J, Page MJ, Elbers RG, Blencowe NS, Boutron I, et al. RoB 2: a revised tool for assessing risk of bias in randomised trials. *BMJ.* (2019) 366:l4898. doi: 10.1136/bmj.l4898
19. Nielsen JC, Johannessen A, Raatikainen P, Hindricks G, Walfridsson H, Pehrson SM, et al. Long-term efficacy of catheter ablation as first-line therapy for paroxysmal atrial fibrillation: 5-year outcome in a randomised clinical trial. *Heart.* (2017) 103:368–76. doi: 10.1136/heartjnl-2016-309781
20. Cheung JW, Yeo I, Cheng EP, Ip JE, Thomas G, Liu CF, et al. Inpatient hospital procedural volume and outcomes following catheter ablation of atrial fibrillation. *J Cardiovasc Electrophysiol.* (2020) 31:1908–19. doi: 10.1111/jce.14584
21. Muthalaly RG, John RM, Schaeffer B, Tanigawa S, Nakamura T, Kapur S, et al. Temporal trends in safety and complication rates of catheter ablation for atrial fibrillation. *J Cardiovasc Electrophysiol.* (2018) 29:854–60. doi: 10.1111/jce.13484
22. Dan GA, Martinez-Rubio A, Agewall S, Boriani G, Borggrefe M, Gaita F, et al. Antiarrhythmic drugs-clinical use and clinical decision making: a consensus document from the European Heart Rhythm Association (EHRA) and European Society of Cardiology (ESC) Working Group on Cardiovascular Pharmacology, endorsed by the Heart Rhythm Society (HRS), Asia-Pacific Heart Rhythm Society (APHRS), and International Society of Cardiovascular Pharmacotherapy (ISCP). *Europace.* (2018) 20:731–2. doi: 10.1093/europace/eux373
23. Saglietto A, De Ponti R, Di Biase L, Matta M, Gaita F, Romero J, et al. Impact of atrial fibrillation catheter ablation on mortality, stroke, and heart failure hospitalizations: a meta-analysis. *J Cardiovasc Electrophysiol.* (2020) 31:1040–7. doi: 10.1111/jce.14429
24. Kuck KH, Fürnkranz A, Chun KRJ, Metzner A, Ouyang F, Schlüter M, et al. Cryoballoon or radiofrequency ablation for symptomatic paroxysmal atrial fibrillation: Reintervention, rehospitalization, and quality-of-life outcomes in the FIRE and ICE trial. *Eur Heart J.* (2016) 37:2858–65. doi: 10.1093/eurheartj/ehw285
25. Arbelo E, Brugada J, Blomström-Lundqvist C, Laroche C, Kautzner J, Pokushalov E, et al. Contemporarymanagement of patients undergoing atrial fibrillation ablation: inhospital and 1-year follow-up findings from the ESC-EHRA atrial fibrillation ablation long-term registry. *Eur Heart J.* (2017) 38:1303–16. doi: 10.1093/eurheartj/ehw564

Conflict of Interest: The authors declare that the research was conducted in the absence of any commercial or financial relationships that could be construed as a potential conflict of interest.

frontiers in Cardiovascular Medicine

ORIGINAL RESEARCH
published: 21 May 2021
doi: 10.3389/fcvm.2021.684461

Association of Heart Rate Variability With Silent Brain Infarcts in Patients With Atrial Fibrillation

Peter Hämmerle[1,2], Christian Eick[3], Sven Poli[4], Steffen Blum[1,2], Vincent Schlageter[2], Axel Bauer[5], Konstantinos D. Rizas[6,7], Ceylan Eken[2], Michael Coslovsky[2], Stefanie Aeschbacher[2], Philipp Krisai[1,2], Pascal Meyre[1,2], Jens Wuerfel[8], Tim Sinnecker[8,9], Jean-Marc Vesin[10], Jürg H. Beer[11], Giorgio Moschovitis[12], Leo H. Bonati[9], Christian Sticherling[1,2], David Conen[2,13], Stefan Osswald[1,2], Michael Kühne[1,2†] and Christine S. Zuern[1,2†] on behalf of the Swiss-AF Study Investigators*

[1] Department of Cardiology, University Hospital Basel, Basel, Switzerland, [2] Cardiovascular Research Institute Basel, University Hospital Basel, Basel, Switzerland, [3] Department of Cardiology, University Hospital Tübingen, Tübingen, Germany, [4] Department of Neurology & Stroke, Hertie Institute for Clinical Brain Research, Eberhard-Karls University Tübingen, Tübingen, Germany, [5] University Clinic of Internal Medicine III, Cardiology and Angiology, Medical University of Innsbruck, Innsbruck, Austria, [6] Medizinische Klinik und Poliklinik I, Munich University Clinic, Munich, Germany, [7] German Center for Cardiovascular Research Partner Site, Munich Heart Alliance, Munich, Germany, [8] Medical Image Analysis Center (MIAC) and Department of Biomedical Engineering, University of Basel, Basel, Switzerland, [9] Department of Neurology and Stroke Center, University Hospital Basel, University of Basel, Basel, Switzerland, [10] Institute of Electrical Engineneering, Swiss Federal Institute of Technology, Lausanne University Hospital, Lausanne, Switzerland, [11] Department of Internal Medicine, Cantonal Hospital Baden, Aargau, Switzerland, [12] Division of Cardiology, Ospedale Regionale di Lugano-Civico e Italiano, Lugano, Switzerland, [13] Population Health Research Institute, McMaster University, Hamilton, ON, Canada

OPEN ACCESS

Edited by:
Daniel M. Johnson, The Open University, United Kingdom

Reviewed by:
Winnie Chua, University of Birmingham, United Kingdom
Irene Escudero-Martinez, Hospital Universitario y Politécnico de La Fe, Spain

***Correspondence:**
Christine S. Zuern
christine.meyerzuern@usb.ch

†These authors have contributed equally to this work and share last authorship

Specialty section:
This article was submitted to Cardiac Rhythmology, a section of the journal Frontiers in Cardiovascular Medicine

Received: *23 March 2021*
Accepted: *20 April 2021*
Published: *21 May 2021*

Citation:
Hämmerle P, Eick C, Poli S, Blum S, Schlageter V, Bauer A, Rizas KD, Eken C, Coslovsky M, Aeschbacher S, Krisai P, Meyre P, Wuerfel J, Sinnecker T, Vesin J-M, Beer JH, Moschovitis G, Bonati LH, Sticherling C, Conen D, Osswald S, Kühne M and Zuern CS (2021) Association of Heart Rate Variability With Silent Brain Infarcts in Patients With Atrial Fibrillation. Front. Cardiovasc. Med. 8:684461. doi: 10.3389/fcvm.2021.684461

Purpose: Silent brain infarcts (SBI) are frequently detected in patients with atrial fibrillation (AF), but it is unknown whether SBI are linked to autonomic dysfunction. We aimed to explore the association of autonomic dysfunction with SBI in AF patients.

Methods: 1,358 AF patients without prior stroke or TIA underwent brain MRI and 5-min resting ECG. We divided our cohort into AF patients who presented in sinus rhythm (SR-group, $n = 816$) or AF (AF-group, $n = 542$). HRV triangular index (HRVI), standard deviation of normal-to-normal intervals, mean heart rate, root mean square root of successive differences of normal-to-normal intervals, 5-min total power and power in the low frequency, high frequency and very low frequency range were calculated. Primary outcome was presence of SBI in the SR group, defined as large non-cortical or cortical infarcts. Secondary outcomes were SBI volumes and topography.

Results: Mean age was 72 ± 9 years, 27% were female. SBI were detected in 10.5% of the SR group and in 19.9% of the AF group ($p < 0.001$). HRVI<15 was the only HRV parameter associated with the presence of SBI after adjustment for clinical covariates in the SR group [odds ratio (OR) 1.67; 95% confidence interval (CI): 1.03–2.70; $p = 0.037$]. HRVI<15 was associated with larger brain infarct volumes [β (95% CI) −0.47 (−0.84; −0.09), $p = 0.016$] in the SR group and was more frequently observed in patients with right- than left-hemispheric SBI ($p = 0.017$).

Conclusion: Impaired HRVI is associated with SBI in AF patients. AF patients with autonomic dysfunction might undergo systematic brain MRI screening to initiate intensified medical treatment.

Clinical Trials Gov Identifier: NCT02105844.

Keywords: atrial fibrillation, autonomic dysfunction, heart rate variability, silent brain infarct, HRV triangular index

INTRODUCTION

Patients with atrial fibrillation (AF) have a high burden of silent brain infarcts (SBI) (1). SBI increase the risk of cognitive decline to a similar degree as overt strokes (1–3). Recently, it has been shown that silent large cortical and non-cortical infarcts (LNCCI) in AF patients were related to a 10-year age difference in cognitive performance (1). Furthermore, individuals with silent subcortical brain infarcts are at high risk for overt stroke (4). Therefore, the prevention and timely identification of SBI is a major public health concern. AF patients with SBI might benefit from an intensive control of vascular risk factors and dedicated neuropsychological treatment. However, systematic brain magnetic resonance imaging (bMRI) screening to detect SBI in patients with AF is not feasible due to reduced availability, costs and contraindications. An easily available tool that would allow for identification of AF patients at high risk for SBI would therefore be of high clinical value.

Overt strokes have been commonly associated with autonomic dysfunction (5–7). The functional status of the autonomic nervous system can be non-invasively assessed by the analysis of heart rate variability (HRV) (8). Parameters of HRV have been shown to predict overt stroke as well as complications and functionality of stroke survivors (9).

However, it is still unknown whether autonomic dysfunction is associated with SBI in AF patients. The primary objective of this analysis was to assess if impaired HRV is associated with presence of SBI in AF patients who were constantly in sinus rhythm (SR) at the time of the ECG recording ("SR group"). Secondary objectives were to (1) investigate the association between impairment of HRV and volumes of SBI and (2) analyze the association of HRV with topography of SBI. Exploratory analyses testing the association of HRV with the presence, volume and topography of SB were conducted in patients who were constantly in AF at the time of ECG recording ("AF group").

MATERIALS AND METHODS

Patient Population

The Swiss Atrial Fibrillation (Swiss-AF) cohort is an ongoing, multicenter prospective cohort study that enrolled 2,415 patients with AF at 14 study sites across Switzerland (10). Detailed information of the design and methodology including sample size calculations have been described elsewhere (ClinicalTrials.gov NCT02105844) (10). In brief, patients were eligible for Swiss-AF if they were aged ≥65 years and had a documented history of AF. A limited subset of patients aged 45–65 years was also enrolled. Main exclusion criteria for Swiss-AF were the presence of provoked, short and reversible AF episodes (e.g., after surgery), the inability to give informed consent as well as any acute illness within 4 weeks prior to enrolment.

Of the 2,415 patients enrolled in Swiss-AF (**Figure 1**), we excluded 480 patients (19.9%) due to known and documented history of stroke or transient ischemic attack (TIA) or due to lack of respective information. From the remaining patients, we excluded 527 due to missing bMRI (mostly patients with cardiac devices or claustrophobia). Finally, we excluded 21 patients due to missing or low-quality baseline ECG, and 29 patients due to rhythm other than SR or AF. Thus, 1,358 patients remained for the present analysis. In order to analyse the association of HRV with SBI during SR and AF separately, the rhythm on the baseline resting ECG was used to allocate patients to two groups: the "SR- group" ($n = 816$) and the AF-group ($n = 542$). Of note, all 1,358 included patients are AF patients. The SR group includes patients with paroxysmal and persistent AF who were in SR at the time of the ECG. The AF group includes patients with paroxysmal, persistent and permanent AF (AF types defined according to ESC guidelines) (11). The study protocol has been approved by the local ethics committees, and all participants provided informed consent.

Clinical Parameters

In order to obtain information on personal characteristics, prior medical history, comorbidities, medical and interventional treatment and other risk factors standardized case report forms were used by trained study personnel.

ECG Recordings

Baseline resting ECG (CS-200 Excellence and CS-200 Touch, Schiller AG, Baar, Switzerland) comprised 16 leads and were recorded for at least 300 seconds. ECG were digitally saved on a central server with a sampling frequency of 1 kHz (signal bandwidth 0.04-387 Hz) and a resolution of 1μV/bit. We used an automated R-peak detection algorithm, based on a Shannon energy envelope estimator and a Hilbert transformation, as described elsewhere (12). The following parameters of HRV were calculated from the total recordings (115 ECG segments with excessive artifact burden from 98 patients were disregarded), according to previously published algorithms (8, 13): heart rate variability triangular index (HRVI), standard deviation of the normal-to-normal intervals (SDNN), mean heart rate (MHR) and root mean square root of successive differences of normal-to-normal intervals (rMSSD). Spectral analysis was performed to calculate the following frequency domain measures of HRV (8):

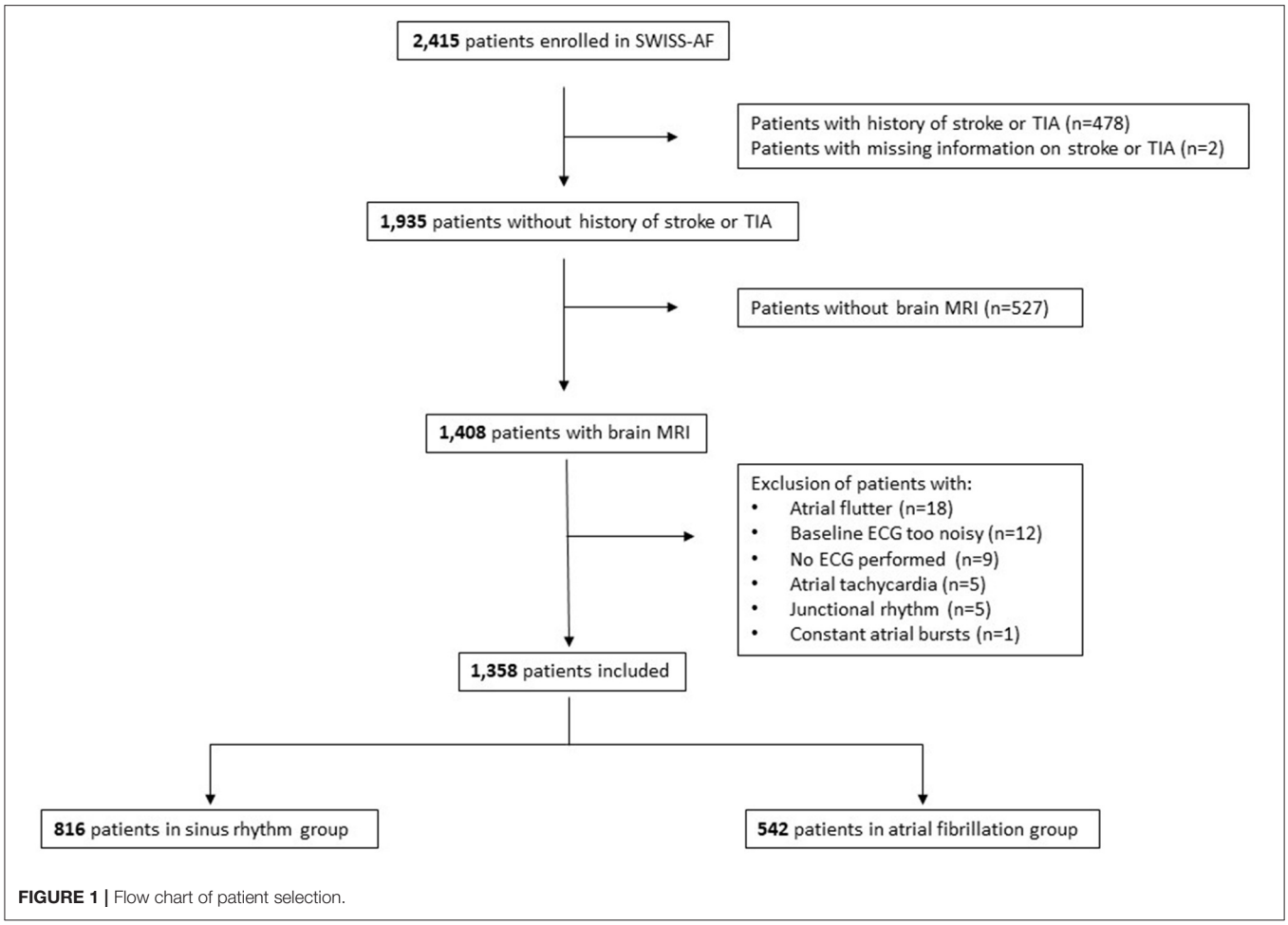

FIGURE 1 | Flow chart of patient selection.

5-min total power, power in the low frequency range (LF, 0.04–0.15 Hz), in the high frequency range (HF, 0.15–0.4 Hz) and in the very low frequency range (VLF, ≤0.04 Hz).

Brain Magnetic Resonance Imaging

The detailed methodology of bMRI analysis within the Swiss-AF cohort study has been described previously (1). In short, bMRI scans were acquired either on 1.5 T or a 3 T scanners with a standardized protocol defining an admissible range of image parameters at all study centers and analyses were performed in the neuroimaging core laboratory at Medical Image Analysis Centre, Basel, Switzerland. Blinded expert raters, who were unaware of the patients' characteristics, analyzed all bMRI scans and board-certified neuroradiologists verified the ratings. Brain infarcts were assessed on MPRAGE, FLAIR, and DWI based on lesion morphology consistent with acute or chronic ischemic infarction.

In more detail, large non-cortical infarcts were defined as hyperintense lesions on FLAIR >20 mm in diameter on axial sections not involving the cortex. These brain lesions had to be in line with an ischemia in the territory of a perforating arteriole located in the white matter, internal or external capsule, deep brain nuclei, thalamus, or brainstem (14). Cortical infarcts were hyperintense lesions on FLAIR involving the cortex regardless of their size (1). We combined large LNCCIs into one category. T2-weighted volumes of non-cortical and cortical infarcts were segmented and quantified by trained specialists in a validated process (software-supported threshold-based segmentation and edge-detection implemented in the Amira software package, Mercury Computer Systems Inc., Chelmsford, Massachusetts) to ensure consistent and reliable lesion and infarct size determination. SBI were defined as LNCCIs detected on bMRI, as all patients with known and documented history of stroke or TIA were a priori excluded from this study (**Figure 1**). Further, SBI were categorized into left-, right- and bi-hemispheric brain infarcts.

Statistical Analysis

Analyses were performed based on a pre-determined statistical analysis plan approved internally by the Swiss-AF steering committee. The patients' clinical characteristics at baseline were stratified according to the baseline ECG rhythm (SR group vs. AF group). Categorical variables are expressed as counts (percentages) and were compared using the chi-square test. The distribution of continuous variables was checked by visual

inspection of the histogram and by assessing skewness and kurtosis. Continuous variables are presented as mean ± standard deviation and are compared using Student's *t*-tests, or presented as median [interquartile range (IQR)] and compared using Mann-Whitney *U*-Test, as appropriate. Outcome analyses were performed in the SR group, whereas in the AF group, outcome analyses were only of exploratory nature. HRV parameters were used as main independent predictor variables in separate binary logistic regression models with the presence of LNCCI as the dependent variable. Study center was included as a random intercept to account for potential differences across study centers. To assess the association of HRV and volumes of SBI in patients who had at least one SBI, we built linear regression models for each predictor. First, we used crude models. Second, multivariable analyses were done by including a set of covariates determined via expert opinion and experience: age, sex, systolic blood pressure, and history of hypertension, history of diabetes, history of heart failure, prior myocardial infarction, prior major bleeding, prior pulmonary vein isolation (PVI) and intake of oral anticoagulation, antiarrhythmic drugs and beta-blockers. We prospectively dichotomized HRVI at 15 according to data of St George's Postinfarction Research Survey Programme and according to previously published data of our Swiss-AF cohort (8, 15), SDNN at 70 ms according to the ATRAMI cut-off (3), that was also used in the GISSI-2 study (16, 17), MHR at 80 bpm according to the ESC guidelines for the management of AF (11, 18) and rMSSD at 42 ms as published previously (19). Frequency domain measures of HRV were log-transformed. We examined whether the association of HRVI and presence of SBI depends on patient characteristics (age < median vs. age ≥ median, males vs. females, paroxysmal vs. persistent AF type, history of diabetes, history of myocardial infarction, intake of antiarrhythmic drugs, history of PVI) first by testing the interaction of HRVI with the relevant characteristic and then by fitting models again within the subgroup. Each interaction was entered to the full multivariable model separately in turn and tested, following with the relevant subgroup analyses with no interactions. Due to the skewed distribution, volumes of clinically SBI were log-transformed. Results are presented as odds ratio (OR) or beta-coefficients (β) with the corresponding 95% confidence intervals (CI). Statistical analyses were performed using SPSS Statistics for Windows, Version 25 (IBM Corp., Armonk, NY, USA) and SAS 9.4 (SAS Corporation, Cary, North Carolina, USA).

RESULTS

Baseline characteristics of the SR group ($n = 816$ patients) and the AF group ($n = 542$ patients) are presented in **Table 1**. Patients in the AF group were older (75 ± 8 vs. 70 ± 9 years) and were less often female (22 vs. 30%) and had higher rates of comorbidities, such as hypertension, diabetes and prior heart failure. Mean CHA_2DS_2-VASc score was 3.2 ± 1.4 in the AF group and 2.8 ± 3.9 in the SR group. The average duration of ECG recording was 300.2 ± 3.5 s in the SR group and 300.3 ± 5.1 s in the AF group. Time domain and frequency domain measures of HRV were higher in the AF group than in the SR group (**Supplementary Table 1**).

In the total study cohort ($n = 1, 358$), the prevalence of SBI was 14.3% ($n = 194$) and the median (IQR) volume was 531 (153–3,510) mm^3. In the AF group, prevalence and median (IQR) volume of SBI was 19.9% ($n = 108$) and 747 (434–4,615) mm^3. In the SR group, prevalence of SBI was 10.5% ($n = 86$) and median (IQR) volume was 354 (132–2,016) mm^3, ($p < 0.001$ for both comparisons between the AF and SR group).

Association of HRV With Presence and Volume of Silent Brain Infarcts in the SR Group

The univariable OR for the association of HRV parameters with presence of SBI are presented in **Table 2**. Only HRVI<15 was associated, yielding an OR of 1.69 (95% CI 1.05–2.70, $p = 0.030$). In the multivariable model, HRVI<15 remained the only HRV parameter associated with the presence of SBI (OR 1.67, 95% CI 1.03–2.70, $p = 0.037$). For HRVI and presence of SBI, no interactions were observed in any of the subgroups (**Table 3**). In multivariable adjusted linear regression models, HRVI was the only HRV parameter related to LNCCI volumes (**Table 4**), with HRVI<15 predicting higher SBI volume [β (95% CI) −0.47 (−0.84; −0.09), $p = 0.016$, **Figure 2**, left panel].

Association of HRV With Topography of Silent Brain Infarcts

Eighty three patients had right-hemispheric, 67 left-hemispheric and 41 bi-hemispheric brain infarcts (**Figure 3**). Three patients had a SBI in a localization, which could not be allocated to one hemisphere. In patients with right-hemispheric infarcts, HRVI was lower compared to patients with left-hemispheric SBI [median 13.6 (IQR 11.3–16.2) vs. 14.9 (12.1–20.0), $p = 0.022$], whereas SDNN, rMSSD, MHR, 5-min total power, LF, HF and VLF did not differ. All HRV parameters were similar in patients with right-hemispheric vs. bi-hemispheric infarcts and in patients with bi-hemispheric vs. left-hemispheric brain infarcts. Sixty nine point nine percentage of the patients with right-hemispheric SBI had an HRVI<15, in comparison to 50.7% of patients with left-hemispheric brain infarct ($p = 0.017$ for comparison of right- vs. left-hemispheric brain infarct) and 61.0% of patients with bi-hemispheric brain infarct ($p = 0.700$ for comparison of right- vs. bi-hemispheric brain infarct and $p = 0.300$ for comparison of left- vs. bi-hemispheric brain infarct).

Exploratory Analyses: Association of HRV With Presence and Volume of Silent Brain Infarcts in the AF Group

The univariable OR for the association of HRV parameters with presence of SBI are presented in **Supplementary Table 2**. The OR was 1.65 (95% CI 1.08–2.53, $p = 0.021$) for HRVI<15 and 1.59 (95% CI 1.01–2.48, $p = 0.046$) for rMSSD. Other HRV parameters were not associated with presence of SBI. In the multivariable model, HRVI<15 was the only HRV parameter associated with the presence of SBI (OR 1.63, 95% CI 1.05–2.55, $p = 0.031$). For HRVI and presence of SBI, we found no

TABLE 1 | Characteristics of the patients stratified by baseline rhythm.

Characteristic	Sinus rhythm group ($n = 816$)	Atrial fibrillation group ($n = 542$)	p-value*
Age, years	70 ± 9	75 ± 8	<0.001
Female sex (%)	242 (30)	118 (22)	0.001
Body mass index, kg/m^2	27.2 ± 4.9	28.5 ± 5.0	<0.001
Systolic/diastolic blood pressure, mmHg	137 ± 18/78 ± 11	133 ± 18/80 ± 13	0.004/0.003
History of hypertension (%)	521 (64)	401 (74)	<0.001
History of diabetes mellitus (%)	100 (12)	99 (18)	0.002
Active and former smokers (%)	459 (56)	302 (56)	0.847
History of electrocardioversion (%)	325 (40)	200 (37)	0.278
History of pulmonary vein isolation (%)	300 (37)	38 (7)	<0.001
History of myocardial infarction (%)	92 (11)	87 (16)	0.011
History of percutaneous coronary intervention (%)	145 (18)	133 (25)	0.002
History of heart failure (%)	121 (15)	171 (32)	<0.001
History of chronic kidney disease (%)	102 (13)	127 (23)	<0.001
CHA_2DS_2-VASc score, points	2.8 ± 3.9	3.2 ± 1.4	<0.001
History of major bleeding (%)	34 (4)	37 (7)	0.031
Paroxysmal atrial fibrillation (%)	531 (65)	66 (12)	<0.001
Persistent atrial fibrillation (%)	285 (35)	167 (31)	0.115
Permanent atrial fibrillation (%)	0 (0)	309 (57)	–
Antiarrhythmic therapy (class Ic and III) (%)	261 (32)	143 (26)	0.027
Beta-blockers (%)	520 (64)	376 (69)	0.031
Non Vitamin K oral anticoagulants (%)	500 (61)	219 (40)	<0.001
Vitamin K antagonists (%)	196 (24)	293 (54)	<0.001

*Data are means ± SD or counts (percentages). *p-value compares sinus rhythm and atrial fibrillation groups. P-values were obtained from Student's t-tests for continuous variables and chi-square tests for categorical variables. CHA_2DS_2-VASc, congestive heart failure, hypertension, age ≥75 yeas (2 points), diabetes, prior stroke or TIA or thromboembolism (2 points), vascular disease, age 65 to 74 years, female sex; n, number.*

interactions in any of the subgroups (**Supplementary Table 3**). None of the HRV parameters were associated with brain infarct volumes (**Supplementary Table 4**, **Figure 2**, right panel).

DISCUSSION

To the best of our knowledge, this is the first study to assess the relationship of HRV with SBI in AF patients. First, in the SR group, impaired HRVI was independently associated with the presence of SBI. Second, patients in the SR group with impaired HRVI had a higher volume of SBI. Moreover, patients with SBI in the right hemisphere showed more pronounced impairment of HRVI compared to patients with left-hemispheric brain infarcts. Exploratory analyses in the AF group showed that impaired HRVI was associated with the presence of SBI, but not with infarct volume.

In patients with AF, SBI have a similar impact on cognitive impairment as overt strokes (1) and are known to enhance the risk of subsequent overt strokes (4). The early identification of SBI or risk factors thereof may be important when risk stratifying AF patients. Few parameters (age, male sex and hypertension) have already been associated with SBI (20). However, the detected SBI in the NOMAS study were mostly small and subcortical (20) and only 4.2% of the participants had a history of AF. Moreover, although higher AF burden has been associated with an increasing risk of stroke (21), its association with SBI warrants further investigation.

Multiple studies have shown that patients with overt stroke show changes of HRV (22–26) that are mainly characterized by the predominance of sympathetic activity (22). Numerous studies suggest that HRV is impaired in stroke patients when compared to controls (23, 25, 26). Furthermore, HRV parameters may have the capacity to predict incident stroke (23, 25, 26). HRV measures can also be used as biomarkers for post-stroke outcomes such as mortality, complications and functionality (9, 27). However, all above mentioned studies have exclusively included SR patients. Only two studies included AF patients. The first study assessed HRV in stroke patients with permanent AF ($n = 173$) to predict overt stroke (28). The second study tested the association of HRV with 3-month post-stroke outcome and included a proportion of AF patients ($n = 77$) (29). Although HRV has already been thoroughly investigated in patients with overt strokes (22–27, 29), no prior investigation has assessed the association of HRV with SBI in AF patients.

In this first study assessing the association of HRV and SBI in patients with AF, we focused our analysis on the SR group, because HRV analysis is very well-established during SR (8), but has not been commonly used during AF so far. From a pathophysiological perspective, the meaning of HRV parameters measured during AF is less well-understood. It is questionable whether HRV calculated from AF recordings

TABLE 2 | Association of heart rate variability and presence of silent brain infarcts in the sinus rhythm group.

HRV parameter	Univariable model OR (95% CI)	*p*-value*	Multivariable model OR (95% CI)	*p*-value*
Time domain measures				
HRVI<15	1.69 (1.05–2.70)	0.030	1.67 (1.03–2.70)	0.037
SDNN<70ms	1.51 (0.93–2.43)	0.093	1.53 (0.90–2.39)	0.087
rMSSD<42ms	1.15 (0.73–1.83)	0.550	1.16 (0.72–1.86)	0.537
MHR>80bpm	1.00 (0.64–1.56)	0.991	1.02 (0.64–1.61)	0.934
Frequency domain measures†				
5-min total power	1.33 (0.97–1.82)	0.078	1.38 (1.00–1.90)	0.050
LF	1.29 (0.96–1.74)	0.090	1.34 (0.99–1.81)	0.057
HF	1.31 (0.95–1.80)	0.103	1.36 (0.98–1.90)	0.066
VLF	1.22 (0.93–1.61)	0.157	1.26 (0.94–1.67)	0.118

*Data are odds ratios (OR) (95% confidence intervals [CI]). *p-values were based on logistic regression models. †Frequency domain measures of HRV have been log-transformed. Study center was included as random intercept. Multivariable model was adjusted for age, sex, systolic blood pressure, history of hypertension, history of diabetes, history of heart failure, prior myocardial infarction, prior major bleeding, history of pulmonary vein isolation, intake of oral anticoagulation, antiarrhythmics and betablockers. HF, high frequency (0.15–0.4 Hz); HRV, heart rate variability; HRVI, heart rate variability triangular index; MHR, mean heart rate; LF, low frequency (0.04–0.15 Hz); OR, odds ratio; rMSSD, root mean square root of successive differences of normal-to-normal intervals; SDNN, standard deviation of the normal-to-normal intervals; VLF, very low frequency (≤0.04 Hz).*

TABLE 3 | Association of heart rate variability triangular index and silent brain infarcts: subgroup analyses in the sinus rhythm group.

Subgroup	No. of events/n	Odds ratio	95% CI	*p*-value	p-interaction
Age					
Age<median	40/408	1.52	0.78–2.95	0.220	0.302
Age≥median	46/408	1.84	0.94–3.61	0.077	
Sex					
Male	66/574	1.48	0.87–2.52	0.146	0.132
Female	20/242	2.64	0.93–7.52	0.068	
AF type					
Paroxysmal	54/531	1.19	0.68–2.10	0.540	0.173
Persistent	32/285	3.77	1.41–10.1	0.008	
History of diabetes					
Yes	13/100	4.90	1.03–23.4	0.046	0.111
No	73/716	1.45	0.88–2.34	0.143	
History of myocardial infarction					
Yes	13/92	1.61	0.46–5.69	0.457	0.381
No	73/724	1.68	1.01–2.79	0.045	
Intake of antiarrhythmic drugs (class Ic, II & III)					
Yes	68/626	1.95	1.14–3.35	0.015	0.271
No	18/190	1.01	0.38–2.69	0.979	
History of pulmonary vein isolation					
Yes	35/300	1.30	0.63–2.66	0.475	0.917
No	51/516	2.05	1.09–3.84	0.026	

Univariable analyses are presented. AF, atrial fibrillation; CI, confidence interval; No, number; n, number of patients included in the subgroup.

directly quantifies autonomic function. However, also in AF, HRV may be modulated by autonomic factors, for example on the level of the AV node (30). Therefore, we also performed exploratory analyses in the AF group to gain more information on the diagnostic meaning of HRV in AF, which might be a potential basis for further research.

HRVI, a geometrical HRV parameter (8), was independently associated with the presence of SBI. Impaired HRVI indicates imbalance of the autonomic nervous system, and is a predictor of adverse events such as malignant arrhythmias and mortality (31–33). Of note, other HRV parameter (including various time and frequency domain measures) were not associated with the presence of SBI in our study. An explanation may be that HRVI can be robustly calculated without manual editing of the RR interval series in a highly reproducible way and is highly insensitive to artifacts and ectopic beats (34).

TABLE 4 | Association of heart rate variability and silent brain infarct volume in the sinus rhythm group.

HRV parameter	Univariable model β (95% CI)	*p*-value*	Multivariable model β (95% CI)	*p*-value*
Time domain measures				
HRVI<15	0.49 (0.14; 0.83)	0.007	−0.47 (−0.84; −0.09)	0.016
SDNN<70ms	0.30 (−0.06; 0.66)	0.103	0.24 (−0.15; 0.63)	0.222
rMSSD<42ms	0.11 (−0.25; 0.47)	0.550	0.01 (−0.39; 0.41)	0.946
MHR>80bpm	0.13 (−0.21; 0.47)	0.453	0.17 (−0.22; 0.55)	0.389
Frequency domain measures†				
5-min total power	0.19 (−0.06; 0.46)	0.140	0.24 (−0.02; 0.50)	0.065
LF	0.21 (−0.03; 0.44)	0.090	0.24 (−0.01; 0.49)	0.061
HF	0.06 (−0.18; 0.31)	0.603	0.12 (−0.15; 0.38)	0.380
VLF	0.12 (−0.10; 0.33)	0.286	0.17 (−0.06; 0.40)	0.149

*Data are beta-coefficients (β) [95% confidence intervals (CI)]. Brain infarct volumes were log-transformed.*p-values were based on linear regression models. †Frequency domain measures of HRV have been log-transformed. Study center was included as random intercept. Multivariable model was adjusted for age, sex, systolic blood pressure, history of hypertension, history of diabetes, history of heart failure, prior myocardial infarction, prior major bleeding, history of pulmonary vein isolation, intake of oral anticoagulation, antiarrhythmics and betablockers. HF, high frequency (0.15–0.4 Hz); HRV, heart rate variability; HRVI, heart rate variability triangular index; MHR, mean heart rate; LF, low frequency (0.04–0.15 Hz); rMSSD, root mean square root of successive differences of normal-to-normal intervals; SDNN, standard deviation of the normal-to-normal intervals; VLF, very low frequency (≤0.04 Hz).*

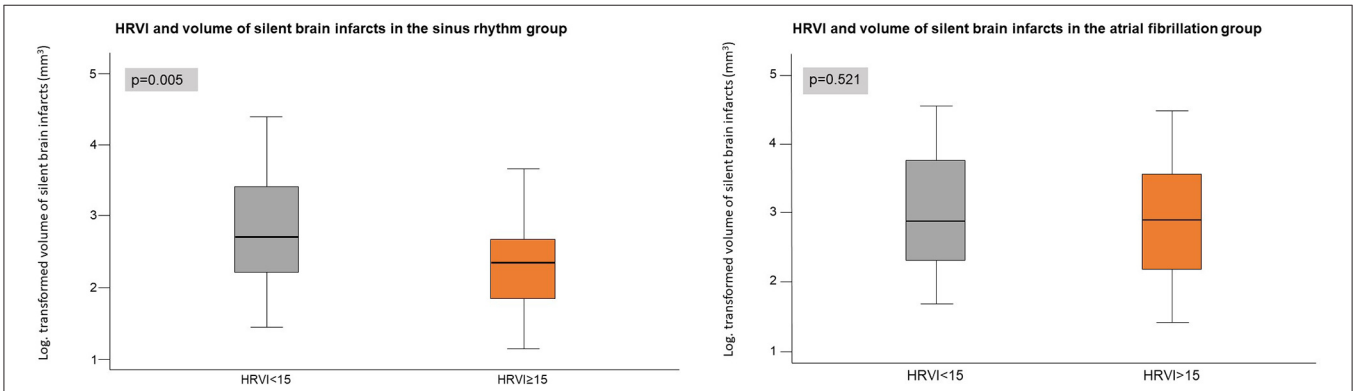

FIGURE 2 | Volumes of silent brain infarcts in the sinus rhythm group **(left)** and in the atrial fibrillation group (**right**,exploratory analysis) stratified by heart rate variability triangular index (HRVI).

In our study, patients with impaired HRVI (assessed during SR) had a higher volume of SBI. A potential mechanism might be that a larger involvement of the infarct area itself contributes to a more prominent impairment autonomic function. However, in the AF group, volumes of SBI did not differ when stratified by HRVI. This shows that analysis of HRV during AF may be less useful for risk stratification. Currently, it remains unclear how assessment of the ANS can be optimized in AF patients.

Furthermore, patients with right-hemispheric brain infarct showed a more pronounced impairment of HRVI compared to left-hemispheric brain infarcts. This finding is in line with previous studies showing that overt strokes in the right hemisphere lead to a derangement of HRV as the right hemisphere, especially the insular region, plays a major role in cardiac autonomic control (27, 35, 36). Our findings confirm that the severity of cardiac autonomic impairment might in part depend on the localization of a stroke.

The directionality of association between impairment of HRV and overt stroke is still unknown. On the one hand, the association could potentially originate from changes of autonomic control directly induced by the stroke, i.e., a complication of stroke (7). On the other hand, the association of HRV and stroke could also be explained by sharing the same cardiovascular risk factors. So far, the exact underlying pathways and mechanisms remain to be determined. Of note, it is unknown if SBI are associated with similar impairment of HRV as overt strokes. In our study, patients with a history of stroke/TIA were excluded (**Figure 1**). However, when comparing patients with a history of stroke/TIA from the Swiss-AF cohort study (n = 337) and patients with a SBI from our analysis (n = 194), HRV parameters were similar (detailed data not shown).

Strengths of our study are the large sample size of well-treated patients with AF who are comprehensively characterized. Limitations of our study are the cross-sectional design

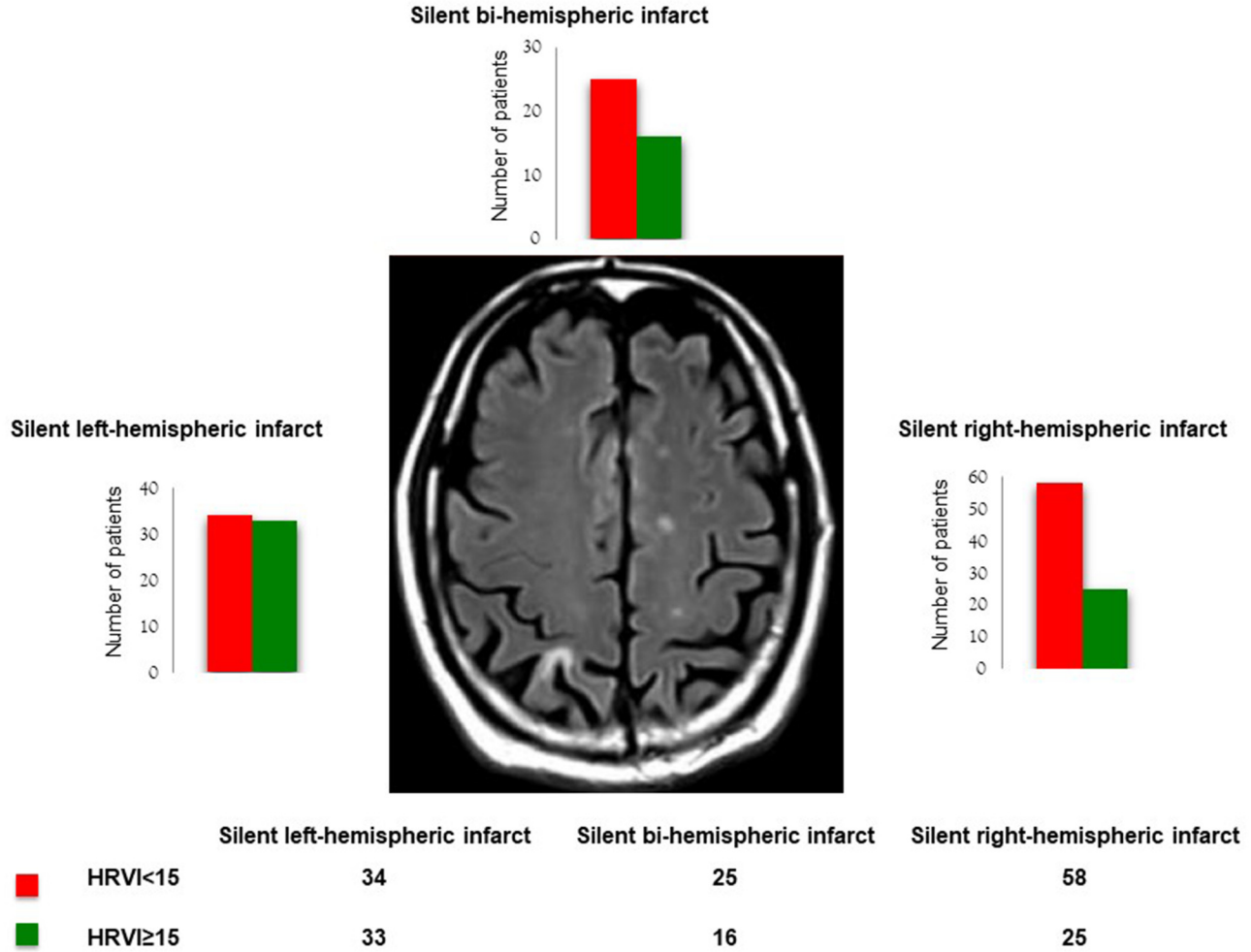

FIGURE 3 | Impairment of heart rate variability triangular index (HRVI) according silent brain infarct topography.

which precludes to assess the directionality of effect between impairment of HRV and SBI. Further, we did not perform 24-h Holter-ECG recordings. Therefore, our results are only valid for 5-min ECG recordings and we cannot judge the association between HRV measures calculated from long-term recordings and SBI. This is particularly relevant for HRVI, which is predominantly established in long-term ECG recordings so far. Further, as comprehensively discussed above, we are aware that HRV during AF may not have the same meaning as in SR. Finally, the generalizability to patients without AF or other population groups remains to be determined. Further studies are needed to validate our observations and cut-offs and clarify its clinical application.

In conclusion, autonomic dysfunction (assessed during SR) is independently associated with the presence and volume of SBI in patients with AF. HRV analysis may be a simple screening tool that enables clinicians to identify patients with an increased risk of SBI. Identified high risk patients may undergo bMRI, and in case SBI are detected, these patients may benefit from intensified treatment beyond standard oral anticoagulation, rhythm control as well as better control of comorbidities such as hypertension and diabetes. However, no study has proven the power of intensified treatment of AF and comorbidities on the occurrence of new brain lesions in AF patients.

DATA AVAILABILITY STATEMENT

Due to restrictions by the ethical committee data is not publicly available. Requests to access the datasets should be directed to christine.meyerzuern@usb.ch.

ETHICS STATEMENT

The studies involving human participants were reviewed and approved by Ethics commitee University of Basel, Switzerland and all local ethics committees at the study sites. The

patients/participants provided their written informed consent to participate in this study.

AUTHOR CONTRIBUTIONS

PH, CSZ, SO, and MK contributed to conception and design of the study. CEi and VS organized the ECG database. SB, SA, PK, and PM organized the clinical database. PH, CSZ, and MC performed the statistical analysis. PH wrote the first draft of the manuscript. CSZ, JW, TS, and MK wrote sections of the manuscript. SP, AB, KR, CEk, J-MV, JB, GM, LB, CS, DC, and SO gave intellectual input for manuscript writing. All authors contributed to the article and approved the submitted version.

FUNDING

The Swiss-AF cohort study is supported by grants of the Swiss National Science Foundation (grant numbers 33CS30_1148474 and 33CS30_177520), the Foundation for Cardiovascular Research Basel (FCVR), and the University of Basel.

SUPPLEMENTARY MATERIAL

The Supplementary Material for this article can be found online at: https://www.frontiersin.org/articles/10.3389/fcvm.2021.684461/full#supplementary-material

REFERENCES

1. Conen D, Rodondi N, Muller A, Beer JH, Ammann P, Moschovitis G, et al. Relationships of overt and silent brain lesions with cognitive function in patients with atrial fibrillation. *J Am Coll Cardiol.* (2019) 73:989–99. doi: 10.1016/j.jacc.2018.12.039
2. Vermeer SE, Prins ND, den Heijer T, Hofman A, Koudstaal PJ, Breteler MM. Silent brain infarcts and the risk of dementia and cognitive decline. *N Engl J Med.* (2003) 348:1215–22. doi: 10.1056/NEJMoa022066
3. Windham BG, Griswold ME, Wilkening SR, Su D, Tingle J, Coker LH, et al. Midlife smaller and larger infarctions, white matter hyperintensities, and 20-Year cognitive decline: a cohort study. *Ann Intern Med.* (2019) 171:389–96. doi: 10.7326/M18-0295
4. Kobayashi S, Okada K, Koide H, Bokura H, Yamaguchi S. Subcortical silent brain infarction as a risk factor for clinical stroke. *Stroke.* (1997) 28:1932–9. doi: 10.1161/01.STR.28.10.1932
5. Korpelainen JT, Sotaniemi KA, Huikuri HV, Myllya VV. Abnormal heart rate variability as a manifestation of autonomic dysfunction in hemispheric brain infarction. *Stroke.* (1996) 27:2059–63. doi: 10.1161/01.STR.27.11.2059
6. Oppenheimer SM, Kedem G, Martin WM. Left-insular cortex lesions perturb cardiac autonomic tone in humans. *Clin Auton Res.* (1996) 6:131–40. doi: 10.1007/BF02281899
7. De Raedt S, De Vos A, De Keyser J. Autonomic dysfunction in acute ischemic stroke: an underexplored therapeutic area? *J Neurol Sci.* (2015) 348:24–34. doi: 10.1016/j.jns.2014.12.007
8. Heart rate variability: standards of measurement, physiological interpretation and clinical use. Task Force of the European Society of Cardiology and the North American Society of Pacing and Electrophysiology. *Circulation.* (1996) 93:1043–65.
9. Lees T, Shad-Kaneez F, Simpson AM, Nassif NT, Lin Y, Lal S. Heart rate variability as a biomarker for predicting stroke, post-stroke complications and functionality. *Biomark Insights.* (2018) 13. doi: 10.1177/1177271918786931
10. Conen D, Rodondi N, Mueller A, Beer J, Auricchio A, Ammann P, et al. Design of the swiss atrial fibrillation cohort study (Swiss-AF): structural brain damage and cognitive decline among patients with atrial fibrillation. *Swiss Med Wkly.* (2017) 147:w14467. doi: 10.4414/smw.2017.14467
11. Kirchhof P, Benussi S, Kotecha D, Ahlsson A, Atar D, Casadei B, et al. 2016 ESC Guidelines for the management of atrial fibrillation developed in collaboration with EACTS. *Eur Heart J.* (2016) 37:2893–962. doi: 10.1093/eurheartj/ehw210
12. Eick C, Rizas KD, Zuern CS, Bauer A. Automated assessment of cardiac autonomic function by means of deceleration capacity from noisy, nonstationary ECG signals: validation study. *Ann Noninvasive Electrocardiol.* (2014) 19:122–8. doi: 10.1111/anec.12107
13. Costa M, Goldberger AL, Peng CK. Multiscale entropy analysis of complex physiologic time series. *Phys Rev Lett.* (2002) 89:068102. doi: 10.1103/PhysRevLett.89.068102
14. Wardlaw JM, Smith EE, Biessels GJ, Cordonnier C, Fazekas F, Frayne R, et al. Neuroimaging standards for research into small vessel disease and its contribution to ageing and neurodegeneration. *Lancet Neurol.* (2013) 12:822–38. doi: 10.1016/S1474-4422(13)70124-8
15. Hammerle P, Eick C, Blum S, Schlageter V, Bauer A, Rizas KD, et al. Heart rate variability triangular index as a predictor of cardiovascular mortality in patients with atrial fibrillation. *J Am Heart Assoc.* (2020) 9:e016075. doi: 10.1161/JAHA.120.016075
16. La Rovere MT, Bigger Jr JT, Marcus FI, Mortara A, Schwartz PJ. Baroreflex sensitivity and heart-rate variability in prediction of total cardiac mortality after myocardial infarction. ATRAMI (Autonomic Tone and Reflexes After Myocardial Infarction) Investigators. *Lancet.* (1998) 351:478–84. doi: 10.1016/S0140-6736(97)11144-8
17. Zuanetti G, Neilson JM, Latini R, Santoro E, Maggioni AP, Ewing DJ. Prognostic significance of heart rate variability in post-myocardial infarction patients in the fibrinolytic era. The GISSI-2 results. Gruppo Italiano per lo Studio della Sopravvivenza nell' Infarto Miocardico. *Circulation.* (1996) 94:432–6. doi: 10.1161/01.CIR.94.3.432
18. Van Gelder IC, Groenveld HF, Crijns HJ, Tuininga YS, Tijssen JG, Alings AM, et al. Lenient versus strict rate control in patients with atrial fibrillation. *N Engl J Med.* (2010) 362:1363–73. doi: 10.1056/NEJMoa1001337
19. Nunan D, Sandercock GR, Brodie DA. A quantitative systematic review of normal values for short-term heart rate variability in healthy adults. *Pacing Clin Electrophysiol.* (2010) 33:1407–17. doi: 10.1111/j.1540-8159.2010.02841.x
20. Prabhakaran S, Wright CB, Yoshita M, Delapaz R, Brown T, DeCarli C, et al. Prevalence and determinants of subclinical brain infarction: the northern manhattan study. *Neurology.* (2008) 70:425–30. doi: 10.1212/01.wnl.0000277521.66947.e5
21. Chen LY, Chung MK, Allen LA, Ezekowitz M, Furie KL, McCabe P, et al. Atrial fibrillation burden: moving beyond atrial fibrillation as a binary entity: a scientific statement from the American heart association. *Circulation.* (2018) 137:e623–44. doi: 10.1161/CIR.0000000000000568
22. Guan L, Collet JP, Mazowita G, Claydon VE. Autonomic nervous system and stress to predict secondary ischemic events after transient ischemic attack or minor stroke: possible implications of heart rate variability. *Front Neurol.* (2018) 9:90. doi: 10.3389/fneur.2018.00090
23. Fyfe-Johnson AL, Muller CJ, Alonso A, Folsom AR, Gottesman RF, Rosamond WD, et al. Heart rate variability and incident stroke: the atherosclerosis risk in communities study. *Stroke.* (2016) 47:1452–8. doi: 10.1161/STROKEAHA.116.012662
24. Chen CF, Lai CL, Lin HF, Liou LM, Lin RT. Reappraisal of heart rate variability in acute ischemic stroke. *Kaohsiung J Med Sci.* (2011) 27:215–21. doi: 10.1016/j.kjms.2010.12.014
25. Kuzemczak M, Bialek-Lawniczak P, Torzynska K, Janowska-Kulinska A, Miechowicz I, Kramer L, et al. Comparison of baseline heart rate variability in stable ischemic heart disease patients with and without stroke in long-term observation. *J Stroke Cerebrovasc Dis.* (2016) 25:2526–34. doi: 10.1016/j.jstrokecerebrovasdis.2016.06.033
26. Korpelainen JT, Sotaniemi KA, Huikuri HV, Myllyla VV. Circadian rhythm of heart rate variability is reversibly abolished in ischemic stroke. *Stroke.* (1997) 28:2150–4. doi: 10.1161/01.STR.28.11.2150

27. Naver HK, Blomstrand C, Wallin BG. Reduced heart rate variability after right-sided stroke. *Stroke.* (1996) 27:247–51. doi: 10.1161/01.STR.27.2.247
28. Watanabe E, Kiyono K, Hayano J, Yamamoto Y, Inamasu J, Yamamoto M, et al. Multiscale entropy of the heart rate variability for the prediction of an ischemic stroke in patients with permanent atrial fibrillation. *PLoS ONE.* (2015) 10:e0137144. doi: 10.1371/journal.pone.0137144
29. Tang SC, Jen HI, Lin YH, Hung CS, Jou WJ, Huang PW, et al. Complexity of heart rate variability predicts outcome in intensive care unit admitted patients with acute stroke. *J Neurol Neurosurg Psychiatry.* (2015) 86:95–100. doi: 10.1136/jnnp-2014-308389
30. Wittkampf FH, de Jongste MJ, Lie HI, Meijler FL. Effect of right ventricular pacing on ventricular rhythm during atrial fibrillation. *J Am Coll Cardiol.* (1988) 11:539–45. doi: 10.1016/0735-1097(88)91528-8
31. Odemuyiwa O, Malik M, Farrell T, Bashir Y, Poloniecki J, Camm J. Comparison of the predictive characteristics of heart rate variability index and left ventricular ejection fraction for all-cause mortality, arrhythmic events and sudden death after acute myocardial infarction. *Am J Cardiol.* (1991) 68:434–9. doi: 10.1016/0002-9149(91)90774-F
32. Wijbenga JA, Balk AH, Meij SH, Simoons ML, Malik M. Heart rate variability index in congestive heart failure: relation to clinical variables and prognosis. *Eur Heart J.* (1998) 19:1719–24. doi: 10.1053/euhj.1998.1148
33. Farrell TG, Bashir Y, Cripps T, Malik M, Poloniecki J, Bennett ED, et al. Risk stratification for arrhythmic events in postinfarction patients based on heart rate variability, ambulatory electrocardiographic variables and the signal-averaged electrocardiogram. *J Am Coll Cardiol.* (1991) 18:687–97. doi: 10.1016/0735-1097(91)90791-7
34. Malik M, Farrell T, Camm AJ. Circadian rhythm of heart rate variability after acute myocardial infarction and its influence on the prognostic value of heart rate variability. *Am J Cardiol.* (1990) 66:1049–54. doi: 10.1016/0002-9149(90)90503-S
35. Tokgozoglu SL, Batur MK, Topcuoglu MA, Saribas O, Kes S, Oto A. Effects of stroke localization on cardiac autonomic balance and sudden death. *Stroke.* (1999) 30:1307–11. doi: 10.1161/01.STR.30.7.1307
36. Colivicchi F, Bassi A, Santini M, Caltagirone C. Cardiac autonomic derangement and arrhythmias in right-sided stroke with insular involvement. *Stroke.* (2004) 35:2094–8. doi: 10.1161/01.STR.0000138452.81003.4c

Conflict of Interest: CSZ reports a research grant from Medtronic and honoraria from Vifor Pharma and Novartis. MK has received grants from the Swiss National Science Foundation, the Swiss Heart Foundation, Daiichi-Sankyo, Bayer, and Pfizer-BMS and lecture/consulting fees from Daiichi-Sankyo, Boehringer Ingelheim, Bayer, Pfizer-BMS, AstraZeneca, Sanofi-Aventis, Novartis, MSD, Medtronic, Boston Scientific, St. Jude Medical, Biotronik, Sorin, Zoll and Biosense Webster. PK is supported by the University of Basel, the Mach-Gaensslen foundation and the Bangerter-Rhyner foundation. SP received research grants from Bristol-Myers Squibb/Pfizer, Daiichi Sankyo, and speakers' honoraria and consulting fees from Bayer, Boehringer Ingelheim, Bristol-Myers Squibb/Pfizer, Daiichi Sankyo and Werfen. JW is CEO of the Medical Image Analysis Center, Basel; has served on advisory boards for Actelion, Biogen, Genzyme-Sanofi, Novartis, Roche, and the Guthy Jackson Charitable Foundation; has received research grants from Novartis; has received speaker honoraria from Bayer, Biogen, Genzyme, Novartis, and Teva.

The remaining authors declare that the research was conducted in the absence of any commercial or financial relationships that could be construed as a potential conflict of interest.

frontiers in Cardiovascular Medicine

SYSTEMATIC REVIEW
published: 24 May 2021
doi: 10.3389/fcvm.2021.669301

Left Bundle Branch Area Pacing vs. Biventricular Pacing for Cardiac Resynchronization Therapy: A Meta-Analysis

Jiyi Liu[1†], Fengzhi Sun[1†], Zefeng Wang[2], Jiao Sun[3], Xue Jiang[4], Weilong Zhao[1], Zhipeng Zhang[1], Lu Liu[1] and Shulong Zhang[1]*

[1] Heart Centre, Affiliated Zhongshan Hospital of Dalian University, Dalian, China, [2] Department of Cardiovascular Medicine, Beijing Anzhen Hospital, Capital Medical University, Beijing, China, [3] Department of Neuroelectrophysiology, Affiliated Zhongshan Hospital of Dalian University, Dalian, China, [4] Cardiovascular Medicine Institute, Beijing Tiantan Hospital, Capital Medical University, Beijing, China

OPEN ACCESS

Edited by:
Mehdi Namdar,
Geneva University Hospitals (HUG), Switzerland

Reviewed by:
Alexander Breitenstein,
University Hospital Zürich, Switzerland
Haran Burri,
Université de Genève, Switzerland

***Correspondence:**
Shulong Zhang
zhangshulong632_dl@21cn.com

[†]These authors have contributed equally to this work

Specialty section:
This article was submitted to Cardiac Rhythmology, a section of the journal Frontiers in Cardiovascular Medicine

Received: 16 March 2021
Accepted: 13 April 2021
Published: 24 May 2021

Citation:
Liu J, Sun F, Wang Z, Sun J, Jiang X, Zhao W, Zhang Z, Liu L and Zhang S (2021) Left Bundle Branch Area Pacing vs. Biventricular Pacing for Cardiac Resynchronization Therapy: A Meta-Analysis. Front. Cardiovasc. Med. 8:669301. doi: 10.3389/fcvm.2021.669301

Background: Left bundle branch area pacing (LBBAP) is a recently proposed method for conduction system pacing. We performed a meta-analysis of controlled studies to compare the clinical outcome in patients who received LBBAP vs. biventricular pacing (BVP) for cardiac resynchronization therapy (CRT).

Methods: PubMed, Embase, and Cochrane's Library databases were searched for relevant controlled studies. A random-effect model incorporating the potential heterogeneity was used to synthesize the results.

Results: Four non-randomized controlled studies including 249 patients with heart failure (HF) for CRT were included, and the patients were followed for 6–12 months. Compared with BVP, LBBAP was associated with significantly shortened QRS duration [mean difference (MD): −29.18 ms, 95% confidence interval (CI): −33.55–24.80, $I^2 = 0\%$, $P < 0.001$], improved left ventricular ejection fraction (MD: 6.93%, 95% CI: 4.69–9.17, $I^2 = 0\%$, $P < 0.001$), reduced left ventricular end-diastolic dimension (MD: −2.96 mm, 95% CI: −5.48 to −0.44, $I^2 = 0\%$, $P = 0.02$), and improved New York Heart Association class (MD: −0.54, 95% CI: −0.84 to −0.24, $I^2 = 65\%$, $P < 0.001$). Moreover, patients who received LBBAP were more likely to achieve echocardiographic [odds ratio (OR): 5.04, 95% CI: 2.17–11.69, $I^2 = 0\%$, $P < 0.001$] and clinical (OR: 7.33, 95% CI: 1.62–33.16, $I^2 = 0\%$, $P = 0.01$) CRT responses.

Conclusion: Current evidence from non-randomized studies suggests that LBBAP appears to be a promising method for CRT, which is associated with more remarkable improvements of symptoms and cardiac function in HF patients with indication for CRT.

Keywords: meta-analysis, heart failure, cardiac resynchronization therapy, biventricular pacing, left bundle branch area pacing

INTRODUCTION

For heart failure (HF) patients with reduced ejection fraction and complete left bundle branch block (LBBB), cardiac resynchronization therapy (CRT) with biventricular pacing (BVP) has been established as an effective therapy that has been associated with improved left ventricular (LV) function and clinical symptoms (1, 2). However, about 30% of patients do not respond to CRT delivered by conventional BVP (3). In addition, the procedure of BVP implantation is complex, and for patients with venous malformations or coronary vein stenosis, implantation of LV pacing leads is sometimes technically difficult (4). Subsequently, physiological pacing approaches have been investigated to achieve CRT, including His-bundle pacing (HBP) and left bundle branch area pacing (LBBAP) (5). Although HBP could achieve physiologic electromechanical synchrony by facilitating conduction through the native His-Purkinje system, HBP is associated with high pacing threshold and risk of abnormal sensing, which limited its use for CRT delivering (6). LBBAP is a newly developed physiological pacing strategy that can effectively achieve narrowed QRS waves and improved LV function in HF patients with indication for CRT (7). In addition, compared with HBP, LBBAP is of lower thresholds, higher R wave amplitude, and easier to perform, which makes it a potential optimal technique to deliver CRT (8). Although primary case series reporting LBBAP delivered CRT showed promising results (9), controlled studies comparing the efficacy and safety of LBBAP vs. BVP in HF patients with indication for CRT are rare (10–13). Moreover, results of these studies were not consistent, probably due to the limited number of HF patients included in each study (10–13). Accordingly, we performed a meta-analysis of controlled studies to compare the influences of CRT delivered by LBBAP vs. BVP on QRS duration (QRSd), LV function, clinical symptoms, and CRT response in these patients.

METHODS

This systematic review and meta-analysis was prepared in accordance with the PRISMA (Preferred Reporting Items for Systematic Reviews and Meta-Analyses) (14) and the Cochrane's Handbook (15) guidelines during the study design, implementation, data analysis, and results reporting processes.

Database Searching

PubMed, Embase, and Cochrane's Library databases were searched for relevant studies using the terms of (1) "left bundle branch pacing" OR "left bundle branch area pacing" and (2) "biventricular" OR "cardiac resynchronization therapy" OR "CRT". The search was limited to human studies published in English. The references of the related original and review articles were also screened manually for potential relevant studies. The final literature searching was performed on January 16, 2021.

Study Selection

Studies were included if they fulfilled the following criteria: (1) published as full-length article in English; (2) designed as randomized or non-randomized controlled studies, without restrictions of the sample size and follow-up duration; (3) including patients with HF who underwent CRT with LBBAP or BVP; and (4) reported at least one of the following outcomes during follow-up, including QRSd, echocardiographic parameters [left ventricular ejection fraction (LVEF) and left ventricular end-diastolic dimension (LVEDD)], New York Heart Association (NYHA) class, echocardiographic or clinical CRT response rates, and the incidence of adverse events including all-cause mortality or HF rehospitalization. Echocardiographic CRT response was defined as an LVEF improvement of at least 5% at follow-up compared with that at baseline, and clinical CRT response was defined as decreasing NYHA functional class for at least one grade at the last follow-up compared with the basal value (16). Reviews, editorials, preclinical studies, and single-arm studies without a BVP control group were excluded. When duplications of the data were found, the results of the most recent publications with longer follow-up durations were included in the meta-analysis.

Data Extraction and Quality Evaluation

Two independent authors performed the literature search, data extraction, and quality assessment according to the predefined inclusion criteria. Discrepancies were resolved by consensus and discussion with another author. The extracted data included the details regarding study and patient characteristics; LVEF, LVEDD, and QRSd at baseline in patients treated with LBBAP or BVP; and follow-up durations. Quality of randomized controlled studies was evaluated with the Cochrane's Risk of Bias Tool (15). Quality of non-randomized controlled studies was evaluated with the Newcastle–Ottawa Scale (NOS) (17). This scale judges the quality of each non-randomized controlled study regarding three aspects: selection of the study groups, the comparability of the groups, and the ascertainment of the outcome of interest.

Statistical Analyses

Mean difference (MD) was used as the general measures for the outcomes of continuous variables, whereas odds ratio (OR) was used for the categorized variables. The 95% confidence intervals (CIs) for MD and OR were also calculated. The heterogeneity among the included studies was detected by the Cochrane's *Q*-test (15, 18) and the I^2-test (19). An $I^2 > 50\%$ indicated significant heterogeneity. A random-effect model was used to pool the results of the included studies because this model was considered to incorporate the potential heterogeneity of the included studies and could therefore retrieve a more generalized outcome (15). Potential publication bias was assessed by visual inspection of the funnel plot as well as the Egger regression asymmetry test (20). RevMan (version 5.1; Cochrane Collaboration, Oxford, UK) software was used for the meta-analysis and statistics.

RESULTS

Searching Results

The process of literature searching is shown in **Figure 1**. Briefly, 98 records were retrieved by initial database searching and exclusion of the duplications. By screening *via* title and abstract of the publications, 78 were subsequently excluded, mainly

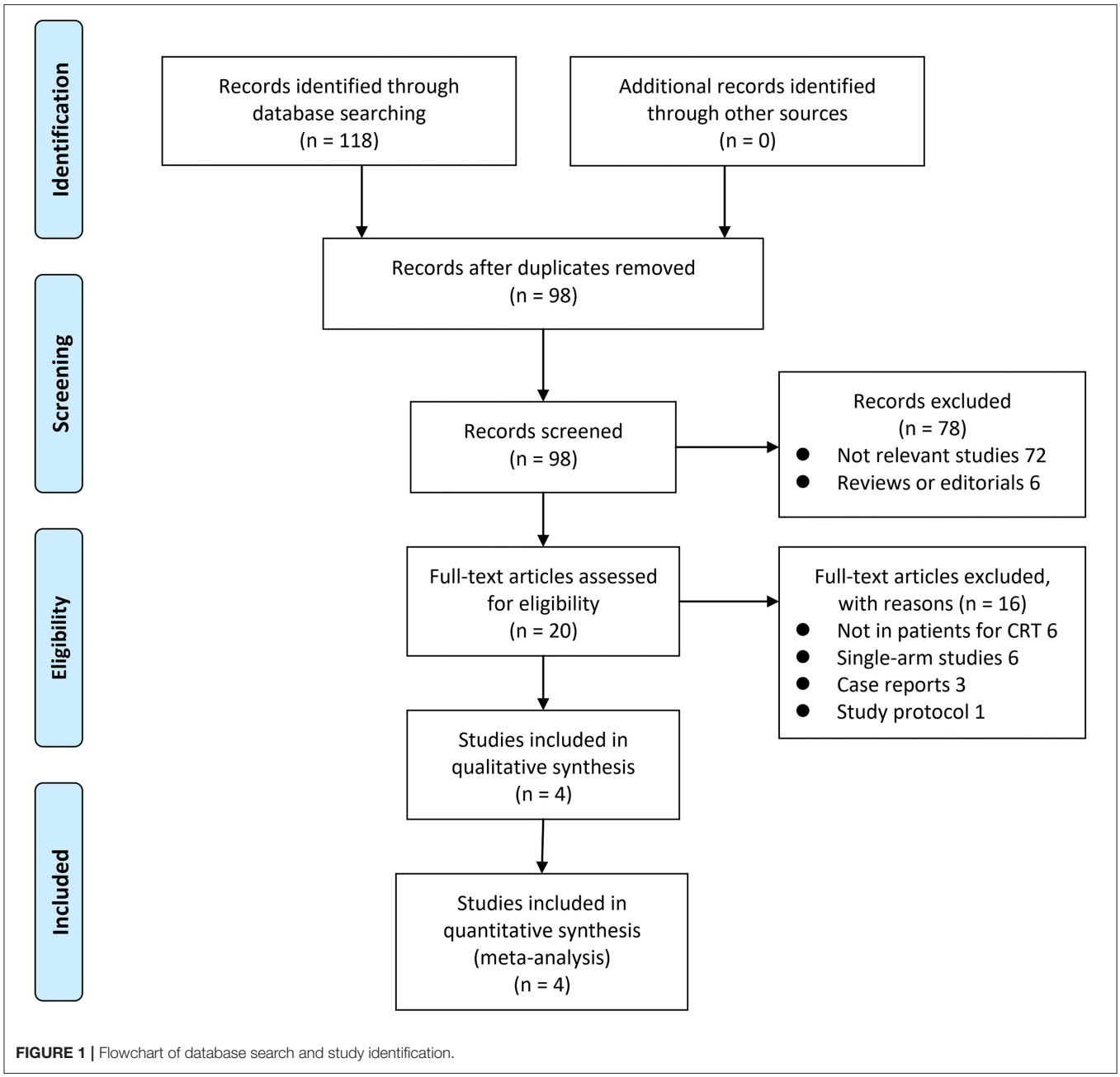

FIGURE 1 | Flowchart of database search and study identification.

because they were irrelevant to the objective of the current study. The remaining 20 records underwent full-text review, and 16 were further excluded for the reasons listed in **Figure 1**. Finally, four studies (10–13) were retrieved.

Study Characteristics and Quality Evaluation

Overall, four prospective non-randomized controlled studies, including 90 HF patients with LBBAP for CRT and 159 patients with BVP for CRT, were included in the meta-analysis (**Table 1**) (10–13). These studies were all performed in China and published between 2020 and 2021. All of the studies included HF patients with indication for CRT. Patients who received LBBAP and BVP were generally frequency-matched on age; sex; histories of ischemic heart disease; NYHA class; QRSd, LVEDD, and LVEF at baseline; and medications for HF (**Table 1**). Patients were followed for 6 months in three studies (10–12) and for 12 months in the other one study (13). The quality of the included studies was generally good, with the NOS varied between 8 and 9 points (**Table 2**).

Changes of QRSd, Cardiac Function, and Clinical Symptoms

Pooled results with a random-effect model showed that compared with BVP, LBBAP was associated with significantly shortened QRSd (MD: −29.18 ms, 95% CI: −33.55–24.80,

TABLE 1 | Characteristics of the included studies.

Study	Country	Design	Patients	Patient number		Mean age (years)		Male (%)		LVEF (%)		LVEDD (mm)		QRSd (mm)		Follow-up duration (months)	Matched variables
				LBBAP	BVP	LBBAP	BVP	LBBAP	BVP	LBBAP	BVP	LBBAP	BVP	LBBAP	BVP		
Guo et al. (10)	China	NRCT	HF patients for CRT	21	21	66.1	65.1	42.9	42.9	30.0	29.8	64.9	66.7	167.7	163.6	6	Age, sex, histories of IHD, DM, HTN, CKD, AF, intrinsic QRSd, LVEDD, LVEF, NYHA class, and medications for HF
Li et al. (11)	China	NRCT	HF patients for CRT	27	54	57.5	58.5	51.9	61.1	28.8	27.2	66.5	69.4	178.2	180.9	6	Age, sex, histories of IHD, DM, HTN, AF, intrinsic QRSd, LVEDD, LVEF, LAD, NYHA class, and medications for HF
Wang et al. (12)	China	NRCT	HF patients for CRT	10	30	64.8	62.9	90.0	76.7	26.8	26.4	68.6	70.4	183.6	174.6	6	Age, sex, histories of IHD, NYHA class, intrinsic QRSd, LVEDD, LVEF, LAD, and medications for HF
Wu et al. (13)	China	NRCT	HF patients for CRT	32	54	67.2	68.3	43.8	53.7	30.9	30.0	NR	NR	166.2	161.1	12	Age, sex, histories of IHD, DM, HTN, CKD, AF, intrinsic QRSd, MR, LVEF, BNP, NYHA class, and medications for HF

LVEF, left ventricular ejection fraction; LVEDD, left ventricular end-diastolic dimension; QRSd, QRS-wave duration; NRCT, non-randomized controlled trials; HF, heart failure; CRT, cardiac resynchronization therapy; LBBAP, left branch bundle area pacing; BVP, biventricular pacing; NR, not reported; IHD, ischemic heart disease; DM, diabetes mellitus; HTN, hypertension; CKD, chronic kidney disease; AF, atrial fibrillation; LVESD, left ventricular end-systolic dimension; NYHA, New York Heart Association; LAD, left atrial dimension; MR, mitral regurgitation; BNP, B-type natriuretic peptide.

TABLE 2 | Details of study quality evaluation *via* the Newcastle–Ottawa Scale.

Study	Representativeness of the patient	Selection of the controls	Ascertainment of intervention	Demonstration that outcome of interest was not present at the start of the study	Comparability-age and gender	Comparability-other factors	Assessment of outcome	Was follow-up long enough for outcomes to occur	Adequacy of follow-up of cohorts	Total
Guo et al. (10)	1	1	1	1	1	1	1	0	1	8
Li et al. (11)	1	1	1	1	1	1	1	0	1	8
Wang et al. (12)	1	1	1	1	1	1	1	0	1	8
Wu et al. (13)	1	1	1	1	1	1	1	1	1	9

$I^2 = 0\%$, $P < 0.001$; **Figure 2A**), improved LVEF (MD: 6.93%, 95% CI: 4.69–9.17, $I^2 = 0\%$, $P < 0.001$; **Figure 2B**), reduced LVEDD (MD: −2.96 mm, 95% CI: −5.48 to −0.44, $I^2 = 0\%$, $P = 0.02$; **Figure 2C**), and improved NYHA class (MD: −0.54, 95% CI: −0.84 to −0.24, $I^2 = 65\%$, $P < 0.001$; **Figure 2D**).

CRT Response Rate and Incidence of Adverse Events During Follow-up

Pooled results with a random-effect model showed that compared with patients who received BVP, patients who received LBBAP were more likely to achieve echocardiographic (OR: 5.04, 95% CI: 2.17–11.69, $I^2 = 0\%$, $P < 0.001$; **Figure 3A**) and clinical (OR: 7.33, 95% CI: 1.62–33.16, $I^2 = 0\%$, $P = 0.01$; **Figure 3B**) CRT responses. No patient died during follow-up, whereas the risk of HF rehospitalization was not statistically different between patients who received LBBAP or BVP (OR: 0.47, 95% CI: 0.05–4.33, $I^2 = 0\%$, $P = 0.51$; **Figure 3C**).

Publication Bias

The publication bias for the current meta-analysis was not estimated since only three to four studies were available for each outcome.

DISCUSSION

In this meta-analysis, by pooling the results of four non-randomized controlled studies, we found that for HF patients with indication for CRT, LBBAP is associated with significantly shortened QRSd, improved LVEF, reduced LVEDD, and decreased NYHA class as compared with conventional BVP at the end of the follow-up. Besides, patients who received LBBAP delivered CRT had higher echocardiographic and clinical response rates than those who received BVP delivered CRT, although the incidence of HF hospitalization was not different between patients from the two groups. These findings suggest that compared with conventional BVP, LBBAP is associated with more remarkable improvements of symptoms and cardiac function in HF patients with indication for CRT, which should be validated in randomized controlled trials (RCTs). Considering the technique feasibility of LBBAP, this novel physiological pacing strategy appears to be promising for HF patients with indication for CRT.

To the best of our knowledge, this study is the first meta-analysis comparing the efficacy between LBBAP and BVP delivered CRT in patients with HF. Since no RCTs regarding the comparative efficacy of LBBAP and BVP delivered CRT have been published, results of the meta-analysis may provide the current evidence-based overview regarding the comparative efficacy of LBBAP and BVP delivered CRT in HF patients during a follow-up of up to 1 year. Previous studies with epicardial activation mapping indicated that electrical dyssynchrony remained despite the use of BVP, suggesting that activation time and pattern could not be corrected to a physiological level by BVP delivered CRT (21). Among new strategies of conduction system pacing, although LBBAP could not achieve normal physiological activation maintained *via* the right bundle as HBP (22, 23), compared with BVP, LBBAP is associated with a significantly further decreased QRSd of −29.2 ms, as evidenced in our meta-analysis. In this meta-analysis, greater improvement of LVEF was achieved by LBBAP delivered CRT compared with BVP delivered CRT, which is paralleled with the more remarkable shortened QRSd in patients after LBBAP delivered CRT. Since a significant association between QRS narrowing and shorter attained QRSd with clinical and echocardiographic CRT responses has been indicated in previous studies, the further shortened QRSd may explain the benefits of LBBAP over BVP on cardiac function and clinical symptoms in HF patients, as well as the increased CRT response during follow-up (24). No significant difference in adverse events, such as HF hospitalization, was observed between groups. However, only four events of HF hospitalization were reported during a follow-up duration of up to 1 year, and our meta-analysis is underpowered for the detection of the potential benefits of LBBAP over BVP on clinical outcomes of HF patients. Large-scale RCTs with longer follow-up durations are warranted.

Although HBP may be more effective to achieve ventricular activation to the physiological level than LBBAP, pilot studies have showed a few technical advantages of LBBAP over HBP, including lower and more stable thresholds, higher implant success rates, and comparable ventricular mechanical synchrony of similar magnitude as HBP (13). With the accumulated experiences and continuous advances in implantation techniques, LBBAP may become an alternative strategy to HBP for CRT delivering with conduction system pacing (25, 26).

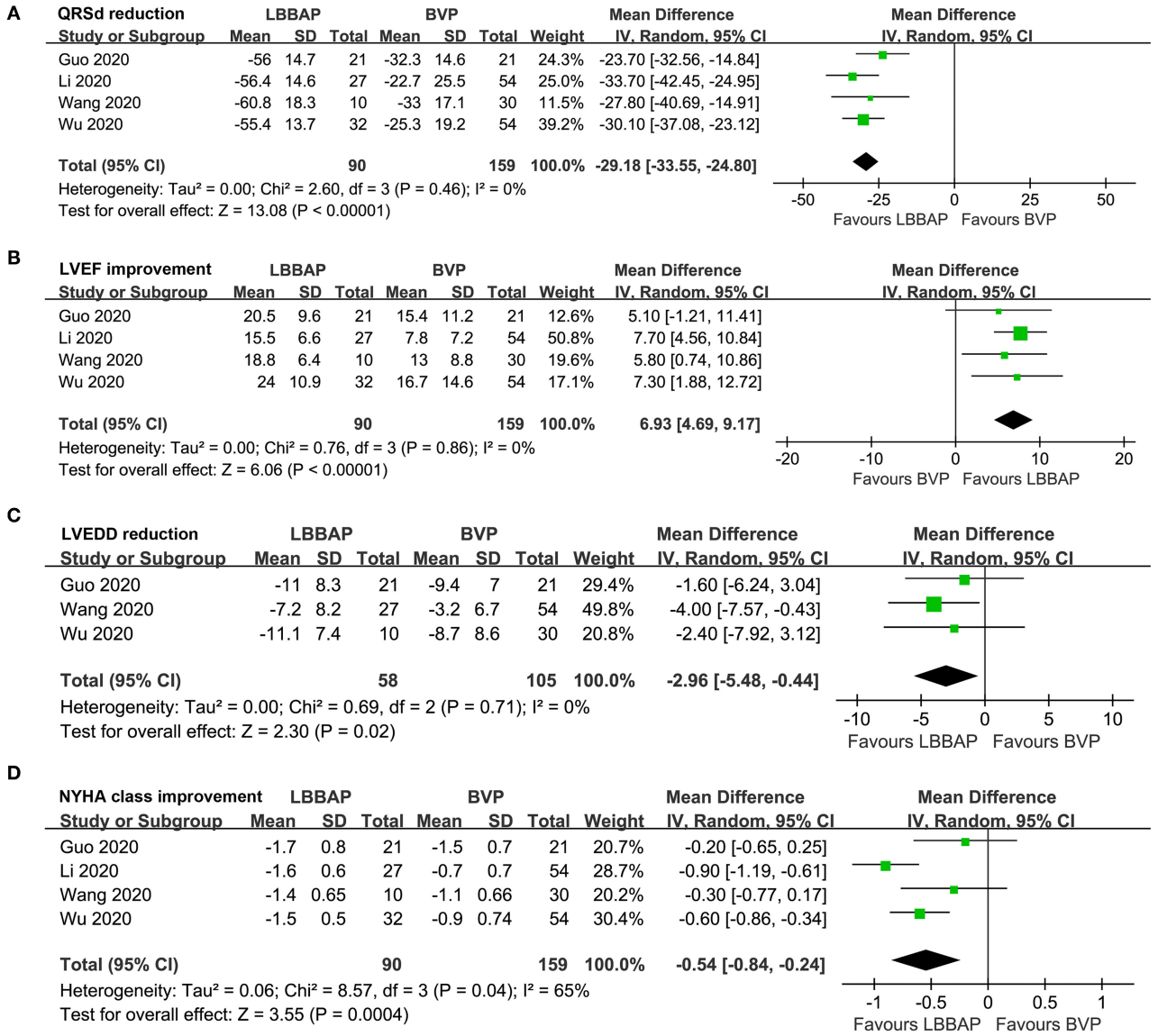

FIGURE 2 | Forest plots for the meta-analysis comparing influences of LBBAP and BVP on QRSd, cardiac function, and clinical symptoms in HF patients with indication for CRT. **(A)** QRSd, **(B)** LVEF, **(C)** LVEDD, and **(D)** NYHA class.

Our study has limitations. Firstly, as a meta-analysis of non-randomized controlled studies, although key variables have been frequency-matched, we acknowledged that the potential imbalance of other clinical characteristic of the patients may confound the findings. Ongoing RCTs may validate our findings (27). Secondly, the number of studies and patients is quite limited, whereas the findings of the studies seemed very consistent. In addition, patients were followed for 6–12 months in the studies included in the meta-analysis; the potential long-term benefits of LBBAP over BVP need to be investigated in studies with longer follow-up durations. Besides, as mentioned before, our meta-analysis is not of adequate statistical power to detect the potential benefits of LBBAP over BVP on clinical outcomes of HF patients, and large-scale RCTs with adequate follow-up durations are needed to validate the clinical benefits of LBBAP. Finally, the four included studies were all performed in Chinese centers with early performance of LBBAP. The experiences and skills of the surgeons may affect the comparative efficacy between LBBAP and BVP in HF patients for CRT.

In conclusion, results of this meta-analysis showed that compared with BVP, LBBAP is associated with more remarkable improvements of symptoms and cardiac function in HF patients with indication for CRT. These findings suggested that LBBAP appears to be a more promising method for CRT. The benefits of LBBAP over BVP for HF

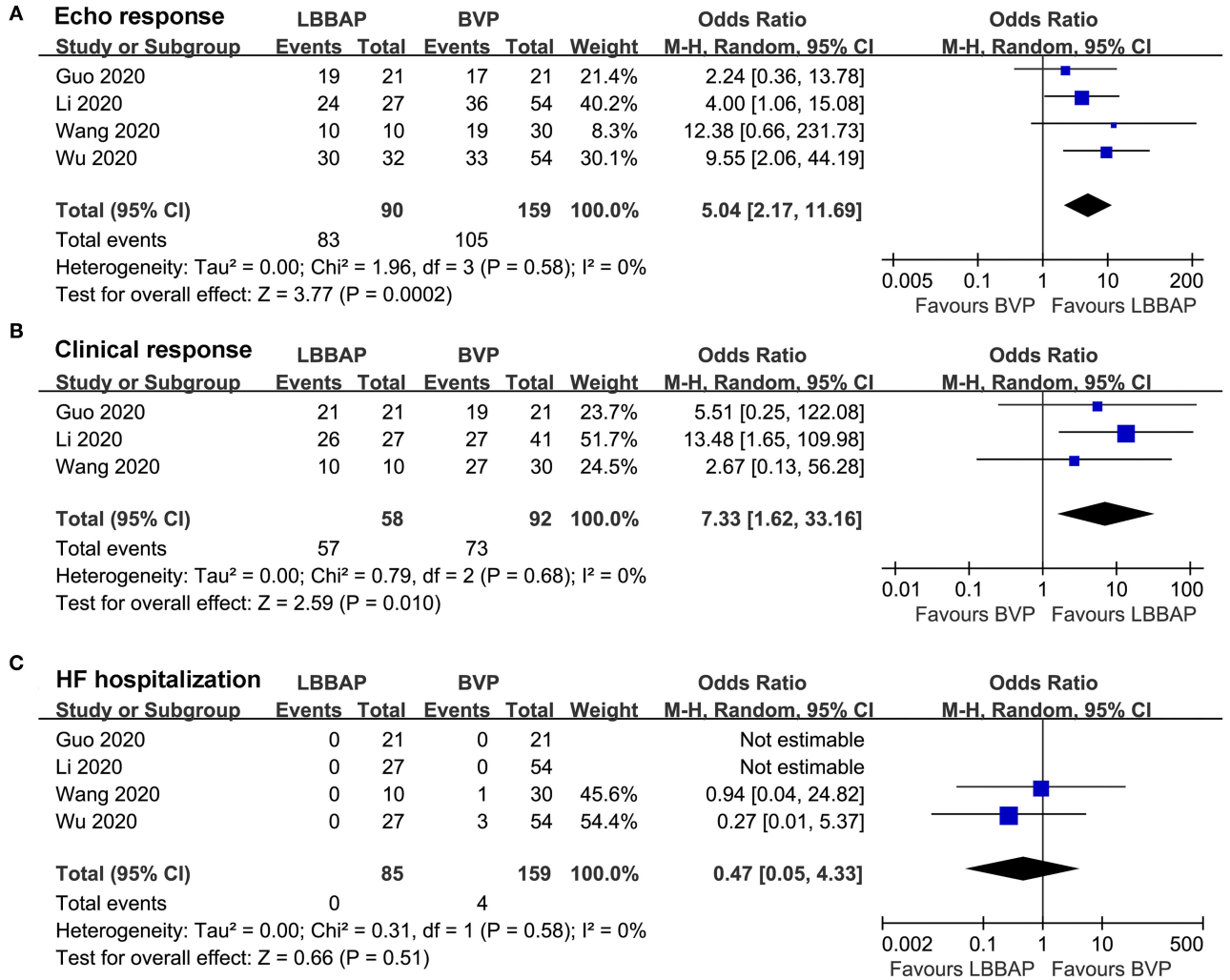

FIGURE 3 | Forest plots for the meta-analysis comparing influences of LBBAP and BVP on CRT response rates and incidence of adverse events during follow-up. **(A)** echocardiographic response, **(B)** clinical response, and **(C)** HF hospitalization.

patients with indication for CRT should be validated in high-quality RCTs.

DATA AVAILABILITY STATEMENT

The original contributions presented in the study are included in the article/supplementary material, further inquiries can be directed to the corresponding author/s.

AUTHOR CONTRIBUTIONS

JL, FS, and SZ designed the study. JL and FS performed the database search, study identification, quality evaluation, data extraction, and drafted the manuscript. ZW, JS, and XJ performed the statistical analyses. All authors interpreted the results, revised, and approved the submission of the manuscript.

REFERENCES

1. Katbeh A, Van Camp G, Barbato E, Galderisi M, Trimarco B, Bartunek J, et al. Cardiac resynchronization therapy optimization: a comprehensive approach. *Cardiology.* (2019) 142:116–28. doi: 10.1159/000499192
2. Wang Z, Wu Y, Zhang J. Cardiac resynchronization therapy in heart failure patients: tough road but clear future. *Heart Fail Rev.* (2021) 26:747. doi: 10.1007/s10741-020-10040-2
3. Zhu H, Zou T, Zhong Y, Yang C, Ren Y, Wang F. Prevention of non-response to cardiac resynchronization therapy: points to remember. *Heart Fail Rev.* (2020) 25:269–75. doi: 10.1007/s10741-019-09834-w
4. Pothineni NVK, Supple GE. Navigating challenging left ventricular lead placements for cardiac resynchronization therapy. *J Innov Card Rhythm Manag.* (2020) 11:4107–17. doi: 10.19102/icrm.2020.110505

5. Ali N, Shin MS, Whinnett Z. The emerging role of cardiac conduction system pacing as a treatment for heart failure. *Curr Heart Fail Rep.* (2020) 17:288–98. doi: 10.1007/s11897-020-00474-y
6. Qi J, Jia X, Wang Z. His bundle pacing for cardiac resynchronization therapy: a systematic literature review and meta-analysis. *J Interv Card Electrophysiol.* (2020) 59:463–70. doi: 10.1007/s10840-020-00827-6
7. Huang W, Su L, Wu S, Xu L, Xiao F, Zhou X, et al. A novel pacing strategy with low and stable output: pacing the left bundle branch immediately beyond the conduction block. *Can J Cardiol.* (2017) 33:1736 e1731–1736 e1733. doi: 10.1016/j.cjca.2017.09.013
8. Huang W, Wu S, Vijayaraman P, Su L, Chen X, Cai B, et al. Cardiac resynchronization therapy in patients with nonischemic cardiomyopathy using left bundle branch pacing. *JACC Clin Electrophysiol.* (2020) 6:849–58. doi: 10.1016/j.jacep.2020.04.011
9. Zhong C, Xu W, Shi S, Zhou X, Zhu Z. Left bundle branch pacing for cardiac resynchronization therapy: a systematic literature review and meta-analysis. *Pacing Clin Electrophysiol*. (2021). doi: 10.1111/pace.14174
10. Guo J, Li L, Xiao G, Ye T, Huang X, Meng F, et al. Remarkable response to cardiac resynchronization therapy via left bundle branch pacing in patients with true left bundle branch block. *Clin Cardiol.* (2020) 43:1460–8. doi: 10.1002/clc.23462
11. Li X, Qiu C, Xie R, Ma W, Wang Z, Li H, et al. Left bundle branch area pacing delivery of cardiac resynchronization therapy and comparison with biventricular pacing. *ESC Heart Fail.* (2020) 7:1711–22. doi: 10.1002/ehf2.12731
12. Wang Y, Gu K, Qian Z, Hou X, Chen X, Qiu Y, et al. The efficacy of left bundle branch area pacing compared with biventricular pacing in patients with heart failure: a matched case-control study. *J Cardiovasc Electrophysiol.* (2020) 31:2068–77. doi: 10.1111/jce.14628
13. Wu S, Su L, Vijayaraman P, Zheng R, Cai M, Xu L, et al. Left bundle branch pacing for cardiac resynchronization therapy: nonrandomized on-treatment comparison with his bundle pacing and biventricular pacing. *Can J Cardiol.* (2021) 37:319–28. doi: 10.1016/j.cjca.2020.04.037
14. Moher D, Liberati A, Tetzlaff J, Altman DG. Preferred reporting items for systematic reviews and meta-analyses: the PRISMA statement. *BMJ.* (2009) 339:b2535. doi: 10.1136/bmj.b2535
15. Higgins J, Green S. *Cochrane Handbook for Systematic Reviews of Interventions Version 5.1.0*. The Cochrane Collaboration(2011). Available online at: www.cochranehandbook.org
16. Parreira L. Assessing response to cardiac resynchronization therapy: time to settle on some definitive criteria. *Rev Port Cardiol.* (2018) 37:971–2. doi: 10.1016/j.repc.2018.11.005
17. Wells GA, Shea B, O'connell D, Peterson J, Welch V, Losos M, et al. The Newcastle-Ottawa Scale (NOS) for assessing the quality of nonrandomised studies in meta-analyses (2010). Available online at: http://www.ohri.ca/programs/clinical_epidemiology/oxford.asp
18. Patsopoulos NA, Evangelou E, Ioannidis JP. Sensitivity of between-study heterogeneity in meta-analysis: proposed metrics and empirical evaluation. *Int J Epidemiol.* (2008) 37:1148–57. doi: 10.1093/ije/dyn065
19. Higgins JP, Thompson SG. Quantifying heterogeneity in a meta-analysis. *Stat Med.* (2002) 21:1539–58. doi: 10.1002/sim.1186
20. Egger M, Davey Smith G, Schneider M, Minder C. Bias in meta-analysis detected by a simple, graphical test. *BMJ.* (1997) 315:629–34. doi: 10.1136/bmj.315.7109.629
21. Ploux S, Eschalier R, Whinnett ZI, Lumens J, Derval N, Sacher F, et al. Electrical dyssynchrony induced by biventricular pacing: implications for patient selection and therapy improvement. *Heart Rhythm.* (2015) 12:782–91. doi: 10.1016/j.hrthm.2014.12.031
22. Elliott MK, Mehta V, Sidhu BS, Niederer S, Rinaldi CA. Electrocardiographic imaging of His bundle, left bundle branch, epicardial, and endocardial left ventricular pacing to achieve cardiac resynchronization therapy. *HeartRhythm Case Rep.* (2020) 6:460–3. doi: 10.1016/j.hrcr.2020.04.012
23. Herweg B, Welter-Frost A, Vijayaraman P. The evolution of cardiac resynchronization therapy and an introduction to conduction system pacing: a conceptual review. *Europace.* (2021) 23:496–510. doi: 10.1093/europace/euaa264
24. Bazoukis G, Naka KK, Alsheikh-Ali A, Tse G, Letsas KP, Korantzopoulos P, et al. Association of QRS narrowing with response to cardiac resynchronization therapy-a systematic review and meta-analysis of observational studies. *Heart Fail Rev.* (2020) 25:745–56. doi: 10.1007/s10741-019-09839-5
25. Su L, Wang S, Wu S, Xu L, Huang Z, Chen X, et al. Long-term safety and feasibility of left bundle branch pacing in a large single-center study. *Circ Arrhythm Electrophysiol.* (2021) 14:e009261. doi: 10.1161/CIRCEP.120.009261
26. Zhang J, Wang Z, Zu L, Cheng L, Su R, Wang X, et al. Simplifying physiological left bundle branch area pacing using a new nine-partition method. *Can J Cardiol.* (2021) 37:329–38. doi: 10.1016/j.cjca.2020.05.011
27. Cheng L, Zhang J, Wang Z, Zhou M, Liang Z, Zhao L, et al. Efficacy and safety of left bundle branch area pacing versus biventricular pacing in heart failure patients with left bundle branch block: study protocol for a randomised controlled trial. *BMJ Open.* (2020) 10:e036972. doi: 10.1136/bmjopen-2020-036972

Conflict of Interest: The authors declare that the research was conducted in the absence of any commercial or financial relationships that could be construed as a potential conflict of interest.

frontiers in Cardiovascular Medicine

ORIGINAL RESEARCH
published: 14 June 2021
doi: 10.3389/fcvm.2021.674452

Feasibility and Outcomes of Upgrading to Left Bundle Branch Pacing in Patients With Pacing-Induced Cardiomyopathy and Infranodal Atrioventricular Block

Yang Ye[1,2†], Shengjie Wu[3,4†], Lan Su[3,4†], Xia Sheng[1,2], Jiefang Zhang[1,2], Bei Wang[5], Parikshit S. Sharma[6], Kenneth A. Ellenbogen[7], Yangang Su[8], Xueying Chen[8], Guosheng Fu[1,2*] and Weijian Huang[3,4*]*

[1] Department of Cardiology, Sir Run Run Shaw Hospital, College of Medicine, Zhejiang University, Hangzhou, China, [2] Key Laboratory of Cardiovascular Intervention and Regenerative Medicine of Zhejiang Province, Hangzhou, China, [3] Department of Cardiology, The First Affiliated Hospital of Wenzhou Medical University, Wenzhou, China, [4] Key Lab of Cardiovascular Disease of Wenzhou, Wenzhou, China, [5] Department of Cardiac Echocardiology, Sir Run Run Shaw Hospital, College of Medicine, Zhejiang University, Hangzhou, China, [6] From the Division of Cardiology, Rush University Medical Center, Chicago, IL, United States, [7] Virginia Commonwealth University Medical Center, Richmond, VA, United States, [8] Department of Cardiology, Shanghai Institution of Cardiovascular Disease, Zhongshan Hospital, Fudan University, Shanghai, China

His bundle pacing (HBP) can reverse left ventricular (LV) remodeling in patients with right ventricular (RV) pacing-induced cardimyopathy (PICM) but may be unable to correct infranodal atrioventricular block (AVB). Left bundle branch pacing (LBBP) results in rapid LV activation and may be able to reliably pace beyond the site of AVB. Our study was conducted to assess the feasibility, safety, and outcomes of permanent LBBP in infranodal AVB and PICM patients. Patients with infranodal AVB and PICM who underwent LBBP for cardiac resynchronization therapy (CRT) were included. Clinical evaluation and echocardiographic and electrocardiographic assessments were recorded at baseline and follow-up. Permanent LBBP upgrade was successful in 19 of 20 patients with a median follow-up duration of 12 months. QRS duration (QRSd) increased from 139.3 ± 28.0 ms at baseline to 176.2 ± 21.4 ms ($P < 0.001$) with right ventricular pacing (RVP) and was shortened to 120.9 ± 15.2 ms after LBBP ($P < 0.001$). The mean LBBP threshold was 0.7 ± 0.3 V at 0.4 ms at implant and remained stable during follow-up. The left ventricular ejection fraction (LVEF) increased from 36.3% ± 6.5% to 51.9% ± 13.0% ($P < 0.001$) with left ventricular end-systolic volume (LVESV) reduced from 180.1 ± 43.5 to 136.8 ± 36.7 ml ($P < 0.001$) during last follow-up. LBBP paced beyond the site of block, which results in a low pacing threshold with a high success rate in infranodal AVB patients. LBBP improved LV function with stable parameters over the 12 months, making it a reasonable alternative to cardiac resynchronization pacing via a coronary sinus lead in infranodal AVB and PICM patients.

Keywords: cardiac pacing, atrioventricular block (AVB), pacing-induced cardiomyopathy (PICM), heart failure (HF), His bundle pacing (HBP), left bundle branch pacing (LBBP), cardiac resynchronization therapy (CRT)

OPEN ACCESS

Edited by:
Hung-Fat Tse,
The University of Hong Kong, China

Reviewed by:
Luigi Pannone,
Vita-Salute San Raffaele University, Italy
Antonio Bisignani,
Catholic University of the Sacred Heart, Italy
Alexandre Almorad,
University Hospital Brussels, Belgium

***Correspondence:**
Weijian Huang
weijianhuang69@126.com
Guosheng Fu
fugs@zju.edu.cn
Xueying Chen
chen.xueying@zs-hospital.sh.cn

†These authors have contributed equally to this work and share first authorship

Specialty section:
This article was submitted to Cardiac Rhythmology, a section of the journal Frontiers in Cardiovascular Medicine

Received: *16 March 2021*
Accepted: *11 May 2021*
Published: *14 June 2021*

Citation:
Ye Y, Wu S, Su L, Sheng X, Zhang J, Wang B, Sharma PS, Ellenbogen KA, Su Y, Chen X, Fu G and Huang W (2021) Feasibility and Outcomes of Upgrading to Left Bundle Branch Pacing in Patients With Pacing-Induced Cardiomyopathy and Infranodal Atrioventricular Block. Front. Cardiovasc. Med. 8:674452. doi: 10.3389/fcvm.2021.674452

INTRODUCTION

Right ventricular pacing (RVP) leads to left ventricular (LV) dyssynchrony and may result in symptoms of heart failure (HF), a syndrome known as pacing-induced cardiomyopathy (PICM) (1, 2). PICM is an important and under-recognized cause of cardiomyopathy and may occur in up to 5–20% of patients with chronic RVP (2, 3). Cardiac resynchronization therapy (CRT) utilizing biventricular pacing (BVP) is recommended for patients who develop a PICM and can result in an improvement in cardiac function and LV remodeling (4). However, the clinical improvement after upgrade from RVP to BVP is limited by cardiac venous anatomy and LV lead positioning (5). BVP may not be the best strategy to maintain synchrony in patients with a native narrow QRS and may not overcome the challenges associated with non-physiological ventricular activation in patients with a narrow QRS and atrioventricular block (AVB) (6). As the most physiological ventricular pacing strategy, permanent His bundle pacing (HBP) improves LV function in PICM patients (7, 8), however is limited by variable success rate, potential high His bundle capture thresholds, low R-wave amplitudes, atrial oversensing, as well as an increased risk of lead revision with late threshold rise (9–11). The HBP has a lower success rate among patients especially with infranodal AVB due to pacing proximal to the site of block and the possibility of the threshold rise due to the progression of conduction disease (9). Left bundle branch pacing (LBBP) was first described in 2017 (12) and has demonstrated clinically promising results including the safety, efficacy, and outcomes in various patient populations with low and stable thresholds (13, 14). LBBP preserves rapid LV activation, and a recent case report demonstrated that LBBP resulted in reverse LV remodeling in a patient with PICM and infranodal AVB (15). LBBP also achieved electric resynchronization in HF and left branch bundle block (LBBB) patients with low and stable pacing thresholds (16). Given the location of LBBP and the theoretical advantage of pacing distal to the site of conduction block, this could be well-suited for patients with infranodal AVB.

The objective of our multicenter study was to assess the feasibility, safety, and clinical outcomes of LBBP in patients with infranodal AVB undergoing a device upgrade for PICM as a result of chronic RVP.

METHODS

Patient Selection

This was a retrospective multicenter study including all consecutive patients undergoing LBBP pacing between December 2017 and June 2019 at three centers (Wenzhou, Hangzhou, and Shanghai) meeting the inclusion criteria. Patients >18 years of age who met the following inclusion criteria were enrolled in this study: (1) PICM patients, which was defined as a >10% decrease in left ventricular ejection fraction (LVEF) after chronic RVP resulting in LVEF ≤50%. (2) The pacing percentage of RVP was >40%. (3) All patients were assessed for the site of conduction block. Then, the patients in whom infranodal AVB was confirmed, LBBP was attempted in order to pace beyond the site of block. Patients with other causes of LV dysfunction, including myocardial infarction, valvular heart disease (>15%), frequent ventricular premature depolarizations, and uncontrolled hypertension (>160/100 mmHg), were not defined to have PICM and were excluded (2). All patients had received standard medical treatments for HF at least 3 months before the upgrade. The hospital institutional review board approved the study procedure, and all patients were provided informed consent and demonstrated the understanding of LBBP therapy as a non-standard approach to achieve physiological pacing. Data analysis was approved by the institutional review board at all three institutions and was retrospectively analyzed.

Implantation Technique and Procedure Details

During the LBBP implantation, intracardiac electrograms (EGM) along with a 12-lead surface ECG GE CardioLab EP Recording System 2000; GE, Milwaukee, Wisconsin, USA. LabSystem PRO, Bard Electrophysiology, 196 Lowell, MA, USA were recorded. The techniques for HBP and LBBP were described in detail in our prior study (17, 18). Briefly, the 3830 lead (SelectSecure, Medtronic, Minneapolis, MN, USA) was advanced through the C315HIS delivery sheath to a spot for unipolar His bundle (HB) site mapping and pacing. Then, the 3830 lead was further advanced to a spot on the interventricular septum that is 1–1.5 cm apical along an axial line between the distal HB site and right ventricular (RV) apex in the right anterior oblique projection on fluoroscopy. The lead was then advanced deep into the septum in order to achieve left conduction system capture. LBBP was confirmed (19) and differentiated from left ventricular septal pacing (LVSP) by the criteria published previously (20).

Infranodal AVB is defined as the intra-Hisian and infra-Hisian block shown as a split His, His potential to ventricle interval (HV) prolongation, or HV dissociation. In patients without an underlying escape rhythm, the pacing rate was decreased to 30–35 bpm to assess for an escape rhythm. If patients had a ventricular escape rhythm due to sinus bradycardia, atrial pacing was used to help test intrinsic conduction to determine the site of block. A HBP lead was used to record the His potential to help assess the site of block.

In patients with AVB, the left bundle branch (LBB) potential was recorded (21), proceeding the ventricular electrogram and pacing at a rate of 130 beats/min (0.5 V above LBB capture threshold) to test the refractory period of the distal conduction system and ensuring capture and 1:1 conduction. In those with LVEF < 35%, a decision to implant an implantable cardiac defibrillator (ICD) was based on shared decision making between the implanter and the patient. LBB potential (s) and/or ventricular electrograms were assessed and lead parameters were analyzed. The pacing lead was then connected with a

Abbreviations: HBP, His bundle pacing; LV, Left ventricular; RV, right ventricular; PICM, pacing-induced cardiomyopathy; AVB, atrioventricular block; LBBP, left bundle branch pacing; QRSd, QRS duration; HF, heart failure; CRT, cardiac resynchronization therapy; BVP, biventricular pacing; LVSP, left ventricular septal pacing; ICD, implantable cardiac defibrillator; RAD, right axis deviation; HFH, heart failure hospitalization; IQR, interquartile range; RBBB, right bundle branch block; LBBB, left branch bundle block; IVCD, interventricular conduction delay.

device (described in **Supplementary Table 1**). At the physician's discretion, the device was programmed to LBBP only.

ECG Evaluation

Electrical dyssynchrony was assessed by QRS width and axis. They were compared between native, RVP, and LBBP configurations. QRS duration (QRSd) was measured in 12 contemporary ECG leads. Paced QRSd was measured from the pacing stimulus to the end of QRS complex. Normal frontal QRS axis was defined as −30° to 90°, left axis deviation (LAD) as −90° to −30°, moderate right axis deviation (RAD) as 90°-180°, and superior RAD as 180°-270°. The precordial lead transition in which the precordial lead R-wave amplitude is equal to or greater than the S wave amplitude was recorded.

Clinical Assessment and Follow-Up

Patients underwent regular follow-up at 3 and 6 months and annually post implantation. Functional status was assessed by the New York Heart Association (NYHA) classification. Device thresholds were checked and adjusted as needed to maximize battery longevity. Echocardiograms were performed as clinically indicated for follow-up. At follow-up visits, R-wave amplitude, capture threshold, pacing impedance, and the percentage of LBBP were collected. Standard echocardiographic indices including LVEF, left ventricular end-diastolic diameter (LVEDD), left ventricular end-systolic volume (LVESV), and valvular regurgitation were acquired by an experienced physician in accordance with the American Society of Echocardiography guidelines (7). Lead-related complications such as a significant increase in pacing threshold, lead dislodgment, or loss of capture were routinely tracked. Heart failure hospitalization (HFH) was determined by the following criteria: admission to hospital for >24 h due to worsening symptoms of HF and requiring intravenous diuretics or intravenous inotropic medications. The echocardiographic response was defined as ≥5% increase in LVEF. Super response was defined as an absolute improvement in LVEF by ≥20% or improvement of LVEF to 50% from a baseline value of <35% (17).

Statistical Analysis

Continuous variables were expressed as mean ± SD or median [interquartile range (IQR)]. Paired comparisons were made with a Student's *t*-test if the data were normally distributed and with the Wilcoxon signed-rank test for non-parametric data. Paired categorical data (NYHA functional class) were compared with the Wilcoxon test. For echocardiographic LVEF, LVEDD, LVESV, and parameters (threshold, sensed R-wave amplitude, and the

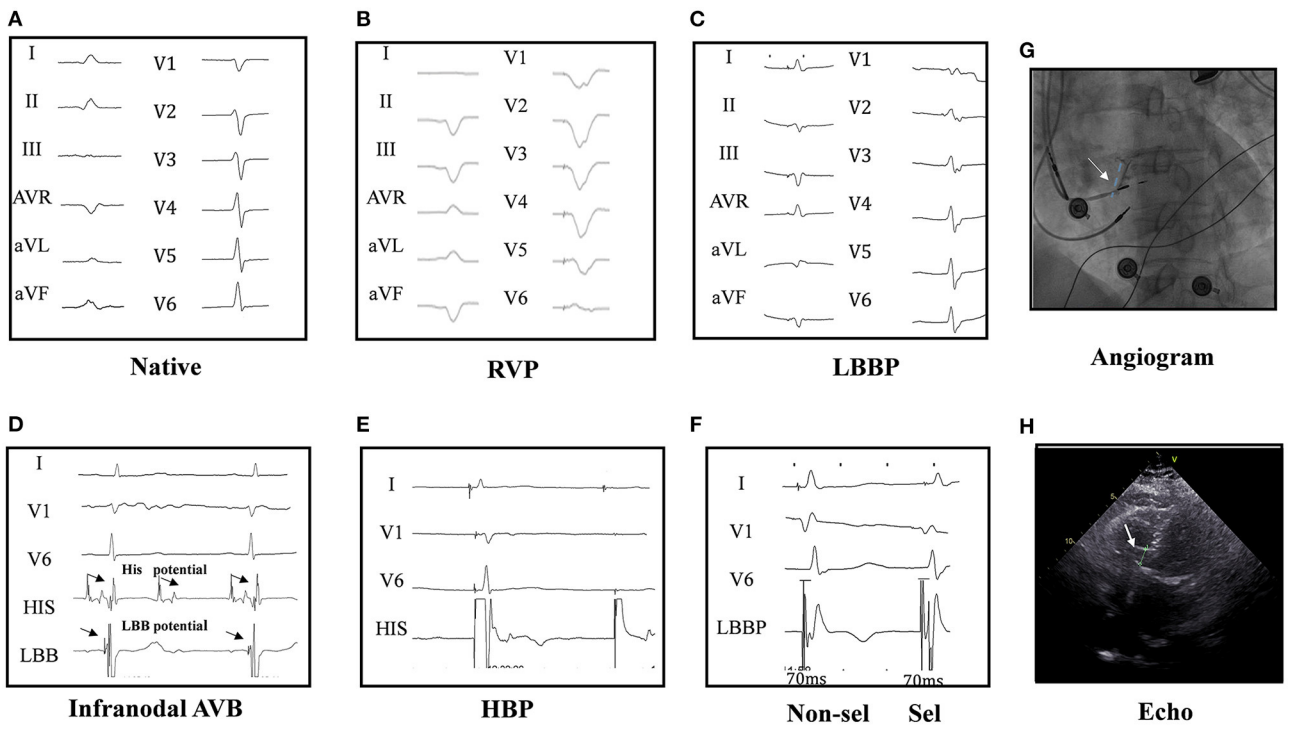

FIGURE 1 | Twelve-lead ECG and intracardiac electrogram (EGM) in a patient. The native cardiac rhythm **(A)**; twelve-lead ECG by right ventricular pacing (RVP) **(B)**; the ECG by left bundle branch pacing (LBBP) **(C)**; narrow ECG QRS with LBB potential in intracardiac electrograms (EGM at the bottom) in a infranodal atrioventricular block (AVB) patient **(D)**. His bundle pacing (HBP) could not pace beyond the block site (2.5 V at 0.4 ms) **(E)**. Selective (0.6 V at 0.4 ms) and non-selective (0.5 V at 0.4 ms) LBBP **(F)** and the angiogram of the sheath to assess the depth of the LBB LBBP lead **(G)** are shown. Echocardiography showed the lead was fixed in the left ventricular septum **(H)**, and LBBP but not HBP could pace beyond the block site in one patient of AVB with infranodal block. HBP at 2.5 V/0.4 ms could induce the loss of capture (2:1) **(E)**, while LBBP could induce pacing (1:1) **(F)**, indicating LBBP but not HBP could pace beyond the block site in infranodal AVB patients. His and LBB potential were seen in the pacing location **(D)**.

percentage of LBBP) that were collected at baseline and later multiple different time points, univariate analysis of variance for repeated measures was used to assess the effects of LBBP. A P value ≤ 0.05 was considered statistically significant. Data analyses were performed using SPSS version 20.0 (SPSS, Chicago, IL, USA).

RESULTS

Patient Characteristics and Implantation Results

Twenty PICM patients with confirmed infranodal AVB were referred for LBBP upgrade. One patient had failed LBBP lead fixation and was left with LVSP (22). Thus, 19 infranodal AVB patients with successful LBBP upgrade were included. As noted in **Figure 1**, in a patient with infranodal AVB, LBBP but not HBP resulted in conduction system capture beyond the site of block. The baseline characteristics of the study population are demonstrated in **Table 1**. The mean age of the successfully implanted patients was 70.2 ± 8.6 years with 57.9% male. The indication for permanent RVP was mostly complete AVB. The median percentage of RVP was 100% (IQR: 97% to 100%), and the mean duration of RVP was 76.4 ± 33.5 months before upgrade to LBBP. Of 19 patients successfully implanted, 52.6% (10/19) patients had LBB potentials with the mean potential to ventricle interval of 19.7 ± 6.6 ms. The median fluoroscopy duration for LBBP lead implantation in all these 19 patients was 7 min (IQR: 6 to 7 min), and the median total procedural time for implantation was 80 min (IQR: 70 to 100 min). The median follow-up after upgrade to LBBP was 12 months (IQR: 12−12 months). The percentage of LBBP was 97.0% ± 16.9% during the median 12-month follow-up. The mean threshold for LBBP capture was 0.7 ± 0.3 V at 0.4 ms and the R-wave amplitude was 12.7 ± 4.2 mv. The mean lead impedance at implant was 625.1 ± 118.8 Ω. There were no complications during the procedure.

TABLE 1 | Baseline clinical characteristics of patients.

	N **(%)/mean ± SD/ median (IQR)**
Successful LBBP	19 (95.0)
Age (years)	70.2 ± 8.6
Male (%)	11 (57.9)
Coronary artery disease	1 (5.3)
Atrial fibrillation	2 (10.5)
Hypertension	6 (31.6)
LVEF (pre-RVP, %)	62.0 ± 6.6
Duration of RVP (months)	75.5 ± 33.3
Percentage of RVP %	100 (97–100)
AVB	
Complete AVB	14 (73.7)
Second degree or higher grade AVB	5 (26.3)
Fluoroscopy duration (min)	7 (6, 7)
QRS duration (ms)	
Baseline	139.3 ± 28.0
RVP	176.2 ± 21.4
LBBP	120.9 ± 15.2
LBBP threshold (V at 0.4 ms)	
LBBP threshold at the implantation	0.7 ± 0.3
LBBP threshold during last follow up	0.8 ± 0.2
Devices	
ICD	1 (5.3)
Pacemaker	9 (47.4)
CRT-P	7 (36.8)
CRT-D	2 (10.5)

Values are mean ±SD or median (IQR). LVEF, left ventricular ejection fraction; RVP, right ventricular pacing; AVB, atrioventricular block; LBBP, left bundle branch pacing; ICD, implantable cardiac defibrillator; CRT-P, cardiac resynchronization therapy-pacing; CRT-D, cardiac resynchronization therapy-defibrillator.

ECG Changes After LBBP Upgrade

Eleven patients had an intrinsic rhythm, with a narrow QRS in five, right bundle branch block (RBBB) in three, LBBB in two, and interventricular conduction delay (IVCD) in one (**Supplementary Table 1**). In patients with an escape rhythm, eight patients had a wide QRSd. Compared with the native QRSd of 139.3 ± 28.0 ms, the mean paced QRSd was wider with RVP (176.2 ± 21.4 ms, $P < 0.001$) and shortened to 120.9 ± 15.2 ms with LBBP ($P = 0.006$). Pre-implant mean QRS axis of all patients was 32.63° (IQR: 0°-70.5°) and was 5.3° by RVP (IQR: −66.00°-80.5°) and kept stable at 63.84° after LBBP (IQR: 41.5°-73°). The percentage of patients with normal QRS axis was 84.2% ($n = 16$) on native and decreased to 26.3% ($n = 5$) on RVP ($p = 0.0001$) and was increased to 78.9% ($n = 15$) on LBBP ($p = 0.001$).

Eleven patients with native conduction had normal R-wave transitions between V3 and V4, while during RVP, 13/19 patients had an R/S transition from V5 to V6. During LBBP, 10 patients were noted to have a normal R/S transition between lead V3 and V4, while nine patients had an R/S transition between leads V1 and V2.

Echocardiographic Changes After LBBP Upgrade

The echocardiographic measurements are summarized in **Figures 2**, **3**. All patients completed 6-month follow-up, and the mean LVEF was increased from 36.3% ± 6.6% to 50.0% ± 11.1% ($p < 0.001$, $n = 18$) (**Figure 2**), and the LVESV was reduced from 179.9 ± 44.8 to 148.4 ± 37.1 ml ($p < 0.001$, $n = 18$) (**Figure 2**). In patients with complete 12-month follow-up, the mean LVEF increased from 36.3% ± 6.8% to 52.9% ± 13.1% ($p < 0.001$, $n = 17$) and the LVESV was reduced from 183.4 ± 44.7 to 137.2 ± 38.7 ml ($p < 0.001$, $n = 17$) (**Figure 2**). The LVEF increased from 36.3% ± 6.5% to 51.9% ± 13.0% ($P < 0.001$) with LVESV reduced from 180.1 ± 43.5 to 136.8 ± 36.7 ml ($P < 0.001$) during last follow-up, while an improvement in LVEF by ≥5% was observed in 17 patients (89.5%) and a super response was observed in five patients (26.3%).

Clinical Outcomes and Lead Complications

During a median follow-up of 12 months, NYHA functional class was improved from 2.8 ± 0.6 to 2.1 ± 0.6 ($p = 0.02$). The number of patients with moderate-to-severe HF (NYHA III–IV)

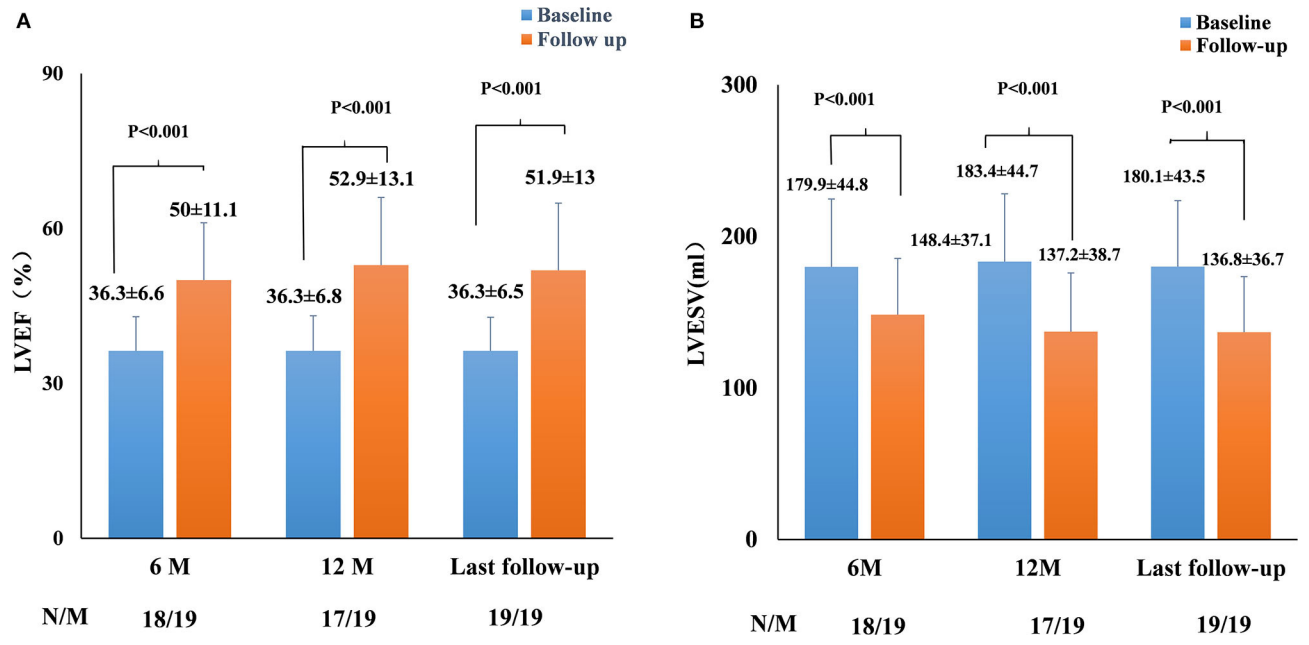

FIGURE 2 | Paired left ventricular ejection fraction (LVEF) **(A)** and left ventricular end-systolic volume (LVESV) **(B)** in all pacing-induced cardiomyopathy (PICM) patients at implant and during the median 12-month follow-up. *N*, the number of patients who had completed the follow-up of 6 and 12 months; *M*, the number of patients who completed the follow-up of 6 and 12 months. Data were available in 18/19 patients at 6-month follow-up, in 17/19 patients at the 12-month follow-up, and in 19/19 patients at the median 12-month follow-up.

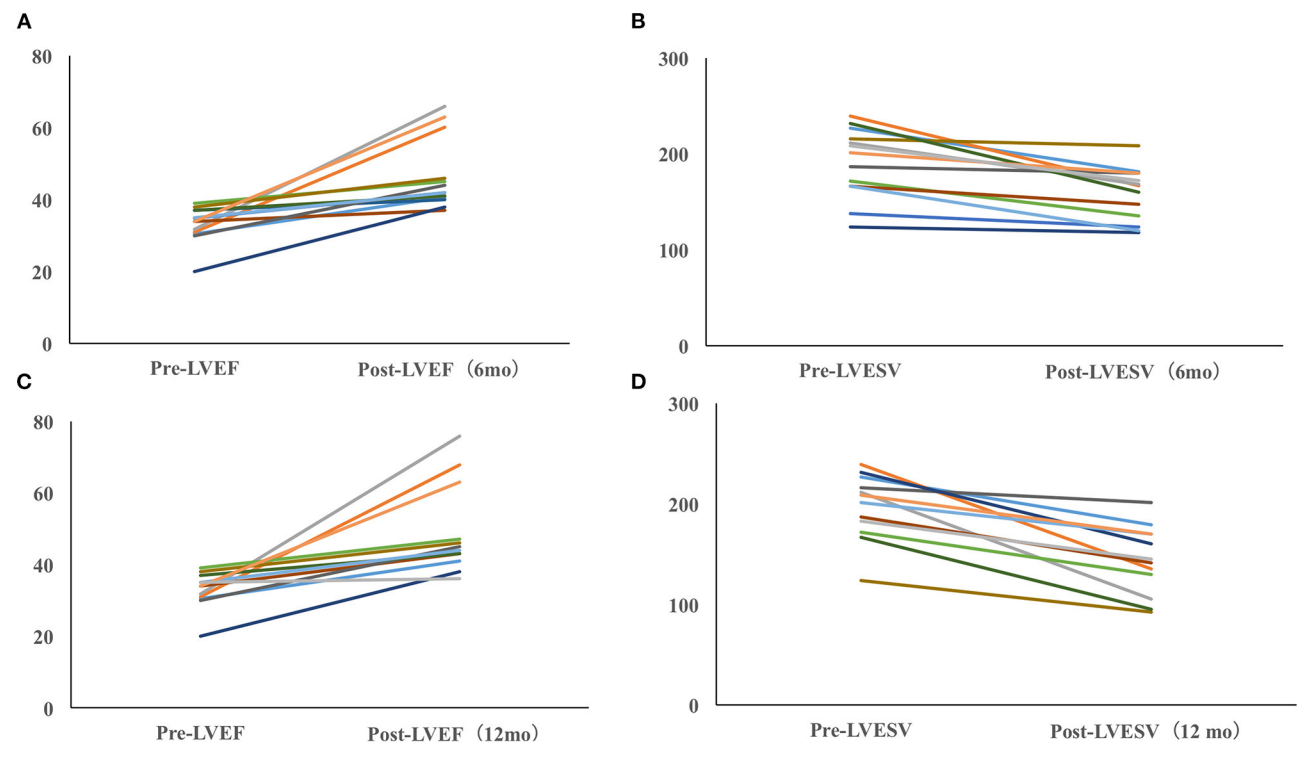

FIGURE 3 | Dynamic echocardiographic changes in PICM patients with baseline LVEF <40%. Improvement of LVEF **(A)** and LVESV **(B)** in PICM patients with LVEF < 40% (6 months). Improvement of LVEF **(C)** and LVESV in PICM patients with LVEF < 40% (12 months) **(D)**. Data were available in 13/14 patients at the 6-month follow-up and in 12/12 patients at the last follow-up.

TABLE 2 | Lead parameters at the baseline and during the follow-up.

LBBP lead	Baseline (*N* = 19)	6-month (*N* = 18)	12-month (*N* = 17)
Pacing threshold, V/0.4 ms	0.7 ± 0.3	0.7 ± 0.2	0.8 ± 0.2
Sensing, mV	12.7 ± 4.2	11.8 ± 3.5	11.5 ± 4.2
Impedance, Ohm	625.1 ± 118.8	621.8 ± 94.1	622.8 ± 92.1

decreased from 73.7% (14/19) at baseline to 21.1% at 12 months (2/19) ($P < 0.001$). Of 18 patients who had diuretics before LBBP upgrade, nine patients were noted to have a reduction in diuretic dosage and another seven patients stopped diuretics completely. There was no difference in the number of patients taking angiotensin-converting enzyme inhibitor/angiotensin receptor antagonist (ACEI/ARB) and β-blockers pre- and post-LBBP. In the year preceding LBBP upgrade, five patients (5/19) experienced at least one HFH, and only one patient (1/19) experienced HFH after LBBP ($P = 0.027$). One patient died 12 months after LBBP implantation due to ischemic stroke.

As shown in **Table 2**, the mean acute LBBP capture threshold, sensed R-wave amplitude, and lead impedance maintained stable. There were no major complications during the implantation or the study period.

DISCUSSION

The key findings from our study are as follows:

1) LBBP could be performed safely in 95% (19/20) of patients with infranodal AVB who developed PICM.
2) LBB pacing beyond the site of AVB had a low threshold and no loss of left bundle branch capture during the median 12-month follow-up.
3) Favorable echocardiographic indices with improvement in EF, reduction in LV size, and improvement in NYHA class were observed in PICM patients by LBBP.

LBBP was feasible in 95% of patients with infranodal AVB regardless of a narrow or wide QRS escape. LBBP captured the conduction system beyond the site of block, maintained LV synchrony, and reversed electrical dyssynchrony caused by RVP. LBBP improved LV function in PICM patients except for one patient with a native IVCD (**Supplementary Table 1**).

After LBBP upgrade, 10 patients developed a normal QRS transition and nine patients demonstrated an R/S transition between leads V1 and V2. In our study, a normal QRS axis was maintained with LBBP in most cases and reversed PICM as we previously reported (14). LBBP deliberately targeted the more proximal left bundle in our study, while some LBBP case reports showed left axis deviation for pacing sites located near the left posterior branch (14, 23).

HBP could improve HF symptoms in LBBB as well as AF patients combined with atrial ventricular nodal (AVN) ablation (24, 25). Shan et al. (7) reported on 11 patients with PICM, after the upgrade to permanent HBP, that average LVEF improved and LVEDD decreased. The concerns regarding lead dislodgement, high threshold, and need for lead revisions remained the main problems of HBP in long-term follow-up (11, 17). HBP was feasible acutely in up to 77% of patients with infranodal block (9). Permanent HBP may not be able to pace truly distal to the site of block, particularly in patients with infranodal AVB, and leaves one with the practical concern for progression of distal His-Purkinje conduction disease (9).

LBBP paced beyond the conduction block (12, 15, 26) is an alternative method for delivering ventricular resynchronization comparable to HBP but with stable and lower capture thresholds and a higher success rate (**Table 2**) (12, 27, 28), while conventional HBP may fail to pace beyond the block site in patients of infranodal AVB (12, 17, 27). In addition, LBBP other than HBP provides more operational space for AVN ablation (29).

In our study, no patients had lead dislodgment, perforation, or threshold increase during a median 12-month follow-up as indicated (14, 30). LBBP is deep enough to penetrate the septum with capture of both the left bundle and the left ventricular septum (22). LVSP provides acute hemodynamic improvement and electrical resynchronization as well as maintains left ventricular function (31).

In a recent case report, LBBP reversed PICM from RVP (15). In our study, PICM patients had a mean drop of 25.9% in LVEF with HF symptoms, and a reduction of LVEF was improved after LBBP upgrade. In our study, all patients completed 6-month follow-up, 89.5% (17/19) patients completed the 12-month follow-up, and the mean follow-up in the study was 13.5 ± 6.2 months, which showed the beneficial effects of LBBP in PICM.

BVP seems to have a beneficial effect on left ventricular reverse remodeling, and the maximal effect of BVP is optimized by maximal fusion from LV lead pacing fusing with the intrinsic right bundle branch in patients with typical LBBB and QRSd longer than 150 ms (32). BVP could not maintain synchrony in patients with a native narrow QRS (6) and leads to non-physiological ventricular activation in AVB patients. Fusion with intrinsic conduction by optimized AV intervals plays an important role in determining the benefit of BVP, which is limited in AF and AVB patients (32), while this could be achieved by HBP or LBBP with narrow QRS or typical LBBB and HF (33, 34). In addition, the role of BVP in patients with AVB and mild-to-moderate impairment in left ventricular function remains controversial, and comparisons of clinical outcomes in such patients with BVP vs. RVP remain mixed (35, 36).

LBBP is a reliable physiological pacing strategy for AVB (13, 14, 26, 27) or HF patients with typical LBBB (16, 28). Maintaining and restoring physiological LV activation is an essential prerequisite in patients with LV dysfunction. Compared with LVSP, LBBP deliverers more physiological LV activation that is comparable to HBP. Moreover, LBBP can be optimized to further improve cardiac synchrony (37). Incorporation and programming of LBBP lead instead of coronary sinus lead into the LV port in a standard cardiac resynchronization therapy-defibrillator (CRT-D) or cardiac resynchronization therapy-pacing (CRT-P) system was feasible for synchronization in PICM patients. We believe that the current data highlights the role for permanent LBBP as a strategy to achieve cardiac synchronization in PICM patients even with infra-Hisian block. Our recent report indicates HBP and LBBP delivered more

effective electrical resynchronization compared to BVP in HF patients with LBBB. LBBP was associated with more stable and lower pacing thresholds than those of HBP (28). However, in our study, there was no randomized or direct comparison of biventricular pacing and LBBP.

Study Limitations

This was a retrospective, multicenter, observational study with limited number of patients. The high success rates of LBBP achieved by experienced operators in our three centers need to be replicated in large pilot studies. Additionally, the success rates and the clinical outcomes of LBBP in this population must be interpreted with caution due to its retrospective study design. A dedicated prospective study is therefore warranted to answer this question. Another limitation of the study was the lack of a direct comparison to BVP as the standard treatment for PICM.

CONCLUSIONS

This retrospective, multicenter, observational study demonstrates the beneficial effect and feasibility of LBBP in PICM patients with infranodal AVB. LBBP paced beyond the site of AV block with a low and stable capture threshold in 12 months as well as a high success rate of implantation in infranodal AVB patients.

DATA AVAILABILITY STATEMENT

The original contributions presented in the study are included in the article/**Supplementary Material**, further inquiries can be directed to the corresponding authors.

ETHICS STATEMENT

The studies involving human participants were reviewed and approved by the institutional review board. The patients/participants provided their written informed consent to participate in this study. Written informed consent was obtained from the individual(s) for the publication of any potentially identifiable images or data included in this article.

AUTHOR CONTRIBUTIONS

WH, GF, and XC conceived and designed the experiments. YY, SW, YS, XS, JZ, and BW analyzed and interpreted the data. YY, SW, XC, PS, and KE wrote or edited the manuscript. All authors contributed to the article and approved the submitted version.

FUNDING

This work was supported by the Key Research and Development Program of Zhejiang (Grant Number 2019C03012), the Major Project of the Science and Technology of Wenzhou (Grant Number ZS2017010), the Natural Science for Youth Foundation (Grant Number 81900345), the funding from Clinical research project of Zhejiang Medical Association (Number 2016ZYC-A28) and Clinical Research Plan of Shanghai Hospital Development Center (Number SHDC2020CR4003).

SUPPLEMENTARY MATERIAL

The Supplementary Material for this article can be found online at: https://www.frontiersin.org/articles/10.3389/fcvm.2021.674452/full#supplementary-material

REFERENCES

1. Nielsen JC, Andersen HR, Thomsen PE, Thuesen L, Mortensen PT, Vesterlund T, et al. Heart failure and echocardiographic changes during long-term follow-up of patients with sick sinus syndrome randomized to single-chamber atrial or ventricular pacing. *Circulation.* (1998) 97:987–95. doi: 10.1161/01.CIR.97.10.987
2. Kiehl EL, Makki T, Kumar R, Gumber D, Kwon DH, Rickard JW, et al. Incidence and predictors of right ventricular pacing-induced cardiomyopathy in patients with complete atrioventricular block and preserved left ventricular systolic function. *Heart Rhythm.* (2016) 13:2272–8. doi: 10.1016/j.hrthm.2016.09.027
3. Kaye G, Ng JY, Ahmed S, Valencia D, Harrop D, Ng ACT. The Prevalence of Pacing-Induced Cardiomyopathy (PICM) in patients with long term right ventricular pacing - is it a matter of definition? *Heart Lung Circ.* (2019) 28:1027–33. doi: 10.1016/j.hlc.2018.05.196
4. Khurshid S, Obeng-Gyimah E, Supple GE, Schaller R, Lin D, Owens AT, et al. Reversal of pacing-induced cardiomyopathy following cardiac resynchronization therapy. *JACC Clin Electrophysiol.* (2018) 4:168–77. doi: 10.1016/j.jacep.2017.10.002
5. Birnie DH, Tang AS. The problem of non-response to cardiac resynchronization therapy. *Curr Opin Cardiol.* (2006) 21:20–6. doi: 10.1097/01.hco.0000198983.93755.99
6. Funck RC, Mueller HH, Lunati M, Piorkowski C, De Roy L, Paul V, et al. Characteristics of a large sample of candidates for permanent ventricular pacing included in the Biventricular Pacing for Atrio-ventricular Block to Prevent Cardiac Desynchronization Study (BioPace). *Europace.* (2014) 16:354–62. doi: 10.1093/europace/eut343
7. Shan P, Su L, Zhou X, Wu S, Xu L, Xiao F, et al. Beneficial effects of upgrading to His bundle pacing in chronically paced patients with left ventricular ejection fraction <50. *Heart Rhythm.* (2018) 15:405–12. doi: 10.1016/j.hrthm.2017.10.031
8. Ye Y, Zhang Z, Sheng X, Wang B, Chen S, Pan Y, et al. Upgrade to his bundle pacing in pacing-dependent patients referred for pulse generator change: Feasibility and intermediate term follow up. *Int J Cardiol.* (2018) 260:88–92. doi: 10.1016/j.ijcard.2018.01.105
9. Vijayaraman P, Naperkowski A, Ellenbogen KA, Dandamudi G. Electrophysiologic insights into site of atrioventricular block: lessons from permanent his bundle pacing. *JACC Clin Electrophysiol.* (2015) 1:571–81. doi: 10.1016/j.jacep.2015.09.012
10. Abdelrahman M, Subzposh FA, Beer D, Durr B, Naperkowski A, Sun H, et al. Clinical Outcomes of his bundle pacing compared to right ventricular pacing. *J Am Coll Cardiol.* (2018) 71:2319–30. doi: 10.1016/j.jacc.2018.02.048
11. Zanon F, Abdelrahman M, Marcantoni L, Naperkowski A, Subzposh FA, Pastore G, et al. Long term performance and safety of his bundle pacing: a multicenter experience. *J Cardiovasc Electrophysiol.* (2019) 30:1594–601. doi: 10.1111/jce.14063
12. Huang W, Su L, Wu S, Xu L, Xiao F, Zhou X, et al. A novel pacing strategy with low and stable output: pacing the left bundle branch immediately beyond the conduction block. *Can J Cardiol.* (2017) 33(:1736 e1–e3. doi: 10.1016/j.cjca.2017.09.013

13. Li X, Li H, Ma W, Ning X, Liang E, Pang K, et al. Permanent left bundle branch area pacing for atrioventricular block: feasibility, safety, and acute effect. *Heart Rhythm.* (2019) 16:1766–73. doi: 10.1016/j.hrthm.2019.04.043
14. Su L, Wang S, Wu S, Xu L, Huang Z, Chen X, et al. Long-term safety and feasibility of left bundle branch pacing in a large single-center study. *Circ Arrhythm Electrophysiol.* (2021) 14:e009261. doi: 10.1161/CIRCEP.120.009261
15. Wu S, Su L, Wang S, Vijayaraman P, Ellenbogen KA, Huang W. Peri-left bundle branch pacing in a patient with right ventricular pacing-induced cardiomyopathy and atrioventricular infra-Hisian block. *Europace.* (2019) 21:1038. doi: 10.1093/europace/euz031
16. Huang W, Wu S, Vijayaraman P, Su L, Chen X, Cai B, et al. Cardiac resynchronization therapy in patients with nonischemic cardiomyopathy using left bundle branch pacing. *JACC Clin Electrophysiol.* (2020) 6:849–58. doi: 10.1016/j.jacep.2020.04.011
17. Vijayaraman P, Herweg B, Dandamudi G, Mittal S, Bhatt AG, Marcantoni L, et al. Outcomes of His-bundle pacing upgrade after long-term right ventricular pacing and/or pacing-induced cardiomyopathy: Insights into disease progression. *Heart Rhythm.* (2019) 16:1554–61. doi: 10.1016/j.hrthm.2019.03.026
18. Huang W, Chen X, Su L, Wu S, Xia X, Vijayaraman P, et al. beginner's guide to permanent left bundle branch pacing. *Heart Rhythm.* (2019). doi: 10.1016/j.hrthm.2019.06.016
19. Chen X, Wu S, Su L, Su Y, Huang W. The characteristics of the electrocardiogram and the intracardiac electrogram in left bundle branch pacing. *J Cardiovasc Electrophysiol.* (2019) 30:1096–101. doi: 10.1111/jce.13956
20. Wu S, Chen X, Wang S, Xu L, Xiao F, Huang Z, et al. Evaluation of the criteria to distinguish left bundle branch pacing from left ventricular septal pacing. *JACC Clin Electrophysiol.* (2021) S2405-500X(21)00202-4. doi: 10.1016/j.jacep.2021.02.018
21. Su L, Xu T, Cai M, Xu L, Vijayaraman P, Sharma PS, et al. Electrophysiological characteristics and clinical values of left bundle branch current of injury in left bundle branch pacing. *J Cardiovasc Electrophysiol.* (2020) 31:834–42. doi: 10.1111/jce.14377
22. Wu S, Sharma PS, Huang W. Novel left ventricular cardiac synchronization: left ventricular septal pacing or left bundle branch pacing? *Europace.* (2020) 22(Suppl_2):ii10–8. doi: 10.1093/europace/euaa297
23. Upadhyay GA, Razminia P, Tung R. His-bundle pacing is the best approach to physiological pacing. *Heart Rhythm O2.* (2020) 1:68–75. doi: 10.1016/j.hroo.2020.03.001
24. Huang W, Su L, Wu S, Xu L, Xiao F, Zhou X, et al. Long-term outcomes of His bundle pacing in patients with heart failure with left bundle branch block. *Heart.* (2019) 105:137–43. doi: 10.1136/heartjnl-2018-313415
25. Huang W, Su L, Wu S, Xu L, Xiao F, Zhou X, et al. Benefits of permanent his bundle pacing combined with atrioventricular node ablation in atrial fibrillation patients with heart failure with both preserved and reduced left ventricular ejection fraction. *J Am Heart Assoc.* (2017) 6. doi: 10.1161/JAHA.116.005309
26. Guo J, Li L, Xiao G, Huang X, Li Q, Wang Y, et al. Feasibility and stability of left bundle branch pacing in patients after prosthetic valve implantation. *Clin Cardiol.* (2020) 43:1110–8. doi: 10.1002/clc.23413
27. Vijayaraman P, Cano O, Koruth JS, Subzposh FA, Nanda S, Pugliese J, et al. His-purkinje conduction system pacing following transcatheter aortic valve replacement: feasibility and safety. *JACC Clin Electrophysiol.* (2020) 6:649–57. doi: 10.1016/j.jacep.2020.02.010
28. Wu S, Su L, Vijayaraman P, Zheng R, Cai M, Xu L, et al. Left bundle branch pacing for cardiac resynchronization therapy: nonrandomized on-treatment comparison with his bundle pacing and biventricular pacing. *Can J Cardiol.* (2021) 37:319–28. doi: 10.1016/j.cjca.2020.04.037
29. Huang W, Su L, Wu S. Pacing treatment of atrial fibrillation patients with heart failure: his bundle pacing combined with atrioventricular node ablation. *Card Electrophysiol Clin.* (2018) 10:519–35. doi: 10.1016/j.ccep.2018.05.016
30. Chen X, Wei L, Bai J, Wang W, Qin S, Wang J, et al. Procedure-related complications of left bundle branch pacing: a single-center experience. *Front Cardiovasc Med.* (2021) 8:645947. doi: 10.3389/fcvm.2021.645947
31. Salden F, Luermans J, Westra SW, Weijs B, Engels EB, Heckman LIB, et al. Short-term hemodynamic and electrophysiological effects of cardiac resynchronization by left ventricular septal pacing. *J Am Coll Cardiol.* (2020) 75:347–59. doi: 10.1016/j.jacc.2019.11.040
32. Vernooy K, van Deursen CJ, Strik M, Prinzen FW. Strategies to improve cardiac resynchronization therapy. *Nat Rev Cardiol.* (2014) 11:481–93. doi: 10.1038/nrcardio.2014.67
33. Wu S, Cai M, Zheng R, Wang S, Jiang L, Xu L, et al. Impact of QRS morphology on response to conduction system pacing after atrioventricular junction ablation. *ESC Heart Fail.* (2021) 8:1195–203. doi: 10.1002/ehf2.13181
34. Wang S, Wu S, Xu L, Xiao F, Whinnett ZI, Vijayaraman P, et al. Feasibility and Efficacy of His bundle pacing or left bundle pacing combined with atrioventricular node ablation in patients with persistent atrial fibrillation and implantable cardioverter-defibrillator therapy. *J Am Heart Assoc.* (2019) 8:e014253. doi: 10.1161/JAHA.119.014253
35. Ebert M, Jander N, Minners J, Blum T, Doering M, Bollmann A, et al. Long-term impact of right ventricular pacing on left ventricular systolic function in pacemaker recipients with preserved ejection fraction: results from a large single-center registry. *J Am Heart Assoc.* (2016) 5:e003485. doi: 10.1161/JAHA.116.003485
36. Gage RM, Burns KV, Bank AJ. Echocardiographic and clinical response to cardiac resynchronization therapy in heart failure patients with and without previous right ventricular pacing. *Eur J Heart Fail.* (2014) 16:1199–205. doi: 10.1002/ejhf.143
37. Huang W, Zhou X, Ellenbogen KA. Pursue physiological pacing therapy -A better understanding of left bundle branch pacing and left ventricular septal myocardial pacing. *Heart Rhythm*. (2021). doi: 10.1016/j.hrthm.2021.05.013

Conflict of Interest: The authors declare that the research was conducted in the absence of any commercial or financial relationships that could be construed as a potential conflict of interest.

frontiers in Cardiovascular Medicine

ORIGINAL RESEARCH
published: 21 September 2021
doi: 10.3389/fcvm.2021.690092

Study on Optimal Parameter and Target for Pulsed-Field Ablation of Atrial Fibrillation

Xuying Ye[1,2], *Shangzhong Liu*[3], *Huijuan Yin*[4], *Qiang He*[2], *Zhixiao Xue*[3,5*], *Chengzhi Lu*[1,2*] *and Siying Su*[5]

[1] The First Central Clinical College of Tianjin Medical University, Tianjin, China, [2] Department of cardiology, Tianjin First Central Hospital, Tianjin, China, [3] School of Biomedical Engineering and Technology, Tianjin Medical University, Tianjin, China, [4] Institute of Biomedical Engineering, Chinese Academy of Medical Sciences & Peking Union Medical College, Tianjin, China, [5] Tianjin Intelligent Health Medical Co., Ltd, Tianjin, China

Pulsed-field ablation (PFA) had potential advantages in atrial fibrillation ablation, and we aim to confirm the optimal parameter and target of PFA for atrial fibrillation. Two ablation modes *in vitro* of single-cell system (ablation in electrode cup) and monolayer cell system (ablation in inserts with electrode tips) were established to perform PFA for myocardial cell H9C2 and smooth muscle cell A7r5. Ablation effect, calcium ion influx, the expression of Cx45, and surface morphological change were observed. Three Bama minipigs were used to verify the *in vivo* ablation effect of PFA. In monolayer cell system, H9C2 was significantly sensitive to PFA compared with A7r5, with shrinking of the whole monolayer. The ablation effect of bidirectional pulse was weaker than that of the two mono-polar pulses. Expressed Cx45 proteins were increased in H9C2 but decreased in A7r5 cells. Bidirectional PFA performed on Bama minipigs was able to effectively block electrical activity from the pulmonary vein to the atrium with week muscle contraction, not generating pulmonary vein stenosis. Bidirectional PFA was able to significantly ablate myocardial cells, maintain cell–cell connection, and reduce muscle contraction, which was a kind of optimized PFA strategy for atrial fibrillation.

Keywords: pulsed field ablation, irreversible electroporation, atrial fibrillation, pulmonary vein ablation, apoptosis

OPEN ACCESS

Edited by:
Henggui Zhang,
The University of Manchester, United Kingdom

Reviewed by:
Silvia Magnani,
New York University, United States
Soufian AlMahameed,
Case Western Reserve University, United States

***Correspondence:**
Zhixiao Xue
xuezhixiao@126.com
Chengzhi Lu
5020200072@nankai.edu.cn

Specialty section:
This article was submitted to Cardiac Rhythmology, a section of the journal Frontiers in Cardiovascular Medicine

Received: *02 April 2021*
Accepted: *16 August 2021*
Published: *21 September 2021*

Citation:
Ye X, Liu S, Yin H, He Q, Xue Z, Lu C and Su S (2021) Study on Optimal Parameter and Target for Pulsed-Field Ablation of Atrial Fibrillation. Front. Cardiovasc. Med. 8:690092. doi: 10.3389/fcvm.2021.690092

INTRODUCTION

Atrial fibrillation (AF) is a kind of common arrhythmia, with around 33.5 million patients globally. The incidence rate of AF is increased along the age. It is predicted that the number of AF patients will double until 2060. In 2019, the American Heart Association (AHA), American College of Cardiology (ACC), and Heart Rhythm Society (HRS) jointly updated the Treatment Guidelines for AF Patients (1) and pointed out that catheter ablation was the first-line therapy scheme for AF. The catheter ablations mainly include radiofrequency (RF) ablation and cryoballoon (CB) ablation. However, there is a zero-sum effect based on cold/hot ablation; overdose will cause complications including pulmonary vein stenosis, esophageal fistula, and phrenic nerve injury; underdose will cause incomplete isolation, and recurrence is likely to happen (2, 3), which limits the application of freezing/thermal catheter ablation.

Pulsed-field ablation (PFA) is a kind of ablation based on irreversible electroporation (IRE). It will form massive nanoscale membrane permeable holes on the cell membrane by virtue of the high-voltage direct current pulse emitted between electrodes (generally, the increasing and falling

time of pulse is 200–800 ns; the pulse width is maintained for 5–100 μs) to lead to apoptosis of cells due to change of permeability (4). The non-thermal ablation of this way and selectivity of electric field intensity for different tissues will avoid damage to vessels and nerves during elimination of tumors (5, 6). The technique has been approved by the Food and Drug Administration (FDA) and National Medical Products Administration (NMPA) to be used for clinical treatment of liver cancer (6), pancreatic cancer (5), kidney cancer (7), and prostate cancer (8).

In recent years, the characteristic of selective ablation of PFA has attracted attentions from experts of cardiac electrophysiology to successively carry out multiple PFA cardiac ablation studies. Witt et al. (9) performed pulmonary vein ablation using catheter balloon IRE on five dogs and demonstrated irreversible transmural myocardial ablation without incidence of pulmonary vein stenosis. Koruth et al. (10, 11) compared the feasibility of RF and PFA in ablation in the pulmonary vein and superior vena vein and discovered that PFA could generate even specific ablation zone with clear boundary in myocardium, without evident damage to the nervous and venous structure. Reddy et al. (12) carried out phase I clinical trial for safety of PFA pulmonary vein ablation in two centers, and the result indicated that the success rate of 15 cases receiving catheter PFA pulmonary vein ablation was 100%, and the success rate of seven cases receiving epicardium PFA was 86%. Although it was proved by these researches that PFA had potential advantages in treatment of AF, the parameters of electric field of PFA varied greatly in different research reports; what is more, there was no comparative study on parameters of electric field, and PFA mechanism was unclear. The muscle convulsions associated with PFA are also a concern for the ablation of AF. Studies have shown that bidirectional pulses can reduce PFA-induced muscle twitches in the tumor ablation (13, 14), but no corresponding studies have been conducted in the application of AF ablation.

Therefore, in the study, we will focus on the comparison of PFA effect in different electric field modes and dose, to verify the optimal parameters for myocardial ablation, providing experiment evidence for PFA clinical treatment strategy planning of AF.

MATERIALS AND METHODS

Materials

The high-frequency alternating PFA equipment, electrode needles, and ablation electrode catheter were developed by Tianjin Intelligent Health Medical Co., Ltd. (<city>Tianjin</city>, China). Rat myocardial cell H9C2(2-1) and rat smooth muscle cell of thoracic aorta A7r5 were purchased from Cell Resource Center of the Institute of Basic Medical Sciences of the Chinese Academy of Medical Sciences (Beijing, China). Dulbecco's modified Eagle medium (8120286) culture mediums were purchased from GIBCO (Grand Island, NY, USA). Electrode cap Disposable Cuvettes (4-mm gap, 45-0126) were purchased from BTX (Holliston, MA, USA). Millicell® 24-well inserts (1-μm pore size, MCRP24H48) were purchased from Merck Millipore (Billerica, MA, USA). LIVE/DEAD® Viability/Cytotoxicity Kit (L3224) and Oregon Green® 488 BAPTA-1 AM (O6807) were purchased from Thermo Fisher Scientific (Waltham, MA, USA). Anti-TNF alpha antibody [EPR21753-109] (ab205587), Anti-Connexin 45/GJA7/Cx45 antibody [5B9.2] (ab78408), Goat Anti-Rabbit IgG H&L (Alexa Fluor® 488) ab150077, and Goat Anti-Mouse IgG H&L (Alexa Fluor® 647, ab150115) were purchased from Abcam (Cambridge, MA, USA). Hematoxylin and eosin/HE Staining Kit and Masson's Trichrome Stain Kit were purchased from Beijing Solarbio Science & Technology Co., Ltd. (Beijing, China). *In Situ* Cell Death Detection Kit, POD (11684817910) was purchased from Sigma-Aldrich (St. Louis, MO, USA).

Cell Experiments

Cell Culture

The H9C2(2-1) and A7r5 cells were used for simulating the targets for PFA AF. DMEM-H complete medium (10% fetal calf serum, 4 mM of L-glutamine, 1% triple antibodies containing penicillin, streptomycin, and amphotericin B) was adopted for H9C2(2-1) cells; DMEM complete medium (10% fetal calf serum and 1% double antibodies containing penicillin and streptomycin) was adopted for A7r5 cells for routine culture. The culture environment was 5% CO_2 37°C incubator, with once passage every 2–4 days.

Pulsed-Field Ablation

Two PFA intervention modes were designed *in vitro*, including single-cell mode and monolayer mode.

Single-Cell Mode

H9C2(2-1) cells or A7r5 cells in logarithmic phase were digested by trypsin and were made into cell suspension of $8 * 10^4$/ml concentration through centrifugation and resuspension; 600 μl of the suspension was added into the electrode cap as shown in (**Supplementary Figure 1A**) for PFA intervention according to the design parameters. Positive and negative anodes were at the two sides of the electrode cap, and the cell suspension was evenly distributed in the space electric field. After intervention, the cell suspension was re-inoculated to a 96-well-plate for 24 h for detection of cellular damage.

Monolayer Cell Mode

H9C2(2-1) cells or A7r5 cells in logarithmic phase were made into the cell suspension of the same concentration and inoculated into 24-well inserts. The cell culture mediums were added into both the inserts and the compartments under the inserts. Forty-eight hours later, PFA intervention was performed when monolayer cell membrane was formed. The intervention equipment is shown in **Supplementary Figure 1B**, equipped with four electrodes, including one positive electrode vertically suspended in the 24-well-inserts with electrode tip 2 mm away from cells, and three negative electrodes inserted to the basolateral compartment through three holes surrounding the inserts, with electrode tip 2 mm away from the well-bottom and 1 mm away from the insert basolateral. Conic electric discharge was formed between positive and negative electrodes. The electric field distribution on monolayer cell membrane was annular

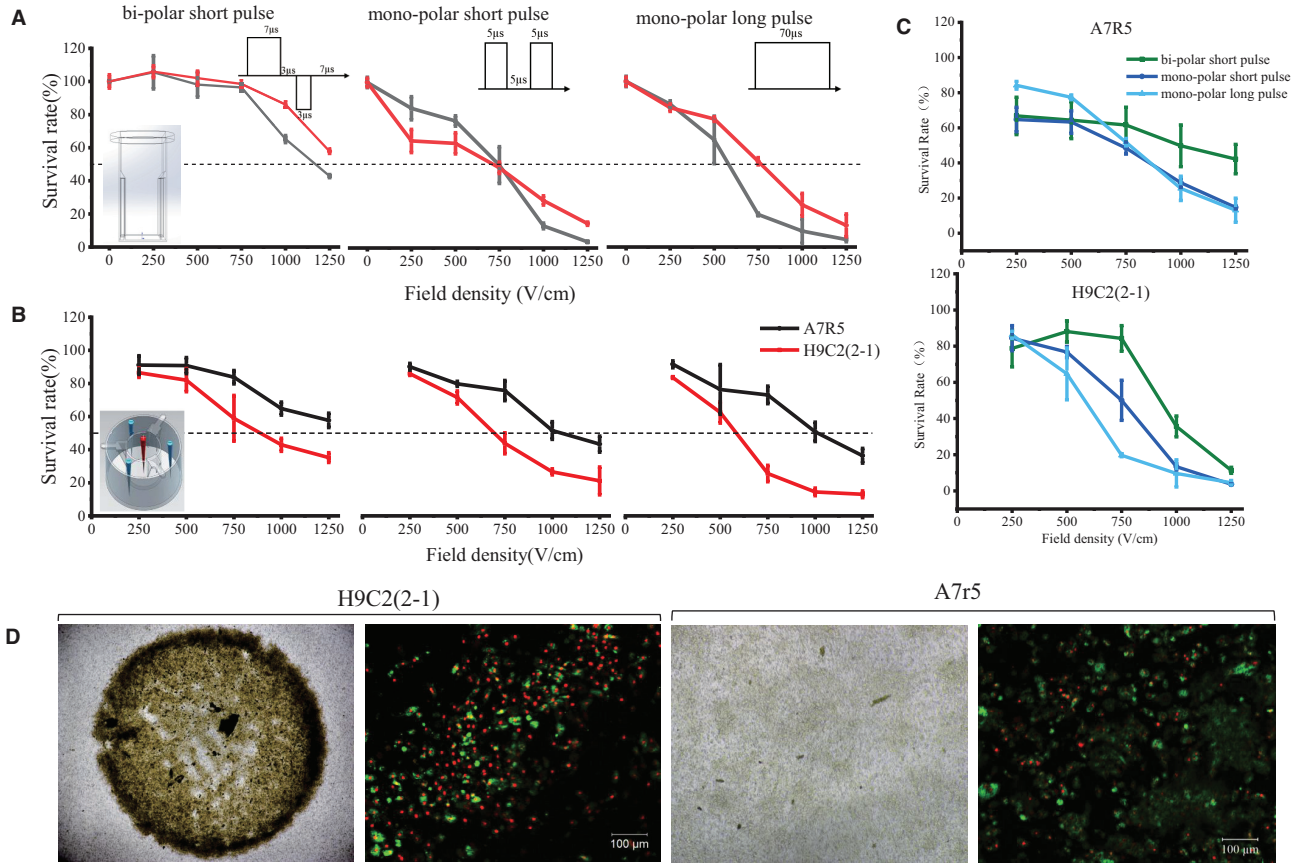

FIGURE 1 | Dose–effect curves of PFA for H9C2(2-1) and A7r5 in single-cell and monolayer systems. **(A)** PFA on single cells. **(B)** PFA on monolayer cells. **(C)** Comparison of cell killing efficiency of three pulsed modes of PFA. **(D)** The morphologic change of cell monolayer after PFA. The top row shows the images under ×4 magnification; the bottom row shows the results of live/dead cell staining under ×10 magnification. PFA, pulsed-field ablation.

through simulation by COMSOL Multiphysics 5.5, and the strength of the electric field gradually increases outward from the center. Ablation was performed according to average field strength. After ablation, the monolayer cells were continued to culture for 24 h for survival detection of cells.

Grouping of Pulsed-Field Ablation Intervention

Three pulse modes were designed in the experiment, as shown in **Supplementary Figure 1C**, including bi-polar short pulse (forward pulse width was 5 μs with pulse interval of 3 μs; reverse pulse width was 3 μs with pulse interval of 5 μs), mono-polar short pulse (pulse width was 5 μs with pulse interval of 5 μs), and mono-polar long pulse (pulse width was 70 μs with pulse interval of 10 μs). Every 10 pulses were included in one group, with between-group interval of 1 s. In short pulse modes, PFA ablated 500 pulses, while in long pulse mode, PFA ablated 70 pulses. The effective acting time was 4,800–5,000 μs, and the field strength was set as 250, 500, 750, 1,000, and 1,250 V/cm.

Detection of Cell Ablation Effect

MTT [3-(4,5-dimethylthiazol-2-yl)-2,5-diphenyltetrazolium bromide] colorimetric method was adopted to detect ablation effect for the cells after PFA in single-cell mode. The details were as follows: in 24 h after ablation, 10 μl of MTT solution (5 mg/ml) was added into every well for continuous incubation for 4 h; the supernatant was carefully absorbed for discard; 100 μl of 50% sodium dodecyl sulfate (SDS)—50% DMF was added into the wells for dissolution for overnight; the optical density value (OD value) under 570 nm wavelength was measured through enzyme-linked immunometric meter. Cell survival rate was calculated by the following formula, in which S means survival rate.

$$S = \frac{OD_{experimental\ group}}{OD_{control\ cell\ group}}$$

Live/dead cell staining method was adopted to detect ablation effect for the cells ablated by PFA in monolayer cell mode. The details were as follows: in 24 h after ablation, cell staining was performed according to the protocol in the specification; after culture medium was discarded, 100 μl of mixed liquid containing 2 μM of calcein AM (for live cells) and 4 μM of EthD-1 (for dead cells) was added for staining for 30 min under room temperature; phosphate-buffered saline (PBS) was used to wash off the extra coloring agent; observation and photography were performed

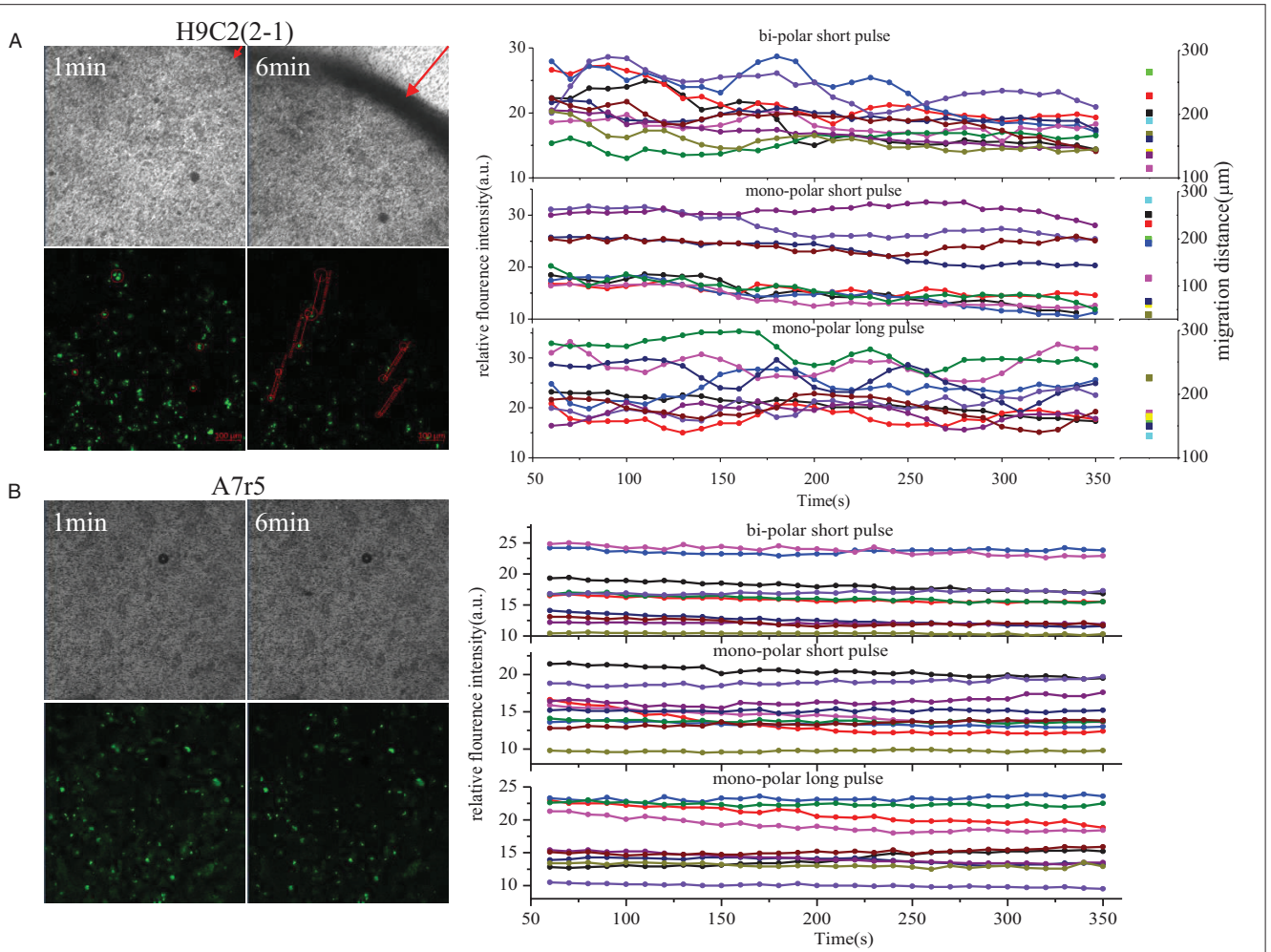

FIGURE 2 | Ca^{2+} influx in H9C2(2-1)and A7r5 after PFA. **(A)** H9C2(2-1). **(B)** A7r5. PFA, pulsed-field ablation.

under confocal microscope. The excitation laser was 488 nm; 500- to 550-nm bandpass was adopted for calcein AM, and 600-nm longpass was adopted for EthD-1. IMAGEJ software was used to analyze the areas of both staining methods. EthD-1 could only stain the cell nucleus; thus, compensation was performed by multiplying the red staining area by 2. Cell survival rate was calculated according to the following formula, in which S means survival rate and A means area.

$$S = \frac{A_{green}}{A_{green} + 2A_{red}}$$

Ca^{2+} Staining

Ten micromolar of OGB-1 (prepared with serum-free DMEM) was used to incubate the H9C2(2-1) cells and A7r5 cells growing into monolayer at both sides of inserts at 37°C for 1 h. After incubation, the serum-free medium was washed off, and new medium was added. Image capture in time-series mode was performed under confocal microscope immediately after PFA of cells in 500 V/cm field strength; λ_{Ex} = 488 nm and λ_{Em} = 490–545 nm; time interval was 10 s; 30 images were captured in total.

Scanning Electron Microscopy

Glutaraldehyde of 2.5% was used to fix monolayer H9C2(2-1) cells and A7r5 cells in insert 30 min and 24 h after PFA (500 V/cm), respectively. Gradient dehydration, drying, and metal spraying were performed. The cell surface appearance was observed under scanning electron microscopy (SEM).

Immunofluorescence Staining

Methyl alcohol was used to fix monolayer H9C2(2-1) cells and A7r5 cells in insert 2 and 24 h after PFA [500 V/cm for H9C2(2-1) and 750 V/cm for A7r5], respectively, for 10 min; and the Tris-buffered saline (TBS) containing 5% goat serum was used for blocking. Anti-Connexin 45 antibody (1:200) was incubated overnight at 4°C; after washing, fluorescent Goat Anti-Mouse IgG H&L (Alexa Fluor® 647) was incubated away from light at 37°C for 1 h; after washing again, the membrane of insert was carefully dissected, and the cells were placed on the

glass slide upside down covered with coverslips for observation under confocal microscope. The condition for signal acquisition of Alexa Fluor® 647 was $\lambda_{Ex} = 647$ nm and $\lambda_{Em} = 660$ nm longpass.

Animal Experiments

Ablation Procedure

Healthy Bama male minipigs (n = 3, 80 ± 10 kg) purchased from Tianjin Yuda Laboratory Animal Breeding Co., Ltd. (Tianjin, China) were fed conventionally. All experimental protocols involving pigs were approved by the animal ethics and welfare committee (approval number: 2017015) of Beijing Tonghe Shengtai Comparative Medical Research Institute, Beijing, China. Before operation, Lumianning (the compound preparation of Jingsongling, edetic acid (EDTA), DHE, and haloperidol) and midazolam injection were mixed by 1:1 and injected to the muscle according to 5 ml/kg (weight). 2,6-Diisopropyl-phenol injection was provided to maintain anesthesia at the speed of 5 ml/h. Skin preparation and sterilization were performed at the groin; femoral vein catheter was inserted under guidance by ultrasound; 8F catheter was inserted into the right atrium through the inferior caval vein with assistance of X-ray contrast radiography, penetrating the interatrial septum to reach the left atrium to find the pulmonary vein. The electrode was sent to the pulmonary vein along the catheter for PFA under 1,600 V/cm in bi-polar short pulse mode (the forward pulse width was 5 μs; reverse pulse width was 3 μs; pulse interval was 3 μs) with 1,000 pulses and 8-A current. ECG monitoring was performed during the operation. After ablation, pacing detection was performed in pulmonary vein and atrium to evaluate ablation effect. X-ray contrast radiography was performed for pulmonary vein to observe if there was spasm or bleeding. Hemostasis by compression was performed on the wound after the operation.

To verify the *in vivo* safety of PFA, PFA was performed on the renal artery of the experimental pigs under different field strengths after the pulmonary vein ablation. The 8F catheter entered the abdominal aorta through the femoral artery channel and then entered both sides of the renal arteries in turn with the assistance of X-ray contrast radiography. The ablation was performed at selected locations before the renal artery branches. The ablation dose of four renal arteries (two experimental pigs) was 1,000, 1,200, 1,600, and 2,000 V/cm, and two for control.

Detection of Blood Indexes

Blood sample was collected before the operation, 30 min and 72 h after the operation for detection of indexes including creatine kinase (CK), creatine kinase isoenzyme (CKMB), troponin (TNI), myoglobin (MYO), creatinine (CRE), low-density lipoprotein cholesterin (LDL-C), high-sensitivity C-reactive protein (hs-CRP), and N-terminal pro-brain natriuretic peptide (NT-pro-BNP).

Pathological Examination

Seventy-two hours after the operation, euthanasia (electric shock) was performed for the experimental pigs. Their heart tissues were taken for fixation and embedding to be as tissue slices. H&E staining, Masson's trichrome staining, and apoptosis staining were performed to observe ablation effect.

Statistics

Origin8.5 software was used for data analysis. All the data were presented by $\chi \pm SD$. Two-tailed *t*-test was adopted for between-group difference. One-way ANOVA was adopted to analyze multigroup difference. $p < 0.05$ was considered statistically significant.

RESULTS

Pulsed-Field Ablation Effects on Cells

In order to screen the optimal PFA dose for clinic, two ablation systems and three ablation modes were designed in this study as shown in **Supplementary Figure 1**. In single-cell system, the field strength was evenly distributed, and PFA energy was received by single cells; while in monolayer system, the field strength was distributed annularly and was becoming weaker when approaching the center, and PFA energy was received by the whole cell monolayer simultaneously. The result is shown in **Figure 1**. In single-cell system (embedding graph of **Figure 1A**), the survival rate of H9C2(2-1) and A7r5 cells depended on the field intensity and pulse mode; cell viability was negatively correlated to the field intensity; i.e., the higher the field strength, the lower the cell survival rate. In the comparison of three pulse modes, the ablation effect of mono-polar short and long pulse was better than that of bi-polar short pulse; the lethal dose of 50% was around 750 and 1,250 V/cm (dotted line in the figure). There was no significant difference in sensitivity of H9C2(2-1) and A7r5 cells for PFA under the single-cell system. The difference was that, in monolayer cell system, although cell vitality still depended on the field intensity and pulse mode, there was significant difference in sensitivity of both cells for PFA; H9C2(2-1) was more sensitive to PFA than A7r5, and the difference was more significant when the field strength was larger. Compared with the three pulse modes (**Figure 1C**), the survival cells under the bidirectional pulse (green line) were slightly more than those of the unidirectional pulse (dark blue and light blue lines), but when the voltage was high enough, such as 1,250 V/cm, the ablation effect of the three pulse modes on H9C2(2-1) cells was similar. There was more significant difference in morphologic change of both cells after PFA. As shown in **Figure 1D**, H9C2(2-1) cell monolayer completely shrunk to the center after ablation, and the live/dead cells in the shrunk cell monolayer took their own proportion. However, disappearing cell–cell junction was found in A7r5 cells after PFA; single-cell shrunk *in situ* and live/dead cell staining indicated that massive cells were survived.

Ca^{2+} Influx

In order to better observe the different morphologic changes of H9C2(2-1) and A7r5 cells after PFA, Ca^{2+} fluorescent probe OGB-1 was used for cell incubation to observe the instant morphologic change of cells and Ca^{2+} influx after PFA. As shown in **Figure 2A** and **Supplementary Video 1**, the whole H9C2(2-1) cell monolayer shrunk to the center immediately after PFA, and the max displacement distance within the scanning period (300 s)

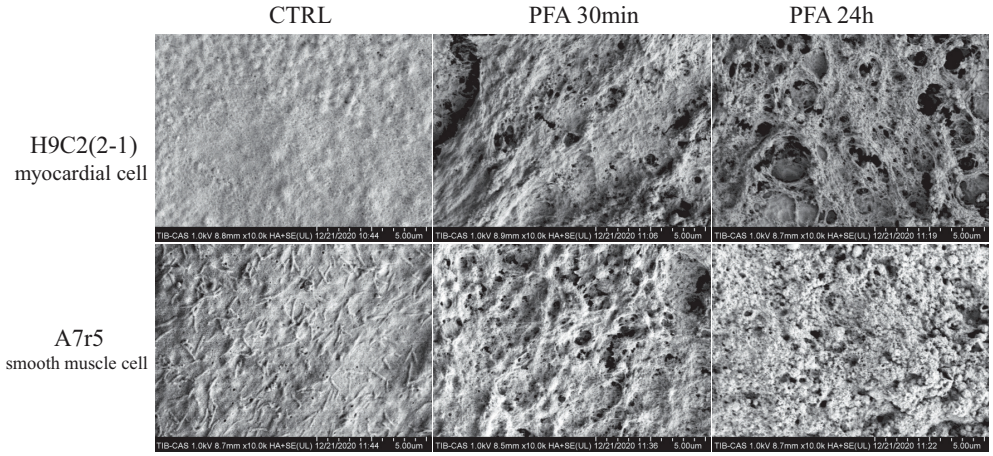

FIGURE 3 | SEM images of H9C2(2-1) and A7r5 cells inoculated in transwell inserts 30 min and 24 h after PFA by ×10,000 magnification. SEM, scanning electron microscopy; PFA, pulsed-field ablation.

was 266 μm. During rapid shrinking and displacement of cells, violent Ca^{2+} flash was found in cells, especially in bi-polar short pulse and mono-polar long pulse mode. Within 300 s, multiple peak values of Ca^{2+} fluorescence intensity were found, indicating multiple Ca^{2+} release and influx; it was also be affected by the movement of cells in and out of the focus during displacement. In mono-polar short pulse mode, shrinking happened to H9C2(2-1) cells as well, but with gentle fluctuation of Ca^{2+} fluorescence intensity. There was no significant difference in displacement distance of cells in the three modes (the scatter plot at the right of **Figure 2A).** Cell monolayer shrunk from peripheral region to the center, and the displacement distance of cells was greatly affected by the subjectivity in selection of visual field; thus, precise comparison failed. No evident displacement of A7r5 cells was observed, and amplitude of Ca^{2+} scintillation was significantly weaker than that of H9C2(2-1).

Ultrastructure of Cell Membrane Perforation

SEM was used to observe the electroporation on surface of myocardial cells and smooth muscle cells after PFA. As shown in **Figure 3**, the surface of H9C2(2-1) cells was smooth, with little pseudopod or villus. Thirty minutes after PFA, micropores of varied sizes were found on cell surface, around 30 micropores under ×10,000 magnification; 24 h later, the micropores on cell surface were enlarged, with fusion of multiple micropores. However, abundant pseudopods were found on surface of A7r5 cells; the pseudopods shrunk to a ball after PFA; massive electroporations were found on cell surface; 24 h later, electroporations were still there, and pseudopods shrunk to form a more evident shape of ball. Compared with the massive pseudopods on surface of A7r5 cells, surface of H9C2(2-1) cells was relatively smooth, which made it fail to closely cling to the transwell membrane. Such kind of ultrastructure explained the phenomenon of shrinking of H9C2(2-1) monolayer after PFA.

Cx45 Expression

Cell–cell junction was the major difference between the two PFA systems *in vitro* (single-cell and monolayer modes) designed in this study. After observation of the fact that in cell monolayer system H9C2(2-1) was more sensitive to PFA than A7r5, and the shrinking of H9C2(2-1) monolayer cells, Cx45 (cell–cell connexin) expression in cells 24 h after PFA was detected. As shown in **Figure 4**, the baseline level of Cx45 expression in H9C2(2-1) cells was lower compared with A7r5. After PFA, with shrinking of cell monolayer, cell–cell junction was closer, and Cx45 fluorescence intensity was significantly reinforced; such phenomena were significantly evident under three modes compared with the control group, and enhancement under bi-polar short pulse mode was even significant, while Cx45 expression level in A7r5 cells was significantly reduced after PFA ($p < 0.05$), with significantly enlarged intercellular space.

Pulsed-Field Ablation With Bi-Polar Short Pulse on Swine

As shown in the embedding image of **Figure 5A**, the self-designed electrode device was in the shape of petal composed of five electrodes. Electric filed was formed between adjacent electrodes for sequential discharge. After PFA (1,600 V/cm) with 1,000 pulses, the manner of cardiac pacing was adopted to verify the instant effect of PFA. As shown in **Figures 5B,C**, when pacing electrode was in the left atrium (non-ablated area), the heart beats simultaneously; however, when pacing electrode was in the left superior pulmonary vein, which was ablated by PFA (**Figures 5D,E**), the heart failed to beat simultaneously, which indicated that the pacing signal in the left superior pulmonary vein was not conducted into atrial tissues, and PFA succeeded. Meanwhile, radiography showed that the structure of left superior pulmonary vein after PFA was intact, without spasm and bleeding, etc. (**Figure 5F**). During intraoperative observation, except mild muscle contraction of pig's chest and abdomen (see **Supplementary Video 2**) in the process of PFA,

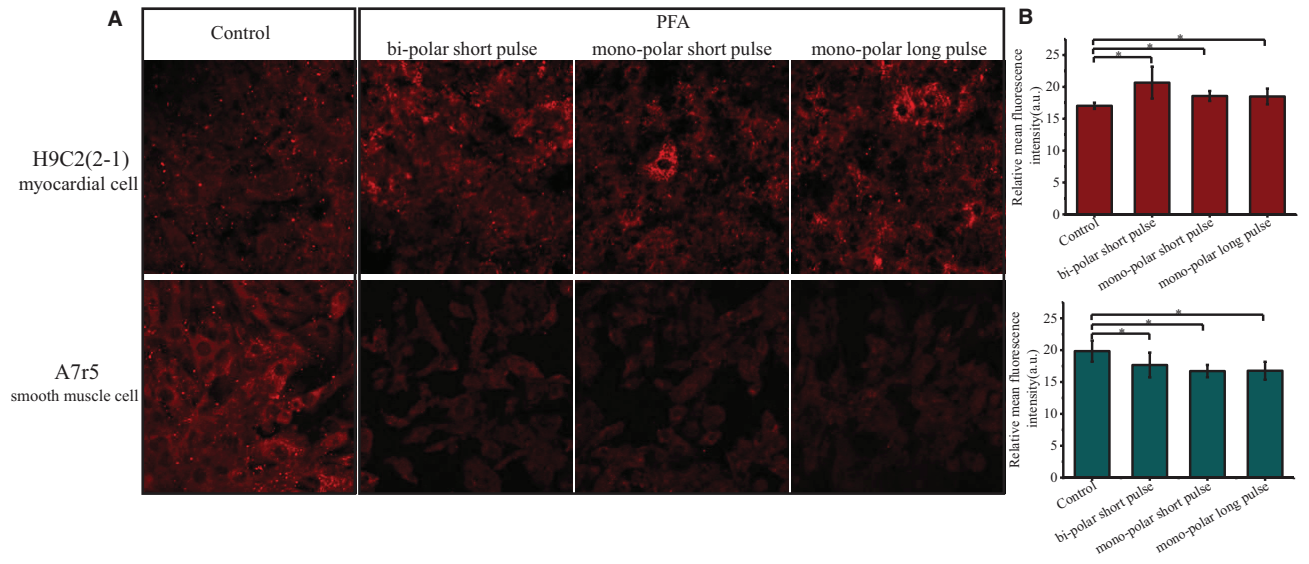

FIGURE 4 | Effect of PFA on Cx45 expression in H9C2(2-1) and A7r5 cells. **(A)** Cx45 expression in H9C2(1, 2) and A7r5 cells 24 h after PFA under three modes. **(B)** Histogram of mean fluorescence intensity of Cx45 expression in H9C2(2-1) (top) and A7r5 (bottom) cells. *$p < 0.05$. PFA, pulsed-field ablation.

there was no other adverse reaction, and the pig was conscious in 30 min after operation.

Pathological Changes of Atrial Tissues After Pulsed-Field Ablation

As shown in **Figure 6** (left), annular ablated zone matching the ablation electrode was seen at the intersection of pulmonary vein and atrium, which was white necrosis-like completely different from the surrounding flesh-colored atrial tissues, with mild swelling. The ablated tissues were dissected along the direction of pulmonary vein for H&E staining, TUNEL staining, and Masson's staining to observe the pathological change. After H&E staining, evident boundary (presented by block dotted line) between ablated and non-ablated tissue was seen under ×20 magnification, and the space between cardiac muscle fibers in ablated tissue was enlarged; under ×200 magnification, the boundary was more clear, and in ablated tissue, the myocardial cell nucleus loss and massive inflammatory cells were infiltrating; ablation depth was transmural. In TUNEL staining, brown hyperchromatism was found in the ablated area, indicating that apoptosis of massive myocardial cells was caused by PFA. In Masson's staining, no significant change was found in the connective tissues between myocardial cells, and the structure of collagenous fibers was intact, infiltrated with massive inflammatory cells. These results indicated that PFA allowed controllable ablated area and transmural ablation depth (around 1 mm) and was able to cause massive apoptosis with mild inflammatory reaction.

In order to observe the safety of PFA, PFA was performed for the renal artery of the pigs under a range of field strengths. As shown in **Supplementary Figure 2**, PFA depth was gradually increased along increase of field strength. The ablation depth reached 4/5 renal arterial wall at 1,600 V/cm. When field strength reached 2,000 V/cm, ablation depth reached 1.45 mm, which was completely transmural, without any damage to the sympathetic nerve 1 mm away from the renal artery.

DISCUSSION

It has been demonstrated in multiple preclinical and clinical researches that PFA is applicable to ablation for AF. Its safety is superior to that of RF ablation due to its characteristic of thermal injury, which made it able to ablate myocardial tissues without damage to the surrounding esophagus and nerves, etc. (10–12). As a new ablation method, PFA is becoming the focus of AF ablation research (15). However, two problems emerge in the previous studies on PFA for AF: (1) Can PFA ablate myocardial tissue without damaging pulmonary veins due to field ablation? (2) Which ablation parameter is better for PFA, especially pulse parameters? There are different pulse parameters designed in reported studies, including pulse frequency from ns to ms, and pulse mode from bi-polar to mono-polar. To solve these problems, two comparative researches were performed in this study: comparison of response of H9C2(2-1) (simulating cardiac tissue) and A7r5 (simulating pulmonary vein) cells to PFA, and comparison of three pulse modes.

The onset and maintenance of AF are closely related to the rapid electrical activity of one or more lesions in the heart, the majority of which are distributed in the pulmonary veins. Thus, AF ablation usually blocks the site of origin of AF by establishing a barrier between the pulmonary vein and the atrium (16). However, ablation of pulmonary vein could cause the risk of stenosis. The best AF ablation method should be selective for cardiomyocytes. In order to verify the sensitivity of PFA to cardiomyocytes, the response of cardiomyocytes and smooth muscle cells to PFA was compared. We found that H9C2(2-1)

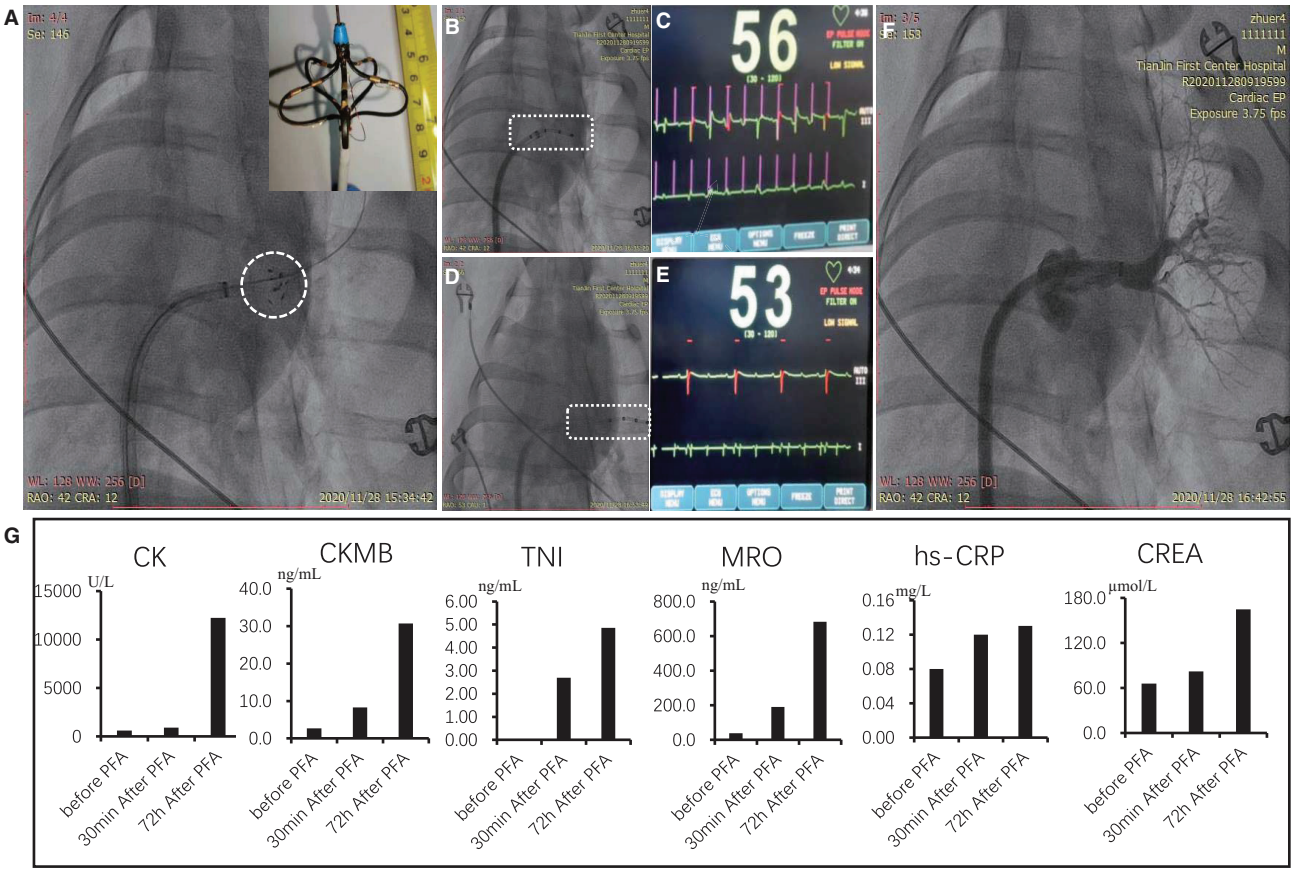

FIGURE 5 | PFA of the left superior pulmonary vein of Bama minipigs. **(A)** Position and shape of PFA electrodes; the embedding graph is the enlarged view of electrode tip. **(B–E)** Effect of PFA verified by cardiac pacing. **(B)** Pacing electrode was in the non-injured part of atrium. **(C)** ECG image after pacing; the first line is pacing signal; the second line is ECG signal. **(D)** Pacing electrode was in the pulmonary vein for PFA. **(E)** ECG image after pacing. **(F)** radiographic image of the ablated pulmonary vein after PFA. **(G)** Indexes of myocardial damage and inflammatory reaction before PFA, 30 min and 72 h after ablation. PFA, pulsed-field ablation.

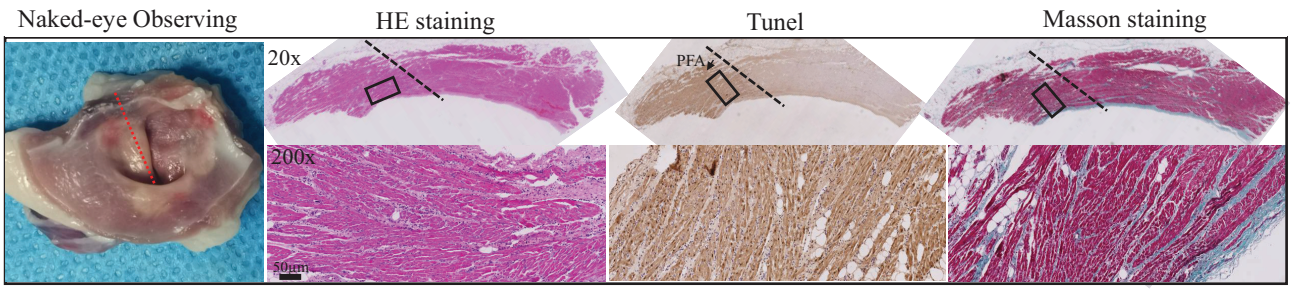

FIGURE 6 | Pathological changes of myocardial tissues after PFA ablation by Gross observation, HE staining, Tunel staining and Masson staining from left to right. Black dotted lines represent the ablation boundary; the images in the black box are shown in the bottom row at 10 times magnification.

not only was more sensitive to PFA than A7r5 but also has a completely different cell morphology. Both cardiomyocytes and smooth muscle cells have an electric field gradient dependence on PFA. When the electric field intensity is >1,000 V/cm, the injury of cardiomyocytes is sharply enhanced, while the injury of smooth muscle cells is <50% (**Figure 1B**), which fully demonstrates the high selectivity of PFA for cardiomyocytes. After PFA, H9C2(2-1) monolayer shrunk completely with intact cell–cell junction and high cell death rate (**Figures 1B,C**,**2**). To explain this phenomenon, we observed the Cx45 expression and

the surface ultrastructure of monolayers, and we found that the pseudopod on the surface of smooth muscle cells seemed to have a protective effect against PFA injury. Fortunately, we first observed the overall ablation effect of PFA on monolayer cell inoculation conductive carriers. In previous studies, single-cell suspension was mostly used as study object because electrode cap was commercialized and easy for setting of ablation system. However, single cells cannot well-simulate the physiological activities of *in vivo* tissues, especially solid organs. Gianulis et al. attempted to study the ablation effect of adherent cells growing on glass coverslips (17). In order to increase the electrical conductivity, a coating of indium tin oxide was added to the non-cellular surface of the glass slides and then was placed into an electrode cup for ablation. But in fact, since glass is a poor conductor of electricity, the added conductivity of the coating makes it difficult to transfer to the cell layer. However, the monolayer system with inserts and electrode array we designed in the study have excellent electrical conductivity. Both sides of the cells are conductive medium, and the no-load resistance is very small. At the same time, the substrate membrane of the insert also simulated the cell matrix. The ablation system is closer to reality, and the membrane shrinkage after PFA of cardiomyocytes we found was also more able to reflect the real situation.

Pulse is the major parameter for PFA, including pulse width, pulse frequency, and pulse mode. Pulse width has been studied for ablation effects in several studies. Dermol-Cerne et al. compared the ablation effect for myocardial cells under ns, μs, and ms pulse width (18). Gianulis et al. studied the ablation effect of PFA for different cells under ns and μs pulse width (17). The μs pulse is generally considered to be more effective. And in the pulse mode, it was found that muscle contraction was likely to be induced by mono-polar pulse, which was one of the main side effects of PFA. However, when bi-polar pulse was adopted, the side effect of muscle contraction was significantly reduced due to depolarization of bi-polar pulse (13, 14). This is particularly important in the ablation of AF. Since the patient is under general anesthesia during tumor ablation, large amounts of muscle relaxants can be used to inhibit muscle convulsions caused by the unidirectional pulse (70–100 μs) PFA. However, AF ablation is performed under local anesthesia in some cases, so muscle relaxants cannot be used to relieve PFA muscle convulsions. Bidirectional pulses that reduce muscle twitching are more suitable for AF ablation than unidirectional pulses. The results of our cell experiments showed that although the damage of bidirectional pulse PFA on myocardial cells was slightly weaker than that of unidirectional pulse, the bidirectional pulse could still achieve the ideal ablation effect by increasing the voltage. Moreover, the effects of bidirectional and unidirectional pulses on the morphology, Ca^{2+} scintillation, and the expression of intercellular junction factor Cx45 were similar. These results suggest that bidirectional pulse can be used for the ablation of cardiomyocytes.

To verify the optimized result of PFA parameters in the cell experiment, *in vivo* experiments of pigs were also conducted in this study. We confirmed that PFA for the atrium by bi-polar short pulse can effectively block the conduction of electrical signals from the pulmonary vein to the atrium and can reduce the side effect of muscle contraction (**Figure 5**). Other findings including PFA-induced apoptosis and completeness of connective tissues, and the relationship between transmural effect and field strength, etc., were consistent with literature reports (19–21).

In conclusion, we found that PFA has a good ablation effect on both cardiomyocytes, which are more sensitive to PFA than smooth muscle cells. PFA can damage myocardial cells without destroying intercellular connections, which is beneficial to the maintenance of tissue structure. At the same degree of myocardial cell damage, the voltage required by bidirectional pulse was higher than that required by unidirectional pulse, but there were no differences in cell morphology, cell–cell injection, and Ca^{2+} activity. The *in vivo* experiment verifies the efficacy and safety of bi-polar short pulse PFA for myocardial cells. These findings answered questions about whether PFA can avoid pulmonary vein injury when ablating myocardial tissue, and the selection of electric field patterns (bidirectional electric field) and pulse parameters (>1,000 V/cm) of PFA. However, due to the small sample size of experimental pigs in this study and no observation of the long-term effects of PFA, more in-depth studies need to be continued. PFA is a novel technique that is promising for the treatment of AF ablation due to its non-thermogenic and selective nature of cardiomyocytes. In the process of clinical transformation, there are still a lot of challenges to be faced. Our team is committed to the research and development of PFA instrument for AF and the clinical transformation of AF PFA and will carry out more in-depth exploration on the basis of this study in the future.

DATA AVAILABILITY STATEMENT

The raw data supporting the conclusions of this article will be made available by the authors, without undue reservation.

ETHICS STATEMENT

The animal study was reviewed and approved by the animal Ethics and Welfare Committee (approval number: 2017015) of Beijing Tonghe Shengtai Comparative Medical Research Institute, Beijing, China.

AUTHOR CONTRIBUTIONS

ZX and CL: conceptualization. XY, SL, QH, and SS: methodology and investigation. XY: data curation. HY: writing—original draft preparation and visualization. ZX: writing—review and editing and funding acquisition. All

authors have read and agreed to the published version of the manuscript.

FUNDING

This research was funded by Tianjin Science and Technology Committee (Grant Nos. 19ZXYXSY00050 and SQ2020YFF0406649) and Tianjin Municipal Health Bureau (Grant No. ZC20165).

SUPPLEMENTARY MATERIAL

The Supplementary Material for this article can be found online at: https://www.frontiersin.org/articles/10.3389/fcvm.2021.690092/full#supplementary-material

REFERENCES

1. January CT, Wann LS, Calkins H, Chen LY, Cigarroa JE, Cleveland JC, et al. 2019 AHA/ACC/HRS focused update of the 2014 AHA/ACC/HRS guideline for the management of patients with atrial fibrillation: a report of the American college of cardiology/American heart association task force on clinical practice guidelines and the heart rhythm society. *J Am Coll Cardiol.* (2019) 74:104–32. doi: 10.1016/j.jacc.2019.01.011
2. Andrade JG, Dubuc M, Guerra PG, Macle L, Mondésert B, Rivard L, et al. The biophysics and biomechanics of cryoballoon ablation. *Pacing Clin Electrophysiol.* (2012) 35:1162–8. doi: 10.1111/j.1540-8159.2012.03436.x
3. Wojtaszczyk A, Caluori G, Pesl M, Melajova K, Starek Z. Irreversible electroporation ablation for atrial fibrillation. *J Cardiovasc Electrophysiol.* (2018) 29:643–51. doi: 10.1111/jce.13454
4. Zhang H, Liu K, Xue Z, Yin H, Dong H, Jin W, et al. High-voltage pulsed electric field plus photodynamic therapy kills breast cancer cells by triggering apoptosis. *Am J Transl Res.* (2018) 10:334–51
5. Paiella S, Salvia R, Girelli R, Frigerio I, Giardino A, D'Onofrio M, et al. Role of local ablative techniques (radiofrequency ablation and irreversible electroporation) in the treatment of pancreatic cancer. *Updates Surg.* (2016) 68:307–11. doi: 10.1007/s13304-016-0385-9
6. Lyu T, Wang X, Su Z, Shangguan J, Sun C, Figini M, et al. Irreversible electroporation in primary and metastatic hepatic malignancies: a review. *Medicine.* (2017) 96:e6386. doi: 10.1097/MD.0000000000006386
7. Narayanan G, Doshi MH. Irreversible electroporation (IRE) in renal tumors. *Curr Urol Rep.* (2016) 17:15. doi: 10.1007/s11934-015-0571-1
8. Wendler JJ, Klink F, Seifert S, Fischbach F, Jandrig B, Porsch M, et al. Irreversible electroporation of prostate cancer: patient-specific pretreatment simulation by electric field measurement in a 3d bioprinted textured prostate cancer model to achieve optimal electroporation parameters for image-guided focal ablation. *Cardiovasc Intervent Radiol.* (2016) 39:1668–71. doi: 10.1007/s00270-016-1390-6
9. Witt CM, Sugrue A, Padmanabhan D, Vaidya V, Gruba S, Rohl J, et al. Intrapulmonary vein ablation without stenosis: a novel balloon-based direct current electroporation approach. *J Am Heart Assoc.* (2018) 7:e009575. doi: 10.1161/JAHA.118.009575
10. Koruth J, Kuroki K, Iwasawa J, Enomoto Y, Viswanathan R, Brose R, et al. Preclinical evaluation of pulsed field ablation: electrophysiological and histological assessment of thoracic vein isolation. *Circ Arrhythm Electrophysiol.* (2019) 12:e007781. doi: 10.1161/CIRCEP.119.007781
11. Koruth JS, Kuroki K, Iwasawa J, Viswanathan R, Brose R, Buck ED, et al. Endocardial ventricular pulsed field ablation: a proof-of-concept preclinical evaluation. *Europace.* (2020) 22:434–9. doi: 10.1093/europace/euz341
12. Reddy VY, Koruth J, Jais P, Petru J, Timko F, Skalsky I, et al. Ablation of atrial fibrillation with pulsed electric fields: an ultra-rapid, tissue-selective modality for cardiac ablation. *JACC Clin Electrophysiol.* (2018) 4:987–95. doi: 10.1016/j.jacep.2018.04.005
13. Arena CB, Sano MB, Rossmeisl, J. H. Jr., Caldwell JL, Garcia PA, et al. High-frequency irreversible electroporation (H-FIRE) for non-thermal ablation without muscle contraction. *Biomed Eng Online.* (2011) 10:102. doi: 10.1186/1475-925X-10-102
14. Aycock KN, Zhao Y, Lorenzo MF, Davalos RV. A theoretical argument for extended interpulse delays in therapeutic high-frequency irreversible electroporation treatments. *IEEE Trans Biomed Eng.* (2021) 68:1999–2010. doi: 10.1109/TBME.2021.3049221
15. Reddy VY, Neuzil P, Koruth JS, Petru J, Funosako M, Cochet H, et al. Pulsed field ablation for pulmonary vein isolation in atrial fibrillation. *J Am Coll Cardiol.* (2019) 74:315–26. doi: 10.1016/j.jacc.2019.04.021
16. Lau DH, Linz D, Sanders P. New findings in atrial fibrillation mechanisms. *Card Electrophysiol Clin.* (2019) 11:563–71. doi: 10.1016/j.ccep.2019.08.007
17. Gianulis EC, Labib C, Saulis G, Novickij V, Pakhomova ON, Pakhomov AG. Selective susceptibility to nanosecond pulsed electric field (nsPEF) across different human cell types. *Cell Mol Life Sci.* (2017) 74:1741–54. doi: 10.1007/s00018-016-2434-4
18. Dermol-Cerne J, Batista Napotnik T, Reberšek M, Miklavčič D. Short microsecond pulses achieve homogeneous electroporation of elongated biological cells irrespective of their orientation in electric field. *Sci Rep.* (2020) 10:9149. doi: 10.1038/s41598-020-65830-3
19. Yao C, Dong S, Zhao Y, Lv Y, Liu H, Gong L, et al. Bipolar microsecond pulses and insulated needle electrodes for reducing muscle contractions during irreversible electroporation. *IEEE Trans Biomed Eng.* (2017) 64:2924–37. doi: 10.1109/TBME.2017.2690624
20. Sano MB, Fan RE, Cheng K, Saenz Y, Sonn GA, Hwang GL, et al. Reduction of muscle contractions during irreversible electroporation therapy using high-frequency bursts of alternating polarity pulses: a laboratory investigation in an ex vivo swine model. *J Vasc Interv Radiol.* (2018) 29:893–8.e4. doi: 10.1016/j.jvir.2017.12.019
21. van Es R, Konings MK, Du Pré BC, Neven K, van Wessel H, van Driel V, et al. High-frequency irreversible electroporation for cardiac ablation using an asymmetrical waveform. *Biomed Eng Online.* (2019) 18:75. doi: 10.1186/s12938-019-0693-7

Conflict of Interest: SS was employed by the company Tianjin Intelligent Health Medical Co., Ltd.

The remaining authors declare that the research was conducted in the absence of any commercial or financial relationships that could be construed as a potential conflict of interest.

Publisher's Note: All claims expressed in this article are solely those of the authors and do not necessarily represent those of their affiliated organizations, or those of the publisher, the editors and the reviewers. Any product that may be evaluated in this article, or claim that may be made by its manufacturer, is not guaranteed or endorsed by the publisher.

frontiers in Cardiovascular Medicine

ORIGINAL RESEARCH
published: 12 October 2021
doi: 10.3389/fcvm.2021.742601

Association Between Apelin and Atrial Fibrillation in Patients With High Risk of Ischemic Stroke

Allan Bohm[1,2,3], Peter Snopek[4,5], Lubomira Tothova[6,7], Branislav Bezak[1,7,8], Nikola Jajcay[3,9], Marianna Vachalcova[10,11], Tomas Uher[3], Marian Kurecko[10], Viera Kissova[12], Katarina Danova[13], Peter Olejnik[1,7], Peter Michalek[3], Tereza Hlavata[2,7], Katarina Petrikova[3], Viliam Mojto[2], Jan Kyselovic[7] and Stefan Farsky[14]*

[1] National Institute of Cardiovascular Diseases, Bratislava, Slovakia, [2] 3rd Department of Internal Medicine, Faculty of Medicine, Comenius University in Bratislava, University Hospital Bratislava, Bratislava, Slovakia, [3] Premedix Academy, Bratislava, Slovakia, [4] Department of Cardiology, Faculty Hospital Nitra, Nitra, Slovakia, [5] St. Elizabeth University of Health and Social Work in Bratislava, Bratislava, Slovakia, [6] Institute of Molecular Biomedicine, Faculty of Medicine, Comenius University, Bratislava, Slovakia, [7] Faculty of Medicine, Comenius University, Bratislava, Slovakia, [8] Faculty of Medicine, Slovak Medical University in Bratislava, Bratislava, Slovakia, [9] Department of Complex Systems, Institute of Computer Science, Czech Academy of Sciences, Prague, Czechia, [10] 1st Department of Cardiology, East Slovak Institute of Cardiovascular Diseases, Košice, Slovakia, [11] Faculty of Medicine, Pavol Jozef Safarik University, Košice, Slovakia, [12] 1st Department of Internal Medicine, Faculty of Medicine, Comenius University, Bratislava, Slovakia, [13] Department of Laboratory Medicine, National Institute of Cardiovascular Diseases, Bratislava, Slovakia, [14] House of the Heart (Dom Srdca), Slovak League Against Hypertension, Martin, Slovakia

OPEN ACCESS

Edited by:
Ana Catarina Fonseca, University of Lisbon, Portugal

Reviewed by:
Maria Baturova, Saint Petersburg State University, Russia
Kuibao Li, Capital Medical University, China

***Correspondence:**
Allan Bohm
allan.bohm@gmail.com

Specialty section:
This article was submitted to Cardiac Rhythmology, a section of the journal Frontiers in Cardiovascular Medicine

Received: *16 July 2021*
Accepted: *13 September 2021*
Published: *12 October 2021*

Citation:
Bohm A, Snopek P, Tothova L, Bezak B, Jajcay N, Vachalcova M, Uher T, Kurecko M, Kissova V, Danova K, Olejnik P, Michalek P, Hlavata T, Petrikova K, Mojto V, Kyselovic J and Farsky S (2021) Association Between Apelin and Atrial Fibrillation in Patients With High Risk of Ischemic Stroke. Front. Cardiovasc. Med. 8:742601. doi: 10.3389/fcvm.2021.742601

Background: Atrial fibrillation (AF) is associated with high risk of stroke preventable by timely initiation of anticoagulation. Currently available screening tools based on ECG are not optimal due to inconvenience and high costs. Aim of this study was to study the diagnostic value of apelin for AF in patients with high risk of stroke.

Methods: We designed a multicenter, matched-cohort study. The population consisted of three study groups: a healthy control group (34 patients) and two matched groups of 60 patients with high risk of stroke (AF and non-AF group). Apelin levels were examined from peripheral blood.

Results: Apelin was significantly lower in AF group compared to non-AF group (*0.694 ± 0.148* vs. *0.975 ± 0.458* ng/ml, $p = 0.001$) and control group (*0.982 ± 0.060* ng/ml, $p < 0.001$), respectively. Receiver operating characteristic (ROC) analysis of apelin as a predictor of AF scored area under the curve (AUC) of *0.658*. Apelin's concentration of *0.969 [ng/ml]* had sensitivity = *0.966* and specificity = *0.467*. Logistic regression based on manual feature selection showed that only apelin and NT-proBNP were independent predictors of AF. Logistic regression based on selection from bivariate analysis showed that only apelin was an independent predictor of AF. A logistic regression model using repeated stratified K-Fold cross-validation strategy scored an AUC of 0.725 ± 0.131.

Conclusions: Our results suggest that apelin might be used to rule out AF in patients with high risk of stroke.

Keywords: atrial fibrillation, apelin, biomarker, electrical atrial remodeling, ischemic stroke

INTRODUCTION

Atrial fibrillation (AF) is associated with high mortality, morbidity, and significant health care costs (1, 2). Despite substantial progress in cardiovascular prevention, constantly increasing incidence and prevalence of AF have reached dimensions of cardiovascular epidemic (3–5). As an independent factor, AF increases the risk of ischemic stroke 5-fold, as well as significantly contributes to the risk of heart failure and death (1, 6). Adequate anticoagulation therapy protects patients from these adverse events, but timely and accurate diagnosis remains a basic precondition (1, 7–11).

Currently available AF diagnostic tools are not sufficient. Standard 12-lead ECG is unreliable because of its low detection rate, especially in the setting of asymptomatic AF, and prolonged ECG monitoring is often impractical due to its high cost and inconvenience. Moreover, it is not always available due to high demand (12–14). There is an increasing need for a new, simple, cost-effective and accurate diagnostic tool, such as a biomarker detectable in peripheral blood.

Our knowledge of AF pathogenesis has evolved and emerging evidence strongly links AF with inflammation, oxidative stress and atrial fibrosis (15–20). Several plasmatic biomarkers for AF have been studied (21–25) and apelin, an endogenous regulatory peptide associated with many physiological and pathophysiological processes (26), has shown promising results (27–29). Among other effects on cardiovascular system, apelin shortens action potential duration in atrial myocytes via its effects on multiple ionic channels. It also affects the renin-angiotensin-aldosterone signaling pathway, acts as a second catalytic substrate for angiotensin-converting enzyme 2 (ACE2) and functions as an inotrope, all of which are processes directly or indirectly associated with AF (30, 31).

In our previous research that included only patients with low risk of stroke, we showed that apelin is significantly decreased in patients with AF compared to patients without AF (27, 28). Whether this result also applies to patients with cardiovascular comorbidities and high risk of stroke is unknown.

Our study sought to further investigate the relationship between apelin and atrial fibrillation and to determine apelin's predictive value for AF in patients with high risk of stroke.

MATERIALS AND METHODS

Study Population

We designed a multicenter, matched-cohort study. Four Slovak hospitals in Bratislava, Malacky, Nitra and Kosice were included. The population consisted of three study groups: A healthy control group consisting of 34 patients without AF (control group) and two matched groups of 60 patients with high risk of stroke: one with atrial fibrillation (AF group) and the other without atrial fibrillation (non-AF group). The healthy control group consisted of random blood donors. Atrial fibrillation was excluded in both control and non-AF group based on the history and 12-lead ECG at the time of enrollment. The inclusion criteria for the AF group were: Age > 17 years, documented, non-valvular paroxysmal AF in the duration of more than 30 s (ECG documented), CHA2DS2-VASc score > 2 for males, CHA2DS2-VASc score > 3 for females and sinus rhythm at the time of inclusion. The inclusion criteria for the non-AF group were: Age > 17 years, CHA2DS2-VASc score > 2 for males, CHA2DS2-VASc score > 3 for females, sinus rhythm at the time of inclusion, no history of palpitations and 30 s AF exclusion using a continuous 7-day ECG Holter and additional 30-day ECG event recorder monitoring three times a day or when the patient felt unwell. Continuous 7-day ECG monitoring was performed using a QardioCore® device and 30-day ECG event recording was performed using a Hartmann Veroval®. The AF group and non-AF group were matched according to these parameters: age, gender, CHA2DS2-VASc parameters, left ventricular ejection fraction (LVEF): reduced (<40%), mid-range (40–49%) and preserved (≥50%), presence of diastolic dysfunction, glomerular filtration rate: (≥1.5 ml/s), (1.4–1 ml/s) and (0.9–0.5 ml/s), drugs (angiotensin-converting enzyme inhibitors and an angiotensin receptor blockers, betablockers, digoxin, amiodarone), body mass index (BMI): (<30 kg/m^2), (30–39 kg/m^2), and (≥40 kg/m^2) and smoking (>5 cigarettes per day). Exclusion criteria for both groups were: electrical cardioversion <7 days prior to inclusion, acute coronary syndrome <1 month prior to inclusion, cardiac surgery <3 months prior to inclusion, acute or decompensated heart failure at the time of inclusion, pregnancy, cardiomyopathy, alcoholism (≥8 drinks/week), thyrotoxicosis, renal disease (dialysis/transplant/CrCl < 0.5 ml/s), liver disease (cirrhosis/transaminase > 3x ULN/bilirubin > 2x ULN), mechanical prosthetic valve, severe mitral stenosis, class I and IV antiarrhythmic drugs usage in the last month, class III antiarrhythmic drugs usage in the last 3 months.

The study was approved by the Ethics Committee of the National Cardiovascular Institute, Bratislava, Slovakia and a written informed consent was obtained from all patients and donors in the control group.

Data Collection and Biochemical Analysis

In AF and non-AF groups, baseline clinical data were obtained during ambulatory visits or during a hospitalization and were recorded into an electronic online case report form. Peripheral fasting blood was taken in the morning using K3EDTA tubes. In the control group, baseline clinical data and fasting blood samples were collected at the time of blood donation. The blood was centrifuged at 2,700 *g* for 5 min and the obtained plasma samples were stored at −80°C. The apelin-12 concentration was measured using a commercially available ELISA kit (Phoenix Pharmaceutical, Karlsruhe, Germany) in plasma samples. Fifty microliters of plasma samples were used for measurement according to the manufacturer's protocol.

Statistical Methods

Continuous variables are presented as sample means and standard deviations. Normality of data was tested using a Shapiro–Wilk test and inspected on Q-Q plots, with homoscedasticity assessed using Levene's test. Classic or Welch ANOVA was employed to analyze the between group differences based on equality of variances, followed by *post-hoc* tests (Tukey-HSD or Games-Howell, respectively) in

order to study pairwise differences between groups. Between group differences for categorical variables were estimated using the χ^2 test of independence with $\lambda = -2$ (Neyman test). All correlations were computed using Spearman's correlation coefficient in order to suppress the effect of tentative outliers. All logistic regression models were fitted either in *sklearn* (with *Elastic-Net* regularization with equal L1 and L2 ratios, and *saga* solver) or *statsmodels* (with the iteratively reweighted least squares method) python libraries, and all receiver operating characteristic (ROC) curves and area under the curve (AUC) statistics were computed using the *sklearn* python library. Before entering the logistic regression, all data were scaled using the standard scaler (to zero mean and unit variance). *P*-values < 0.05 were considered statistically significant.

Based upon our previous research, the expected mean difference in apelin concentration was 0.15 ng/ml with a standard deviation of 0.14. Assuming an alpha of 0.05 and 90% power, the minimum sample size was 24 patients in each matched group.

Data were analyzed using Python version 3.7.9 (https://www.python.org/) with appropriate libraries (for statistical analyses *pingouin* package version 0.3.8: https://pingouin-stats.org/, for

TABLE 1 | Baseline demographics of the study population.

	Non-AF group ($n = 30$)	AF group ($n = 30$)	*p*-value
Age (years)	71.83 ± 8.00	73.63 ± 7.40	0.378
Male gender (%)	19 (63.3%)	19 (63.3%)	> 0.999
Weight (kg)	83.93 ± 12.20	82.63 ± 15.89	0.728
Height (cm)	170.57 ± 9.04	171.10 ± 9.68	0.829
BMI (kg/m^2)	28.86 ± 3.53	28.10 ± 4.09	0.45
Smoking (>5 cigarettes per day) (%)	2 (6.7%)	1 (3.3%)	> 0.999
Systolic blood pressure (mmHg)	134.13 ± 12.48	131.37 ± 9.77	0.366
Diastolic blood pressure (mmHg)	79.13 ± 7.23	75.70 ± 8.36	0.214

Data in the table are presented as mean ± standard deviation or n (%).
AF, atrial fibrillation; BMI, body mass index.

TABLE 2A | Patient characteristics: echocardiography and laboratory parameters.

	Non-AF group ($n = 30$)	AF group ($n = 30$)	*p*-value
Echocardiography			
Left ventricular end-diastolic diameter (mm)	48.73 ± 4.73	48.80 ± 5.34	0.96
Diameter of left atrium in PLAX (Parasternal long axis) (mm)	42.87 ± 5.16	43.00 ± 5.12	0.922
Diastolic dysfunction	0.93 ± 0.73	1.17 ± 0.73	0.295
Left ventricular hypertrophy (%)	13 (43.3%)	14 (46.7%)	> 0.999
Laboratory parameters			
D-dimer (ug/ml)	314.22 ± 391.99	308.33 ± 443.38	> 0.999
Fibrinogen (g/l)	3.71 ± 1.24	3.56 ± 0.58	0.605
CRP (mg/l)	7.62 ± 25.83	4.94 ± 5.31	0.012
NT-proBNP (ng/l)	286.84 ± 297.27	664.82 ± 773.48	0.026
Hs-troponin (ng/l)	11.55 ± 6.77	36.02 ± 96.97	0.071
Apelin (ng/ml)	0.98 ± 0.45	0.69 ± 0.15	0.032
Creatinine (umol/l)	82.00 ± 15.80	85.42 ± 16.53	0.425
Creatinine clearance (ml/s)	1.25 ± 0.21	1.20 ± 0.22	0.376

Data in the table are presented as mean ± standard deviation or n (%).
AF, atrial fibrillation; CRP, C-reactive protein; Hs-troponin, High-sensitivity troponin; NT-proBNP, N-terminal fragment of brain natriuretic peptide.

TABLE 2B | Patient characteristics: medical history and medication.

	Non-AF group ($n = 30$)	AF group ($n = 30$)	*p*-value
Medical history			
AF burden (months)	0	29.85 ± 28.43	N/A
Ischemic stroke/TIA	1.14 ± 0.35	1.25 ± 0.43	0.677
STEMI	1.20 ± 0.40	1.00 ± 0.00	0.606
NSTEMI	1.33 ± 0.47	1.33 ± 0.47	0.792
Ventricular tachycardia/ventricular fibrillation (%)	1 (3.3%)	2 (6.7%)	> 0.999
Arterial hypertension (%)	29 (96.7%)	29 (96.7%)	> 0.999
Pulmonary embolism (%)	0 (0.0%)	1 (3.3%)	> 0.999
Deep vein thrombosis (%)	0 (0.0%)	3 (10.0%)	0.116
Peripheral arterial disease/aortic plaque (%)	10 (33.3%)	13 (43.3%)	0.594
Left ventricular hypertrophy (%)	13 (43.3%)	14 (46.7%)	> 0.999
Stable coronary artery disease (%)	8 (26.7%)	4 (13.3%)	0.32
Chronic obstructive pulmonary disease (COPD) (%)	1 (3.3%)	5 (16.7%)	0.141
Obstructive sleep apnea (OSA) (%)	1 (3.3%)	0 (0.0%)	> 0.999
Severe valvulopathy (%)	0 (0.0%)	0 (0.0%)	> 0.999
Electrical cardioversion (%)	0 (0.0%)	2 (6.7%)	0.408
Pharmacological cardioversion (%)	0 (0.0%)	3 (10.0%)	0.116
CHADS2-VASc	3.7	3.7	N/A
Medication			
ACE- inhibitor/ARB (%)	28 (93.3%)	26 (86.7%)	0.663
Spironolactone/Eplerenone (%)	1 (3.3%)	1 (3.3%)	> 0.999
Beta-blocker (%)	26 (86.7%)	26 (86.7%)	> 0.999
Digoxin (%)	1 (3.3%)	1 (3.3%)	> 0.999
Proton pump inhibitors (%)	6 (20.0%)	13 (43.3%)	0.083
Antidepressants/Antipsychotics (%)	0 (0.0%)	2 (6.7%)	0.408
Acetylsalicylic acid (%)	16 (53.3%)	8 (26.7%)	0.056
Clopidogrel (%)	7 (23.3%)	3 (10.0%)	0.279
Prasugrel (%)	1 (3.3%)	0 (0.0%)	> 0.999
Ticagrelor (%)	0 (0.0%)	0 (0.0%)	> 0.999
Warfarin (%)	1 (3.3%)	9 (30.0%)	0.001
Dabigatran etexilat (%)	0 (0.0%)	4 (13.3%)	0.021
Rivaroxaban (%)	0 (0.0%)	0 (0.0%)	> 0.999
Apixaban (%)	0 (0.0%)	8 (26.7%)	0.001
Edoxaban (%)	0 (0.0%)	1 (3.3%)	> 0.999

Data in the table are presented as mean ± standard deviation or n (%).
ACE, Angiotensin-converting enzyme; ARB, angiotensin receptor blocker; NSTEMI, Non-ST-elevation myocardial infarction; STEMI, ST-Elevation myocardial infarction; TIA, transient ischemic attack.

regression models and their statistics *statsmodels* package version 0.12.1: https://www.statsmodels.org/, *scikit-learn* package version 0.23.2: https://scikit-learn.org/, and *RStudio* 1.2.5033 (32) which was also used for sample size calculation.

RESULTS

Baseline Characteristics

A total of 94 patients were enrolled in the study: 30 in the AF group, 30 in the non-AF group and 34 in the healthy control group. Patient characteristics are presented in **Tables 1**, **2A**–**C**. There were statistically significant differences between the AF and non-AF groups in CRP levels [4.94 ± 5.31 vs. 7.62 ± 25.83 (mg/l), respectively, $p = 0.012$], NT-proBNP levels (664.82 ± 773.48 vs. 286.84 ± 297.27, respectively, $p = 0.026$), Apelin levels (0.69 ± 0.15 vs. 0.98 ± 0.45, respectively, $p = 0.032$) and antithrombotic therapy (see **Tables 1**, **2A**,**B**). Patients in the control group were significantly younger than patients in the AF and non-AF groups.

The analysis of variance test (ANOVA) for all three groups showed a significant group effect on apelin concentrations with $F_{(2, 90)} = 10.67, p < 0.001, \eta_p^2 = 0.192$ with statistical power *0.994* given our number of participants. Subsequent analysis showed significant difference in apelin concentration between healthy controls and patients with AF (*0.982 ± 0.060* vs. *0.694 ± 0.148* ng/ml, $p = 0.001$, $d = 1.044$) as well as between patients with and without AF (*0.694 ± 0.148* vs. *0.975 ± 0.458* ng/ml, $p = 0.001$, $d = -1.021$), respectively. The difference between healthy controls and patients without AF was not significant (*0.982 ± 0.060* vs. *0.975 ± 0.458* ng/ml, $p = 0.900$, $d = 0.023$) (**Figure 1**).

There was no significant correlation between apelin concentration and diastolic dysfunction [*Spearman's r = −0.126, CI 95% (−0.37, 0.13), p* = 0.341], left atrium diameter in parasternal short axis [mm] [*Spearman's r = −0.097, CI 95% (−0.34, 0.16), p* = 0.466], and NT-proBNP [ng/l] [*Spearman's r = −0.147, CI 95% (−0.39, 0.11), p* = 0.267] (**Figure 2**).

ROC analysis of apelin as a predictor of AF scored AUC = 0.658. T = 0.658. The ideal threshold of *apelin concentration was 0.969 [ng/ml] with* accuracy of *0.712*, sensitivity of *0.966*, and specificity of *0.467*, respectively (**Figure 3**).

Finally, we built a logistic regression model for classifying AF using multiple predictors, including apelin. We compared two approaches to this problem, with the first being the manual feature selection based on known predictors of AF from available literature. We selected 16 predictors from our gathered data and fitted a logistic regression model using our patients' data. The model trained on all data scored *AUC = 0.875* (**Figure 4**).

The full list of predictors with their coefficients and *p*-values can be seen in **Table 3A**. Only two predictors were statistically significant with *p*-values lower than 0.05: *apelin*, and *NT-proBNP*.

The second, data-driven route was to compute bivariate analysis (significant differences in our dataset between AF and no AF patients) and include all predictors, whose differences between groups had *p*-value lower than 0.1 (based on *t*-test, Mann-Whitney *U*-test, or χ^2 test where appropriate). Differences in medication were not included in this analysis because they directly depend on the presence of AF. This landed us with four predictors (of course, including apelin) and the final model scored *AUC = 0.825* (**Figure 5**). In this model, only apelin scored

TABLE 2C | Patient characteristics: atrial fibrillation patients vs. non-atrial fibrillation patients vs. control group.

Characteristics	Non-AF group ($n = 30$)	AF group ($n = 30$)	Control group ($n = 34$)	*p*-value
Age (years)	71.83 ± 8.00	73.63 ± 7.40	41.03 ± 9.34	<0.001
Apelin (ng/ml)	0.98 ± 0.45	0.69 ± 0.15	0.98 ± 0.06	= 0.001
Male gender (%)	19 (63.3%)	19 (63.3%)	13 (38.2%)	0.0544

Data in the table are presented as mean ± standard deviation or n (%).
AF, atrial fibrillation.

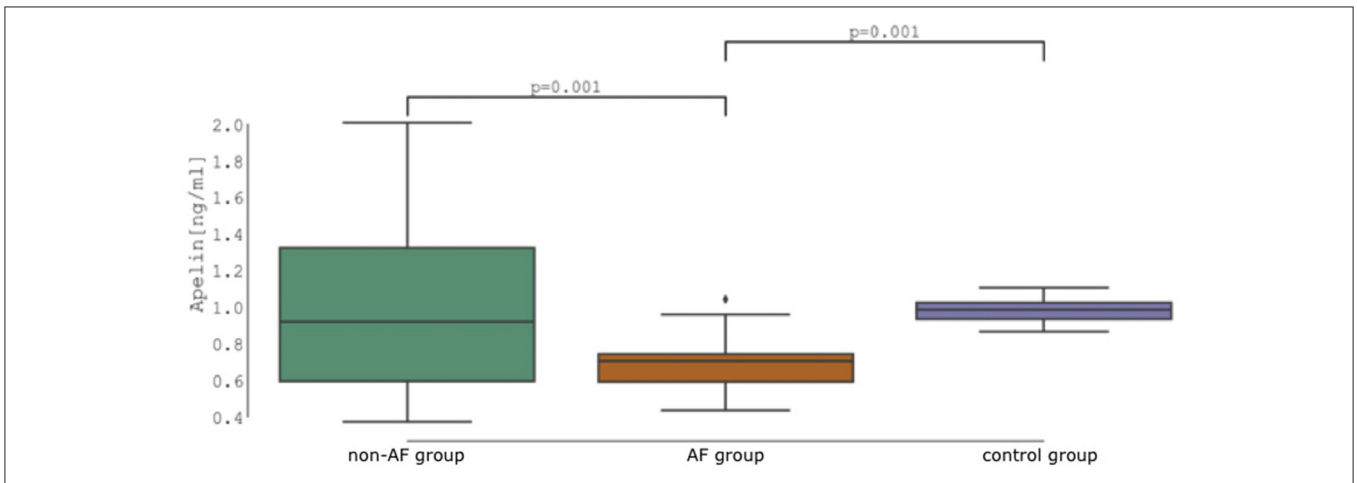

FIGURE 1 | Apelin concentration: Non-atrial fibrillation patients (non-AF group) vs. atrial fibrillation patients (AF group) vs. control group.

p-value lower than preselected threshold of 0.05. The full list of predictors with their coefficients and *p*-values can be seen in **Table 3B**.

To assess the true model performance, we selected predictors from our bivariate analysis with *p*-value < 0.1, and repeatedly trained logistic regression model using repeated stratified K-Fold cross-validation strategy. The receiver operating characteristic (ROC) was computed only from testing dataset. Our final model scored $AUC = 0.725 \pm 0.131$, *with improved sensitivity:* 0.851 ± 0.209 *and specificity:* 0.685 ± 0.250. Full ROC curve showed as mean $\pm$ one standard deviation can be seen in **Figure 6**.

DISCUSSION

Our study demonstrated that in matched cohorts of patients with cardiovascular comorbidities and high risk of stroke, the cohort with AF had significantly lower concentration of apelin compared to the cohort without AF. Similar, there was a statistically significant difference in apelin concentration between patients with AF and the healthy control group.

Further analysis of known AF contributors (1, 33) in our dataset demonstrated that only apelin and NT-proBNP were independent predictors of AF. Increased levels of NT-proBNP in patients suffering from AF have been observed in several studies and their association is well-established (34–36). There

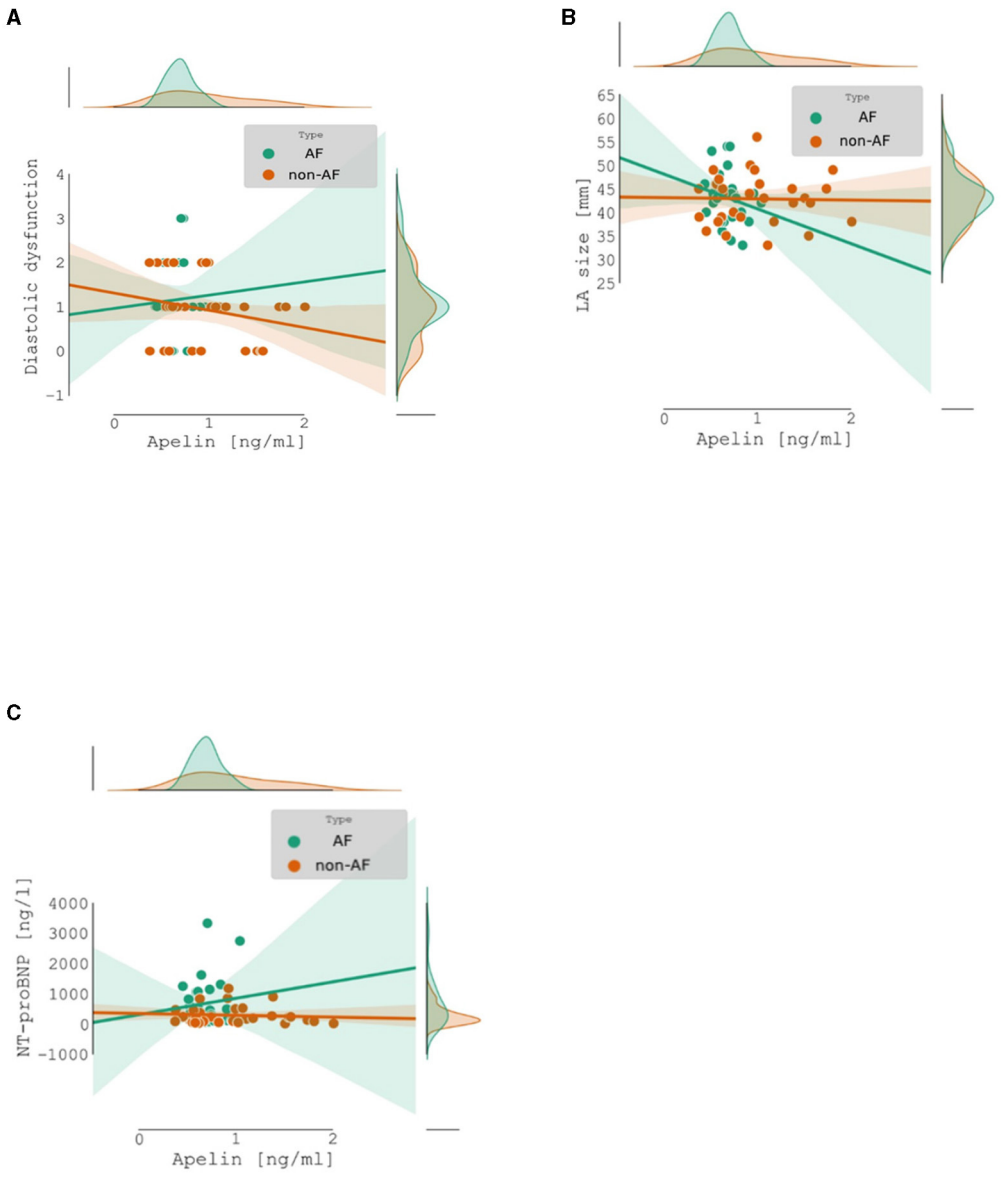

FIGURE 2 | Apelin concentration: Non-atrial fibrillation patients (no-AF) vs. atrial fibrillation patients (AF): **(A)** correlation between apelin concentration and diastolic dysfunction; **(B)** correlation between apelin concentration and left atrium diameter; **(C)** correlation between apelin concentration and NT-proBNP.

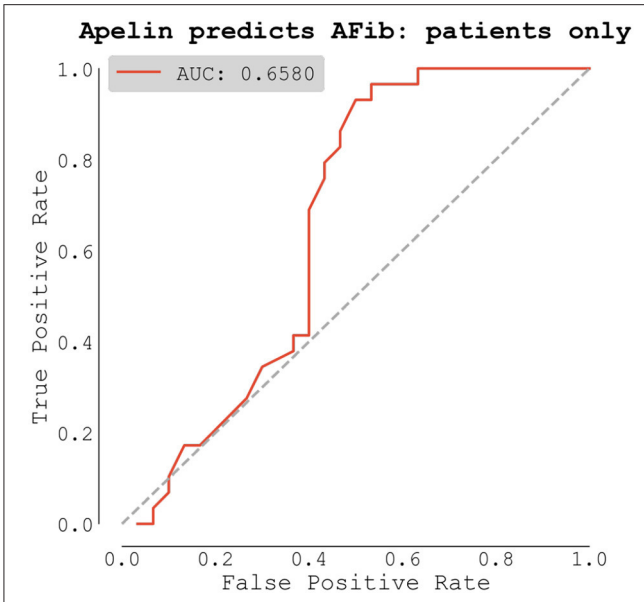

FIGURE 3 | Receiver operating characteristic (ROC) analysis of apelin as a predictor of atrial fibrillation (AF).

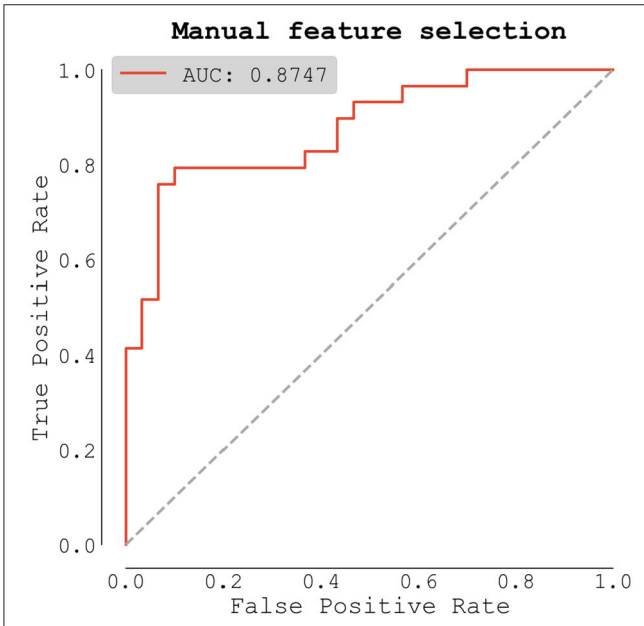

FIGURE 4 | Logistic regression model (all patient data).

TABLE 3A | Logistic regression model for AF predictors.

Predictor	Coef	(95% CI)	*p*-value
(Intercept)	−2.875	(−5.958 to 0.209)	0.068
Signs of heart failure (%)	−0.606	(−2.856 to 1.645)	0.598
Diastolic dysfunction (Grade)	1.512	(−0.622 to 3.647)	0.165
Chronic obstructive pulmonary disease (COPD) (%)	3.745	(0.005 to 7.485)	0.05
Vascular disease (%)	−0.175	(−2.005 to 1.656)	0.852
Gender (%)	1.64	(−0.495 to 3.775)	0.132
Diabetes Mellitus (%)	1.252	(−1.073 to 3.577)	0.291
D-Dimer (ug/ml)	−0.325	(−1.19 to 0.541)	0.462
Systolic blood pressure (mmHg)	0.263	(−0.701 to 1.228)	0.593
Age (years)	−0.47	(−1.398 to 0.457)	0.320
NT-proBNP (ng/l)	1.823	(0.251 to 3.396)	0.023
Diastolic blood pressure (mmHg)	−0.45	(−1.447 to 0.548)	0.377
BMI (kg/m^2)	0.047	(−0.916 to 1.011)	0.923
Apelin (ng/ml)	−1.936	(−3.551 to −0.320)	0.019
CRP (mg/l)	−0.222	(−1.068 to 0.624)	0.607
Creatinine (umol/l)	0.464	(−0.605 to 1.534)	0.395
Diameter of left atrium in PLAX (Parasternal long axis) (mm)	−0.645	(−1.81 to 0.520)	0.278

Data in the table are presented as mean ± standard deviation or n (%).
AF, atrial fibrillation; BMI, body mass index; CRP, C-reactive protein; NT-proBNP, N-terminal fragment of brain natriuretic peptide.

TABLE 3B | Logistic regression model for AF predictors based on selection from bivariate analysis (predictors with $p < 0.1$).

Predictor	Coef	(95% CI)	*p*-value
(Intercept)	0.409	(−0.653 to 1.471)	0.450
Apelin (ng/ml)	−1.019	(−1.915 to −0.123)	0.026
Hs-troponin (ng/l)	3.907	(−1.512 to 9.327)	0.158
NT-proBNP (ng/l)	0.777	(−0.142 to 1.696)	0.097
CRP (mg/l)	−0.321	(−1.061 to 0.418)	0.395

Data in the table are presented as mean ± standard deviation or n (%).
AF, atrial fibrillation; CRP, C-reactive protein; Hs-troponin, High-sensitivity troponin; NT-proBNP, N-terminal fragment of brain natriuretic peptide.

are several unmeasured factors such as amount of exercise (37, 38) or dietary intake (39–41) which may alter apelin plasmatic levels. These changes may be pronounced between patient and healthy control group, however, should not be significant between matched cohorts. Additionally, it is not possible to completely eliminate the potential influence of medication on plasmatic levels of apelin. However, there was no statistically significant difference between plasmatic levels of apelin when comparing high risk patients in non-AF group and healthy donors receiving no chronic medication.

Based on ROC analysis, apelin was able to predict AF with an AUC of 66%. By setting the apelin level threshold to 0.969 [ng/ml] with the aim of maximizing sensitivity we demonstrated a classification accuracy of 0.712, sensitivity of 0.966, and specificity of 0.467.

Our previous research confirmed that apelin has high sensitivity and specificity to predict and quantify AF in patients with minimal cardiovascular comorbidities and low risk of stroke (27, 28). However, this result is not sufficient for use in clinical practice where there would be more complex cases and it would not be known whether apelin would be able to provide sufficient diagnostic power in patients with multiple comorbidities who

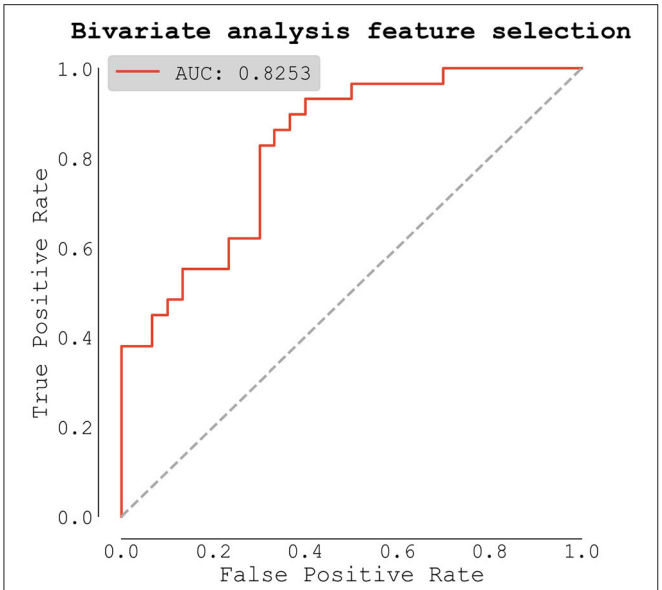

FIGURE 5 | Logistic regression model based on selection from bivariate analysis (predictors with $p < 0.1$).

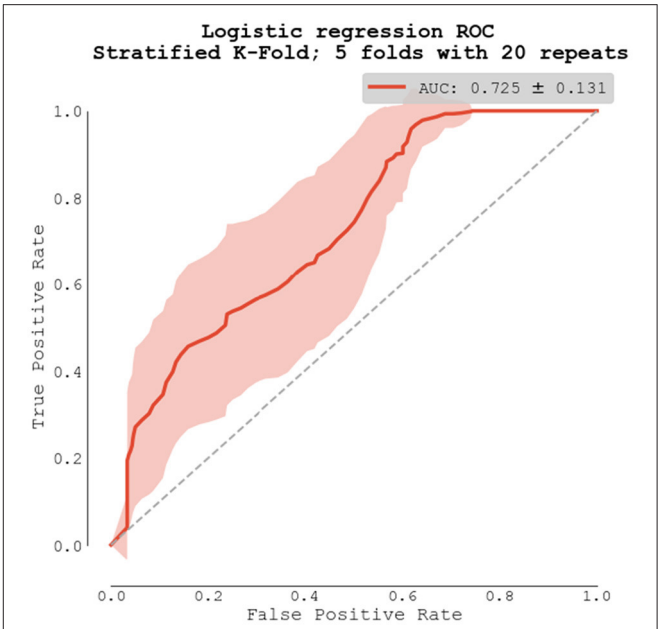

FIGURE 6 | Logistic regression model using repeated stratified K-Fold cross-validation strategy.

are at high risk of stroke. Furthermore, young patients with a low risk profile and lone AF *(reflected in low CHA2DS2-VASc score)* do not meet existing criteria for anticoagulation treatment. To address these questions, we designed a study where apelin was studied in a high-risk cohort of patients with AF and multiple cardiovascular comorbidities. Patients with persistent/permanent AF were not included in this study because we wanted to study if apelin is reduced in the setting of paroxysmal AF and therefore if it potentially can be used for AF detection (e.g., in patients after cryptogenic stroke with no symptoms of arrhythmia).

We were able to confirm good sensitivity, however specificity for AF was low. The APJ receptor for apelin is detectable in many central and peripheral tissues (42, 43) and compelling evidence demonstrates that this complex is involved in a large number of physiological and pathophysiological processes (44, 45). Specificity for AF is therefore limited in patients with comorbidities. This situation could be overcome by including variables besides apelin in a classification model for AF detection.

The Stratified K-Fold cross-validation strategy was performed to ascertain the performance of logistic regression models and to compare this result with the performance of apelin alone. The overall predictive value increased from 66 to 73% *with improved sensitivity: 0.851 ± 0.209 and specificity: 0.685 ± 0.250.* These results suggest a potential improvement in the predictive value of apelin when incorporate into a multi-factor scoring system. The potential benefit of multi-factorial biomarker-based prediction models has already been described in several studies (36, 46, 47).

Optimal patient selection could improve the predictive value of apelin or apelin-based scoring systems for AF. For example, in the case of heart failure with decreased LV ejection fraction, some studies have reported decreased, unaltered or even increased plasma levels compared to control subjects (48, 49). Therefore, patients with reduced LVEF were excluded from our study. On the other hand, patients with heart failure with preserved ejection fraction (HFpEF) were included in our study and they did not show any association with apelin levels. Our observations suggest that apelin, despite its low specificity in the presence of several comorbidities indicating high risk of stroke, could still be used to rule out AF due to its high sensitivity. This, however, should be validated further in a larger cohort of patients.

We also hypothesized about the potential cause of apelin reduction in AF. Previous studies including our findings (28, 50) showed that increased stretch might play a pathophysiological role in decreased apelin concentration. However, in the present study, apelin showed no statistically significant correlation with left atrium (LA) size, NT-proBNP and diastolic dysfunction, all of which are known and verified risk factors for AF development and continuation, and reflect elevated pressure and volume in the atrium. In the context of our present findings, we hypothesize that these previously reported correlations were not causal and that apelin more likely reflects electrical remodeling rather than structural remodeling. This theory also corresponds with experimental findings showing that apelin increases atrial conduction velocity, refractoriness, shortens action potential, affects multiple ionic currents and prevents the inducibility of atrial fibrillation (51, 52).

We believe that our results encourage further research of apelin as a biomarker that might be used to rule out atrial fibrillation.

Study Limitations

Our study had several limitations. The predictive value of apelin with multiple risk factors model was not validated on an independent cohort. However, the cross-validation strategy using repeated K-Fold was used to substitute the independent cohort validation. Secondly, although our inclusion criteria were relatively broad, there are still many unmeasured factors that could alter apelin plasmatic levels. Thirdly, apelin levels may change during the natural history of atrial fibrillation and our study did not follow changes of apelin levels over time. Lastly, a matched-cohort design cannot assess a causal relationship between apelin and AF. Thus, while our results are provocative, they need to be confirmed in future studies.

CONCLUSION

Our results showed that low level of apelin has good sensitivity for atrial fibrillation even in the setting of multiple cardiovascular comorbidities that increase the risk of ischemic stroke. Additional research is needed to verify whether apelin could be used in clinical practice to rule out atrial fibrillation and to improve AF screening in patients with increased risk of ischemic stroke.

DATA AVAILABILITY STATEMENT

The original contributions presented in the study are included in the article/**Supplementary Material**, further inquiries can be directed to the corresponding author.

ETHICS STATEMENT

The studies involving human participants were reviewed and approved by Ethics Committee of the National Cardiovascular Institute, Bratislava, Slovakia. The patients/participants provided their written informed consent to participate in this study.

AUTHOR CONTRIBUTIONS

AB conceived the ideas and designed the study. AB, PS, MV, MK, and TU conducted the study. AB, BB, and NJ analyzed the data. LT performed biochemical analyses. AB, BB, NJ, TH, and KP wrote the manuscript. SF, JK, VM, VK, PM, KD, and PO provided supervision. All the authors have read and approved the final version for publication.

FUNDING

This work was supported by independent research grants provided by the Ministry of Education, Science, Research and Sport of the Slovak Republic VEGA [Grant Number 1/0563/21] and by Pfizer. There was no involvement of grantors in the collection, analysis and interpretation of data, writing of the manuscript, and in the decision to submit the article for publication.

ACKNOWLEDGMENTS

We would like to thank our collaborators at Comenius University Science Park, Bratislava, Slovakia and Assoc. Prof. Eric Eisenstein for valuable help with language editing and proofreading the manuscript.

SUPPLEMENTARY MATERIAL

The Supplementary Material for this article can be found online at: https://www.frontiersin.org/articles/10.3389/fcvm.2021.742601/full#supplementary-material

REFERENCES

1. Hindricks G, Potpara T, Dagres N, Arbelo E, Bax JJ, Blomström-Lundqvist C, et al. 2020 ESC guidelines for the diagnosis and management of atrial fibrillation developed in collaboration with the European association for cardio-thoracic surgery (EACTS): the task force for the diagnosis and management of atrial fibrillation of the European society of cardiology (ESC) developed with the special contribution of the European heart rhythm association (EHRA) of the ESC. *Eur Heart J*. (2021) 42:373–498. doi: 10.1093/eurheartj/ehaa612
2. Vermond RA, Geelhoed B, Verweij N, Tieleman RG, Van der Harst P, Hillege HL, et al. Incidence of atrial fibrillation and relationship with cardiovascular events, heart failure, and mortality: a community-based study from the Netherlands. *J Am Coll Cardiol*. (2015) 66:1000–7. doi: 10.1016/j.jacc.2015.06.1314
3. Chamberlain AM, Brown RD Jr, Alonso A, Gersh BJ, Killian JM, Weston SA, et al. No decline in the risk of stroke following incident atrial fibrillation since 2000 in the community: a concerning trend. *J Am Heart Assoc*. (2016) 5:e003408. doi: 10.1161/JAHA.116.003408
4. Lippi G, Sanchis-Gomar F, Cervellin G. Global epidemiology of atrial fibrillation: an increasing epidemic and public health challenge. *Int J Stroke*. (2021) 16:217–21. doi: 10.1177/1747493019897870
5. Wilhelm M. How to best prevent cardioembolic stroke? *Eur J Prev Cardiol*. (2020) 26:961–63. doi: 10.1177/2047487319842250
6. Song Z, Xu K, Hu X, Jiang W, Wu S, Qin M, et al. A study of cardiogenic stroke risk in non-valvular atrial fibrillation patients. *Front Cardiovasc Med*. (2020) 7:604795. doi: 10.3389/fcvm.2020.604795
7. Saglietto A, Gaita F, De Ponti R, De Ferrari GM, Anselmino M. Catheter ablation vs. Anti-arrhythmic drugs as first-line treatment in symptomatic paroxysmal atrial fibrillation: a systematic review and meta-analysis of randomized clinical trials. *Front Cardiovasc Med*. (2021) 8:664647. doi: 10.3389/fcvm.2021.664647
8. Asad ZUA, Yousif A, Khan MS, Al-Khatib SM, Stavrakis S. Catheter ablation versus medical therapy for atrial fibrillation: a systematic review and meta-analysis of randomized controlled trials. *Circ Arrhythm Electrophysiol*. (2019) 12:e007414. doi: 10.1161/CIRCEP.119.007414
9. Barnett AS, Kim S, Fonarow GC, Thomas LE, Reiffel JA, Allen LA, et al. Treatment of atrial fibrillation and concordance with the American heart association/American college of cardiology/heart rhythm society guidelines: findings from ORBIT-AF (outcomes registry for better informed treatment of atrial fibrillation). *Circ Arrhythm Electrophysiol*. (2017) 10:e005051. doi: 10.1161/CIRCEP.117.005051
10. Taggar JS, Coleman T. Screening for atrial fibrillation in primary care: from recommendation to implementation. *Eur J Prev Cardiol*. (2016) 23:1880–2. doi: 10.1177/2047487316652976

11. Kovacs RJ, Flaker GC, Saxonhouse SJ, Doherty JU, Birtcher KK, Cuker A, et al. Practical management of anticoagulation in patients with atrial fibrillation. *J Am Coll Cardiol*. (2015) 65:1340–60. doi: 10.1016/j.jacc.2015.01.049
12. Murali S, Brugger N, Rincon F, Mashru M, Cook S, Goy JJ. Cardiac ambulatory monitoring: new wireless device validated against conventional holter monitoring in a case series. *Front Cardiovasc Med*. (2020) 7:587945. doi: 10.3389/fcvm.2020.587945
13. Young B. New standards for ECG equipment. *J Electrocardiol*. (2019) 57:S1–S4. doi: 10.1016/j.jelectrocard.2019.07.013
14. Freedman B, Camm J, Calkins H, Healey JS, Rosenqvist M, Wang J, et al. Screening for atrial fibrillation: a report of the AF-screen international collaboration. *Circulation*. (2017) 135:1851–67. doi: 10.1161/CIRCULATIONAHA.116.026693
15. Segers VFM, De Keulenaer GW. Autocrine signaling in cardiac remodeling: a rich source of therapeutic targets. *J Am Heart Assoc*. (2021) 10:e019169. doi: 10.1161/JAHA.120.019169
16. Xiao Z, Reddy DPK, Xue C, Liu X, Chen X, Li J, et al. Profiling of miR-205/P4Ha3 following angiotensin II-induced atrial fibrosis: implications for atrial fibrillation. *Front Cardiovasc Med*. (2021) 8:609300. doi: 10.3389/fcvm.2021.609300
17. Deng Y, Liu F, Yang X, Xia Y. The key role of uric acid in oxidative stress, inflammation, fibrosis, apoptosis, and immunity in the pathogenesis of atrial fibrillation. *Front Cardiovasc Med*. (2021) 8:641136. doi: 10.3389/fcvm.2021.641136
18. Zhou X, Dudley SC, Jr. Evidence for inflammation as a driver of atrial fibrillation. *Front Cardiovasc Med*. (2020) 7:62. doi: 10.3389/fcvm.2020.00062
19. Scott L Jr, Li N, Dobrev D. Role of inflammatory signaling in atrial fibrillation. *Int J Cardiol*. (2019) 287:195–200. doi: 10.1016/j.ijcard.2018.10.020
20. Korantzopoulos P, Letsas KP, Tse G, Fragakis N, Goudis CA, Liu T. Inflammation and atrial fibrillation: a comprehensive review. *J Arrhythm*. (2018) 34:394–401. doi: 10.1002/joa3.12077
21. Staerk L, Preis SR, Lin H, Lubitz SA, Ellinor PT, Levy D, et al. Protein biomarkers and risk of atrial fibrillation: the FHS. *Circ Arrhythm Electrophysiol*. (2020) 13:e007607. doi: 10.1161/CIRCEP.119.007607
22. Yamagishi S-I. Role of advanced glycation endproduct (AGE)-receptor for advanced glycation endproduct (RAGE) axis in cardiovascular disease and its therapeutic intervention. *Circ J*. (2019) 83:1822–28. doi: 10.1253/circj.CJ-19-0618
23. Yamagishi SI, Sotokawauchi A, Matsui T. Pathological role of advanced glycation end products (ages) and their receptor axis in atrial fibrillation. *Mini Rev Med Chem*. (2019) 19:1040–48. doi: 10.2174/1389557519666190311140737
24. Berntsson J, Smith JG, Nilsson PM, Hedblad B, Melander O, Engström G. Pro-atrial natriuretic peptide and prediction of atrial fibrillation and stroke: the malmö preventive project. *Eur J Prev Cardiol*. (2017) 24:788–95. doi: 10.1177/2047487317693948
25. Lubbers ER, Murphy NP, Mohler PJ. Defining the links between oxidative stress-based biomarkers and postoperative atrial fibrillation. *J Am Heart Assoc*. (2015) 4:e002110. doi: 10.1161/JAHA.115.002110
26. Audebrand A, Désaubry L, Nebigil CG. Targeting GPCRs against cardiotoxicity induced by anticancer treatments. *Front Cardiovasc Med*. (2019) 6:194. doi: 10.3389/fcvm.2019.00194
27. Böhm A, Urban L, Tothova L, Bezak B, Uher T, Musil P, et al. Concentration of apelin inversely correlates with atrial fibrillation burden. *Bratisl Lek Listy*. (2021) 122:165–71. doi: 10.4149/BLL_2021_026
28. Uher T, Bohm A, Urban L, Tothova L, Bacharova L, Musil P, et al. Association of apelin and AF in patients with implanted loop recorders undergoing catheter ablation. *Bratisl Lek Listy*. (2020) 121:484–7. doi: 10.4149/BLL_2020_079
29. Wang YZ, Fan J, Zhong B, Xu Q. Apelin: a novel prognostic predictor for atrial fibrillation recurrence after pulmonary vein isolation. *Medicine*. (2018) 97:e12580. doi: 10.1097/MD.0000000000012580
30. Folino A, Montarolo PG, Samaja M, Rastaldo R. Effects of apelin on the cardiovascular system. *Heart Fail Rev*. (2015) 20:505–18. doi: 10.1007/s10741-015-9475-x
31. Cheng CC, Weerateerangkul P, Lu YY, Chen YC, Lin YK, Chen SA, et al. Apelin regulates the electrophysiological characteristics of atrial myocytes. *Eur J Clin Invest*. (2013) 43:34–40. doi: 10.1111/eci.12012
32. RStudio Team. *RStudio: Integrated Development for R*. Boston, MA: RStudio, PBC (2020). Available online at: https://support.rstudio.com/hc/en-us/articles/206212048-Citing-Rstudio?mobile_site=true
33. Casaclang-Verzosa G, Gersh BJ, Tsang TS. Structural and functional remodeling of the left atrium: clinical and therapeutic implications for atrial fibrillation. *J Am Coll Cardiol*. (2008) 51:1–11. doi: 10.1016/j.jacc.2007.09.026
34. Almuwaqqat Z, O'Neal WT, Norby FL, Lutsey PL, Selvin E, Soliman EZ, et al. Joint associations of obesity and NT-proBNP with the incidence of atrial fibrillation in the ARIC study. *J Am Heart Assoc*. (2019) 8:e013294. doi: 10.1161/JAHA.119.013294
35. Büttner P, Schumacher K, Dinov B, Zeynalova S, Sommer P, Bollmann A, et al. Role of NT-proANP and NT-proBNP in patients with atrial fibrillation: association with atrial fibrillation progression phenotypes. *Heart Rhythm*. (2018) 15:1132–37. doi: 10.1016/j.hrthm.2018.03.021
36. Svennberg E, Lindahl B, Berglund L, Eggers KM, Venge P, Zethelius B, et al. NT-proBNP is a powerful predictor for incident atrial fibrillation - validation of a multimarker approach. *Int J Cardiol*. (2016) 223:74–81. doi: 10.1016/j.ijcard.2016.08.001
37. Izadi MR, Ghardashi Afousi A, Asvadi Fard M, Babaee Bigi MA. High-intensity interval training lowers blood pressure and improves apelin and NOx plasma levels in older treated hypertensive individuals. *J Physiol Biochem*. (2018) 74:47–55. doi: 10.1007/s13105-017-0602-0
38. Fujie S, Sato K, Miyamoto-Mikami E, Hasegawa N, Fujita S, Sanada K, et al. Reduction of arterial stiffness by exercise training is associated with increasing plasma apelin level in middle-aged and older adults. *PLoS ONE*. (2014) 9:e93545. doi: 10.1371/journal.pone.0093545
39. Yuzbashian E, Zarkesh M, Asghari G, Hedayati M, Safarian M, Mirmiran P, et al. Is apelin gene expression and concentration affected by dietary intakes? a systematic review. *Crit Rev Food Sci Nutr*. (2018) 58:680–8. doi: 10.1080/10408398.2016.1262325
40. Zuo H, Svingen GFT, Tell GS, Ueland PM, Vollset SE, Pedersen ER, et al. Plasma concentrations and dietary intakes of choline and betaine in association with atrial fibrillation risk: results from 3 prospective cohorts with different health profiles. *J Am Heart Assoc*. (2018) 7:e008190. doi: 10.1161/JAHA.117.008190
41. Bertrand C, Pignalosa A, Wanecq E, Rancoule C, Batut A, Deleruyelle S, et al. Effects of dietary eicosapentaenoic acid (EPA) supplementation in high-fat fed mice on lipid metabolism and apelin/APJ system in skeletal muscle. *PLoS ONE*. (2013) 8:e78874. doi: 10.1371/journal.pone.0078874
42. Kleinz MJ, Davenport AP. Emerging roles of apelin in biology and medicine. *Pharmacol Ther*. (2005) 107:198–211. doi: 10.1016/j.pharmthera.2005.04.001
43. Kawamata Y, Habata Y, Fukusumi S, Hosoya M, Fujii R, Hinuma S, et al. Molecular properties of apelin: tissue distribution and receptor binding. *Biochim Biophys Acta*. (2001) 1538:162–71. doi: 10.1016/S0167-4889(00)00143-9
44. Castan-Laurell I, Dray C, Attané C, Duparc T, Knauf C, Valet P. Apelin, diabetes, and obesity. *Endocrine*. (2011) 40:1–9. doi: 10.1007/s12020-011-9507-9
45. Japp AG, Cruden NL, Barnes G, van Gemeren N, Mathews J, Adamson J, et al. Acute cardiovascular effects of apelin in humans: potential role in patients with chronic heart failure. *Circulation*. (2010) 121:1818–27. doi: 10.1161/CIRCULATIONAHA.109.911339
46. Sepehri Shamloo A, Bollmann A, Dagres N, Hindricks G, Arya A. Natriuretic peptides: biomarkers for atrial fibrillation management. *Clin Res Cardiol*. (2020) 109:957–66. doi: 10.1007/s00392-020-01608-x
47. O'Neal WT, Venkatesh S, Broughton ST, Griffin WF, Soliman EZ. Biomarkers and the prediction of atrial fibrillation: state of the art. *Vasc Health Risk Manag*. (2016) 12:297–303. doi: 10.2147/VHRM.S75537
48. Chong KS, Gardner RS, Morton JJ, Ashley EA, McDonagh TA. Plasma concentrations of the novel peptide apelin are decreased in patients with chronic heart failure. *Eur J Heart Fail*. (2006) 8:355–60. doi: 10.1016/j.ejheart.2005.10.007
49. Földes G, Horkay F, Szokodi I, Vuolteenaho O, Ilves M, Lindstedt KA, et al. Circulating and cardiac levels of apelin, the novel ligand of the orphan receptor APJ, in patients with heart failure. *Biochem Biophys Res Commun*. (2003) 308:480–5. doi: 10.1016/S0006-291X(03)01424-4

50. Scimia MC, Hurtado C, Ray S, Metzler S, Wei K, Wang J, et al. APJ acts as a dual receptor in cardiac hypertrophy. *Nature*. (2012) 488:394–8. doi: 10.1038/nature11263
51. Kim YM, Lakin R, Zhang H, Liu J, Sachedina A, Singh M, et al. Apelin increases atrial conduction velocity, refractoriness, and prevents inducibility of atrial fibrillation. *JCI Insight*. (2020) 5:e126525. doi: 10.1172/jci.insight.126525
52. Chamberland C, Barajas-Martinez H, Haufe V, Fecteau MH, Delabre JF, Burashnikov A, et al. Modulation of canine cardiac sodium current by apelin. *J Mol Cell Cardiol*. (2010) 48:694–701. doi: 10.1016/j.yjmcc.2009.12.011

Conflict of Interest: The authors declare that the research was conducted in the absence of any commercial or financial relationships that could be construed as a potential conflict of interest.

Advantages of publishing in Frontiers

OPEN ACCESS
Articles are free to read for greatest visibility and readership

FAST PUBLICATION
Around 90 days from submission to decision

HIGH QUALITY PEER-REVIEW
Rigorous, collaborative, and constructive peer-review

TRANSPARENT PEER-REVIEW
Editors and reviewers acknowledged by name on published articles

Frontiers
Avenue du Tribunal-Fédéral 34
1005 Lausanne | Switzerland

Visit us: www.frontiersin.org
Contact us: frontiersin.org/about/contact

REPRODUCIBILITY OF RESEARCH
Support open data and methods to enhance research reproducibility

DIGITAL PUBLISHING
Articles designed for optimal readership across devices

FOLLOW US
@frontiersin

IMPACT METRICS
Advanced article metrics track visibility across digital media

EXTENSIVE PROMOTION
Marketing and promotion of impactful research

LOOP RESEARCH NETWORK
Our network increases your article's readership